COMETABOLIC DEGRADATION OF TRICHLOROETHYLENE (TCE) AND 1,2-DICHLOROETHANE (1,2-DCA) IN NITRIFICATION SYSTEMS

by

BİLGE ALPASLAN KOCAMEMİ

BS. in Environmental Engineering, Marmara University, 1996

M.S. in Environmental Engineering, Marmara University, 1999

Submitted to the Institute of Environmental Sciences in partial fulfillment of the requirements for the degree of

Doctor

of

Philosophy

in

Environmental Technology

Boğaziçi University

2005

ACKNOWLEDGEMENTS

I would like to express my sincere thanks to my supervisor Prof. Dr. Ferhan Çeçen for her guidance, support and encouragement, for sharing her vast knowledge and experience with me, for her valuable comments and generous time in proof readings and for providing me a ready-to-use nitrifying biofilm set-up.

I would also like to thank my jury members for spending their valuable time to evaluate this thesis.

I would like to thank my undergraduate students for their help in laboratory works in the scope of their graduation projects under my supervision. Marmara University Environmental Engineering Laboratory staffs are also acknowledged for their help. Thanks to Bülent Mertoğlu and Nuray Güler for molecular analyses of biofilm samples.

The financial supports of this study by the Research Fund of Boğazici University (B.A.P. 02Y101D) and TÜBİTAK (İÇTAG A027, A038, A052) are gratefully acknowledged.

Special thanks to Prof. Dr. Ahmet Saatçi for his continued support in the development of my academic career and for his kindness and interest throughout this thesis.

Special thanks to Neslihan Semerci for her endless support and friendship. Thank you being with me during my hard times. Sincere thanks to Aslıhan Kerç for sharing her knowledge in GC analysis and for her nice friendship.

I am deeply grateful to Ercüment Aktuz for GC calibrations, helpful advices on the use of GC, arrangement for the supply of all GC standards and a hollow fiber membrane module from U.S., and most importantly for standing by me in good and bad times like my family.

Lastly, and most importantly, I am forever indebted to my parents, brother, sister-in-law, mother-in-law and my husband for their never-ending support and unconditional love. To my husband Hakan, thank you for your incredible patience and tremendous encouragement. Without your support, this study would have been much more difficult.

ABSTRACT

Trichloroethylene (TCE) and 1,2-dichloroethane (1,2-DCA), which are extensively used in various industries, are commonly detected organohalogen pollutants in industrial effluents, groundwater and soil. In recent years, biodegradation of TCE and 1,2-DCA by cometabolic processes has received much attention as a promising alternative to other available treatment techniques. To date, cometabolic degradation of these compounds was mainly studied by methane, toluene and phenol oxidizers. On the other hand, nitrifying bacteria, which ubiquitously present in wastewater treatment plants and soil, have been studied to a much smaller extent compared to other organisms. The aim of the present study was to investigate the cometabolic removal of TCE and 1,2-DCA by enriched nitrifier cultures and to assess their inhibitory effects on nitrification. For this purpose, batch suspended-growth experiments and continuous-flow biofilm experiments were performed using enriched nitrifier cultures. These experiments demonstrated that both TCE and 1,2-DCA are cometabolically degradable by enriched nitrifier cultures using ammonium as the primary substrate. However, the presence of these compounds inhibited ammonium utilization. Cometabolic TCE or 1,2-DCA degradation in parallel to ammonium oxidation was found to be dependent on various factors.

ÖZET

Çeşitli endüstriyel faaliyetlerde yaygın olarak kullanılmakta olan trikloroetilen (TCE) ve 1,2-dikloroetan (1,2-DCA) endüstriyel atıksularda, yeraltı suyunda ve toprakta sıklıkla karşılaşılan organik halojen kirleticilerdir. Son yıllarda TCE ve 1,2-DCA'nın kometabolik prosesler ile biyolojik arıtımı diğer mevcut arıtma tekniklerine göre gelecek vadeden bir alternatif olarak oldukça önem kazanmıştır. Bugüne kadar bu maddelerin kometabolik ayrışımı esasen metan, toluen ve fenol gideren organizmalar ile gerçekleştirilmiştir. Diğer taraftan, atıksu arıtma tesislerinde ve toprakta bulunan nitrifikayon bakterileri ile yürütülmüş çalışmaların sayısı diğer bakteri türleri ile gerçekleştirilmiş çalışmalara göre oldukça düşüktür. Bu çalışma kapsamında TCE ve 1,2-DCA'nın nitrifikasyon açısından zenginleştirilmiş kültürler ile kometabolik ayrışımı ve bu maddelerin nitrifkasyon üzerinde yarattığı inhibisyon incelenmiştir. Bu amaç doğrultusunda zenginleştirilmiş nitrifikasyon kültürleri ile kesikli askıda çoğalan deneyler ve sürekli biyofilm deneyleri gerçekleştirilmiştir. Bu deneyler TCE ve 1,2-DCA'nın amonyağı besi maddesi olarak kullanan zenginleştirilmiş nitrifikasyon kültürleri tarafından kometabolik olarak ayrıştırılabildiğini göstermiştir. Ancak, bu maddeler amonyak gideriminin inhibisyonuna sebep olmuştur. TCE ve 1,2-DCA'nın amonyak giderimine paralel olarak kometabolik ayrışımlarının çeşitli faktörlere bağlı olduğu belirlenmiştir.

TABLE OF CONTENTS

LIST OF FIGURES

LIST OF TABLES

LIST OF SYMBOLS / ABBREVIATIONS

Symbol	Explanation	Units used
1,1,1-TCA	1,1,1-Trichloroethane	
1,1,2-TCA	1,1,2- Trichloroethane	
1,1-DCA	1,1-Dichloroethane	
1,2-DCA	1,2-Dichloroethane	
AMO	Ammonia monooxygenase enzyme	
CA	Chloroethane	
C_{DO}	Bulk dissolved oxygen concentration	mg/L
CF	Trichloromethane (chloroform)	
C_{FA}	Bulk free ammonia concentration	mg/L
CM	Chloromethane	
C_{NH4-N}	Bulk ammonium concentration	mg/L
CT	Carbontetrachloride	
DCE	Dichloroethene	
DCM	Dichloromethane	
DGGE	Denaturing Gradient Gel Electrophoresis	
DO	Dissolved oxygen	mg/L
EI	Enzyme-inhibitory compound complex	
EIS	Enzyme-substrate-inhibitory compound complex	
FA	Free ammonia	mg/L
FISH	Fluorescence In-Situ Hybridization	
FNA	Free nitrous acid	mg/L
HAO	Hydroxylamine oxidoreductase enzyme	
HCA	Hexachloroethane	
I	Free inhibitor concentration	mol/L (µg/L)
k	maximum specific growth substrate utilization rate	mg/g.h
k_I	maximum specific non-growth substrate utilization rate	µg/mg.h
K_{ic}	Dissociation constant of EI complex	mol/L (µg/L)
K_{iu}	Dissociation constant of EIS complex	mol/L (µg/L)

K_m	Half-velocity (half-saturation) constant	mol/L (mg/L)
K_m^{app}	Apparent half velocity constant	mol/L (µg/L)
K_N	Half-saturation constant for ammonia	mg/L
K_o	Half-saturation constant for DO	mg/L
K_s	Half-saturation constant	mg/L
K_S^{app}	Apparent half velocity constant	mg/L
K_I	Inhibition constant	µg/L
MLVSS	Mixed Liquor Volatile Suspended Solids	mg/L
MMO	Methane monooxygenase enzyme	
N	Nitrogen concentration	mg/L
NADP	Nicotinamide Adenine Dinucleotide Phosphate	
NH_4^+	Ammonium	mg/L
NH_4-N	Ammonium nitrogen	mg/L
NLSR	Nonlinear Least Square Regression	
NO_2-N	Nitrite nitrogen	mg/L
NO_3-N	Nitrate nitrogen	mg/L
OUR	Oxygen Uptake Rate	mg/L.min
p	Probability value	
PCA	Pentachloroethane	
PCE	Perchloroethene (tetrachloroethene)	
PCR	Polymerase Chain Reaction	
pMMO	Particulate methane monooxygenase enzyme	
r_{NH4-N}	Surface ammonium removal rate	$g/m^2.d$
r_{DCA}	Surface 1,2-DCA removal rate	$mg/m^2.d$
q_{NH4-N}	Specific ammonium utilization rate	mg/g.h
$q_{max,N}$	Maximum specific ammonium oxidation rate	mg /g.h
$q_{max,\ NH4-N}$	Maximum specific ammonium utilization rate	mg/g.h
$q_{mas,NH4-N}^{app}$	Apparent maximum specific ammonium utilization rate	mg/g.h
q_N	Specific ammonium oxidation rate	g /g.d
q_{TCE}	Specific degradation rate of TCE	µg /g .h
q_{DCA}	Specific degradation rate of 1,2-DCA	mg/g.h
r_{NH4-N}	Surface NH_4-N removal rate	$g/m^2.d$

r_{NO2-N}	Surface NO_2-N accumulation rate	$g/m^2.d$
r_{NO3-N}	Surface NO_3-N production rate	$g/m^2.d$
S	Substrate concentration	mol/L (mg/L)
sMMO	Soluble methane monooxygenase enzyme	
SOUR	Specific Oxygen Uptake Rate	mg/mg.min
T	Temperature	^0C
T_y	Transformation yield	mg/mg
TCE	Trichloroethylene	
TeCA	Tetrachloroethane	
V	Reaction velocity	mol/L.time
VC	Vinyl chloride (Monochlorinated ethene)	
V_m	Maximum reaction velocity	mol/L.time
V_m^{app}	Apparent maximum reaction velocity	mol/L.time
VSS	Volatile suspended solids	mg/L
Y_N	Yield coefficient for nitrifiers	g/g
α	Type I error, significance level	
ε	Ratio of the pseudo-first-order reaction rate constants for the growth substrate and non-growth substrate	
$\mu_{max,a}$	Maximum specific growth rate of autotrophic biomass	1/day
$\mu_{max,N}$	Maximum specific growth rate of nitrifying bacteria	1/day
μ_N	Specific growth rate of nitrifying bacteria	1/day

1. INTRODUCTION

Trichloroethylene (TCE), which is extensively used in degreasing of fabricated metal parts, industrial dry-cleaning and textile manufacturing (CEPA, 1993), and 1,2-dichloroethane (1,2-DCA) which is extensively used in the production of vinyl chloride and organic solvents (e.g., trichloroethylene, tetrachloroethylene) (ATSDR, 2001a), are two of the most commonly detected organohalogen pollutants in industrial effluents, groundwater and soil. The widespread occurrence of TCE and 1,2-DCA in industrial effluents and subsurface media is an important environmental issue due to their carcinogenic and other serious health effects on humans (ATSDR 1997; 2001a; 2001b; 2003). Therefore, in recent years, their discharges into the environment have been strictly regulated and great effort has been spent to remediate subsurface media contaminated with these compounds in the past.

Among the available treatment techniques, air stripping and carbon adsorption simply transfer these compounds from one medium to another without any significant reduction in volume or toxicity (EPA 1992), while the chemical oxidation techniques are energy intensive and expensive (EPA 1993a). Therefore, in recent years, elimination of TCE and 1,2-DCA by biological processes has gained importance as an attractive solution due to lower cost and capability of toxicity reduction.

Research efforts to date clearly demonstrate that TCE is resistant to biodegradation because it can not be used as an energy and growth-substrate by microorganisms. In contrast to TCE, 1,2-DCA is known to be utilized by some pure aerobic bacterial strains [e.g., *Xanthobacter autotrophicus GJ10* (Inguva and Shreve, 1999)]. However, these pure bacterial strains isolated under sterile conditions and adapted to 1,2-DCA are not widespread in the environment. Therefore, in recent years, the cometabolic degradation process has appeared as a promising alternative for biological treatment of TCE and 1,2-DCA. During cometabolic degradation, one organism, which is growing on a particular substrate also oxidizes a second substrate (non-growth substrate) that cannot be used as a carbon and energy source by the organism (Singleton, 1994). Therefore, cometabolic degradation of a non-growth substrate requires the presence of another growth-supporting

substrate. But, the presence of a non-growth substrate may also inhibit the degradation of growth-substrate.

To date, cometabolic degradations of TCE and 1,2-DCA under aerobic conditions were mainly studied by organisms, which utilize slightly soluble methane gas and toxic aromatic compounds (e.g., toluene and phenol) as primary growth-substrates. Although the nitrifying bacteria, which is ubiquitously present in almost all environment (particularly in soil and wastewater treatment plants), are particularly attractive for the cometabolic treatment of TCE (or 1,2-DCA), they have been studied to a much smaller extent compared to other organisms. Much of these limited number of studies were performed with pure *Nitrosomonas europaea* species rather than mixed nitrifying cultures although the latter represent a more realistic case. There is almost no detailed study evaluating both the cometabolism of these compounds and their inhibitory effects on nitrification for a broad ammonium and TCE (or 1,2-DCA) range. Additionally, in the former studies the interest was focused on suspended-growth systems and in literature there is still lack of information about the cometabolic degradation of TCE (or 1,2-DCA) in biofilm systems containing nitrifying cultures.

In the present study, cometabolic degradation of TCE and 1,2-DCA and their inhibitory effects on nitrification were studied in batch suspended-growth systems enriched for nitrifiers. The cometabolic degradation 1,2-DCA and its inhibitory effects on nitrification were also studied in a continuous-flow nitrifying biofilm reactor. The findings of this research demonstrate the cometabolic degradation of TCE and 1,2-DCA with nitrifying cultures and dependence of the process on various factors. Therefore, this study could fill a gap in literature and be useful in the design of engineered TCE (or 1,2-DCA) remediation/treatment systems.

2. CHLORINATED ORGANIC COMPOUNDS

Chlorinated organics are a broad class of compounds, which are manufactured in bulk quantities and used for a wide range of applications in various industries. Some of the industrially important chlorinated organics and their major applications in industry are summarized in Table 2.1.

While these compounds are widely used in various industries, they are transported to the environment through discharge of industrial wastewaters, seepage from landfills, leakage from underground storage tanks and accidental spillages. Many of these compounds are important environmental pollutants because they have been introduced into the environment in large quantities, have potentially high carcinogenic potency factors and/or other toxicity, and exhibit slow breakdown rates in the environment (Ely et al., 1995a). Therefore, in recent years, discharges of chlorinated organics have been subject to stringent environmental regulations. However, the long history of use and improper disposal of chlorinated organics has caused contamination of many soil and groundwater sources in the past. Nowadays, trichloroethylene (TCE) and 1,2-dichloroethane (1,2-DCA), which were chosen as the model compounds in this study, are among the most frequently detected chlorinated organic contaminants in groundwater and soil media.

All these factors lead to an intense interest in the treatment of chlorinated organics to limit their discharges into the environment and to remediate subsurface media contaminated in the past. Up to date, different treatment techniques such as air stripping, carbon adsorption and chemical oxidation have been developed. However, air stripping and carbon adsorption simply transfer contaminants from one medium to another without any significant reduction in volume or toxicity (EPA, 1992), while the chemical oxidation techniques are energy intensive and expensive (EPA, 1993a). Therefore, in recent years, biological treatment techniques, which may provide partial or full degradation of chlorinated organics rather than transferring them from one phase to another have received much attention as a cost-effective alternative.

Table 2.1. Industrially important chlorinated organics and their major applications (Fetzner, 1998)

Chlorinated Organic	Major Applications
Chloromethanes	
Monochloromethane (CM)	Production of silicones, tetramethyllead, methylcellulose; other methylation reactions
Dichloromethane (DCM)	Degreasing agent; paint remover; pressure mediator in aerosols; extraction technology
Trichloromethane (CF) (chloroform)	Production of monochlorodifluoromethane (used for the manufacture of Teflon); extractant of pharmaceutical products
Tetrachloromethane (CT) (carbontetrachloride)	Production of trichloromonofluoromethane and dichlorodifluoromethane; solvent
Chloroethanes	
Monochloroethane	Production of tetraethyllead; production of ethylcellulose; ethylating agent for fine chemical production; solvent for extraction processes
1,1-Dichloroethane (1,1-DCA)	Feedstock for the production of 1,1,1-trichloroethane
1,2-Dichloroethane (1,2-DCA)	Production of vinylchloride; production of chlorinated solvents; synthesis of ethylenediamines
1,1,1-Trichloroethane (1,1,1-TCA)	Dry cleaning; vapor degreasing; solvent for adhesives and metal cutting fluids; textile processing
1,1,2-Trichloroethane (1,1,2-TCA)	Intermediate for production of 1,1,1-trichloroethane and 1,1-dichloroethane
Chloroethenes	
Monochloroethene (VC) (vinylchloride)	Production of polyvinylchloride (PVC); production of chlorinated solvents
1,1-Dichloroethene (1,1-DCE)	Basic material for polyvinylidine chloride and its copolymers; production of 1,1,1- trichloroethane
Trichloroethene (TCE)	Solvent for vapor degreasing in the metal industry and for dry cleaning; extraction solvent; solvent in formulations for rubbers, elastomers, and industrial paints
Tetrachloroethene (PCE)	Solvent for dry cleaning, metal degreasing, textile finishing, dyeing, extraction processes; intermediate for the production of trichloroacetic acid and some fluorocarbons
2-Chloro-1,3- butadiene (chloroprene)	Starting monomer for polychloroprene rubber

Table 2.1. continued (Fetzner, 1998)

Chlorinated Organic	Major Applications
Nucleus-chlorinated aromatic hydrocarbons	
Monochlorobenzene	Production of nitrophenol, nitroanisole, chloroaniline, and phenylenediamine for the manufacture of dyes, crop protection products, pharmaceuticals, and rubber chemicals
1,2-Dichlorobenzene	Production of 1,2-dichloro-4-nitrobenzene for the production of dyes and pesticide; production of disinfectants, deodorants
1,4-Dichlorobenzene	Production of disinfectants, room deodorants; moth control agent; production of insecticide; production of 2,5-dichloronitrobenzene for the manufacture of dyes; production of polyphenylenesulfide-based plastics
Chlorinated toluenes	Hydrolysis to cresol; solvents for dyes; precursors for dyes, pharmaceuticals, pesticides, preservatives, and disinfectants
Chlorophenols (CP)	Preparation of agricultural chemicals (herbicides, insecticides, fungicides), pharmaceuticals, biocides, and dyes
Chlorophenoxy-alkanoic acids	Herbicides
Side-chain chlorinated aromatic hydrocarbons	Production of plasticizers, benzyl alcohol, benzaldehyde, benzoylchloride, pesticides, and dyes.

2.1. Trichloroethylene (TCE)

2.1.1. Chemical and Physical Properties

Trichloroethylene (TCE, CAS No.79-01-6) is a colorless, non-flammable liquid having a sweet, chloroform-like odor and a molecular formula of C_2HCl_3 (131.4 g/mol). It is a volatile, synthetic chemical with a vapor pressure of 8.0 to 9.9 kPa (at 20-25^{0}C), water solubility of 1.1 to 1.4 g/L (at 20-25^{0}C), density of 1.46 g/mL (at 20^{0}C), Henry's constant of 0.020 atm.m^3/mol (at 20^{0}C), boiling point of 86.7^{0}C, melting point of –87.1^{0}C and log partition coefficients (log K_{ow} and log K_{oc}) of 2.42 and 2.03-2.66, respectively. In air, 1 ppm is equivalent to 5.41 mg/m^3 (at 20°C and 101.3 kPa) (ATSDR, 1997; CEPA, 1993).

2.1.2. Production, Use, Release and Environmental Fate

TCE is a synthetic product with no known natural sources. It is generally produced by chlorinating ethylene or ethylene dichloride. The major use of TCE is for the vapor-degreasing and cold-cleaning of fabricated metal parts in the automotive and metals industries. TCE is also used in the production of adhesives and copolymers, household and industrial dry-cleaning, textile manufacturing, the cleaning of electronic components, petroleum industry processes involving refining catalysts, paint removers coatings and vinyl resins, and in laboratory reagent/solvent applications. Household or consumer products that may contain TCE include typewriter correction fluids, paint removers/strippers, adhesives, spot removers and rug-cleaning fluids (CEPA, 1993).

TCE releases into the atmosphere through evaporation from degreasing operations, volatilization from water treatment facilities, gaseous emissions from landfills and stack emissions from the incineration of municipal and hazardous waste. TCE does not readily undergo chemical oxidation or hydrolysis in the atmosphere, and direct photolysis is a minor transformation process (ATSDR, 1997). In the air, it reacts with photochemically produced hydroxyl radicals to produce phosgene, dichloroacetyl chloride, formyl chloride etc. (CEPA, 1993). The estimated half-life for this process is approximately 7 days (Papp, 1996). Although this relatively short half-life indicates that TCE is not a persistent atmospheric compound, the actual half-life varies with latitude, season and concentration of hydroxyl radicals (CEPA, 1993). Moreover, it should be noted that the half-lives determined by assuming first-order kinetics represent the calculated time for loss of the first 50% of TCE; the time required for the loss of the remaining 50% may be substantially longer (ATSDR, 1997).

TCE is released to surface water from industrial discharges of wastewater streams of manufacturing and processing facilities. Oxidation of TCE in the aquatic environment does not appear to be significant, probably because of its already oxidized form by the chlorine atoms. The rate of hydrolysis is also too slow to be an important transformation process. Since neither biodegradation nor hydrolysis occurs at a rapid rate and TCE has a high Henry's constant of $2x10^{-2}$ atm.m^3/mol, most TCE present in surface water can be expected to volatilize into the atmosphere. However, TCE is denser than water and only

moderately soluble in water. Therefore, it is not immediately volatilized and may be expected to submerge and thus be removed by contact with the surface (ATSDR, 1997). The estimated half-life for volatilization of TCE dissolved in surface water is approximately several minutes to several hours (Papp, 1996). Although volatilization is rapid, the actual volatilization rates in the natural environment depend on a number of parameters such as the depth of water, its flowrate and the airspeed above it, the temperature of water and the air, and the possibility of stratification caused by the salinity/density of seawater, freshwater or effluents (Papp, 1996). Based on its low n-octanol/water partition coefficient and the results of field studies, TCE is unlikely to significantly bioaccumulate in aquatic biota (CEPA, 1993).

TCE can be released to the soil through industrial discharges and improper disposal of industrial wastes and TCE-containing products (e.g, glues, paints). Releases to the ground will result in either evaporation or percolation into the subsurface. Volatilization of TCE from soil is slower than from water (ATSDR, 1997). The low K_{oc} value of 2.42 translates into little retardation by soil or aquifer organic materials. Since it is heavier than water and has a low solubility, TCE is classified as a dense non-aqueous phase liquid (DNAPL); therefore, it is likely to move downward through the subsurface until lower permeability features impedes its progress (EPA, 1992). Its high mobility in soil may result in substantial percolation towards subsurface regions before volatilization can occur (ATSDR, 1997). In the subsurface region, TCE can become associated with soil pore water, enter the gas phase, or exist as a non-aqueous phase liquid (NAPL). Areas containing insoluble TCE, i.e., DNAPL pools, can serve as sources for contamination. As groundwater moves through and/or around these source areas, the pollutant partitions into the aqueous phase. Aqueous phase TCE is then spread through the aquifer by advection and dispersion (EPA, 1992). TCE can also be formed in groundwater as a biodegradation product of tetrachloroethylene (CEPA, 1993).

2.1.3. Levels Monitored in the Water Media

The TCE concentrations monitored in surface water, groundwater and leachate samples at various locations are presented in Table 2.2.

2.1.4. Health Effects, Regulations and Guidelines

People can be exposed to TCE by inhalation, oral and dermal routes. In most circumstances, the inhalation route and ingestion of drinking water are the primary routes of exposure to TCE (http://www.toronto.ca). Breathing small amounts of TCE may cause headaches, lung irritation, dizziness, poor coordination, and difficulty in concentrating. Breathing large amounts of TCE may cause impaired heart function, unconsciousness, and death. Breathing it for long periods may cause nerve, kidney, and liver damage. Drinking large amounts of TCE may cause nausea, liver damage, unconsciousness, impaired heart function, or death. Drinking small amounts of TCE for long periods may cause liver and kidney damage, impaired immune system function, and impaired fetal development in pregnant women, although the extent of some of these effects is not yet clear. Skin contact with TCE for short periods may cause skin rashes (ATSDR, 2003). Based on the limited data in humans regarding TCE exposure and cancer, and evidence that high doses of TCE can cause cancer in animals, the International Agency for Research on Cancer (IARC) has determined that TCE is probably carcinogenic to humans (Class 2A). TCE has been nominated for listing in the National Toxicology Program (NTP) 9th Report on Carcinogens. Evaluation of this substance by the NTP review committee is ongoing. In the past, EPA assigned a classification of B2 (probable human carcinogen) to TCE. In 1988, EPA's Scientific Advisory Board offered an opinion that the weight of evidence was on a C-B2 continuum (possible-probable human carcinogen). The agency has not restated a more current position on the weight-of-evidence classification and is reflecting this by posting an "under review" status in the Integrated Risk Information System (IRIS) (ATSDR, 1997).

Regulation of TCE by the EPA began in the 1980s. TCE is listed as a priority pollutant under the Clean Water Act (CWA) and has a Safe Drinking Water Act (SDWA) maximum contaminant limit of 5 µg/L. It is regulated under the Resource Conservation and Recovery Act (RCRA) as a spent solvent process waste and as a characteristically toxic waste (any material leaching greater than 0.5 mg/L). The Comprehensive Environmental Response, Compensation, and Liability Act (CERCLA) requires reporting of releases of TCE above 100 pounds (about 8 gallons), while the Superfund Amendments and Reauthorization Act (SARA) lists TCE as a chemical requiring reporting under its

community right-to-know provisions (http://www.clu-in.org). The Occupational Safety and Health Administration (OSHA) has set an exposure limit of 100 parts of TCE per million parts of air (100 ppm) for an 8-hour workday, 40-hour workweek (ATSDR, 2003).

2.2. 1,2-Dichloroethane (1,2-DCA)

2.2.1. Chemical and Physical Properties

1,2-Dichloroethane (1,2-DCA; CAS Registry No.107-06-2) is a colorless, flammable liquid having a sweet, chloroform-like odor and a molecular formula of $C_2H_4Cl_2$ (98.96 g/mol). It is a volatile, synthetic chemical having a vapor pressure of 8.5 to 10.5 kPa (at 20-25^{0}C), water solubility of 8.69 g/L (at 20^{0}C), density of 1.23 g/mL (at 20^{0}C), Henry's constant of 0.0011 atm.m^3/mol (at 20^{0}C), boiling point of 83.5^{0}C, melting point of –35.5^{0}C and log partition coefficients (log K_{ow} and log K_{oc}) of 1.76 and 1.28, respectively. In air, 1 ppm is equivalent to 4.05 mg/m^3 (at 25°C) (ATSDR, 2001a; CEPA, 1994).

2.2.2. Production, Use, Release and Environmental Fate

1,2-DCA does not occur naturally (ATSDR, 2001a). It is produced by either the catalytic vapor-or liquid-phase chlorination of ethylene or by oxychlorination of ethylene (CEPA, 1994). 1,2-DCA is mainly used as a chemical intermediate in the synthesis of vinyl chloride (ATSDR, 2001a; CEPA, 1994), which in turn is used in the manufacture of polymers. It is also added to leaded gasoline as a lead scavenger; however, this use has declined significantly as leaded gasoline use has attenuated. It is also used in the synthesis of vinylidene chloride, 1,1,1-trichloroethane, trichloroethene, tetrachloroethene, aziridines, and ethylene diamines and in chlorinated solvents. Formerly, 1,2-DCA was used in varnish and finish removers, in soaps and scouring compounds, in organic synthesis for extraction and cleaning purposes, in metal degreasers, in ore flotation, and in paints, coatings, and adhesives It was also formerly used as a grain, household, and soil fumigant (ATSDR, 2001a).

Releases of 1,2-DCA to the environment may result from the manufacture, use, storage, distribution, and disposal of 1,2-DCA. Older consumer goods containing 1,2-DCA that are still in use or have been discarded as waste also represent potential emission sources. 1,2-DCA may also be released to the environment from the microbial degradation of other chlorinated alkanes. For example, 1,2-DCA is a known product of the anaerobic biodegradation of 1,1,2,2-tetrachloroethane (ATSDR, 2001a).

In the atmosphere, 1,2-DCA is degraded by reaction with photochemically produced hydroxyl radicals. The estimated atmospheric lifetime of 1,2-DCA was reported to be >5 months with formyl chloride, chloroacetyl chloride, hydrogen chloride, and chloroethanol reported as degradation products. 1,2-DCA is not expected to undergo significant atmospheric removal by oxidation with ozone or nitrate radicals, and it will not undergo removal by direct photolysis. 1,2-DCA released to the atmosphere may be transported long distances before being washed out in precipitation or degraded (ATSDR, 2001a).

Based on the high vapor pressure and volatility, 1,2-DCA is expected to volatilize rapidly from water surfaces. The estimated half-life for volatilization of 1,2-DCA in surface water is approximately 30 minutes to 4 hours (Papp, 1996). No information was found regarding partitioning of 1,2-DCA from the water column onto sediments. Based on log K_{oc} value of 1.28, 1,2-DCA is not expected to adsorb to sediment in the water column. The n-octanol/water partition value (log K_{ow}) of 1.76 indicates that 1,2-DCA will not bioconcentrate in fish and aquatic organisms (ATSDR, 2001a). Hydrolysis of 1,2-DCA can occur in the aquatic environment; however, with an estimated half-life of 72 years at neutral pH and at 25^0C, this process cannot be considered as a major removal pathway from surface waters (CEPA, 1994).

1,2-DCA released to land surfaces is expected to volatilize into atmosphere or leach into groundwater. Based on log K_{oc} value of 1.28, 1,2-DCA is expected to have very high mobility in soil surfaces and should be available for transport into groundwater. Environmental surveys conducted by EPA have detected 1,2-DCA in groundwater sources in the vicinity of contaminated sites. Large spills of 1,2-DCA may contaminate

groundwater because of the high density of this compound, which makes it sink into the aquifer in a vertical gravity-driven process (ATSDR, 2001a).

2.2.3. Levels Monitored in the Water Media

The 1,2-DCA concentrations monitored in surface water, groundwater and industrial wastewater samples at various locations are presented in Table 2.3.

2.2.4. Health Effects, Regulations and Guidelines

People can be exposed to 1,2-DCA by inhalation, oral and dermal routes. Nervous system disorders, liver and kidney diseases, and lung effects have been reported in humans ingesting or inhaling large amounts of 1,2-DCA. In laboratory animals, breathing or ingesting large amounts of 1,2-DCA have also caused nervous system disorders and liver, kidney, and lung effects. Animal studies also suggest that 1,2-DCA may damage the immune system. Kidney disease has also been seen in animals ingesting low doses of 1,2-DCA for a long time. Studies in animals indicate that 1,2-DCA does not affect reproduction (ATSDR, 2001b). So far, exposure to 1,2-DCA has not been associated with cancer in humans. Cancer was found in laboratory animals who were fed large doses of 1,2-DCA. When 1,2-DCA was put on the skin of laboratory animals, they developed lung tumors. Because of the cancer findings in animals, the possibility of cancer in humans cannot be ruled out. The Department of Health and Human Services (DHHS) has determined that 1,2-DCA may reasonably be anticipated to be a human carcinogen. The International Agency Research on Cancer (IARC) has placed 1,2-DCA in Group 2B (possibly carcinogenic to humans), and the EPA has classified 1,2-DCA as a Group B2 carcinogen (probable human carcinogen) (ATSDR, 2001a).

The EPA allows 5 μg/L 1,2-DCA in drinking water. The Occupational Safety and Health Administration (OSHA) has set a limit of 50 parts of 1,2-DCA per million parts of air (50 ppm) in workplace air for 8 hour shifts and 40 hour work weeks (ATSDR, 2001 b).

Table 2.2. TCE levels monitored in water media

Media	Site Description	Location	TCE detected (µg/L)	Reference
Groundwater	West Central Phoenix Site -Glenrosa Avenue	Arizona, U.S.	11.5	http://www.azdeq.gov
Groundwater	Savannah River Site	USA	60	EPA, 2000
Groundwater	West Central Phoenix Site-42nd Avenue	Arizona, U.S.	2.6-86	http://www.azdeq.gov
Groundwater	Municipal Landfill	Minnesota, U.S.	0.2-144	ATSDR, 1997
Groundwater	West Central Phoenix Site- Turney Avenue	Arizona, U.S.	480	http://www.azdeq.gov
Groundwater	Former Site of American Beryllium Company	Tallevast, Flourida, U.S.	500	http://www.braytonlaw.com
Groundwater	Site 11,NSB Kings Bay	USA	550	EPA, 2000
Groundwater	Butler Cleaners Site (#2)	Florida, U.S.	830	http://www.drycleancoalition.org
Groundwater	Chemical Transfer and Storage Facility	Toronto, Canada	1165-1654	CEPA, 1993
Groundwater	Gloucester Ontario Municipal Landfill	Ontario, Canada	1-2480	CEPA, 1993
Groundwater	Former site of Denver Colorado Dry Cleaner	Colorado, U.S.	12600	http://www.drycleancoalition.org
Groundwater	Ville Mercier Landfill	Quebec, Canada	102-12950	CEPA, 1993
Groundwater	Industrial site	Vancouver, Canada	59.5-21900	CEPA, 1993
Groundwater	not mentioned	Pennsylvania-NewYork-Massachusetts, U.S.	900-27300	ATSDR, 1997
Groundwater	U.S. Army Cold Regions Research and Engineering Laboratory	Hanover, U.S.	44-180000	ATSDR, 1997
Groundwater	Industrial site	Manitoba, Canada	425000	CEPA, 1993
Leachate	Municipal Landfill	Minnesota, U.S.	0.7-125	ATSDR, 1997
Leachate	not mentioned	New Jersey, U.S.	7700	ATSDR, 1997
Surface water	not mentioned	New Jersey, U.S.	32.6	ATSDR, 1997
Surface water	St. Clair River	Canada	42	CEPA, 1993
Surface water	St. Lawrence River	Canada	90	CEPA, 1993

Table 2.3. 1,2-DCA levels monitored in water media

Media	Site Description	Location	1,2-DCA detected (µg/L)	Reference
Groundwater	Gloucester-Ontario Landfill Site	Canada	3.9-58	CEPA, 1994
Groundwater	West Central Phoenix Site –Glenrosa Avenue	Arizona, U.S.	119	http://www.azdeq.gov
Groundwater	Hazardous Waste Landfill	Germany	40-830	ATSDR, 2001a
Groundwater	Fallon Naval Air Station	Nevada, U.S.	1400	ATSDR, 2001a
Groundwater	Aviex Superfund Site	Niles, Michigan, U.S.	1600	http://www.costperformance.org
Groundwater	Jasco Chemical Superfund Site	California, U.S.	2600	http://www.lanl.gov
Groundwater	Du Pont Necco Park Landfill in Niagara Falls	Newyork, U.S.	14-4250	ATSDR, 2001a
Groundwater	Ville Mercier Hazardous Waste Site	Quebec, Canada	41800	CEPA, 1994
Groundwater	Ott-Story-Cordova Supefund Site	Michigan, U.S.	110000	http://www.costperformance .org
Groundwater	Botlek Area of Rotterdam Harbor	The Netherlands	300000	Dyer et al., 2000
Groundwater	French Ltd Superfund Site	Texas, U.S.	920000	http://www.costperformance.org
Industrial Wastewater	Not mentioned	England and Wales	117	ATSDR, 2001a
Industrial Wastewater	Synthetec Inc. of Albany	Oregon, U.S.	1000-8000	http://www.synthetech.com
Surface Water	Tees Estuary	England	0.72-4.02	ATSDR, 2001a
Surface Water	St. Clair River	Ontario, Canada	16	CEPA, 1994

2.3. Biodegradation of Chlorinated Organics

Most commonly used chlorinated aliphatic compounds are not natural compounds, perhaps for this reason, enzyme systems capable of their degradation have not evolved sufficiently to make them widely biodegradable. This refractory nature also is related to the fact that they are highly resistant to chemical breakdown, which is the major reason for their widespread commercial use. Although chlorinated aliphatic organics are recalcitrant, many can be transformed biologically under suitable conditions (Rittmann and McCarty, 2001). First, some can be used as an electron donor for energy generation and growth, either under aerobic or anaerobic conditions. Second, some can serve as an electron acceptor to support respiration of anaerobic microorganisms utilizing simple electron donating substrates, which is also referred to as halorespiration. Lastly, some are biotransformed cometabolically either under aerobic conditions or anaerobic conditions without any benefit for the organisms (Field and Sierra Alvarez, 2004; Rittmann and McCarty, 2001). This section mainly emphasizes the first and second processes. The last process “cometabolism” is discussed in Chapter 3.

In the research work performed to evaluate the growth-based biodegradability of chlorinated organics under aerobic conditions, it was shown that the lower chlorinated methanes, which include chloromethane (CM) and dichloromethane (DCM), are growth-substrates for several aerobic bacterial strains. In contrast to them, higher chlorinated methanes, which include chloroform (CF) and carbon tetrachloride (CT), are not utilized as sole sources of carbon and energy supporting growth under aerobic conditions. Also, lower chlorinated ethanes, which include chloroethane (CA), 1,1-dichloroethane (1,1-DCA) and 1,2-dichloroethane (1,2-DCA), can be utilized as primary growth-substrates by aerobic bacteria (Field and Sierra-Alvarez, 2004). The possible use of CA and 1,1-DCA as growth-substrates has not yet been studied. However, up to date, several pure bacterial strains have been isolated that can grow with 1,2-DCA as a substrate, such as *Xanthobacter autotrophicus GJ10*, *Ancylobacter aquaticus AD25*, *Pseudomonas sp. Strain* DCA1 (Hage and Hartmanns, 1999; Inguva and Shreve, 1999; Janssen et al., 1985; Klecka et al., 1998). On the other hand, no aerobic biodegradation is yet known for the higher chlorinated ethanes, which include 1,1,1-trichloroethane (1,1,1-TCA), 1,1,2-trichloroethane (1,1,2-

TCA), various isomers of tetrachloroethane (TeCA), pentachloroethane (PCA), and hexachloroethane (HCA) (Field and Sierra-Alvarez, 2004). Lower chlorinated ethenes, which include monochlorinated ethene (vinyl chloride, VC) and dichlorinated ethenes (DCE), can be utilized as primary growth-substrate under aerobic conditions. In many researches, aerobic degradation of DCE and VC as primary substrates has been shown for several aerobic bacterial strains. In contrast, the higher chlorinated ethenes, which include trichloroethylene (TCE) and perchloroethylene (PCE), are not utilized as aerobic growth-substrates (Bradley, 2003; Field and Sierra-Alvarez, 2004).

In the researches performed to evaluate the anaerobic growth on chlorinated organics as electron donor or acceptor, the lower chlorinated methanes (CM and DCM) were observed to be growth-substrates for anaerobic bacteria. In contrast to this, under anaerobic conditions, higher chlorinated methanes (CF and CT) are not utilized as sole sources of carbon and energy. Among the chloroethanes, halorespiration has been reported for 1,2-DCA and 1,1,1-TCA. To date, no isolates or enrichment cultures capable of oxidizing lower chlorinated ethenes (VC and DCE) under anaerobic conditions have yet been obtained. However, both VC and DCE are known to serve as terminal electron acceptors to support the growth of halorespiring bacteria. Similarly, biodegradation of higher chlorinated ethenes (PCE and TCE) was demonstrated which was linked to growth-supporting halorespiration. However, the anaerobic metabolism of higher chlorinated ethene proceeds through sequential reductive dechlorination in which hydrogen replaces the chloro-group, leading to progressively more dechlorinated intermediates. These include TCE, DCE, VC and eventually ethene (Field and Sierra-Alvarez, 2004). Due to the fact that degradation rates under anaerobic conditions decrease with a decreasing degree of halogen substitution, in the reductive dechlorination of higher chlorinated ethenes (PCE and TCE) there is a risk of accumulation of the carcinogen VC, which is more toxic than the parent compounds (PCE or TCE) (McCarty, 2000; Van Hylckama Vlieg et al., 2001).

Biodegradation of chlorinated organics linked to growth is important, since under such conditions, rates of degradation will increase as the microbial population increases (Field and Sierra-Alvarez, 2004). However, as discussed above, many chlorinated organics, especially highly chlorinated ones, cannot be utilized as primary growth-substrate under aerobic and anaerobic conditions. Moreover, biological transformation of these

compounds linked to growth-supporting halorespiration under anaerobic conditions has a potential for the accumulation of intermediate chlorinated compounds, which are more toxic than the parent compounds. Therefore, in recent years, biodegradation of chlorinated organics by cometabolic processes, especially under aerobic conditions, have received much attention as a promising alternative.

3. COMETABOLIC DEGRADATION OF CHLORINATED ORGANIC COMPOUNDS

3.1. Cometabolism

Cometabolism is the biological transformation of a non-growth-substrate by bacteria through the catalysis of nonspecific enzymes of which synthesis in microbial cell can only be induced by a growth-substrate providing reducing power and energy for cell growth and maintenance of bacteria. Cometabolic transformation of a non-growth-substrate yields no carbon and energy benefits to the cells and hence cannot induce production of enzymes. Therefore, a growth-substrate must be available at least periodically to grow new cells and to induce production of the enzymes necessary for cometabolic transformation of non-growth substrate (Alvarez-Cohen and Speitel, 2001).

Cometabolism can be accomplished by (Criddle, 1993):

- growing cells in the presence of growth-substrate,
- resting cells in the absence of a growth-substrate,
- resting cells in the presence of an energy substrate, which is an electron donor that provides reducing power and energy, but does not by itself support growth.

Cometabolism can bring about biodegradation of compounds that otherwise would be broken down only very slowly if at all in the environment. Also, lower residual contaminant levels may be achieved by cometabolic treatment than could otherwise be attained. However, cometabolism inherently tends to be an unsustainable process. For example, the presence of a non-growth substrate can inhibit metabolism of the natural growth-substrate, thereby decreasing or preventing bacterial growth. In addition, cometabolic transformations consume reductant (e.g., NADH) that otherwise would be available to support metabolism of the growth-substrate. Moreover, cometabolic transformation of some non-growth substrates can lead to injury and inactivation of bacteria by damaging important cellular constituents. However, cells can recover from cometabolism associated injuries, even in the presence of the injury-inducing non-growth substrate (Ely et al., 1997).

Since the cometabolic biotransformations of non-growth substrates are catalyzed by non-specific enzymes induced by growth-substrates, having knowledge about the general nature, mechanism and kinetics of enzymes provides better understanding of the cometabolic degradation processes.

3.1.1. Enzymes

Enzymes are organic catalysts, globular protein molecules that are synthesized in the cytoplasm and speed up chemical reactions by lowering the energy of activation that must be supplied to cause molecules to react with each other. They do this by forming an enzyme-substrate complex (Figure 3.1). Substrates are attracted to the enzyme because their shapes fit together like a *key fits a lock*. The region where the substrate(s) attach is called the "active site", and it is here where the reaction takes place. After the reaction has been completed, the product(s) is (are) released and the active site returns to its original state (Mader, 1990).

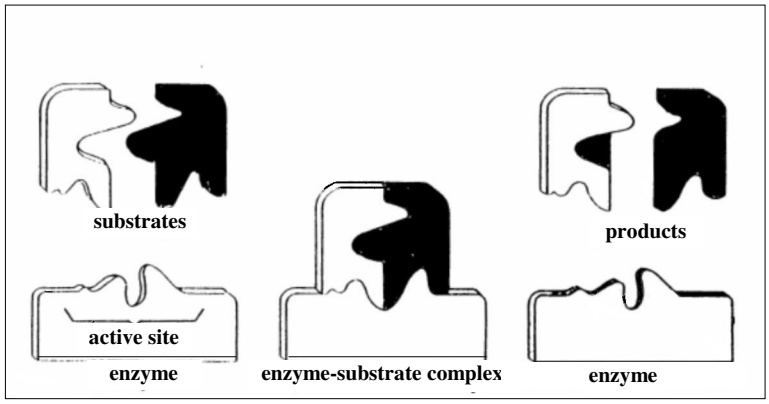

Figure 3.1. Enzyme-Substrate complex formation (Mader, 1990)

Enzymatic reactions are affected by substrate concentration, temperature and pH. Generally, an enzyme's activity increases with greater substrate concentration because there are more collisions between substrate molecules and the enzyme. But when the concentration of substrate is so great that the enzyme's active sites are almost continuously filled with substrate, the enzyme's rate of activity cannot increase any more. A higher temperature generally results in an increase in enzyme activity. However, if the temperature rises beyond a certain point, the enzyme is denaturated. A change in pH can

also affect enzyme activity. Each enzyme has an optimal pH, which helps maintain its normal configuration. (Mader, 1990).

Some enzymes depend for their activity only upon their structure as proteins. Others require, in addition, a nonprotein component for their activity. When the nonprotein portion is a metal ion (e.g., Co, Cu, Fe, Mn, Ni, Zn), it is called a *cofactor*. If the nonprotein structure is organic, it is called a *coenzyme*. Coenzymes generally serve in the transfer of electrons, elements, or functional groups from one molecule to another or from one place in the cell to another (Rittmann and McCarty, 2001). NAD^+ (nicotinamide adenine dinucleotide) and $NADP^+$ (nicotinamide adenine dinucleotide phosphate) are common coenzymes that function as an electron and hydrogen ion carrier in cellular oxidation-reduction reactions. NAD^+ accept electrons from certain substrates and carry them to an electron transport system for producing ATP (adenosine triphosphate) that is the common energy currency of cells. During this process, they remove 2 hydrogen atoms ($2e^- + 2H^+$) from its substrate, both electrons and only one hydrogen atom are passed to NAD^+ as shown in Figure 3.2. $NADP^+$ has a structure similar to NAD^+ but its function is slightly different. It does carry electrons and a hydrogen ion just like NAD^+ but its electrons are used to bring about reduction synthesis with the supply of necessary energy from ATP as shown in Figure 3.3 (Mader, 1990).

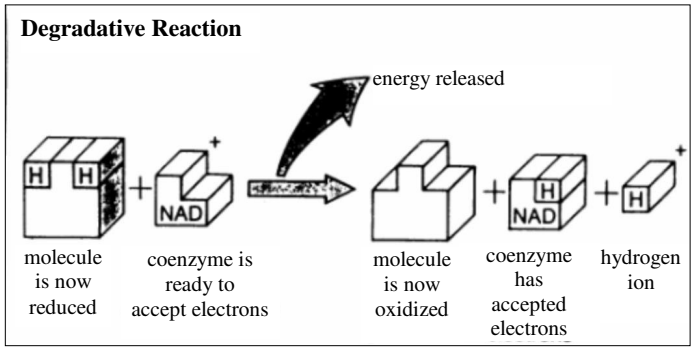

Figure 3.2. Degradative reaction pathway (Mader, 1990)

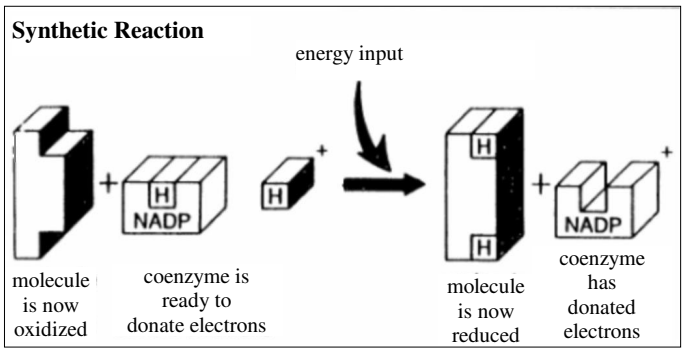

Figure 3.3. Synthetic reaction pathway (Mader, 1990)

3.1.1.1. Kinetics of Enzyme-Catalyzed Reactions. A characteristic of enzyme reactions is substrate saturation. Figure 3.4 illustrates the observed effect of substrate concentration on the rate of an enzyme-catalyzed reaction.

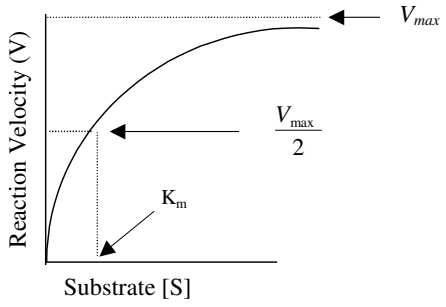

Figure 3.4. Effect of substrate concentration on enzymatic transformation rate based upon Michaelis-Menten kinetics (adapted from Rittmann and McCarty, 2001)

At very low substrate concentrations, the rate increases in direct proportion to substrate concentration. Thus, the rate here is first-order with respect to substrate concentration. As substrate concentration increases, however, the rate of increase begins to decline, giving a mixed-order reaction. At higher substrate concentrations, the enzyme becomes saturated with the substrate, and the rate increases no further. This rate is the maximum rate for the reaction. Here, the rate becomes zero-order with respect to substrate concentration. This saturation effect is typical of all enzyme-catalyzed reactions. The quantitative relationship between the substrate concentration and the reaction rate in relation to the maximum possible rate is defined by Michaelis-Menten equation as follows (Rittmann and McCarty, 2001):

$$V = V_m \frac{S}{K_m + S} \tag{3.1}$$

where V is the reaction velocity; V_m is the maximum reaction velocity; S is the substrate concentration and K_m is the half-velocity constant.

The coefficient K_m in Eqn. 3.1 equals the substrate concentration at which the velocity of the reaction is one-half of the maximum velocity. K_m represents the affinity between the substrate and the enzyme. A low value of K_m indicates a very strong affinity, such that the maximum rate is reached at a relatively low substrate concentration. A large value of K_m, on the other hand, shows a poor affinity. When an enzyme transforms more than one substrate, the values for K_m and V_m are different for each substrate. However, these coefficients are independent of the enzyme concentration (Rittmann and McCarty, 2001).

3.1.1.2. Inhibition of Enzymes. Substances that decrease the rate of an enzyme-catalyzed reaction when present in the reaction mixture are called inhibitors (Cornish-Bowden, 1995). Inhibition types may in principle be sub-classified as competitive, uncompetitive and mixed.

In competitive inhibition (Figure 3.5), a chemical that is similar in structure to the normal enzyme substrate competes with the substrate for the active site of the enzyme (Rittmann and McCarty, 2001).

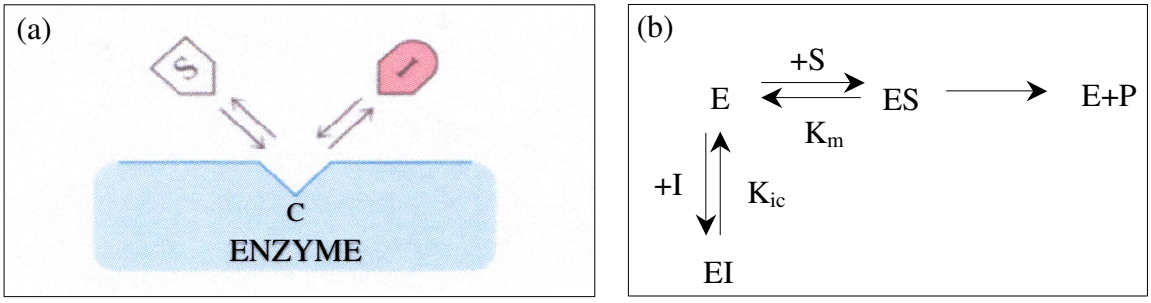

Figure 3.5. Mechanism of competitive inhibition [adapted from (a) Moran et al., 1994; (b) Cornish-Bowden, 1995]

The competitive inhibition can be defined in the form of Michaelis-Menten equation by using the apparent values of V_m and K_m as shown in Eqn. 3.2. As seen from the equation, the net effect of a competitive inhibitor is to increase K_m with a factor $(1+I/K_{ic})$ while leaving that of V_m unchanged (Cornish-Bowden, 1995). Stated in different terms, the rate reduction caused by a competitive inhibitor can be completely offset by increasing the substrate concentration sufficiently, the maximum possible reaction velocity is not affected by the competitive inhibitor (Bailey and Ollis, 1986).

$$V = \frac{V_m^{app} S}{K_m^{app} + S} = \frac{V_m S}{K_m(1 + \frac{I}{K_{ic}}) + S} \tag{3.2}$$

where V is the reaction velocity; V_m is the maximum reaction velocity; S is the substrate concentration, K_m is the half-velocity constant; I is the free inhibitor concentration, K_{ic} is the dissociation constant of enzyme- inhibitory compound (EI) complex, V_m^{app} and K_m^{app} are the apparent values of V_m and K_m and are given by $V_m^{app} = V_m$, $K_m^{app} = K_m(1 + \frac{I}{K_{ic}})$.

In uncompetitive inhibition (Figure 3.6), the inhibitor binds only to the enzyme–substrate (ES) complex and not to the free enzyme (Cornish-Bowden, 1995).

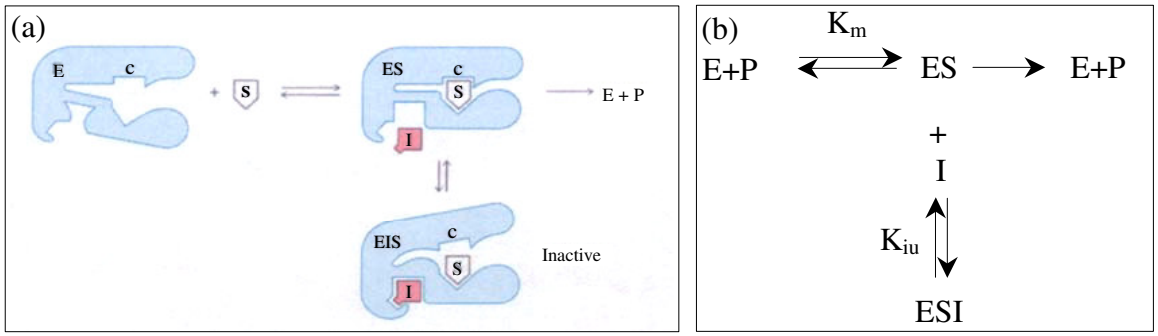

Figure 3.6. Mechanism of uncompetitive inhibition [adapted from (a) Moran et al., 1994; (b) Cornish-Bowden, 1995]

Eqn. 3.3 defines the uncompetitive inhibition in the form of Michaelis-Menten equation by using the apparent values of V_m and K_m. As seen from the equation, the net

effect of an uncompetitive inhibitor is to decrease both V_m and K_m with a factor $1/(1+I/K_{iu})$ (Cornish-Bowden, 1995).

$$V = \frac{V_m^{app} S}{K_m^{app} + S} = \frac{V_m \left[1/(1 + \frac{I}{K_{iu}}) \right] S}{K_m \left[1/(1 + \frac{I}{K_{iu}}) \right] + S} \tag{3.3}$$

where V is the reaction velocity; V_m is the maximum reaction velocity; S is the substrate concentration, K_m is the half-velocity constant, I is the free inhibitor concentration, K_{iu} is the dissociation constant of enzyme-substrate-inhibitory compound (ESI) complex, V_m^{app} and K_m^{app} are the apparent values of V_m and K_m and are given by $V_m^{app} = V_m \left[1/(1 + \frac{I}{K_{iu}} \right]$, $K_m^{app} = K_m \left[1/(1 + \frac{I}{K_{iu}}) \right]$.

In mixed inhibition (Figure 3.7), the inhibitor can bind both to the free enzyme (E) to build the enzyme-inhibitory substance (EI) complex with a dissociation constant K_{ic} and to the enzyme-substrate (ES) complex to build the enzyme-substrate-inhibitory substance (ESI) complex with a dissociation constant K_{iu}. Hence, depending on the binding constants (K_{ic}, K_{iu}) of the inhibitor, both competitive and uncompetitive effects can be observed (Cornish-Bowden, 1995).

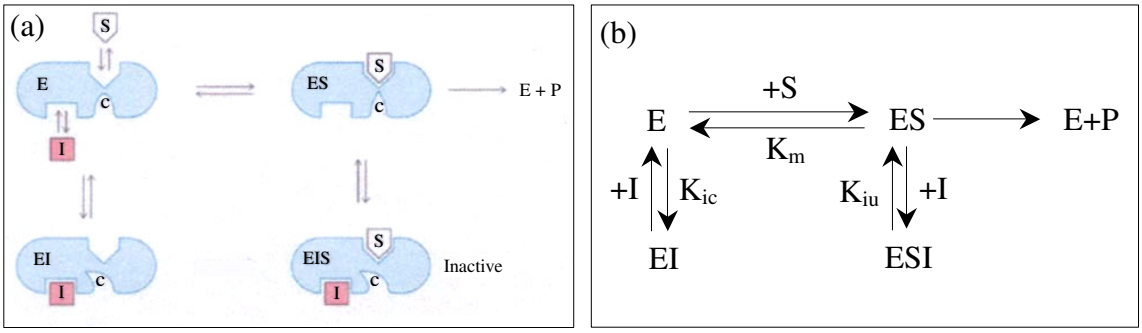

Figure 3.7. Mechanism of mixed inhibition [adapted from (a) Moran et al., 1994; (b) Cornish-Bowden, 1995]

Eqn. 3.4 defines the mixed inhibition in the form of Michaelis-Menten equation by using the apparent values of V_m and K_m. As seen from the equation, the net effect of a mixed inhibitor is to increase or decrease K_m with a factor $(1+I/K_{ic})/(1+I/K_{iu})$ while decreasing V_m with a factor of $1/(1+I/K_{iu})$. Comparison of Eqn. 3.4 with Eqn. 3.2 shows that competitive inhibition is the limiting case of mixed inhibition in which K_{iu} approaches infinity, i.e. I/K_{iu} is negligible at all values of I and hence disappears from Eqn. 3.4. Similarly, comparison of Eqn. 3.4 with Eqn. 3.3 shows that uncompetitive inhibition is the other limiting case of mixed inhibition in which K_{ic} approaches infinity, i.e. I/K_{ic} is negligible at all values of I and hence disappears from Eqn. 3.4 (Cornish-Bowden, 1995).

$$V = \frac{V_m^{app} S}{K_m^{app} + S} = \frac{V_m \left[1/(1 + \frac{I}{K_{iu}}) \right] S}{K_m \left[(1 + \frac{I}{K_{ic}}) / (1 + \frac{I}{K_{iu}}) \right] + S} \qquad (3.4)$$

where V is the reaction velocity; V_m is the maximum reaction velocity; S is the substrate concentration, K_m is the half-velocity constant, I is the free inhibitor concentration, K_{ic} is the dissociation constant of enzyme-inhibitory compound (EI) complex, K_{iu} is the dissociation constant of enzyme-substrate-inhibitory compound (EIS) complex, V_m^{app} and K_m^{app} are the apparent values of V_m and K_m and are given by $V_m^{app} = V_m \left[1/(1 + \frac{I}{K_{iu}}) \right]$, $K_m^{app} = K_m \left[(1 + \frac{I}{K_{ic}}) / (1 + \frac{I}{K_{iu}}) \right]$.

A special type of mixed inhibition is the non-competitive inhibition, which results in a decrease of V_m with a factor of $1/(1+I/K_{iu})$ while leaving K_m unchanged due to the equal binding constants of E and ES complex (K_{ic} and K_{iu}, respectively) for the inhibitor. This type of inhibition might be possible for very small inhibitors, such as protons and metal ions, but seems most unlikely otherwise (Cornish-Bowden, 1995). In the presence of a non-competitive inhibitor, no amount of substrate addition to the reaction mixture can provide the maximum reaction rate, which is possible without the inhibitor (Bailey and Ollis, 1986).

3.2. Cometabolism of Chlorinated Organics

As an alternative to growth-based biodegradation, cometabolic degradation of chlorinated compounds has received much attention in the recent years. Up to date, numerous researches have been carried out to investigate the cometabolic degradability of various chlorinated organic compounds by using anaerobic and aerobic bacterial strains.

3.2.1. Anaerobic Cometabolism of Chlorinated Organics

Under anaerobic conditions, a common form of cometabolism is the reaction of reduced enzyme cofactors with chlorinated organics, resulting in their reductive dehalogenation (Field and Sierra-Alvarez, 2004).

In the researches performed to evaluate the cometabolic degradability of chlorinated organics under anaerobic conditions, it was shown that higher chlorinated methanes, chloroform (CF) and carbon tetrachloride (CT), were cometabolized by pure cultures of methanogens, fermentative bacteria, sulfate-reducing bacteria and iron-reducing bacteria resulting in formation of lower chlorinated methanes (Field and Sierra-Alvarez, 2004).

Lower chlorinated ethanes [chloroethane (CA), 1,1-dichloroethane (1,1-DCA) and 1,2-dichloroethane (1,2-DCA)] were shown to be cometabolically degraded by unadapted methanogenic sludge and enrichment cultures. In these experiments, 1,1-DCA was converted to CA and ethane. CA was converted to ethane. On the other hand, 1,2-DCA was converted to CA and ethene. Anaerobic cometabolism of higher chlorinated ethanes [1,1,1-trichloroethane (1,1,1-TCA), 1,1,2-trichloroethane (1,1,2-TCA), various isomers of tetrachloroethane (TeCA), pentachloroethane (PCA), and hexachloroethane (HCA)] were mainly studied in mixed methanogenic cultures. In these experiments, HCA, PCA, TeCA were converted to chlorinated ethenes. On the other hand, cometabolism of trichlorinated ethanes resulted in the formation of both lower chlorinated ethenes and ethanes as the main products. 1,1,2-TCA was predominantly converted to vinyl chloride and 1,2-DCA. 1,1,1-TCA was primarily transformed to 1,1-DCA and CA (Field and Sierra-Alvarez, 2004).

Both lower and higher chlorinated ethenes [monochlorinated ethene (vinyl chloride, VC), dichlorinated ethenes (DCE), trichloroethylene (TCE) and perchloroethylene (PCE)] are slowly cometabolized under anaerobic conditions to lower chlorinated ethenes and ethene (Field and Sierra-Alvarez, 2004). Cometabolically mediated sequential reductive dechlorination of PCE and TCE to less-chlorinated ethenes has been widely observed by a variety of anaerobic bacteria, including methanogens and sulfate reducers (Magnuson et al., 1998). Several acetogenic bacteria have also been shown to dechlorinate PCE to TCE (Field and Sierra-Alvarez, 2004). The tendency of chloroethene compounds to undergo reductive dechlorination appears to decrease with a decreasing number of chlorine constituents, therefore, reductive dechlorination of lower chlorinated ethenes (DCE and VC) is characteristically slow and generally associated with highly reducing, methanogenic conditions. Therefore, reductive dechlorination of chloroethene contaminants is often incomplete and frequently leads to the accumulation of cis-DCE and VC (Bradley, 2003).

3.2.2. Aerobic Cometabolism of Chlorinated Organics

The aerobic cometabolic transformation of chlorinated organics (Figure 3.8) are catalyzed by nonspecific oxygenase enzymes that use molecular oxygen as the electron acceptor and NAD(P)H as the reducing energy (electron) donor to oxidize both growth-substrates and nonbeneficial cometabolic (non-growth) substrates (Chang and Alvarez-Cohen, 1995a; Chang and Alvarez-Cohen, 1995b).

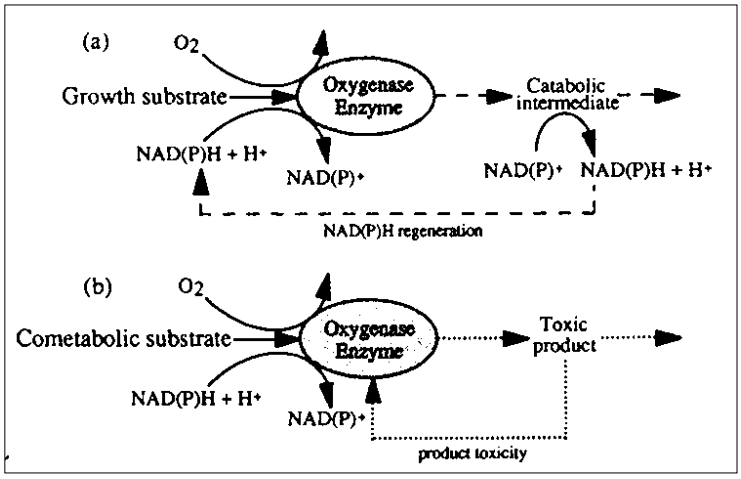

Figure 3.8. Typical oxygenase enzyme reactions for growth-substrate and cometabolic (non-growth) substrate (Chang and Alvarez-Cohen, 1995b)

Oxygenases constitute a subset of the enzyme classified as oxidoreductases, which is one of the six major classes of enzymes. Oxygenases serve a myriad of functions in cells including biosynthesis, detoxification, and catabolism. They catalyze the reduction of O_2 with incorporation of one (monooxygenases) or two (dioxygenases) of the O atoms into the substrate that is being oxidized. Monooxygenases require an input of reductant, which is used to reduce the second atom of O to H_2O. Dioxygenases do not necessarily require reductant as both atoms of O_2 are reduced upon incorporation into the substrate. However, some dioxygenases do use reductant to further reduce the substrate (e.g, toluene dioxygenase) (Arp et al., 2001).

Any organism with an active mono- or di-oxygenase has the potential for cometabolic transformation of chlorinated organics (Ward et al., 1997). However, some factors may adversely affect the cometabolic degradation of chlorinated organics by oxygenase-expressing microorganisms. These factors include chlorinated organic product toxicity, enzyme inhibition by growth or other cometabolic substrates and reducing energy or reductant shortages (Alvarez-Cohen and Speitel, 2001).

a) Product Toxicity: The oxidation of some chlorinated organics by oxygenase enzymes generates short-lived toxic intermediate products that may cause enzyme and/or cell damage as shown in Figure 3.8 (Chang and Alvarez-Cohen, 1995b). Although the specific chlorinated solvent products responsible for the observed product toxicity are not known, toxic effects have been shown to include damage directly to the oxygenase enzymes as well as to general cell constituents. Studies conducted with a wide range of oxygenase utilizing cultures suggest that both the extent of product toxicity and the mode of action are highly variable across species and genera. However, for the cultures in which toxicity has been quantified, the attack of toxic products on the enzyme and/or cellular materials has resulted in activity and viability that decreases in proportion to the amount of compound degraded (Alvarez-Cohen and Speitel, 2001).

b) Enzyme Inhibition: Because a single enzyme is responsible for the oxidation of both growth-substrate and cometabolic substrate, the presence of cometabolic substrate can inhibit the oxidation rate of growth-substrate and vice versa (Chang and Alvarez-Cohen, 1995a). Among the inhibition types discussed in Section 3.1.1.2, competitive inhibition

between growth-substrates and cometabolic substrates has been most widely observed for many oxygenase-utilizing organisms. However, there are also few studies in which non-competitive inhibition of growth-substrate was observed for ammonia monooxygenase utilizing pure cultures degrading monohalogenated methanes, ethanes and highly chlorinated organics (carbon tetrachloride and tetrachloroethylene) (Alvarez-Cohen and Speitel, 2001).

c) Reducing Energy Limitation: Cometabolic oxidation of the non-growth substrate consumes reductant [NAD(P)H] and the products of the reaction do not regenerate NAD(P)H (Figure 3.8b). Thus, reducing energy [(NAD(P)H], which is a potentially limiting reactant during cometabolic reactions, are provided by external or endogenous NAD(P)H regenerants mentioned below.

External NAD(P)H regenerants:

Growth-substrate: It is known that the products of the growth-substrate oxidation undergo further degradations that regenerate NAD(P)H for additional substrate oxidations (Figure 3.8a). Thus, presence of growth-substrate may prolong cometabolic degradation reactions by regenerating NAD(P)H as well as prompt the growth of new cells. However, in this case, competitive inhibition may also occur between growth and cometabolic substrates, causing lower cometabolic degradation rates or vice versa (Chang and Alvarez-Cohen, 1995b).

Energy substrate: Some oxygenase expressing cultures can regenerate reductant by using alternate energy substrates that are not oxidized by the oxygenase enzymes, and therefore do not result in competitive inhibition with either growth or non-growth substrates. The utilization of an alternate energy substrate for the regeneration of reductant allows cometabolic oxidations to be carried out without limitations due to either reducing energy depletion or competitive inhibition. However, growth-substrate must be provided at least periodically, because oxygenase enzyme levels may diminish and biosynthesis of these enzymes cannot proceed in the absence of growth-substrate (Alvarez-Cohen and Speitel, 2001).

Endogenous NAD(P)H regenerant :

When cometabolic degradations occur in the absence of external NAD(P)H regenerants (resting cells condition; i.e. separation of microbial growth and cometabolite oxidation), the reducing energy required to sustain the oxidation of cometabolites could only be provided by endogenous energy sources, such as poly-β-hydroxybutyrate or general biomass, and cometabolic degradation may be limited by the depletion of endogenous cellular reducing energy (Chang and Alvarez-Cohen, 1995b).

Up to date, methanotrophs, phenol oxidizers and toluene oxidizers, which express methane monooxygenase, phenol monooxygenase and toluene monooxygenase enzymes respectively are the most widely studied group of organisms for cometabolic degradation of chlorinated organics. Some of these studies are briefly discussed in the next section.

3.2.3. Aerobic Cometabolism of Chlorinated Organics by Phenol, Toluene, Propane and Methane Oxidizers

Different studies have been conducted about the cometabolic degradation of various chlorinated organics, especially trichloroethylene (TCE), by phenol, toluene or propane oxidizers. Chang and Alvarez-Cohen (1995a, 1995b) conducted studies to investigate the observed transformation capacities (the maximum mass of compound that can be degraded per mass of cells prior to inactivation) of TCE, chloroform (CF), and 1,2-dichloroethane (1,2-DCA) for resting cells (in the absence of growth and energy substrates; under reducing energy and product toxicity limitations) of propane, toluene and phenol oxidizers. The results showed that CF and 1,2-DCA were not degraded by toluene and phenol oxidizers whereas TCE was degraded for all microorganisms studied. Ranking of microorganisms with respect to transformation capacity of TCE (mg TCE/mg cells) was obtained as propane oxidizers < toluene oxidizers < phenol oxidizers. Transformation capacities of chlorinated organics (mg of chlorinated organic/mg of cells) by propane oxidizers were observed in the order of CF < TCE < 1,2-DCA. Further experiments performed to investigate TCE degradation by propane/toluene/phenol oxidizers in the presence of growth-substrates (propane/toluene, phenol) without the addition of any other external reducing energy regenerant showed that TCE degradation rates were increased by

the addition of low growth-substrate concentrations, possibly due to NAD(P)H regeneration, but were decreased at high growth-substrate concentrations, possibly due to competitive inhibition between growth-substrate and chlorinated organic (non-growth substrate).

Speitel and Segar (1995) studied the cometabolic degradation of TCE, perchloroethylene (PCE), 1,1-dichloroethene (1,1-DCE), cis-1,2-DCE and trans-1,2-DCE by a mixed culture of phenol degraders, predominantly consisting of *Pseudomonas putida*, in upflow packed-bed biofilm reactors filled with glass beads. Initially, they simultaneously fed growth-substrate and chlorinated organic to the reactor. However, they encountered significant operating problems because of the slower kinetics of cometabolism in comparison to that of metabolism. Moreover, reactor plugging, poor rates of cometabolism and enzyme competition between growth-substrate and non-growth substrate were also observed. Thus, later they performed experiments in sequencing biofilm reactor(s) which cycles between two modes of operation once the biofilm is established: 1st mode: degradation of chlorinated organic in the absence of growth-substrate, 2nd mode: rejuvenation of the biofilm by supplying growth-substrate in the absence of chlorinated organic. Degradation of chlorinated organics in this type of reactor takes place while the microorganisms are in a state of endogenous decay. The results of experiments showed that PCE could not be cometabolically degraded under the conditions studied. Ranking of chloroethenes with respect to maximum specific degradation rates (mg chlorinated organic/mg cells/time) was obtained as cis1,2-DCE > TCE > 1,1-DCE > trans1,2-DCE. Transformation capacities of chlorinated organics (the maximum mass of compound that can be degraded per mass of cells prior to inactivation, mg chlorinated organic/mg cells) were observed in the order of cis1,2-DCE > TCE > trans1,2-DCE > 1,1-DCE. In the same study, degradation of chloroethene mixtures was also studied. For this purpose, three sequencing biofilm reactors were used. One reactor was always fed with TCE as the sole contaminant, whereas another reactor received either PCE, 1,1-DCE, cis1,2-DCE or trans1,2-DCE as the sole contaminant. The third reactor received a mixture of the feeds used for each sole-feed reactor. The degradation rates observed in the first and second reactors showed a decrease in the third reactor receiving a mixture of chloroethenes in the first and second reactors. TCE removal was strongly inhibited by the presence of 1,1-DCE.

In the study of Yeager et al. (2004), TCE degrading capacity of five toluene-oxidizing strains was examined which were grown on non-aromatic substrates. The results demonstrated that each strain harboring distinct toluene-oxidizing systems were capable of degrading TCE when grown on non-aromatic substrates. However, significant strain dependent and substrate dependent differences were observed in the amount of TCE degraded.

In other studies, evidence for cometabolic degradation of 1,1,1-trichloroethane (1,1,1-TCA) has been observed with either pure cultures or enrichment cultures with propane. The cometabolic degradation of vinyl chloride (VC) and DCE has been observed with toluene eliciting monooxygenase activity. One research group has noticed slow PCE cometabolism with the bacterium *Pseudomonas stutzeri* OX1 expressing tolune-o-xylene monooxygenase. TCE oxidation was found to be feasible with microorganisms expressing certain dioxygenases, such as toluene dioxygenase of *Pseudomonas putida* F1 (Field and Sierra-Alvarez, 2004)**.**

By far, aerobic cometabolism of chlorinated organics has been most widely studied with methanotrophs. Methanotrophs are obligate aerobes, using oxygen as the terminal electron acceptor, and require methane (CH_4) or methanol as carbon and energy source. They are unable to grow on other "organic media". Since methane (CH_4) and methanol are considered to be organic compound, these organisms are technically heterotrophs but they are in many ways similar to chemolithotrophic autotrophs. One species of them can fix atmospheric nitrogen; others use NH_3 or nitrate as nitrogen source. These organisms commonly occur in aerobic layers of soil or water above the anaerobic sediments where CH_4 is produced (Gaudy and Gaudy, 1980). All methanotrophic bacteria produce the copper-containing particulate methane monooxygenase (pMMO). However, under copper-limited conditions, some methanotrophs express the soluble MMO (sMMO). Studies conducted by methanotrophs expressing either sMMO or pMMO showed that sMMO is much more nonspecific with respect to potential substrates and can rapidly oxidize all the chlorinated ethenes except PCE. On the other hand, pMMO has a 10- to 100-fold higher specificity for methane and generally oxidizes TCE and cis1,2-DCE at a much lower rate than sMMO does. However, trans1,2-DCE, is oxidized at rates similar to that by sMMO (Anderson and McCarty, 1997).

In the study of Oldenhius et al. (1989), TCE was found to be degradable by the methanotrophic bacterium *Methylosinus trichosporium OB3b* only when grown under copper limitation. During TCE degradation, nearly total dechlorination occurred. Dichloromethane (DCM), CF, 1,1-dichloroethane (1,1-DCA) and 1,2-DCA were completely degraded, with the release of stoichiometric amounts of chloride. Trans1,2-DCE and cis1,2-DCE were completely converted, but not all the chloride was released because of the formation of chlorinated intermediates. 1,1,1-TCA and 1,1-DCE were incompletely converted, and 1,1,1-TCA yielded 2,2,2-trichloroethanol as a chlorinated intermediate. The two perchlorinated compounds tested, carbontetrachloride (CT) and PCE, were not converted.

Chang and Alvarez-Cohen (1995b) carried out a study to investigate the transformation capacities (the maximum mass of compound that can be degraded per mass of cells prior to inactivation) for TCE, 1,2-DCA and CF by methane oxidizers in the absence of external NAD(P)H regenerants (resting cells condition; absence of growth and energy substrates) and for only TCE (a) in the presence of a reducing energy substrate (formate); (b) in the presence of growth-substrate under conditions of excess NAD(P)H regenerant (formate); (c) in the presence of growth-substrate without the addition of any other external reducing energy regenerant. The experiments performed in resting cell conditions showed the transformation capacities of chlorinated organics in the order of 1,2-DCA > TCE > CF, similar to the results for propane oxidizers discussed in the first paragraph of this section. In later experiments, transformation capacity of TCE increased with the addition of formate (a reducing energy substrate that produces no competitive inhibition or cell growth) and reached a saturation value at a certain formate concentration (20 mM), suggesting that reducing energy limitation was eliminated with formate addition. Measurement of TCE degradation by methane oxidizers in the presence of CH_4 (growth-substrate) and excess NAD(P)H regenerant (20 mM formate) showed a decrease in TCE degradation rate as CH_4 concentration increased, indicating the occurrence of competitive inhibition between CH_4 and TCE. Finally, TCE degradation by methane oxidizers in the presence of CH_4 (growth-substrate) was studied without the addition of any other external reducing energy regenerant. Similar results were found as in the case of phenol, toluene and propane oxidizers discussed in the first paragraph of this section. TCE degradation rates were increased by the addition of low growth-substrate concentrations, possibly due

to NAD(P)H regeneration, but were decreased at high CH_4 concentrations, possibly due to competitive inhibition between CH_4 and TCE.

A study conducted on inactivation of MMO enzyme during cometabolic transformation of chlorinated organics by methanotrophs showed that the rate of 1,1-DCE inactivation of sMMO was about twice that caused by TCE. In another study, it was reported that 1,1-DCE was about three times more "acutely toxic" than TCE to whole cells expressing sMMO and much more potent inactivation of a methane oxidizing mixed culture was observed with 1,1-DCE than with TCE (Ely et al., 1997).

Speitel and Segar (1995) investigated the cometabolic degradation of TCE by pure culture of methanotrophs including *Methylosinus trichosporium OB3b* and copper resistant mutants of this organism in sequencing upflow packed-bed biofilm reactors. The operation conditions were discussed in the second paragraph of this section. The results showed that *Methylosinus trichosporium OB3b* mutants were not very successful because of the organism's slow growth rate and relatively poor ability to attach to surfaces. The experiments, however, illustrated that the addition of organic polymers to biofilm reactors can assist in promoting the attachment of organisms to the media.

In another study, Anderson and McCarty (1997) observed the transformation yields (expressed as moles of chlorinated organic degraded per mole of CH_4 consumed) for the aerobic cometabolic degradation of trans1,2-DCE, VC, cis1,2-DCE, TCE and 1,1-DCE by using a methanotrophic mixed culture expressing pMMO. As a result, the transformation yields were obtained in the order of trans1,2-DCE > VC > cis1,2-DCE > TCE > 1,1-DCE. Although the transformation yields of cis1,2-DCE, TCE and 1,1-DCE were similar to or less than those for cultures expressing sMMO, exceptionally high transformation yields were observed for trans1,2-DCE and VC, which were 20 times greater than those reported for cultures expressing sMMO. Therefore, it was concluded that pMMO can be more effective than sMMO for trans1,2-DCE and VC cometabolism and further experiments for various combinations of CH_4 and VC/trans1,2-DCE; formate (energy substrate) and VC/trans1,2-DCE; CH_4, formate and VC/ trans1,2-DCE were carried out to determine the conditions yielding the highest transformation yields for trans1,2-DCE and VC. Results showed that CH_4 and VC/trans1,2-DCE fractional degradation varied with the initial CH_4

concentration. Formate addition increased the transformation yields of VC and trans1,2-DCE slightly if CH_4 was not present since the CH_4 is needed to induce pMMO production. However, with CH_4 present, formate increased the transformation yields considerably, especially at the highest concentration. From these results it was concluded that the availability of reducing-power is an important aspect in the extent of chlorinated organics oxidation but that enzyme induction is also required.

Chang and Alvarez-Cohen (1996) investigated the degradation of chlorinated methanes [chloromethane (CM), DCM, CT, CF], chloroethanes [chloroethane (CA), 1,2-DCA, 1,1,1-TCA, 1,1,2,2-tetrachloroethane (TeCA), 1,1,1,2-TeCA] and chlorinated ethenes [VC, 1,1-DCE, cis1,2-DCE, trans1,2-DCE, TCE, PCE] by two mixed and two pure methane-oxidizing cultures. None of the cultures were found to be able to degrade the fully chlorinated aliphatics such as PCE and CT. Within similar carbon structure groups (methanes, ethanes and ethenes), measured T_c values (the maximum mass of compound that can be degraded per mass of cells prior to inactivation) were generally in inverse proportion to the chlorine content, whereas similar trends were not observed for degradation rate constants. A notable exception to this relationship was observed with 1,1-DCE, which exerted a much higher toxicity than dichloroethylenes (cis1,2-DCE and trans1,2-DCE) with all four cultures.

The study conducted by Chu and Alvarez-Cohen (2000) to compare the feasibility of employing nitrogen-fixing and nitrate-supplied methane oxidizing cultures in unsaturated porous media to degrade cis-1,2-DCE and TCE in gas streams showed that nitrate-supplied columns were not able to recover from TCE or cis1,2-DCE product toxicity as effectively as nitrogen-fixing columns, suggesting that a higher resistance to chlorinated solvent product toxicity was obtained when cells fixed molecular nitrogen. Moreover, although CH_4 is a competitive inhibitor during the cometabolic degradation of chlorinated solvents by methanotrophs, significant TCE and cis1,2-DCE removals were observed in both nitrate-supplied and nitrogen-fixing columns even though they were continuously supplied with CH_4. This suggests that the amount of CH_4 provided under the test conditions was not sufficient to cause significant inhibition during chlorinated solvent degradation. Furthermore, the continuous supply of low CH_4 concentrations during

chlorinated solvent treatment might actually enhance degradation in the system by providing the reducing energy to fuel the cometabolic reaction.

Although the above discussed studies showed that various chlorinated organics can successfully be cometabolized by methanotrophs, it is difficult to handle CH_4 which is the primary substrate for methanotrophs due to low solubility of CH_4 gas. Thus, cometabolism of chlorinated organics by bacterial species using more soluble substrates (e.g., ammonia /ammonium for nitrifiers) may increase the operational efficiencies (Yang et al., 1999).

3.3. Cometabolic Degradation of Chlorinated Organics in Nitrification Systems

3.3.1. Fundamentals of Nitrification

3.3.1.1. Process Description and Physiology of Nitrifying Bacteria. Nitrification is a two-step biological process in which ammonium (NH_4^+) is oxidized to nitrite (NO_2^-) and nitrite is oxidized to nitrate (NO_3^-). The nitrifying bacteria that carry out both the first and second steps of nitrification are autotrophs, chemolithotrophs, and obligate aerobes (Rittmann and McCarty, 2001).

The most commonly recognized genus of bacteria that carries out the first step of nitrification, i.e., ammonium oxidation, is *Nitrosomonas*; however *Nitrosococcus*, *Nitrosospira*, *Nitrosovibrio*, and *Nitrosolobus* are also able to oxidize NH_4^+ to NO_2^-. The ammonium oxidizing nitrifiers, which all have the genus prefix *Nitroso,* are genetically diverse, but related to each other in the beta subdivision of the proteobacteria (Rittmann and McCarty, 2001).

The most famous genus of bacteria that carries out the second step of nitrification, i.e., nitrite oxidation, is *Nitrobacter*, however, *Nitrospira*, *Nitrospina*, *Nitrococcus*, and *Nitrocystis* are also known to sustain themselves in the second step of nitrification. Recent findings using oligonucleotide probes targeted to the 16S rRNA of *Nitrobacter* indicate that *Nitrobacter* is not the most important nitrite-oxidizing genus in most wastewater-treatment processes. *Nitrospira* was more often identified as the dominant nitrite oxidizer (Rittmann and McCarty, 2001).

3.3.1.2. Stoichiometry of Nitrification. The energy yielding two-step oxidation of ammonium to nitrate is as follows (Metcalf and Eddy, 2003):

Nitroso-bacteria:

$$2NH_4^+ + 3O_2 \rightarrow 2NO_2^- + 4H^+ + 2H_2O \quad (3.5)$$

Nitro-bacteria:

$$2NO_2^- + O_2 \rightarrow 2NO_3^- \quad (3.6)$$

Total oxidation reaction:

$$NH_4^+ + 2O_2 \rightarrow NO_3^- + 2H^+ + H_2O \quad (3.7)$$

Based on Reaction 3.7, the oxygen required for complete oxidation of ammonium 4.57 g O_2/g N oxidized with 3.43 g O_2/g used for nitrite production and 1.14 g O_2/g NO_2 oxidized. When synthesis is considered, the amount of oxygen required is less than 4.57 g O_2/g N (Metcalf and Eddy, 2003).

Neglecting cell tissue, the amount of alkalinity required to carry out the reaction given in 3.7 is as follows (Metcalf and Eddy, 2003):

$$NH_4^+ + 2HCO_3^- + 2O_2 \rightarrow NO_3^- + 2CO_2 + 3H_2O \quad (3.8)$$

In Reaction 3.8, for each g of ammonium nitrogen (as N) converted, 7.14 g of alkalinity as $CaCO_3$ will be required (Metcalf and Eddy, 2003).

Along with obtaining energy, a portion of the ammonium ion is assimilated into cell tissue. By using the chemical formula $C_5H_7O_2N$ to represent the synthesized bacterial cells, the biomass synthesis reaction can be written as follows (Metcalf and Eddy, 2003):

$$4CO_2 + HCO_3^- + NH_4^+ + H_2O \rightarrow C_5H_7O_2N + 5O_2 \quad (3.9)$$

The overall synthesis and energy reaction for nitrification can be developed by considering the following relationship (Metcalf and Eddy, 2003):

$$R = f_e R_a + f_s R_{cs} - R_d \tag{3.10}$$

in which R is the overall balanced equation; f_e is the fraction of e^- donor used for energy, R_a is the half reaction for e^- acceptor; f_s is the fraction of e^- donor used for cell synthesis; R_{cs} is the half reaction for synthesis of cell tissue; R_d is the half reaction for e^-donor; $f_s+f_e=1$.

The half reactions for cell synthesis, oxidation of ammonium to nitrate, and the reduction of oxygen to water are given in Reactions 3.11, 3.12, and 3.13, respectively.

$$\frac{1}{5}CO_2 + \frac{1}{20}HCO_3^- + \frac{1}{20}NH_4^+ + H^+ + e^- = \frac{1}{20}C_5H_7O_2N + \frac{9}{20}H_2O \tag{3.11}$$

$$\frac{1}{8}NO_3^- + \frac{5}{4}H^+ + e^- = \frac{1}{8}NH_4^+ + \frac{3}{8}H_2O \tag{3.12}$$

$$\frac{1}{4}O_2 + H^+ + e^- = \frac{1}{2}H_2O \tag{3.13}$$

By combining Reactions 3.11, 3.12 and 3.13 according to Reaction 3.10 for the f_s value of 0.05 (f_c=0.95), the overall nitrification reaction is shown as follows (Metcalf and Eddy, 2003):

$$NH_4^+ + 1.863O_2 + 0.098CO_2 \rightarrow 0.0196C_5H_7NO_2 + 0.98NO_3^- + 0.0941H_2O + 1.98H^+ \tag{3.14}$$

From Reaction 3.14, it will be noted that for each g of ammonium nitrogen converted, 4.25 g of O_2 are utilized, 0.16 g of new cells are formed, 7.07 g of alkalinity as $CaCO_3$ are removed, and 0.08 g of inorganic carbon are utilized in the formation of new cells. The oxygen required to oxidize 1.0 g of ammonium nitrogen to nitrate (4.25 g) is less than the theoretical value of 4.57 g computed using Reaction 3.7, because the ammonium for cell synthesis is not considered in Reaction 3.7. Similarly, the alkalinity required for nitrification in Reaction 3.14 (7.07 g as $CaCO_3$/g NH_4-N) is less than the value of 7.14 g

calculated from Reaction 3.8 without considering the conversion of some of the ammonium to cellular nitrogen. It should be recognized that the coefficient values in Reaction 3.14 are dependent upon the value of f_s that is used.

3.3.1.3. The Role of the Ammonia Monooxygenase (AMO) Enzyme in Nitrification. The conversion of NH_3 to nitrite is accomplished by the catalysis of ammonia monooxygenase (AMO) and hydroxylamine oxidoreductase (HAO) enzymes as shown in Figure 3.9.

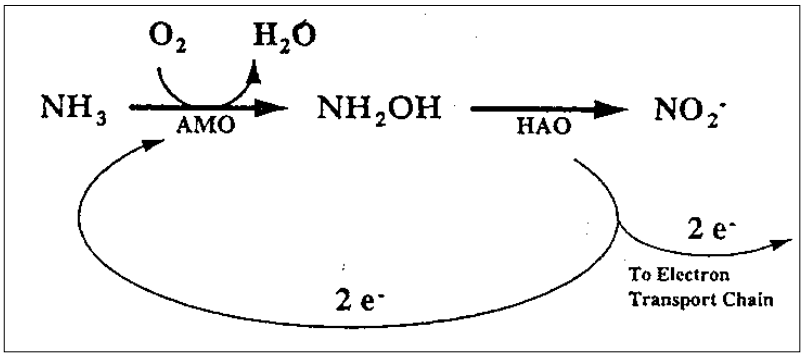

Figure 3.9. Conversion of ammonia to nitrite by *Nitrosomonas* by the catalysis of AMO and HAO (Ely et al., 1995b).

AMO catalyzes the reduction and insertion of an oxygen atom from molecular O_2 into ammonia, oxidizing ammonia to hydroxylamine (NH_2OH (Ely et al., 1995b; Arciero et al., 1989):

$$NH_3 + O_2 + 2H^+ + 2e^- \rightarrow NH_2OH + H_2O \qquad (3.15)$$

The further four-electron oxidation of hydroxylamine to nitrite is catalyzed by HAO as follows (Arciero et al., 1989):

$$NH_2OH + H_2O \rightarrow 4e^- + NO_2^- + 5\,H^+ \qquad (3.16)$$

Two of four electrons supplied by the oxidation of hydroxylamine to nitrite used to maintain steady-state AMO activity. The remaining two electrons enter the electron transport chain to synthesize ATP providing energy for cell growth and maintenance (Ely et al., 1995b; Hyman et al., 1995).

Although many metabolic and phylogenetic similarities exist between ammonia-oxidizing and methane-oxidizing bacteria, much more is known about the sMMO and pMMO found in methane oxidizing bacteria than about AMO (Ely et al., 1995b). AMO has not yet been purified to homogeneity with activity, so the detailed properties of this enzyme are not available (Arp et al., 2001). AMO is membrane bound as is pMMO and its substrate is thought to be ammonia (NH_3) rather than ammonium ion (NH_4^+). It catalyzes the oxidation of many non-growth substrates such as methane, and other n-alkanes (to C_8), n-alkenes (to C_5), aromatics, and halogenated hydrocarbons. Although evidence suggests considerable similarity between AMO and pMMO; its ability to catalyze the oxidation of aromatic hydrocarbons and straight-chain alkanes above C_5 indicates that, catalytically, AMO may be more similar to sMMO than to the less versatile pMMO (Ely et al., 1995b).

3.3.1.4. Growth Kinetics of Nitrifying Bacteria. The kinetic equation (3.17) proposed by Monod is used to describe the kinetics of biological growth of either *Nitrosomonas* or *Nitrobacter* (EPA, 1993b):

$$\mu_n = \mu_{\max,N} \frac{N}{K_N + N} \tag{3.17}$$

where μ_N is the specific growth rate of nitrifying bacteria, d^{-1}, $\mu_{max,N}$ is the maximum specific growth rate of nitrifying bacteria, d^{-1}; K_N is the half-saturation or half-velocity coefficient (equivalent to the growth-limiting substrate concentration at half the maximum specific growth rate), mg/L; N is the nitrogen concentration, mg/L.

Nitrite normally does not accumulate in large amounts under steady-state conditions. This is because the maximum growth rate of *Nitrobacter* is considerably higher than the maximum growth rate of *Nitrosomonas* and K_N values for both organisms are less than 1 mg/L N at temperatures below 20^0C. For this reason, the rate of nitrifier growth can be modeled using the conversion of ammonium to nitrite as the rate-limiting step. The relationship between the ammonium oxidation rate and the growth rate of *Nitrosomonas* can be expressed as follows (EPA, 1993b):

$$q_N = \frac{\mu_N}{Y_N} = q_{\max,N} \frac{N}{K_N + N} \tag{3.18}$$

where q_N is the specific ammonium oxidation rate, g NH_4^+ oxidized/gVSS.d; $q_{max,N}$ is the maximum specific ammonium oxidation rate, g NH_4^+ oxidized/gVSS.d; K_N is the half-saturation coefficient for *Nitrosomonas*, mg/L; N is the NH_4^+-N concentration, mg/L; Y_N is the organism yield coefficient , g *Nitrosomonas* grown (VSS)/g NH_4^+-N removed; μ_N is the specific growth rate of *Nitrosomonas*, d^{-1}.

3.3.1.5. Factors Affecting Nitrification. Nitrification is affected by a number of environmental factors including temperature, pH, alkalinity, dissolved oxygen (DO), un-ionized ammonia (free ammonia, FA), un-ionized nitrous acid (free nitrous acid, FNA) and toxicity as discussed below:

Temperature Effects

The nitrification process occurs over a range of approximately 4-45^{0}C with about 35^{0}C optimum for *Nitrosomonas* and 35-42^{0}C optimum for *Nitrobacter* (EPA, 1993b).

pH and Alkalinity

Nitrification is pH-sensitive and rates decline significantly at pH values below 6.8. At pH values near 5.8-6.0, the rates may be 10 to 20 percent of the rate at pH 7.0. Optimal nitrification rates occur at pH values in the range of 7.5 to 8.0. A pH of 7.0-7.2 is normally used to maintain reasonable nitrification rates, and for locations with low alkalinity waters, alkalinity is added at the wastewater-treatment plant to maintain acceptable pH values. The amount of alkalinity added depends on the initial alkalinity concentration and amount of NH_4-N to be oxidized (Metcalf and Eddy, 2003). Overall energy and synthesis reaction of nitrification Reaction (3.14) shows that, nitrification consumes alkalinity (7.07 g as $CaCO_3$/ g NH_4^+-N) and also results in production of free acid which will tend to depress pH. The alkalinity of wastewater must be 10 times greater the amount of ammonium nitrified in order to maintain a pH greater than 6 (EPA, 1993b).

Dissolved Oxygen (DO) concentration

Nitrification rates are affected by the liquid DO concentration. In contrast to what has been observed for heterotrophic degradation of organic compounds, nitrification rate increases up to DO concentrations of 3 to 4 mg/L. To account for these effects of DO, the expression for the specific growth rate (Eqn. 3.17) is modified as follows (Metcalf and Eddy, 2003):

$$\mu_N = \left[\frac{\mu_{\max,N} N}{K_N + N}\right]\left[\frac{DO}{K_o + DO}\right] \tag{3.19}$$

where DO is the dissolved oxygen concentration, mg/L and K_o is the half-saturation coefficient for DO, mg/L and the other terms as defined previously.

At low DO concentrations (< 0.50 mg/L) where nitrification rates are greatly inhibited, the low DO inhibition effect has been shown to be greater for *Nitrobacter* than for *Nitrosomonas*. In such cases, incomplete nitrification will occur with increased NO_2-N concentrations in the effluent (Metcalf and Eddy, 2003).

Free Ammonia (FA) and Free Nitrous Acid (FNA)

Free ammonia (FA, un-ionized ammonia, NH_3) and free nitrous acid (FNA, un-ionized nitrous acid) are believed to be inhibitory to nitrifiers above certain concentrations. FA begins to inhibit to *Nitrosomonas* at a concentration of 10-150 mg/L and *Nitrobacter* in the range of 0.1-1.0 mg/L. FNA begins to inhibit *Nitrosomonas* and *Nitrobacter* at concentrations of 0.22-2.8 mg/L. The FA and FNA concentrations are directly correlated to pH and temperature and the concentration of ammonia plus ammonium and nitrite plus nitrous acid, respectively (EPA, 1993b).

Toxicity

Nitrifying organisms are sensitive to a wide range of organic and inorganic compounds and at concentrations well below those concentrations that would affect

aerobic heterotrophic organisms. In many cases, nitrification rates are inhibited even though bacteria continue to grow and oxidize ammonia and nitrite, but at significantly reduced rates. In some cases, toxicity may be sufficient to kill nitrifying bacteria. Compounds that are toxic include solvent organic chemicals, amines, proteins, tannins, phenolic compounds, alcohols, cyanates, ethers, carbamates, benzene and metals (Metcalf and Eddy, 2003). Aliphatic chlorinated solvents are the major issue in this study.

3.3.1.6. Nitrification in Attached-Growth Systems. Attached-growth reactors (biofilm reactors) involve a solid media to which bacteria are fixed as a matrix called the biofilm, the surface of which is exposed to water passing through the reactor (Arvin and Harremoes, 1990). Main advantages of biofilm reactors with respect to suspended growth reactors are as follows:

- simplicity of operation and maintenance
- capability to remove slowly decomposable substrates
- slower response and quicker recovery to sudden changes of influent
- less sensitivity to toxic compounds
- less area requirement
- high effect on low concentration wastewater
- operation at high sludge ages
- low cost

Since nitrifying organisms show relatively slow growth rates, they require longer sludge ages. Moreover, they are very sensitive to various industrially discharged organic and inorganic toxic chemicals Thus, there is an increasing trend for nitrification of industrial wastewaters in biofilm systems which provides long sludge ages and can function in response to loadings of toxic chemicals.

However, the mechanisms of biofilm systems are more complicated than suspended growth systems because of mass-transport and diffusional resistances. As shown in Figure 3.10, indiffusion of substrates from bulk liquid to liquid film and then to biofilm in which reactions take place and products are formed and outdiffusion of products from biofilm to bulk water are the main mechanisms involved in biofilm systems.

Therefore, the performance of biofilm reactors heavily depends on whether the substrate can penetrate the biofilm fully or partly. In order for the substrate to move into the film by diffusion there has to be a concentration gradient. If the rate of removal per unit volume is high and the diffusion is slow, the concentration may reach zero and the substrate penetrates the film only partly. Only part of the biofilm is active and the rate of reaction per unit surface is much slower than with a fully penetrated film. It is the bulk concentration that determines the transition from full to part penetration (Arvin and Harremoes, 1990). These aspects have been applied in the analyses of biofilm data in Section 6.9.2

Although the factors described in Section 3.3.1.5 are valid for both attached growth and suspended growth nitrifier systems, different mechanisms involved in biofilm systems necessitates considering additional factors when dealing with attached growth nitrifier systems. According to Boller et al. (1994), the numerous environmental factors affecting the performance of nitrifying biofilms can be divided into two set of parameters as summarized in Table 3.1. A first set includes transport and reaction processes within the biofilm on a microscopic level which are primarily independent of the reactor. With the second set of parameters describing the hydraulics and the nutrient transport conditions to the biofilm surface, gas exchange processes, reactor configuration and operational features, the reactor specific conditions in each reactor are taken into account on a macroscopic level.

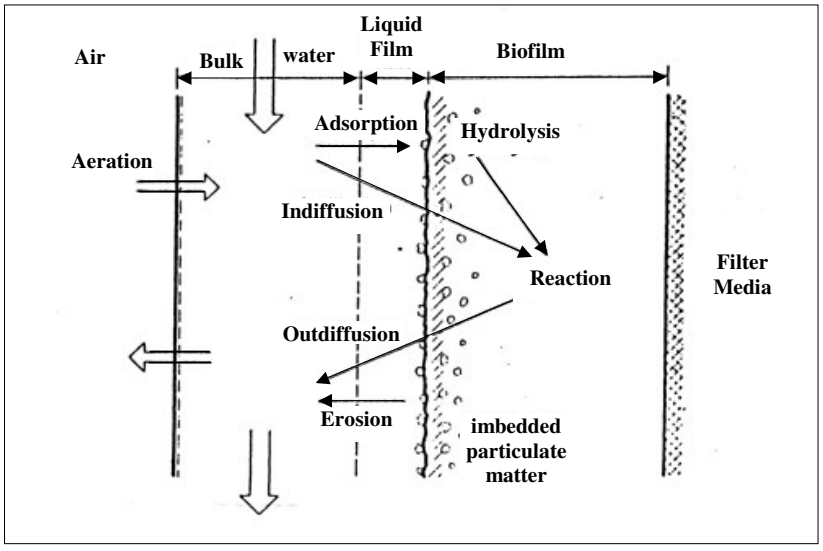

Figure 3.10. Mechanisms in biofilm systems (Arvin and Harremoes, 1990)

Table 3.1. Parameters affecting the performance of nitrifying biofilms on a biofilm oriented (microscopic) and a reactor specific (macroscopic) level (Boller et al., 1994)

biofilm specific parameters	reactor specific elements
• concentration of dissolved nutrients (e.g., COD, NH_4^+, NO_2^-, NO_3^-, O_2) at and in the biofilm	• reactor configuration (completely stirred, plug flow, mixed
• concentration of particulate substances (e.g., TSS, COD, heterotrophs)	• reactor hydraulics (laminar, turbulent flow)
• concentrations of HCO_3^- and pH	• oxygen transfer
• diffusion coefficients for COD, NH_4^+, NO_2^-, NO_3^-, HCO_3^-, O_2	• biofilm sloughing
• maximum growth rates of microbial species (e.g., heterotrophs, Nitrosomonas, Nitrobacter)	• biofilm grazing
• saturation coefficients for COD, NH_4^+, NO_2^-, NO_3^-, HCO_3^-, O_2	
• biomass density and biofilm thickness	

Among various types of biofilm reactors, the followings are considered to be the most feasible and economical for practical applications at the present time (Boller et al., 1994).

- *Trickling filters* packed with volcanic rock or plastic media in the form of random packings or corrugated plastic sheets.
- *Rotating biologic contactors (RBC)* with different types of biomass carrier elements like discs or plastic media drums exerting different hydraulic flow pattern.
- *Biofilters (BF)* with different granulated media or corrugated sheets in the up or downflow mode and mostly internally aerated with compressed air.
- *Fluidized bed reactors* where the biomass carrier material is suspended by the upflowing water and aerated by compressed air or pure oxygen.

Several long term experiments carried out to investigate maximum non-NH_4^+-limited nitrification rates of secondary non-nitrified effluent wastewater with activated sludge systems, trickling filters, RBCs and biofilters showed that nitrification potential of aerated biofilters is considerably larger than of the other reactors tested. Therefore, area

and space requirements of biofilters are much smaller than any alternative systems. However, the oxygen transfer is relatively low and the air input leads to higher operating costs. Therefore, if energy consumption can be reduced, biofilters will certainly be a favorable solution to perform nitrification (Boller et al., 1994).

3.3.2. Review of Studies on Cometabolic Degradation of Chlorinated Organics by Nitrifiers

The cometabolic degradation of chlorinated organics by nitrifier species has been studied to a much smaller extent compared to the studies with methanotrophs and aromatic substance (e.g. toluene and phenol) oxidizers. The majority of these limited studies have been performed with pure *Nitrosomonas europaea* species. In these studies, the primary focus was on trichloroethylene (TCE). A brief information on the findings of these studies is given below.

The study of Arciero et al. (1989) is the first demonstration that the ammonia oxidizing bacteria (*Nitrosomonas europaea*) catalyze the degradation of TCE. In this study, the rate of oxygen utilization by *Nitrosomonas europaea* cell suspensions with 1mM ammonia (14 mg/L NH_4-N) was inhibited by 98% in the presence of 1.1 mM (144540 mg/L) TCE. In contrast, the rate of oxygen utilization coupled to the oxidation of 2mM hydroxylamine (NH_2OH) was not inhibited by 1.1 mM TCE. This suggested that TCE may specifically interact with the ammonia monooxygenase (AMO) enzyme. Incubation of *Nitrosomonas europaea* cell suspension with 11 μM (1445 μg/L) TCE and 1 mM (14 mg/L NH_4-N) ammonia resulted in the disappearance of TCE at an initial rate of at least 1.1 nmoles/mg protein/min and slower nitrite production rate with respect to that observed for cells incubated with only ammonia.

Ely et al. (1995b) investigated the inhibition (caused by the presence of a cometabolic compound), inactivation (resulting from toxicity of cometabolic product) and recovery (associated with bacterial synthesis of new enzyme in response to inactivation) of AMO enzyme during cometabolism of TCE by *Nitrosomonas europaea* with a series of experiments and the solution of the enzyme kinetics model (Ely et. al, 1995a). NO_2^-, TCE, O_2 uptake rate, protein content and cell viability (analyzed by hydroxylamine

oxidoreductases, HAO, activity experiments) measurements were done by the quasi-steady-state batch experiments with pulse injections of TCE (590-3500 μg/L) and constant rate delivery of NH_3 (quasi-steady-state NH_4-N concentration=0.14-0.57 mg/L). The results showed that a large decrease in NH_3 oxidizing activity was evident immediately after TCE injection. Similarly, the solution of enzyme kinetics model showed that TCE was a competitive inhibitor of NH_3 oxidation, with TCE affinity for AMO being about four times greater than that of NH_3 for the AMO. By using the proposed model, half-saturation constant (K_I) and the maximum degradation rate (k_I) of TCE were estimated as 1400 μg/L and 11 nmol TCE/mg protein.min, respectively. Based on the assumption that the dry cell mass consists of 50% protein, these estimated parameters result in a first-order TCE degradation rate constant of 0.74 L/mg.d (Alvarez-Cohen and Speitel, 2001).

In the same study (Ely et al., 1995b), as TCE was oxidized, decreases in both NH_3 and TCE oxidation rates were observed due to inactivation of the AMO enzyme. Decreased TCE oxidation rates caused TCE concentrations to remain higher for longer periods of time, indirectly reducing NH_3 oxidation rates by prolonging inhibitory effects. In addition, model solution results showed that TCE oxidation was relatively slow compared to NH_3 oxidation, with the maximum specific oxidation rate of TCE being roughly 100 to 200 times less than the that of NH_3, causing inactivation of AMO to be a more gradual process. It was concluded that inhibition reduces NH_3 oxidizing activity more severely in the short term. However, inactivation of AMO that hinders the ability of bacteria to regain activity as the TCE concentration decreases, may become more critical in the long term.

Throughout this study (Ely et al., 1995b), it was also observed that bacterial recovery (i.e., synthesis of new enzymes in the absence of detectable cell growth) in response to inhibition and/or inactivation was initiated even in the presence of TCE. It is a very significant observation because it suggests that electron transport proteins were functioning and cell membranes were intact (allowing the cells to realize energy from NH_3 oxidation) and that protein synthesis components (e.g., DNA, mRNA) were functional. The relative importance of the two activity-decreasing mechanisms (inhibition and inactivation) was reported to be dependent on NH_3 and TCE concentrations, amount and rate of TCE oxidation, and ability of cells to recover. In view of these findings, researchers suggested that under appropriate conditions, the bacteria potentially could oxidize TCE while

concurrently coping with AMO damage. If NH_3 and TCE concentrations were controlled within specific ranges to limit the rate of TCE oxidation (and enzyme inactivation), while maintaining a necessary minimum rate of NH_3 oxidation (and recovery rate), it may be possible that TCE degradation could be sustained by ammonia oxidizing bacteria.

In another study, Hyman et al. (1995) investigated the cometabolism of TCE by *Nitrosomonas europaea* in short term (< 10 min) incubations. First, the effects of a range of TCE concentrations (3000-24000 μg/L) on ammonia-dependent O_2 uptake rates were examined with cells incubated in the presence of 1, 2.5 or 10 mM NH_4Cl (14, 35 or 140 mg/L NH_4-N). The increasing concentrations of TCE led to increased inhibition of O_2 uptake for cells incubated at all NH_4Cl concentrations. Demonstration of results by Dixon plot indicated that TCE was a potent competitive inhibitor of ammonia oxidation by *Nitrosomonas europaea*. The K_I value for TCE was estimated as 30 μM (3942 μg/L which was very similar to K_m for ammonia [40 μM (0.56 mg/L NH_4-N)]. Further experiments performed to investigate the inactivation of ammonia-oxidizing activity of the cells incubated with 5 mM (70 mg/L NH_4-N) and varying concentrations of TCE [57.5 μM (7555 μg/L) - 2.08 mM (273312 μg/L)] demonstrated that chloride ion release from TCE oxidation is a saturable process and is closely associated with a TCE-dependent inactivation of ammonia-oxidizing activity. The amount of TCE required to inactivate AMO varied with the specific AMO activity, which is dependent on factors such as the phase of growth cycle when the cells were harvested. The amount of TCE oxidation required for full AMO inactivation varied from 30 nmol TCE/mg protein for cells harvested in the late stationary phase, with low specific rates of ammonia-oxidizing activity, to 105 nmol TCE/mg protein for cells harvested during the logarithmic growth, which exhibited high specific rates of ammonia-oxidizing activity.

In the same study (Hyman et al., 1995), the effect of ammonia concentration on inactivation of ammonia oxidizing activity by TCE was evaluated with cells incubated with varying concentrations of ammonium [5 mM (70 mg/L NH_4-N), 10 mM (140 mg/L NH_4-N), 25 mM (350 mg/L NH_4-N)] and TCE [57.5 μM (7555 μg/L) and 230 μM (30222 μg/L)]. The results showed that ammonium concentration had little effect on the extent of TCE dependent inactivation of ammonia-oxidizing activity. At the TCE concentrations studied, increased ammonium concentration did not prevent TCE dependent inactivation of

ammonia oxidizing activity. Evaluation of the ability of cells to recover ammonia-oxidizing activity after exposure to TCE demonstrated that the rate of recovery was dependent on the initial level of inactivation of ammonia-oxidizing activity. A greater extent of inactivation entailed a longer recovery phase.

Yang (1997) and Yang et al. (1999) investigated the efficiencies of TCE cometabolism by AMO generated in enriched nitrifying culture through the analysis of relationships between specific growth-substrate utilization rate (q_{NH3}), specific non-growth substrate cometabolic rate (q_{TCE}), NH_3 and TCE concentrations, NH_3/TCE and TCE/NH_3 ratios. In the study of Yang (1997), the amounts of TCE removed through cometabolism were proportional to the initial concentrations of TCE applied to the systems and concentrations of biomass, and thus the amounts of AMO, applied to the system. However, no relationship was found between the amounts of TCE removed and the initially applied NH_3. Under sufficient oxygen supply, TCE showed inhibition to NH_3 oxidation at an initial level of above 200 μg/L. In a system containing 4 mg/L NH_4-N and 4.8 mg/L enriched nitrifier culture, ammonium oxidation activity was completely halted when the initial TCE concentration was at 200 μg/L. In the study of Yang et al. (1999), the oxygen was found to be important in the cometabolism of TCE by AMO, for which an oxygen deficiency would limit both NH_3 and TCE oxidation. The results of kinetic analysis showed that qNH_3 presented a positive linear relationship with NH_3 concentration in the absence or presence of TCE. In the absence of NH_3, specific TCE degradation rate (q_{TCE}) decreased linearly with TCE due to enzyme inactivation. It was also found that the NH_3/TCE ratio rather than TCE concentration alone exhibited a strong correlation with the specific ammonium utilization rate (q_{NH3}). Finally, they concluded that an enriched nitrifying culture might cometabolize TCE well as long as an environment was provided with sufficient oxygen, some NH_3 (to keep the enzyme AMO active to cometabolize TCE), enriched nitrifying biomass, suitable pH level and TCE concentrations below the inhibitory levels to NH_3 oxidation.

In the study of Juliastuti et al. (2003), the inhibitory effect of TCE on the net maximum specific growth rate of autotrophic biomass ($\mu_{max,a}$) was investigated with a respirometric technique. An activated sludge sample was taken from a municipal wastewater treatment plant. Oxygen uptake rate experiments performed at various TCE

concentrations (500, 750, 1000 μg/L) but at a fixed NH_4-N concentration (15 mg/L), showed that increasing concentrations of TCE resulted in constantly decreasing values of $\mu_{max,a}$. 50% inhibition of $\mu_{max,a}$ was reached at 750 μg/L TCE.

In another study, Ginestet et al. (2001) investigated the biodegradability of TCE, chloroform (CF) and 1,1-trichloroethane (1,1,1-TCA) by an enriched nitrifying biomass obtained from an activated sludge inoculum. The experiments were performed with varying concentrations of ammonium [0 to 8 mM (112 mg/L NH_4-N)] for a fixed chlorocarbon concentration of 4 μM (corresponds to 525 μg/L TCE, 478 μg/L CF and 530 μg/L 1,1,1-TCA). Specific initial degradation rate of each chlorinated organic studied were significantly increased with increasing ammonium concentration because of electron supply from ammonia oxidation. Maximal rates were observed at 4.3 mM (60 mg/L NH_4-N) for TCE [24 μmol TCE/h.g protein (3.15 mg TCE/h.g protein)], at 4.3 mM (60 mg/L NH_4-N) for CF [10 μmol CF/h.g protein (1.19 mg CF/h.g protein)] and at 7.6 mM (106 mg/L NH_4-N) for 1,1,1-TCA [3 μmol TCA/h.g protein (0.39 mg TCA/h.g protein)]. However, at higher ammonium concentrations [4-8 mM (56-112 mg/L NH_4-N)] chlorocarbon degradation rates were lower because of competitive inhibition between ammonia and chlorinated organics for the AMO active site. In the same study, the biodegradation of CF and TCE led to an inactivation of ammonia oxidizers with inactivation yields of around 30 to 40 mg of proteins inactivated per μmol of chlorocarbon oxidized. In the case of 1,1,1-TCA, no inactivation was observed. It was explained with the possibility of systematic compensation of TCA mediated inactivation by ammonia oxidation. For both CF and TCE, re-activation yields were found to be very close to each other (around 25 mg protein/μmol N). This suggested that re-activation was independent of the inactivating compound and its mechanism was related to the usual turnover rate of AMO.

Vannelli et al. (1990) studied the transformation of dichloromethane (DCM), trichloromethane (chloroform, CF), tetrachloromethane (carbon tetrachloride, CT), 1,1,2-trichloroethane (1,1,2-TCA), 1,1,1-trichloroethane (1,1,1-TCA), monochloroethylene (vinyl chloride, VC), cis1,2-dichloroethylene (1,2-DCE), trans1,2-DCE, trichloroethylene (TCE), tetrachloroethylene (perchloroethene, PCE) with suspensions of *Nitrosomonas*

europaea. All the compounds, except CT and PCE, were degraded. In all cases, the presence of chlorinated organic compound decreased the rate of nitrite production from ammonia, consistent with competition for an active site. Degradation of chlorinated organic compounds was also observed in the absence of ammonia, although the rates and extent were always greater with ammonia. CT was not degraded by *Nitrosomonas europaea*, nor was the compound a good inhibitor of nitrite production. On the other hand, PCE was not degraded by *Nitrosomonas europaea* but was an effective inhibitor of nitrite production. Oxidation of hydroxylamine (NH_2OH) to nitrite was not inhibited by CT or PCE.

In another study, Rasche et al. (1991) investigated the cometabolic degradation of 16 chlorinated aliphatic compounds [chloromethane (CM), dichloromethane (DCM), trichloromethane (chloroform, CF), tetrachloromethane (carbon tetrachloride, CT), chloroethane (CA), 1,1-dichloroethane (1,1-DCA), 1,2-DCA, 1,1,1-trichloroethane (1,1,1-TCA), 1,1,2-TCA, 1,1,2,2-tetrachloroethane (1,1,2,2-TeCA), monochlorinated ethene (vinylchloride, VC), 1,1-dichloroethylene (1,1-DCE), cis1,2-DCE, trans1,2-DCE, trichloroethylene (TCE), tetrachloroethylene (perchloroethene, PCE)] and their inactivating potential for ammonia oxidation by *Nitrosomonas europaea.* For this purpose, *Nitrosomonas europaea* cells were initially incubated for 1 h with ammonium and the individual chlorocarbons. During the incubation period, chlorocarbon, chloride and nitrite measurements were performed. Co-oxidation products of chlorocarbons were also identified whenever possible. The cells preincubated for 1 h with ammonium and individual chlorocarbon were then washed and the ammonia-dependent and hydrazine (alternative substrate for HAO enzyme) dependent oxygen uptake rates were measured. The results of oxygen uptake rate measurements were compared with control cells that had been pretreated with ammonium alone for 1 h. During incubation period, all of the chlorinated methanes (except CT), ethanes and ethenes (except PCE) containing up to four chlorine substituents were cometabolized by *Nitrosomonas europaea.* Co-oxidation of the degradable chlorocarbons was accompanied by the release of chloride ions into the medium in all cases except 1,1,1-TCA and trans1,2-DCE. The organic products detected (formaldehyde for CM; CO for DCM; acetaldehyde for CA; acetic acid for 1,1-DCA; chloroacetaldehyde for 1,2-DCA; 2,2,2-trichloroethanol for 1,1,1-TCA) were all consistent with the simple hydroxylation of a carbon-hydrogen bond or an oxidative dehalogenation

mechanism. On the basis of the ability of *Nitrosomonas europaea* to co-oxidize the compound and the tendency of chlorocarbon cometabolism to inactivate O_2 uptake by cells, three classes of chlorocarbons were identified as follows:

- Class 1 compounds (not biodegradable, no inactivation): The first class of chlorocarbons included CT and PCE, which were not co-oxidized by *Nitrosomonas europaea*. No chlorocarbon depletion or chloride release was detected. Incubation of *Nitrosomonas europaea* cells with CT and PCE at the concentrations tested did not prevent AMO from oxidizing ammonia during the time course of the assay and did not affect the ammonia-dependent and hydrazine-dependent oxygen uptake. This indicated that the inability to degrade the compounds was not due to the inactivation of AMO or a general toxic effect on the cell.

- Class 2 compounds (biodegradable, minimal inactivation): This class included the compounds CM, CA and 1,2-DCA, which did not inactivate oxygen uptake by cells to a great extent, but were co-substrates for AMO, as determined by chlorocarbon depletion, chloride release, and product formation. The partial inactivation of ammonia-dependent and hydrazine-dependent oxygen uptake rates may reflect damage of *Nitrosomonas europaea* cells due to prolonged (1 h) exposure to the aldehyde products (formaldehyde as product of CM, acetaldehyde as product of CA and chloroacetaldehyde as product 1,2-DCA cometabolism), which were not toxic to the cell during short-term (10-min) exposures in a previous study.

- Class 3 compounds (biodegradable, substantial inactivation): The final class included the compounds DCM, CF, 1,1-DCA, 1,1,1-TCA, 1,1-2-TCA, 1,1,2,2,-TeCA, VC, 1,1-DCE, cis1,2-DCE, trans1,2-DCE and TCE, which were co-substrates for AMO, as indicated by substrate depletion and chloride production, and produced a turnover-dependent inactivation of one or both of the ammonia-dependent and hydrazine-dependent oxygen uptake activities. In this group, an effect both the ammonia-dependent and hydrazine-dependent oxygen uptake activities accompanied the co-oxidation of CF, 1,1-DCA, 1,1-DCE and TCE. Moderate or severe inhibition of ammonia-oxidizing activity with little or no effect on hydrazine oxidation occurred when cells were preincubated with 1,1,2-TCA, 1,1,2,2-TeCA, 1,1,-TCA, VC, cis1,2-DCE, trans1,2-DCE. Interestingly, DCM

was the only halocarbon, which strongly inhibited hydrazine-dependent oxygen uptake while only moderately affecting the rate of ammonia-dependent uptake. For all co-substrates, which had a deleterious effect on O_2 uptake activities, the addition of ATU (allylthiourea, specific inhibitor for AMO) during the 1 h preincubations with the chlorocarbon protected the cells against inactivation, suggesting that turnover conditions (i.e., oxidation of the co-substrate) were necessary for inactivation.

In another study, Ely et al. (1997) investigated the cometabolism of representative compounds of Class 1 (CT), Class 2 (1,2-DCA) and Class 3 (CF, TCE, 1,1-DCE) by *Nitrosomonas europaea* in terms of cometabolite and NH_3 oxidation rates, inhibition of NH_3 oxidation, AMO inactivation and synthesis of new enzymes. The experiments were performed in a quasi- steady–state bioreactor with pulse injections of TCE [15.6 μM (2050 μg/L)], 1,2-DCA [25.1-1390 μM (2483-137554 μg/L)], 1,1-DCE (1-7.6 μM (97-737 μg/L), CF (5.4-13.7 μM (645-1637 μg/L)], CT [19.2 μM (2956 μg/L)] and constant rate delivery of NH_3 (quasi-steady-state NH_4-N concentration=0.14-0.57 mg/L). The results showed that when TCE [15.6 μM (2050 μg/L)] was added to the system, TCE competition for AMO caused almost instantaneous inhibition of NH_3 oxidation. NH_3 oxidizing activity continued to decline, due to progressive inactivation of AMO, as TCE was oxidized. By using the enzyme kinetics model developed in a previous study (Ely et al., 1995a), the half-saturation constant (K_I) and the maximum degradation rate (k_I) of TCE were estimated as 1563 μg/L and 16.9 nmol TCE/mg protein.min, respectively. Based on the assumption that the dry cell mass consists of 50% protein, these estimated parameters result in a first-order TCE degradation rate constant of 1.02 L/mg.d (Alvarez-Cohen and Speitel, 2001).

In the same study (Ely et al., 1997), with 1,2-DCA [25.1 μM (2483 μg/L), no inhibition or inactivation of the NH_3 oxidizing culture were observed. 1,2-DCA hampered ammonia-oxidizing activity so little in these experiments that very high initial concentrations [up to nearly 1390 μM (137554 μg/L)] were required to cause a substantial deleterious effect. By using the enzyme kinetics model (Ely et al., 1995a), the half-saturation constant (K_I) and the maximum degradation rate (k_I) of 1,2-DCA were estimated as 98972 μg/L and 510 nmol DCA/mg protein.min, respectively. Based on the assumption that the dry cell mass consists of 50% protein, these estimated parameters result in a first-

order 1,2-DCA degradation rate constant of 0.37 L/mg.d (Alvarez-Cohen and Speitel, 2001).

Injection of 1,1-DCE [7,6 μM (737 μg/L) at one half of the initial TCE concentration hampered NH_3 oxidizing activity more strongly than TCE and nearly complete cessation of NH_3 oxidizing activity was observed over time. Although CF injection [13.7 μM (1637 μg/L)] caused less inhibition of NH_3 oxidizing activity, significant inactivation occurred with time and CF oxidation and total decline in NH_3 oxidizing activity during the experiment were nearly as severe as with a comparable initial TCE concentration.

In the case of CT injection [19.2 μM (2956 μg/L)], an initial drop in NH_3 oxidizing activity was observed. However, NH_3 oxidizing activity rebounded relatively quickly. CT was not oxidized by AMO and hence its concentration remained constant during the experiment.

As a summary, the half-saturation constants (K_I) and the maximum degradation rates (k_I) estimated for each of the chlorinated organic compounds showed the relative enzyme affinities for AMO in the order of 1,1-DCE ≅ TCE > CT > NH_3 > CF > 1,2-DCA and relative maximum specific substrate transformation rates in the order of NH_3>1,2-DCA >CF > 1,1-DCE ≅ TCE > CT(=0). In broad terms, the data may suggest lower transformation rates with higher chlorination per carbon atom, especially for the chlorinated alkanes. Of the compounds tested, the alkenes showed higher affinity for AMO than did the alkanes. Among the alkanes, high chlorination correlated with higher enzyme affinity. Hydroxylamine oxidoreductase (HAO) enzyme activity experiments carried out to investigate the nature of cellular injury showed that TCE exposure led to a severe loss of ammonia-oxidizing activity, but hydrazine-dependent activity remained unchanged. Even with the complete loss of NH_3 oxidizing activity brought about by exposure to 1,1-DCE, hydrazine-dependent O_2 uptake did not decline significantly. With CF present, ammonia-dependent and hydrazine-dependent O_2 uptake rates both declined. With both 1,2-DCA and CT, hydrazine-dependent activity remained unchanged while NH_3-dependent activity increased. Moreover, recovery capabilities of all solvents, except CF, were also demonstrated in this study. Undiminished hydrazine-dependent oxygen uptake together

with demonstrated recovery capability (except with CF) suggest that (1) cellular injury was limited primarily to AMO under the conditions of these experiments, (2) the electron transport chain continued to support O_2 uptake, (3) essentially all other cellular functions necessary for CO_2 fixation, RNA synthesis, and protein synthesis were active. Therefore, although TCE or 1,1-DCE oxidation caused severe injuries to AMO, cellular processes apparently were initiated to compensate for and/or recover from the injuries. This potential to recover activity by new enzyme synthesis is important primarily because synthesis of specific proteins and enzymes requires much less time and/or energy than growth of new cells. Thus, to maintain activity in a system treating compounds that cause enzyme inactivation, conditions must be controlled to allow the bacteria to cope with inactivation effects. In other words, the inactivation rate must be kept less than or equal to the recovery rate.

4. STATEMENT OF PROBLEM

As reported in Section 3.2, in recent years, biodegradation of TCE and 1,2-DCA by cometabolic processes, especially under aerobic conditions, have received much attention as a promising alternative to other available techniques. To date, the cometabolic degradations of TCE and 1,2-DCA under aerobic conditions were mainly studied by methane, toluene and phenol oxidizers, which utilize slightly soluble methane gas and toxic aromatic compounds toluene and phenol as primary growth substrates, respectively. On the other hand, the cometabolic degradation of TCE and 1,2-DCA by nitrifiers species, which are ubiquitously present in almost all environments (particularly in natural soil and wastewater treatment plants), have been studied to a much smaller extent compared to the studies with methane, toluene and phenol oxidizers. The majority of these limited studies, which have been performed with pure *Nitrosomonas europaea* species, do not represent a realistic case since in full-scale biological treatment and bioremediation systems pure nitrifying cultures are hardly employed and are difficult to maintain. Moreover, in these studies, the emphasis was on the inhibitory effect of TCE or 1,2-DCA on nitrification. There is almost no detailed study evaluating both the cometabolism of these compounds and the inhibitory effects of them on nitrification for a broad growth substrate (NH_4-N) and cometabolic substrate (TCE or 1,2-DCA) ranges in a systematic way. Therefore, the data presented in the literature are insufficient to evaluate the effectiveness and practical applicability of these processes in treatment and bioremediation systems. Additionally, all of the studies presented in the literature were performed in suspended-growth nitrifying systems and no information is available on cometabolic degradation of TCE or 1,2-DCA in nitrifying biofilm systems. However, several advantages of biofilm systems compared to suspended-growth ones (e.g, less sensitivity to toxic chemicals, operation at high sludge ages) make these systems attractive for the implementation of TCE or 1,2-DCA cometabolism via nitrifier species in practice.

The aim of the present study was to investigate the cometabolic removal of TCE and 1,2-DCA and to assess their inhibitory effects on nitrification. For this purpose, batch suspended-growth experiments and continuous-flow biofilm experiments were performed by using mixed cultures enriched for nitrifiers for a time period of about 3.5 years. The

methodology of the study is shown in Table 4.1. As seen from the table, the experiments were started with the enrichment of a mixed culture for nitrifiers. This culture was then used in suspended-growth batch experiments. As a next phase, various oxygenation methods were evaluated in order to find an appropriate oxygenation method to satisfy the high oxygen requirement of nitrifiers without causing stripping of chlorinated organics (TCE or 1,2-DCA) in batch experiments. In Phases III and IV, suspended-growth batch experiments were performed with TCE and 1,2-DCA in order to evaluate the cometabolic removal of these compounds and their inhibitory effects on nitrification. For this purpose, experiments were performed in a systematic way. Initially, immediate inhibitory effects of these compounds were evaluated in terms of specific oxygen uptake rates (SOUR). TCE and 1,2-DCA ranges determined in these experiments were further evaluated in long-term experiments in terms of specific ammonium utilization rates, SOUR and specific cometabolic degradation rates of TCE and 1,2-DCA to have an idea about the cometabolic degradation of TCE and 1,2-DCA by nitrifiers and the inhibitory effect on ammonium oxidation. In view of these results, the kinetics of cometabolic TCE and 1,2-DCA degradation and the impacts of these compounds on nitrification were then studied in detail. In Phase V, considering the results of suspended-growth batch experiments, cometabolic degradation of 1,2-DCA was also evaluated in a continuous-flow nitrifying biofilm reactor, which simulates the applicability of this process under field conditions. Prior to these experiments, nitrification efficiency and kinetics of the nitrifying biofilm reactor enriched for nitrifiers since 1994 was studied in detail. This constituted a base of continuous-flow experiments with 1,2-DCA. Finally, in Phase VI performed by Mertoğlu (2005b), biofilm samples taken during continuous-flow experiments were investigated by molecular biology techniques in order to characterize the microbial community in the reactor and to observe the community shifts and bacterial quantity changes as a result of 1,2-DCA degradation.

Table 4.1. Methodology of the study

Phase	Description
Phase I	Enrichment of a mixed culture for nitrifiers – measurements during the enrichment period – batch kinetic experiments with the enriched nitrifier culture
Phase II	Evaluation of the various oxygenation methods – experiments with diffused aeration systems, hydrogen peroxide, ORC®, silicon gas permeable tubing and gas permeable membrane module
Phase III	Suspended-growth batch experiments with TCE – preliminary oxygen uptake rate (OUR) experiments – batch experiments – batch experiments directed to kinetic modelling
Phase IV	Suspended-growth batch experiments with 1,2-DCA – preliminary oxygen uptake rate (OUR) experiments – batch experiments – batch experiments directed to kinetic modelling
Phase V	Continuous-flow experiments in the nitrifying biofilm reactor – preliminary experiments to investigate nitrification efficiency and kinetics of the biofilm reactor – evaluation of cometabolic degradation of 1,2-DCA and inhibitory effect of 1,2-DCA on nitrification
Phase VI	Characterization of the microbial community in the nitrifying biofilm reactor by molecular biology techniques

5. MATERIALS AND METHODS

5.1. Enrichment of a Mixed Culture for Nitrifiers

A mixed liquor was taken from the aeration tank recycle line of the Istanbul Pasakoy Advanced Biological Sewage Treatment Plant and enriched for nitrifiers in a 16 L batch reactor (Figure 5.1) for 4 months. This activated sludge was daily fed based on a fill-and-draw principle with the stock synthetic feed and mineral solutions described in Table 5.9 and the initial NH_4-N concentration was kept in the range of 150-200 mg/L. Dissolved oxygen (DO) concentration in the reactor was maintained above 4 mg/L by the airflow coming through an airstone diffuser connected to an air pump at a rate of 5.5 L/min. The airflow also provided complete mixing conditions in the reactor. The temperature of wastewater was held in the range of 20-25^{0}C by an aquarium heater placed into the reactor. The pH value in the reactor was kept in the range of 7-8.

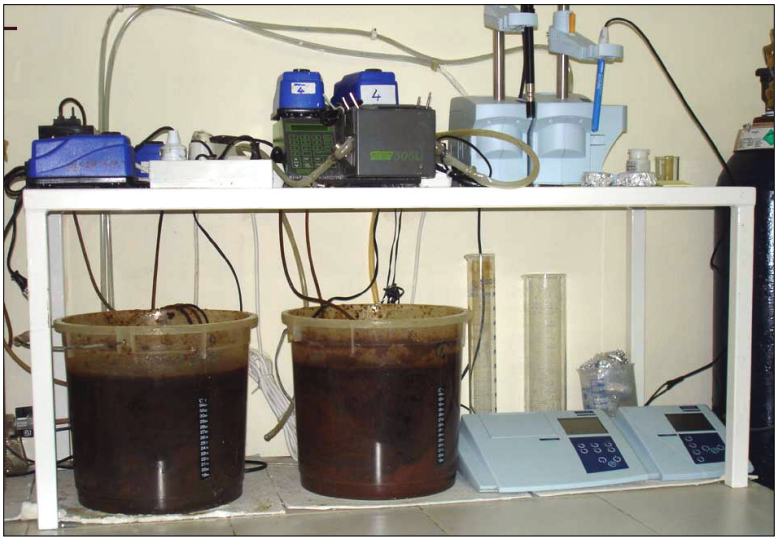

Figure 5.1. Batch reactor set-up used for the enrichment of nitrifiers

During the enrichment period, hourly NH_4-N, NO_2-N, NO_3-N and mixed liquor volatile suspended solids (MLVSS) measurements were performed at certain days. The data were processed by plotting NH_4-N values versus time as shown in Figures A.1 and A.2 in Appendix A. The specific ammonium utilization rates ($q_{NH4\text{-}N}$) were then calculated from the slopes of plottings through linear regression analysis and division of slopes by the

present MLVSS values. NO_2-N and NO_3-N measurements (Figure A.3 in Appendix A) were not used in the data analysis, since high NO_2-N concentrations caused interferences in NO_3-N measurements. This problem was compensated in later experiments as indicated in Section 5.7.

5.1.1. Batch Kinetic Experiments with the Enriched Nitrifier Culture [in the Absence of TCE and 1,2-DCA under Diffused Air Conditions]

These experiments were performed to determine the maximum specific ammonium utilization rate ($q_{max, NH4-N}$) and half-saturation constant (K_s) of the enriched nitrifier culture (in the absence of TCE and 1,2-DCA) under diffused aeration conditions. For this purpose, five experiments were performed at an initial NH_4-N concentration of 25, 50, 100, 200 and 400 mg/L.

Each experiment was performed in a 200 mL capped glass bottle at a constant wastewater temperature of 25^0C. The test bottle was placed into a water bath equipped with an aquarium heater under required conditions. The pH was kept in the range of 7-8.5. The dissolved oxygen (DO) concentration in the bottle was maintained above 4 mg/L by the airflow. The airflow also provided complete mixing conditions in the reactor.

In each experiment, the stock enriched nitrifier culture rinsed and diluted with deionized water to a MLVSS concentration of 250-420 mg/L was fed with the stock synthetic feed and mineral solutions to maintain the initial NH_4-N concentration of 25-400 mg/L. During the test period, NH_4-N measurements were carried out at certain time intervals. MLVSS measurement was also performed at the end of experiment. The NH_4-N measurements were plotted against time as shown in Figures B.1-B.5 in Appendix B. In these graphs, initial NH_4-N values decreased linearly till a certain bulk NH_4-N concentration was reached. NH_4-N measurements in the linear portion of this graph were then divided by the present MLVSS value and plotted against time. The specific ammonium utilization rate (q_{NH4-N}) was calculated from the slope of NH_4-N/VSS versus time plotting through linear regression analysis. q_{NH4-N} values were further processed with respect to the bulk NH_4-N concentrations and also with respect to the initial NH_4-N

concentrations to determine the exact $q_{max, NH4-N}$ and K_s values and apparent $q_{max, NH4-N}$ and K_s values, respectively.

5.2. Evaluation of Various Oxygenation Methods

The high oxygen requirement of nitrifier species (see Section 3.3.1.2) necessitates the selection of an efficient oxygenation method. If the wastewater contains volatile organic compounds, as in our case, then diffused aeration causes the volatile organics to be released into the bubbles and then into the air rather than be treated by bacteria. Nevertheless, in this study, diffused aeration systems were investigated as a first option for oxygenation.

Initially, fine-bubble diffused aeration was evaluated in terms of its effect on TCE stripping. For this purpose, the two test bottles filled with deionized water were only fed with TCE at an initial TCE concentration of 1000 µg/L. The test bottles were then aerated with the airflow coming through a 11.5 cm-diameter fine bubble airstone diffuser (Figure 5.2a) at a rate of 0.75 L/min and 0.65 L/min, respectively. The air flowrates of 0.65 and 0.75 L/min were chosen according to the results of preliminary trials in which short-time ammonium utilization experiments were performed at different air flows to find the lowest air flowrate satisfying the minimum 2 mg/L DO concentration through experiments (data not shown). TCE measurements were performed at certain time intervals to observe the stripped amount of TCE at the studied air flowrates.

The next trial was performed with a micro-bubble ceramic diffused aeration system by pure oxygen supply. For this purpose, two test bottles filled with deionized water were only fed with TCE at an initial TCE concentration of 200 µg/L. The test bottles were then aerated with the pure oxygen gas flow coming through 4” (10.16 cm) long RENA micro-bubble diffusers (Figure 5.2b) supplied from Foster & Smith Inc., Wisconsin, U.S. The pure oxygen gas flow rate was adjusted as 0.65 L/min and 0.16 L/min for the first and second bottles, respectively. The gas flowrate of 0.16 L/min was decided by considering the fact that the usage of 99.5% pure oxygen instead of air (20.9% oxygen by volume) increases the driving force by a factor of 4.76 (476%). During the test period of 3 h, TCE

measurements were performed at certain time intervals to observe the stripped amount of TCE.

Since the trials with diffused aeration systems resulted in significant stripping of TCE in a short time, as a next trial, hydrogen peroxide (H_2O_2, 50%) was investigated as a source of dissolved oxygen for nitrification. Two different experiments were performed to investigate the effect of H_2O_2 on nitrification efficiency. For this purpose, two bottles containing 600 mg/L (MLVSS) enriched nitrifier culture were initially fed with the stock synthetic feed and mineral solutions to maintain the initial NH_4-N concentration of 100 mg/L. During the experiments, the first bottle was used as a blank and aerated with the diffused aeration system. In the second bottle, oxygen was supplied by the addition of 110 µL 1/500 diluted H_2O_2 (50%) for five seconds at seven minutes intervals. Complete mixing of this bottle was achieved by magnetic stirring. During the test period of 140 min, the DO concentration in both bottles varied between 4-6 mg/L. In data analysis, the specific ammonium utilization rates in both conditions were calculated as described in Section 5.1.

Oxygen Release Compound, ORC ® supplied from Regenesis Inc., San Clemente, U.S. was also investigated as an oxygenation method. ORC® (Figure 5.2c), which is an insoluble powdery material less than 10 microns in diameter, is a patented formulation of phosphate-intercalated magnesium peroxide that produces a slow and sustained release of molecular oxygen when in contact with soil moisture or groundwater. The term "intercalation" describes the permeation of phosphates into the crystal structure of the magnesium peroxide, which allows for a continued release of the oxygen for a long period of time. ORC ® was first introduced to the environmental remediation market in 1995. It has now been used on over 5000 soil and groundwater restoration projects in the U.S. and in several countries (http://www.regenesis.com). For the evaluation of the oxygen release rate of ORC®, 0.5 g of ORC® was added into a 250 mL test bottle filled with deionized water. Complete mixing was achieved by magnetic stirring. DO concentration was continuously monitored for a test period of 90 min. Due to insoluble characteristics, even a small quantity of ORC® addition (0.5 g) into water resulted in a chalk like slurry. Therefore, no more trials were performed with higher amounts.

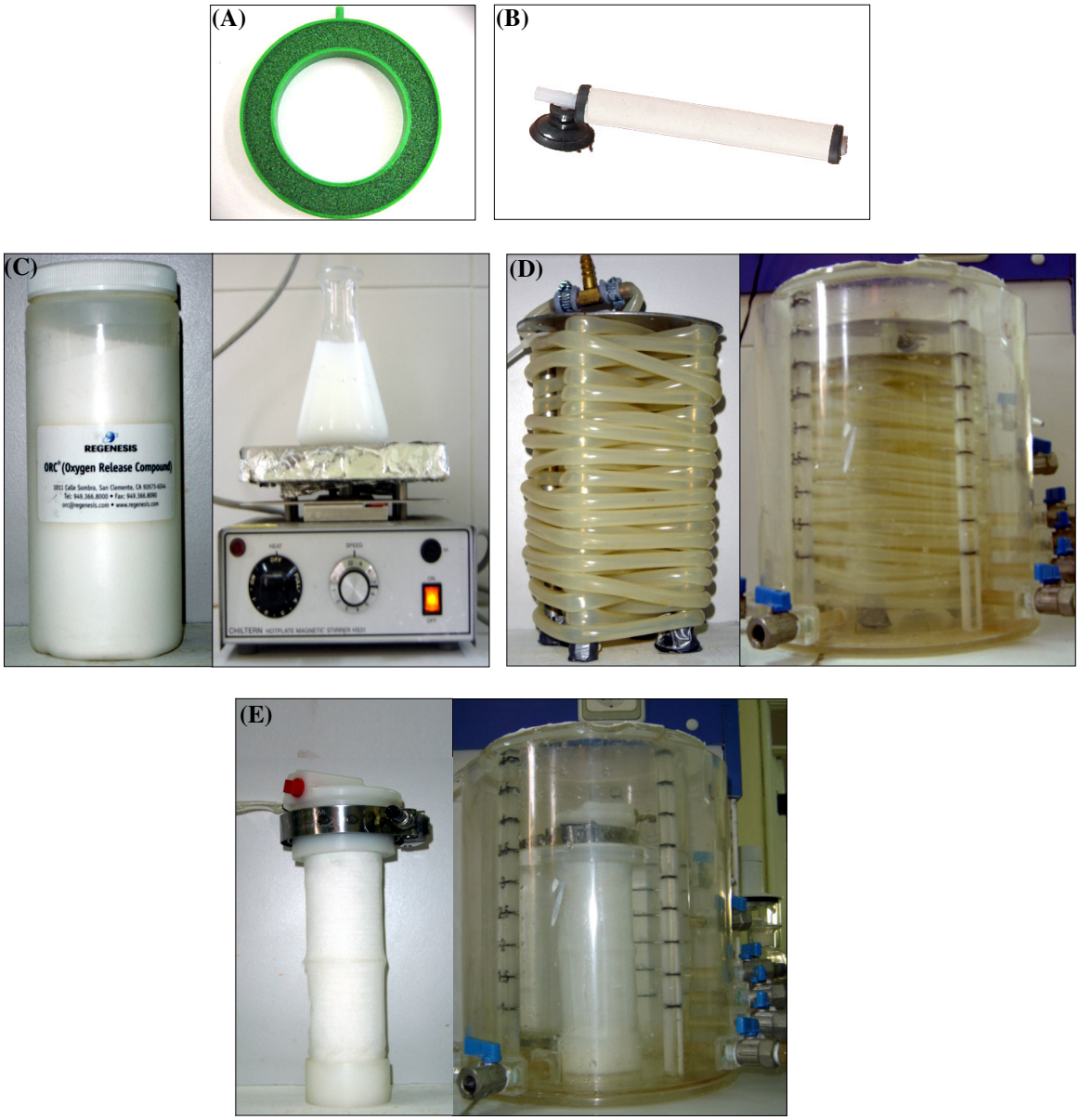

Figure 5.2. Oxygenation systems (a) fine-bubble airstone diffuser (Has Tropikal Ltd.), (b) micro bubble ceramic diffuser (Foster&Smith Inc., U.S.), (c) oxygen releasing compound (ORC) (Regenesis Inc., U.S.), (d) gas permeable silicon-tubing (McMaster-Carr, Inc., U.S.) and (e) gas permeable hollow fiber membrane module (Celgard Inc., U.S.)

Finally, bubble-free (or bubbleless) oxygenation via gas-permeable membranes was investigated as an option for efficient oxygenation. For this purpose, initially, gas permeable silicon-tubing (6 m long, 0.635 cm (1/4") diameter, Part No: 51135K28) supplied from McMaster-Carr, Inc., U.S. was wrapped around a metal plate and placed into a reactor shown in Figure 5.2d. The tubing was connected to pure oxygen. The reactor was then filled with deionized water and fed with TCE at an initial concentration of 350 µg/L.

Complete mixing was provided by magnetic stirring. The outlet pressure of pure oxygen gas supply was regulated as low as possible (< 0.1 bar) by using needle valve. TCE measurements were performed at certain intervals during a test period of 30 min. As an alternative to silicon tubing, the next trial was performed with a gas permeable hollow fiber membrane module (Figure 5.2e) supplied from Celgard Inc., North Caroline, U.S. This membrane module was also connected to the pure oxygen gas supply and placed into the reactor filled with deionized water. The outlet pressure of pure oxygen gas supply was regulated as low as possible (< 0.1 bar) as in the case of silicon tubing experiments to observe whether bubbles are formed or not.

5.3. Batch Experiments with TCE in Suspended-Growth Enriched Nitrifying Systems

5.3.1. Preliminary Oxygen Uptake Rate (OUR) Experiments with TCE

Since the oxygen consumption as an electron acceptor is a key activity in nitrification (see Section 3.3.1.2), respirometric methods based on oxygen uptake rate measurements provide easy and rapid tracking of viability and activity of nitrifiers. Therefore, it is very common to monitor the inhibitory effects of certain inorganic/organic compounds on nitrification via oxygen uptake rate (OUR) measurements.

As seen from Table 2.2, TCE levels monitored in the environment (e.g, in groundwater and leachate) exhibit a significant variance (0.2-425000 μg/L) depending on the history and extent of contamination. In the previous studies performed to evaluate the cometabolic degradation of TCE by various types of microorganisms including *Nitrosomonas europaea* species, TCE concentrations varied from 30 to 273000 μg/L (Section 3.3.2; Alvarez-Cohen and Speitel, 2001). However, there is almost no study evaluating the inhibitory effects of a broad TCE range on nitrification at the same experimental conditions.

In this study, preliminary OUR experiments were initially started with 50 μg/L TCE. In later runs, TCE concentration was increased gradually up to the detection of 90%

inhibition of OUR. The main aim was to assess the immediate inhibitory effect of TCE on nitrification and have an idea about the inhibitory range. For this purpose eight sets of OUR experiments were performed in 300 mL capped glass bottles without headspace as described in Table 5.1. The experimental set-up is shown in Figure 5.3.

Table 5.1. Operating conditions in OUR experiments with TCE

Experiment No	MLVSS mg/L	NH_4-N mg/L	TCE µg/L
Blank	103	40	-
1	132	40	50
2	131	40	100
3	153	40	500
4	149	40	1000
5	145	40	2500
6	146	40	5000
7	138	40	10000
8	144	40	50000

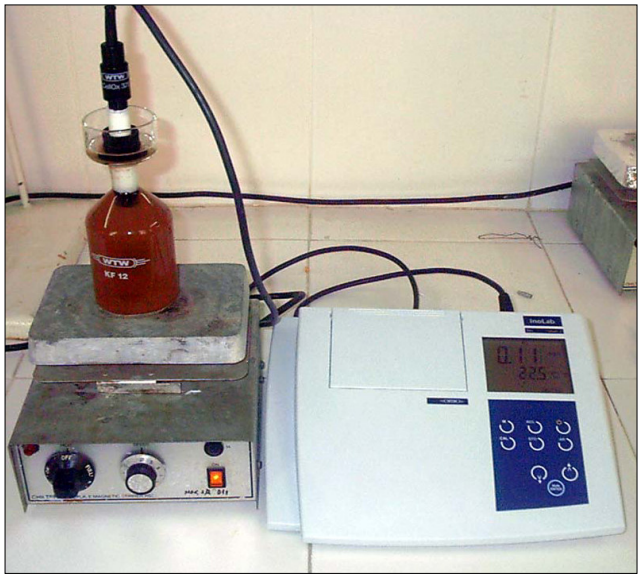

Figure 5.3. Experimental set-up of oxygen uptake rate (OUR) experiments

All experiments were performed at a constant wastewater temperature of 20^0C. The test bottles were placed into a water bath equipped with an aquarium heater under required conditions. Complete mixing condition was provided by magnetic stirring. The pH value

was kept in the range of 7-8. In each experiment, the stock enriched nitrifier culture rinsed and diluted by deionized water was aerated till saturation (7-8 mg/L DO) and then fed with the stock feed, mineral and TCE solutions. The initial TCE concentrations varied between 50-50000 µg/L whereas the initial NH_4-N was fixed at 40 mg/L. A blank experiment was also carried out in the absence of TCE. In each set of experiments, the DO concentrations were recorded at 15 s intervals over a 10 min test period as shown in Figures C.1-C.2 in Appendix C. The MLVSS concentrations were also measured at the end of each test. The OUR values were calculated from the slopes of DO versus time plottings through linear regression analysis. The specific oxygen uptake rate values (SOUR) were calculated by dividing the OUR values to the present MLVSS values.

5.3.2. Batch Experiments with TCE

Batch experiments were performed to investigate the cometabolic degradation of TCE by nitrifiers and the inhibitory effect of TCE on ammonium oxidation. Based on the results of preliminary OUR experiments, six sets of batch experiments (Table 5.2) were performed at an initial TCE concentration between 50-4500 µg/L and a fixed initial NH_4-N concentration of 40 mg/L. The experimental set-up is shown in Figure 5.4.

Table 5.2. Operating conditions in batch experiments with TCE

Exp. No.	1st bottle (Blank)			2nd bottle (Blank)			3rd bottle		
	VSS (mg/L)	NH_4-N (mg/L)	TCE (µg/L)	VSS (mg/L)	NH_4-N (mg/L)	TCE (µg/L)	VSS (mg/L)	NH_4-N (mg/L)	TCE (µg/L)
1	135	40	-	-	-	50	123	40	50
2	131	40	-	-	-	100	134	40	100
3	131	40	-	-	-	500	130	40	500
4	131	40	-	-	-	1000	137	40	1000
5	135	40	-	-	-	2000	133	40	2000
6	135	40	-	-	-	4500	144	40	4500

Figure 5.4. Experimental set-up of batch experiments with TCE

In all experiments, the enriched nitrifier culture was initially supersaturated to a DO concentration of 30-35 mg/L with pure O_2 gas. Aeration with diffuser was not used since TCE was highly volatile under diffused aeration conditions. The experiments were finished when the DO concentration in the bottles reached about 4 mg/L to avoid oxygen limited conditions. Each experiment was performed in a 2 L capped glass bottle at a constant wastewater temperature of 20^0C. The test bottle was placed into a water bath equipped with an aquarium heater under required conditions. Complete mixing was achieved by magnetic stirring. The pH was kept in the range of 7-8.5. Since the duration of experiments was too short (maximum 4-5 hours) and the initial NH_4-N/VSS ratio in these experiments was too small, the change in cell concentrations was considered insignificant and the MLVSS measurements were performed at the end of each experiment.

In each set of experiments, three bottles were run over a test period of 4-5 h as described in Table 5.2. The first bottle was used as a blank to investigate the specific ammonium utilization rate ($q_{NH4\text{-}N}$) and SOUR of the culture in the absence of TCE by performing NH_4-N and DO measurements at certain time intervals. For this purpose, the stock enriched nitrifier culture rinsed and diluted with deionized water was supersaturated with pure oxygen gas and then fed with stock feed and mineral solutions to maintain the initial NH_4-N concentration of 40 mg/L. The second bottle was used as a blank to determine the transfer rate of TCE from the liquid phase into the head space of the capped bottle due to magnetic stirring by performing TCE measurements at certain time intervals. For this purpose, the bottles filled with deionized water were only fed with stock TCE

solution to maintain an initial TCE range of 50-4500 µg/L. The third bottle was used to investigate the q_{NH4-N} in the presence of TCE and the specific cometabolic degradation rates of TCE (q_{TCE}) by performing NH_4-N, DO and TCE measurements at certain time intervals. For this purpose, the stock enriched nitrifier culture rinsed and diluted with deionized water was supersaturated with pure oxygen gas and then fed with stock feed, mineral and TCE solutions such that the initial NH_4-N was 40 mg/L while the initial TCE ranged from 50 to 4500 µg/L.

The q_{NH4-N} values in the first and third bottles of each run were calculated from the slopes of NH_4-N/VSS versus time plottings (Figure D.1 in Appendix D) through linear regression analysis.

For the calculation of the SOUR values in the first and third bottles of each run, the measured DO concentrations were corrected by an oxygen exchange rate of 0.294 mg/L.h which was determined between the reaction liquid and the overhead gas through a control experiment (data not shown) as shown in Eqn. 5.1.

$$DO_C = DO_M + 0.294 \times t \qquad (5.1)$$

where DO_C is the corrected DO concentration (mg/L) at time t, DO_M is the measured DO concentration (mg/L), t is time (h).

The SOUR values were then calculated from the slopes of DO_C/VSS versus time plottings (Figure E.1 in Appendix E) through linear regression analysis. The SOUR values were calculated by dividing the OUR values to the present MLVSS values.

Under the experimental conditions described above, volatilization of TCE was due to transfer of TCE from the liquid phase into the headspace of the capped bottle which was very low (6-8 %) compared with the volatilization of TCE under diffused aeration. Since the second blank bottle of each run did not contain microorganisms, the decreases observed (Figure F.1 in Appendix F) directly reflected the volatilization losses. On the other hand, the decreases in the TCE concentration in the third bottle containing microorganisms, TCE and NH_4-N were due to both cometabolic degradation and volatilization. Therefore, the

measured TCE concentrations in the third bottles were corrected for the volatilized amount of TCE as shown in Eqn. 5.2.

$$TCE_C = TCE_M + r_{vol,\ TCE} \times t \qquad (5.2)$$

where TCE_C is the corrected TCE concentration (µg/L), TCE_M is the measured TCE concentration (µg/L), $r_{tce,\ vol}$ is the volatilization rate of TCE (µg/L.h) and t is the time (h).

The q_{TCE} values in the third bottles of each run were then calculated from the slopes of TCE_C/VSS versus time plottings (Figure G.1 in Appendix G) through linear regression analysis.

5.3.3. Batch Experiments with TCE Directed to Kinetic Modelling

These experiments were performed to investigate the effect of TCE on the maximum specific ammonium utilization rate ($q_{max,\ NH4\text{-}N}$) and half-saturation constant (K_s) of the enriched nitrifier culture, type of TCE inhibition on nitrification and inhibition constant (K_I) of TCE. Based on the results of batch experiments, five sets of experiments were performed in a TCE range of 40-845 µg/L and a NH_4-N range of 25-400 mg/L as described in Table 5.3.

In all experiments, aeration, mixing and pH conditions were the same as in Section 5.3.2. Each test was performed in a 200 mL capped glass bottle at a constant wastewater temperature of 25^0C in a similar experimental set-up shown in Figure 5.4. The duration of each experiment was maximum 2 h. Therefore, MLVSS measurements were performed at the end of each experiment due to the reasons described in Section 5.3.2.

The first set of batch kinetic experiments was performed as a blank to determine the $q_{max,\ NH4\text{-}N}$ and K_s of the enriched nitrifier culture in the absence of TCE under saturated oxygen conditions. For this purpose, the stock enriched nitrifier culture rinsed and diluted with deionized water was supersaturated with pure oxygen gas and then fed with stock feed and mineral solutions to maintain the initial NH_4-N concentrations ranging between 25-400 mg/L. During the test period, NH_4-N measurements were carried out at certain time

intervals. The q_{NH4-N} values were calculated from Figure H.1 in Appendix H as described in Section 5.3.2. q_{NH4-N} values were further processed to determine the apparent $q_{max, NH4-N}$ and K_s values.

Prior to experiments with TCE, a set of blank experiments was performed to determine the transfer rate of TCE from the liquid phase into the headspace of the capped bottle due to magnetic stirring. For this purpose, the bottles filled with deionized water were only fed with the stock TCE solution to maintain the initial TCE concentrations ranging between 40-700 µg/L and TCE measurements were performed at certain time intervals. Volatilization rates of TCE were then calculated from the slope of TCE versus time plottings (Figure I.1 in Appendix I) through linear regression.

The other sets of experiments were performed for the NH_4-N concentrations varied for a fixed TCE concentration. In each experiment, the stock enriched nitrifier culture rinsed and diluted with deionized water was supersaturated with pure oxygen gas and then fed with stock feed, mineral and TCE solutions to maintain the initial NH_4-N concentrations ranging between 25-400 mg/L and the initial TCE concentration of 40µg/L for the second set, 110 µg/L for the third set, 325 µg/L for the fourth set and 845 µg/L for the fifth set of the experiments. During the test period, NH_4-N and TCE measurements were performed at certain time intervals. The q_{NH4-N} values were calculated from Figures H.2-H.5 in Appendix H as described in Section 5.3.2. The measured TCE concentrations were corrected for the volatilized amount of TCE as described in Equation 5.2. The q_{TCE} values were then calculated from Figures J.1-J.4 in Appendix J as described in Section 5.3.2.

Table 5.3. Operating conditions in batch experiments with TCE directed to kinetic modelling

Exp. No	1st bottle			2nd bottle			3rd bottle			4th bottle			5th bottle		
	VSS mg/L	NH_4-N mg/L	TCE µg/L	VSS mg/L	NH_4-N mg/L	TCE µg/L	VSS mg/L	NH_4-N mg/L	TCE µg/L	VSS mg/L	NH_4-N mg/L	TCE µg/L	VSS mg/L	NH_4-N mg/L	TCE µg/L
1	420	25	-	510	50	-	365	100	-	330	200	-	320	400	-
2	420	25	40	370	50	40	330	100	40	380	200	40	390	400	40
3	280	25	110	260	50	110	210	100	110	350	200	110	480	400	110
4	350	25	325	510	50	325	530	100	325	490	200	325	495	400	325
5	420	25	845	400	50	845	450	100	845	420	200	845	460	400	845

5.4. Batch Experiments with 1,2-DCA in Suspended-Growth Enriched Nitrifying Systems

5.4.1. Preliminary Oxygen Uptake Rate (OUR) Experiments with 1, 2 DCA

As seen from Table 2.3, 1,2-DCA levels monitored in the environment (e.g, in groundwater and leachate) exhibit a significant variance (0.72-920000 μg/L) depending on the history and extent of contamination. In the previous studies performed to evaluate the cometabolic degradation of 1,2-DCA by various types of microorganisms including *Nitrosomonas europaea* species, 1,2-DCA concentrations varied from 0.4 to 140000 μg/L (Section 3.3.2; Alvarez-Cohen and Speitel, 2001). However, there is almost no study evaluating the inhibitory effects of a broad 1,2-DCA range on nitrification at the same experimental conditions.

In this study, preliminary OUR experiments were initially started with 70 μg/L 1,2-DCA. In later runs, 1,2-DCA concentration was increased gradually up to detection of 94 % inhibition of OUR. The main aim was to assess the immediate inhibitory effect of 1,2-DCA on nitrification and have an idea about the inhibitory range. For this purpose twenty OUR experiments were performed in five sets in 300 mL capped glass bottles without headspace as described in Table 5.4. The experimental set-up is shown in Figure 5.3.

In all experiments, the initial 1,2-DCA concentrations varied between 70-380000 μg/L whereas the initial NH_4-N was fixed at 40 mg/L. The mixing and pH conditions were same as in Section 5.3.1. The wastewater temperature was kept at a constant value of 25^0C as described in Section 5.3.1. In each experiment, the stock enriched nitrifier culture rinsed and diluted by deionized water was supersaturated with pure O_2 gas to DO concentration of 8-11 mg/L and then the procedure described in Section 5.3.1 was followed. The DO concentrations recorded at 15 s intervals over a 10 min test period are shown in Figures K.1-K.5 in Appendix K.

Table 5.4. Operating conditions in OUR experiments with 1,2-DCA

Experiment No	VSS mg/L	NH_4-N mg/L	1,2-DCA µg/L
1st SET			
Blank	170	40	-
1	185	40	70
2	190	40	350
3	190	40	17000
4	190	40	35000
5	170	40	52000
6	280	40	70000
7	220	40	140000
2nd SET			
Blank	250	40	-
8	230	40	370
9	271	40	3600
10	230	40	36000
3rd SET			
Blank	184	40	-
11	120	40	85
12	172	40	170000
13	192	40	380000
4th SET			
Blank	156	40	-
14	152	40	225
15	188	40	4200
16	190	40	42000
17	204	40	60000
5th SET			
Blank	248	40	-
18	196	40	6000
19	184	40	150000
20	232	40	175000

5.4.2. Batch Experiments with 1,2-DCA

These experiments were performed to investigate the cometabolic degradation of 1,2-DCA by nitrifiers and the inhibitory effect of 1,2-DCA on ammonium oxidation. Based on preliminary OUR experiments, six batch experiments (Table 5.5) were performed with initial 1,2-DCA concentrations ranging between 1600-100000 µg/L at a fixed initial NH_4-N concentration of 50 mg/L.

Table 5.5. Operating conditions in batch experiments with 1,2-DCA

Experiment No	VSS mg/L	NH_4-N mg/L	1,2-DCA µg/L
1	214	50	-
2	247	50	1600
3	160	50	15000
4	176	50	50000
5	340	50	75000
6	256	50	100000

In all experiments, aeration, mixing and pH conditions were the same as in Section 5.3.2. Each test was performed in a 200 mL capped glass bottle at a constant wastewater temperature of 25^0C in a similar experimental set-up shown in Figure 5.4. The duration of each experiment was maximum 4 h. Therefore, MLVSS measurements were performed at the end of each experiment due to the reasons described in Section 5.3.2.

The first experiment was performed as a blank at an ammonium concentration of 50 mg/L NH_4-N in the absence of 1,2-DCA. The stock enriched nitrifier culture rinsed and diluted with deionized water was supersaturated with pure oxygen gas and then fed with stock feed and mineral solutions. During the test period, NH_4-N and DO measurements were performed at certain time intervals as shown in Figure L.1a in Appendix L and Figure M.1a in Appendix M, respectively. The $q_{NH4\text{-}N}$ and SOUR values were calculated as described in Section 5.3.2.

Prior to experiments with 1,2-DCA, a set of blank experiments was performed to determine the transfer rate of 1,2-DCA from the liquid phase into the headspace of the capped bottle due to magnetic stirring (Figure N.1 in Appendix N). In these experiments, the initial 1,2-DCA concentration ranged between 2500-130000 µg/L and the procedure described in Section 5.3.3 was followed.

In the experiments performed at various 1,2-DCA concentrations (1600-100000 µg/L) and at a fixed NH_4-N of 50 mg/L, the stock enriched nitrifier culture rinsed and diluted with deionized water was supersaturated with pure oxygen gas and then fed with

stock feed, mineral and 1,2-DCA solutions. During the test period, DO, NH_4-N and 1,2-DCA measurements were performed at certain time intervals. The SOUR, q_{NH4-N} and q_{DCA} values were calculated from Figure L.1 in Appendix L, Figure M.1 in Appendix M and Figure O.1 in Appendix O, respectively, as described in Section 5.3.2.

5.4.3. Batch Experiments with 1,2-DCA Directed to Kinetic Modelling

These experiments were performed as a continuation of batch experiments discussed in Section 5.4.2 to investigate the effect of 1,2-DCA on the maximum specific ammonium utilization rate ($q_{max,NH4-N}$) and half-saturation constant (K_s) of the enriched nitrifier culture, type of 1,2-DCA inhibition on nitrification and inhibition constant (K_I) of 1,2-DCA.

Three sets of experiments were performed as described in Table 5.6 in a similar experimental set-up shown in Figure 5.4. In each set of experiments, six different runs were carried out with the initial 1,2-DCA concentration ranging between 1600-100000 µg/L at a fixed initial NH_4-N concentration of 100 mg/L in the first set, 200 mg/L in the second set and 400 mg/L NH_4-N in the third set of experiments. In each set of experiments, the procedure described in Section 5.4.2 was followed. In data analysis, the results of these experiments (Figures P.1-P.6 in Appendix P and Figures Q1-Q5 in Appendix Q) were evaluated together with those determined through batch experiments in Section 5.4.2.

Table 5.6. Operating conditions batch experiments with 1,2-DCA directed to kinetic modelling

Run	1st Set Experiments			2nd Set Experiments			3rd Set Experiments		
No	VSS mg/L	NH_4-N mg/L	1,2-DCA µg/L	VSS mg/L	NH_4-N mg/L	1,2-DCA µg/L	VSS mg/L	NH_4-N mg/L	1,2-DCA µg/L
1	200	100	-	320	200	-	192	400	-
2	308	100	1600	220	200	1600	132	400	1600
3	268	100	15000	220	200	15000	324	400	15000
4	136	100	50000	220	200	50000	170	400	50000
5	592	100	75000	590	200	75000	543	400	75000
6	222	100	100000	120	200	100000	148	400	100000

5.5. Continuous-Flow Experiments in a Nitrifying Biofilm Reactor

The continuous-flow experiments were performed in an upflow aerated submerged biofilm system shown in Figure 5.5. This system was started-up in 1994 as described by Orak (1994) and Çeçen and Orak (1996) and was used in different studies until 1998 (Çeçen et al., 1995; Çeçen, 1996; Çeçen and Orak, 1996; Çeçen and Ipek, 1998). Since the start-up in 1994, the reactor has been fed with synthetic inorganic ammonium and mineral solutions and hence has been enriched for nitrifiers. The detailed technical information about the system is given in Table 5.7.

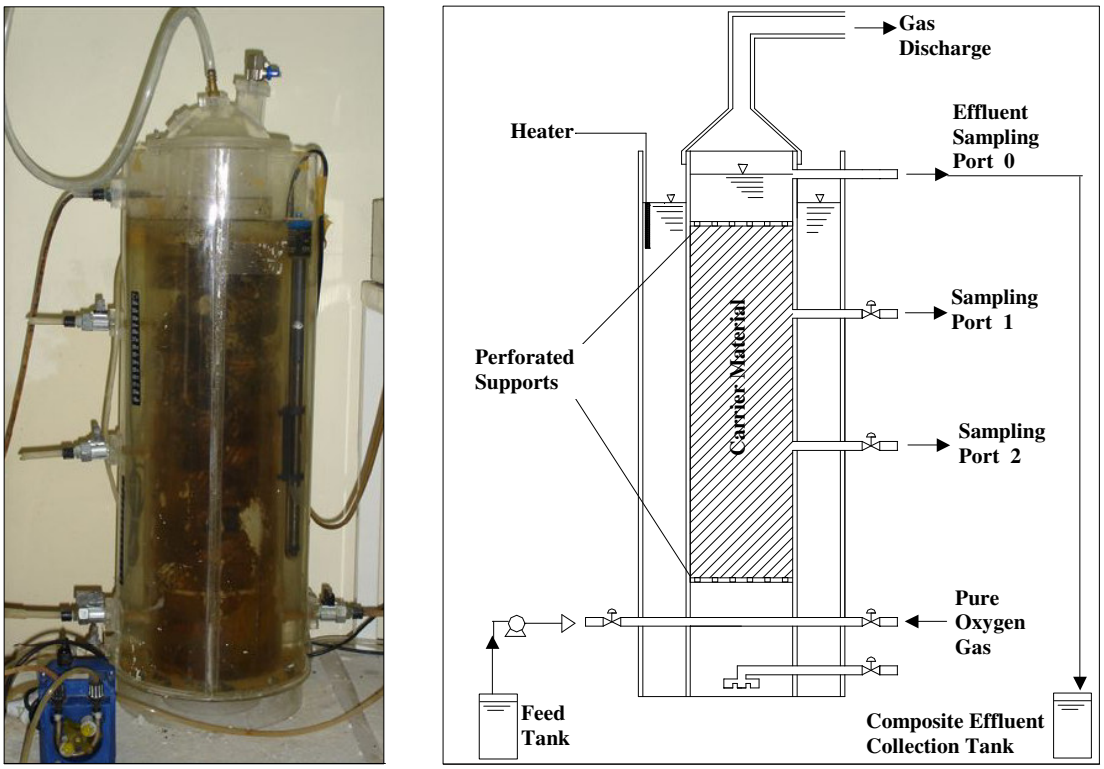

Figure 5.5. Experimental set-up of the nitrifying biofilm reactor

Table 5.7. Technical details of the nitrifying biofilm reactor

Construction material: plexiglass		Carrier material	: Bio-Pac15, polyethylene (Envicon Eng. GmbH)
Inner diameter	: 11.65 cm	No. of carrier materials	: 30
Outer diameter	: 22.5 cm	Length of carrier material	: 3 cm
Working height	: 40 cm	Specific surface area of carrier material	: 150 m^2/m^3
Total height	: 55 cm	Total surface area of the carrier materials in the reactor	: 0.192 m^2
Working volume	: 4.25 L	Total volume occupied by the carrier materials in the reactor	: 0.52 L
Total volume	: 5.85 L	Total volume of the packed part in the reactor	: 4.25 L
		Void volume of the packed part in the reactor	: 3.73 L

5.5.1. Evaluation of Nitrification Efficiency and Kinetics of the Nitrifying Biofilm Reactor

Continuous-flow biofilm experiments were initially carried out at various influent ammonium concentrations (60 to 400 mg/L NH_4-N) to investigate the nitrification efficiency and kinetics in the nitrifying biofilm reactor.

In each run, the feed solution prepared with stock synthetic feed and mineral solutions described in Table 5.9 was continuously fed into the system through a peristaltic pump with a flowrate of 6 L/day, which corresponds to an average hydraulic retention time of 17 h at the working volume of 4.25 L. The duration of each run was in the range of 6-12 days. The wastewater temperature in the filter was kept in the range of 23-26 ^{0}C. The aquarium heater placed into the water jacket around the reactor was adjusted as required. The DO in the bulk liquid was maintained in the range of 2.5-4 mg/L with pure oxygen supply at a rate of 40-45 mL/min. Inside the reactor pH was kept in the range of 7-8.5.

Before starting with the experiments, the hydraulic behavior of the reactor was investigated. For this purpose, the reactor was continuously fed with an influent NH_4-N

concentration of 35-55 mg/L for a month. During this period, grab samples taken from the effluent line (port 0), first port and second port were daily analyzed for NH_4-N. The measurements showed negligible concentration gradients in NH_4-N concentrations (see Section 6.9.1). Therefore, the filter was accepted as a completely stirred tank reactor (CSTR).

Throughout the experiments, samples were taken daily from the feed tank, effluent collection tank (composite sample) and the effluent line port 0 (grab sample). These samples were analyzed for NH_4-N, NO_2-N and NO_3-N as illustrated in Figures R.1-R.12 in Appendix R. Ammonium removal, nitrite accumulation and nitrate production rates were calculated after the filter reached steady-state with respect to effluent NH_4-N concentration as shown in Appendix R. The time period necessary to reach steady-state conditions varied in the range of 2-6 days depending on the variations in environmental conditions (e.g., temperature, DO).

In data analysis, volumetric and surface loading and removal rates of ammonium (Eqns. 5.3-5.6); volumetric and surface nitrite accumulation rate and nitrate production rates (Eqns. 5.7-5.10); and free ammonia (FA) concentrations (Eqn. 5.11) were calculated as described below. Since the synthetic feed solution did not contain NO_2-N and NO_3-N, in the calculation of nitrite accumulation (Eqns. 5.7 and 5.8) and nitrate production rates (Eqns. 5.9 and 5.10), influent NO_2-N and NO_3-N concentrations were not taken into consideration.

$$Volumetric\ \ Loading\ \ Rate = \frac{QS_{\inf}}{V} \tag{5.3}$$

$$Surface\ \ Loading\ \ Rate = \frac{QS_{\inf}}{A} \tag{5.4}$$

$$Volumetric\ \ \mathrm{Re}moval\ \ Rate = \frac{Q(S_{\inf} - S_{eff})}{V} \tag{5.5}$$

$$Surface\ \ \mathrm{Re}moval\ \ Rate = \frac{Q(S_{\inf} - S_{eff})}{A} \tag{5.6}$$

$$Volumetric\ \ Nitrite\ \ Accumulation\ \ Rate = \frac{Q(NO_{2\_}N)_{eff}}{V} \tag{5.7}$$

$$Surface\ \ Nitrite\ \ Accumulation\ \ Rate = \frac{Q(NO_{2\_}N)_{eff}}{A} \tag{5.8}$$

$$Volumetric\ \ Nitrate\ \ \Pr oduction\ \ Rate = \frac{Q(NO_{3\_}N)_{eff}}{V} \tag{5.9}$$

$$Surface\ \ Nitrate\ \ \Pr oduction\ \ Rate = \frac{Q(NO_{3\_}N)_{eff}}{A} \tag{5.10}$$

where Q is the influent flowrate (m^3/day); S_{inf} is the influent substrate (NH_4-N or 1,2-DCA) concentration (mg/L); S_{eff} is the effluent substrate (NH_4-N or 1,2-DCA) concentration (mg/L); V is the volume of the packed part of reactor (m^3) = 4.25 L; A is the total surface area of the carrier materials in the filter (m^2)=0.192 m^2; $(NO_2\text{-}N)_{eff}$ is the effluent NO_2-N concentration (mg/L); and $(NO_3\text{-}N)_{eff}$ is the effluent NO_3-N concentration (mg/L).

$$Free\ \ Ammonia\ \ (FA)\ \ Concentration\ \ (mg/L) = \frac{Total\ \ NH_{4\_}N}{1+10^{(pK-pH)}} \tag{5.11}$$

where $pK = 0.09018 + \frac{2729.92}{(273 +^0 C)}$

5.5.2. Evaluation of Cometabolic Degradation of 1,2-DCA and Inhibitory Effect of 1,2-DCA on Nitrification

Continuous-flow experiments with 1,2-DCA were performed to investigate the cometabolic degradation of 1,2-DCA, the inhibitory effect of 1,2-DCA on nitrification and recovery of cells from 1,2-DCA inhibition. These experiments were mainly performed at two different influent NH_4-N concentrations (152 mg/L and 50 mg/L) as two sets to evaluate the effects of low and high ammonium loadings on 1,2-DCA degradation. The 1,2-DCA concentrations in the first runs of these experiments were chosen close to the concentrations which caused about 10% inhibition of ammonium utilization in batch experiments directed to kinetic modelling (Section 6.8). The 1,2-DCA concentrations in later runs were increased gradually. Each set of experiment was ended at the 1,2-DCA concentration causing significant (about 30-50%) inhibition of ammonium utilization.

The operating conditions in these two sets of experiments are given in Table 5.8. In the first set of experiments, 1,2-DCA concentrations varied between 1539-8087 μg/L for an average influent NH_4-N concentration of 152 mg/L. In the second set of experiments, 1,2-DCA concentrations varied between 1352-68087 μg/L for an average influent NH_4-N concentration of 50 mg/L. Daily measurements are given in Figures S.1-S.21 in Appendix S.

Table 5.8. Operating conditions in the continuous-flow experiments with 1,2-DCA

Exp. No	Influent Flowrate (L/d)	Influent NH_4-N mg/L	Influent 1,2-DCA μg/L
1st SET			
1	6	156	-
2	6	153	1539
3	6	152	-
4	6	153	4728
5	6	151	-
6	6	152	8087
7	6	149	-
2nd SET			
8	6	52	-
9	6	53	1352
10	6	51	-
11	6	54	3844
12	6	50	-
13	6	51	5891
14	6	48	-
15	6	50	9791
16	6	46	-
17	6	51	14337
18	6	51	29116
19	6	49	-
20	6	53	68087
21	6	42	-

In all experiments, the feed solution prepared with stock synthetic feed and mineral solutions (Table 5.9) and the stock 1,2–DCA solution (Section 5.8.3) were continuously fed into the system through a peristaltic pump with a flowrate of 6 L/day which corresponded to an average hydraulic retention time of 17 h at the working volume of 4.25 L. The duration of each run was in the range of 5-19 days. The wastewater temperature in the filter was kept in the range of 24-28^{0}C. The aquarium heater placed into the water

jacket around the reactor was adjusted as required. The DO in the bulk liquid was maintained in the range of 2-4 mg/L with pure oxygen supply at a rate of 40-45 mL/min. Inside the reactor pH was kept in the range of 7-8.

At the beginning of experimental set, the system was initially fed with the NH_4-N concentration to be studied at that set for a certain period of time. These runs are indicated as Exp. No:1 and Exp No:8 in Table 5.8. The aim was to investigate the nitrification efficiency of the system at that load before 1,2-DCA injection. During this period, influent samples and composite effluent samples were taken daily and analyzed for NH_4-N, NO_2-N and NO_3-N. Ammonium removal, nitrite accumulation and nitrate production rates were calculated using Eqns. 5.5-5.10 after the filter reached steady-state with respect to effluent NH_4-N concentration as shown in Appendix S. The time period necessary to reach steady-state conditions varied in the range of 4-5 days.

The later experiments of each set (Table 5.8) consisted of two phases. In the first phase experiments (Exp. No: 2, 4, 6 for the first set; Exp. No: 9, 11, 13, 15, 17, 18, 20 for the second set) the biofilm system was continuously fed with both ammonium and 1,2-DCA for a certain period of time. The aim was to investigate the cometabolic degradation of 1,2-DCA and the inhibitory effect of 1,2-DCA on nitrification. During this period, influent samples and composite effluent samples were daily taken and analyzed for NH_4-N, NO_2-N, NO_3-N, 1,2-DCA and Cl^-. In general, cometabolic degradation of chlorinated organics under aerobic conditions occurs through oxidative dechlorination. Oxidative dechlorination is thought to result from spontaneous elimination of chloride ion from an unstable chlorinated organic epoxide, which is generated in the monooxygenation of a chlorinated organic (Fetzner, 1998). Therefore, in these experiments, the measurements of chloride (Cl^-) releases were used as an indicator for the initiation of cometabolic degradation through dechlorination. Ammonium removal, 1,2-DCA removal, nitrite accumulation and nitrate production rates were calculated using Eqns. 5.5-5.10 after the filter reached steady-state with respect to effluent NH_4-N concentration as shown in Appendix S. The time period necessary to reach steady-state conditions varied in the range of 2-11 days. Volumetric and surface chloride production rates were calculated by using Eqns. 5.12 and 5.13 given below.

$$Volumetric\ \ Chloride\ \ \Pr oduction\ \ Rate = \frac{Q(Cl_{eff} - Cl_{\inf})}{V} \qquad (5.12)$$

$$Surface\ \ Chloride\ \ \Pr oduction\ \ Rate = \frac{Q(Cl_{eff} - Cl_{\inf})}{A} \qquad (5.13)$$

where Cl_{inf} is the chloride concentration in the feed solution, μg/L and Cl_{eff} is the chloride concentration in the effluent, μg/L.

In the second phase experiments (Exp. No: 3, 5, 7 for the first set; Exp. No: 10, 12, 14, 16, 19, 21 for the second set), 1,2-DCA feeding was stopped and the biofilm system was only fed with ammonium for a certain period of time. The aim was to investigate the recovery of cells from 1,2-DCA inhibition occurring in the first phase of experiments. During this period, influent samples and composite effluent samples were daily taken and analyzed for NH_4-N, NO_2-N and NO_3-N. Ammonium removal, nitrite accumulation and nitrate production rates were calculated using Eqns. 5.5-5.10 after the filter reached steady-state with respect to effluent NH_4-N concentration as shown in Appendix R. The time period necessary to reach steady-state conditions varied in the range of 2-17 days.

5.6. Characterization of the Microbial Community in the Nitrifying Biofilm Reactor by Molecular Biology Techniques

Throughout continuous-flow experiments, microbial ecology, community shifts and quantity changes of the microbial community in the nitrifying biofilm reactor were investigated with Fluorescence In-Situ Hybridization (FISH), Slot-Blot Hybridization, Polymerase Chain Reaction (PCR), and Denaturing Gradient Gel Electrophoresis (DGGE) techniques discussed briefly in the below sections. The detailed description of these techniques are given in the Ph.D. thesis of Mertoğlu (2005a).

All samplings and analyses for molecular characterization were done by Mertoğlu (2005b). Also, the interpretation of results was done by Mertoglu (2005b).

5.6.1. Sample Collection and Preparation

Biofilm samples were taken at regular time intervals during preliminary continuous–flow experiments with ammonium only (Section 5.5.1) and at the end of each continuous-flow experiment with 1,2-DCA (Table 5.8). Biofilm samples were scraped from the carrier materials located between Port 1 and Port 2 of the reactor (see Figure 5.5). Samples were then concentrated by centrifuging for 0.5 h at 7,000 rpm. Concentrated sludge samples were extracted and fixed for DNA extractions and FISH experiments immediately after centrifugation. The fixed cells were stored at - 20 °C (Mertoğlu, 2005a).

5.6.2. FISH (Fluorescence In-Situ Hybridization)

Fluorescence In Situ Hybridization (FISH) is a molecular technique used for the detection of target Bacterial groups or species of interest. In this study, FISH analyses were performed to detect, identify and characterize the Bacteria domain and ammonia-and nitrite-oxidizing species in the nitrifying biofilm reactor. Oligonucleotide probes used in these analyses are as follows: EUB338 for Bacteria domain, NSO1225 and NSO190 for *Ammonia oxidizing β-proteobacteria*, NSM156 for *Nitrosomonas species*, NIT3 for *Nitrobacter species*, NTSPA662 for *Nitrospira genus.* The sequences of these oligonucleotide probes are given in Mertoğlu (2005a). For detection of all microorganisms, biofilm samples were stained with 4,6-diamidino-2-phenylindole (DAPI) (Mertoğlu, 2005a).

The slides were examined with Leica DM-LB fluorescent microscope and digital images of the slides were captured with Leica DC350F digital camera as outlined by Mertoğlu (2005a).

5.6.3. DNA Extraction

The procedure followed for the cell lysis and DNA purification was mainly based on the FastDNA® kit protocol. However, this protocol was applied as modified by Mertoğlu (2005a).

5.6.4. Slot- Blot Hybridization

Slot blot hybridization was performed with DNA isolates to investigate the diversity and activity of all microbial populations and also to quantify the relative abundance of *Nitrosomonas*, *Nitrobacter* and *Nitrospira* populations during the operational period of the biofilm reactor. The analyses were performed with the oligonucleotide probes given in Section 5.6.2. Hybridization and detection of oligonucleotide probes were achieved by DIG (digoxigenin) System (Boehringer Mannheim GmbH, Biochemica) according to the manufacturer's protocol (Mertoğlu, 2005a).

5.6.5. PCR (Polymerase Chain Reaction)

The variable regions of the ribosomal DNA and amoA genes of the DNA isolates were amplified for DGGE analyses. The PCR primers used for the partial amplification of 16S rRNA gene sequences of *Bacteria* are *27* for (5'- AGA GTT TGA TCC TGG CTC AG-3') and 1510 rev (5'- GGT TAC CTT GTT ACG ACT T-3'). The PCR primers used for the partial amplification of amoA gene sequence are amoA – 1F (5'- GGG GTT TCT ACT GGT GGT-3') and amoA – 2R (5'- CCC CTC KGS AAA GCC TTC TTC-3') (Mertoğlu, 2005a).

5.6.6. DGGE (Denaturing Gradient Gel Electrophoresis)

DGGE is a gel-electrophoretic separation procedure for double stranded DNA's of equal size but with different base-pair composition or sequence. In principle, the method is sensitive enough to separate DNA's on the basis of single point mutations (Mertoğlu, 2005a). In this study, DGGE analyses were used to assess whether any changes occurred in the diversity of Bacteria domain and ammonia oxidizing community during the operation of the nitrifying biofilm reactor.

Prior to DGGE, the bacterial 16S rRNA and amoA genes were amplified with PCR (Section 5.6.5) using the appropriate primer pairs. One primer in each primer pair had a G+C "clamp" attached to the 5' end that prevented the two DNA strands from completely dissociating even under strong denaturing conditions. During electrophoresis through a

polyacrylamide gel containing denaturants, migration of the molecule was essentially arrested once a domain in a PCR product reached its melting temperature. Following staining of the DNA, a banding pattern emerged that represented the diversity of the rRNA and amoA gene sequences present in the sample (Mertoğlu, 2005a).

In this study, DGGE of PCR amplified bacterial 16S rRNA and amoA genes were performed with the Biorad D-Code Universal Mutation Detection System in accordance with the procedure described by Mertoğlu (2005a).

5.7. Analytical Methods

The analytical methods throughout all experiments are as follows:

(a) NH_4-N Analysis: NH_4-N concentrations were analyzed by Method 4500-NH_3 C (Nesslerization Method) in Standard Methods (APHA, AWWA, WEF, 1998) with Hach DR/2000 spectrophotometer using the Nessler reagent, mineral stabilizer and polyvinyl alcohol dispersing agent.

(b) NO_2-N Analysis: NO_2-N concentrations ranging between 0 to 150 mg/L NO_2 were analyzed by Ferrous Sulfate Method (Method 8153) with Hach DR/2000 spectrophotometer by using NitriVer 2 powder pillows. NO_2-N concentrations ranging between 0 to 0.3 mg/L NO_2-N were analyzed by Diazotization Method (Method 8507) with Hach DR/2000 spectrophotometer using NitriVer3 powder pillows.

(c) NO_3-N Analysis: NO_3-N concentrations were analyzed by Cadmium Reduction Method (Method 8039) with Hach DR/2000 spectrophotometer by using NitraVer 5 powder pillows. Nitrite interferences were compensated by the addition of bromine water and phenol solution as indicated in the method.

(d) SS and VSS Analyses: SS and VSS analyses were performed using Method 2540D (Total Suspended Solids Dried at 103-105^{0}C) and Method 2540E (Fixed and Volatile Solids Ignited at 550^{0}C) in Standard Methods (APHA, AWWA, WEF, 1998), respectively.

(e) TCE Analysis: Liquid samples for TCE analysis were extracted into n-pentane by EPA Method 502.1. The extracts were analyzed by Hewlett Packard 5890 Gas Chromatograph (GC) equipped with a J&W prosteel megabore column (0.53 mm ID, 30 m length) and an electron capture detector (ECD). The chromatograph was operated isothermally at 100^0C oven, 250^0C injection port and 250^0C detector temperatures for 5 minutes with a nitrogen carrier gas flow of 10 mL/min. Nitrogen gas (extra pure, >99.99%) were obtained from BOS Inc., Turkey. The GC calibration standards were prepared with TCE solution (200 μg/mL) supplied from Crescent Chemical Company, Inc., Newyork.

(f) 1,2-DCA Analysis: Liquid samples for 1,2-DCA analysis were extracted into n-pentane by EPA Method 502.1. The extracts were analyzed by Hewlett Packard 5890 Gas Chromatograph (GC) equipped with a J&W prosteel megabore column (0.53 mm ID, 30 m length) and an electron capture detector (ECD). The chromatograph was operated for 4.5 minutes at an oven temperature increasing from 40^0C to 80^0C (Ramp time: 10^0C/min). Nitrogen gas with a flow of 16 mL/min was used as carrier gas. Injection port and detector temperatures were kept at 250^0C. Nitrogen gas (extra pure, >99.99%) were obtained from BOS Inc., Turkey. The GC calibration standards were prepared with 1,2-DCA solution (200 μg/mL) supplied from Crescent Chemical Company, Inc., New York.

(g) Chloride (Cl^-) Analysis: The chloride ion concentrations generated from the degradation of TCE and 1,2-DCA were measured spectrophotometrically with the procedure developed by Florence and Farrar (1971). According to this procedure, 15.1 g of $Fe(NO_3)_3.9H_2O$ was dissolved in 45 mL of 72% perchloric acid ($HClO_4$) and diluted to 100 mL with distilled deionized water. Saturated solution of $HgSCN_2$ in ethanol was prepared by dissolving 0.1 g $HgSCN_2$ in 100 mL ethanol. In each measurement, 20 mL of sample was placed into a 25 mL volumetric flask. 2 mL of $Fe(NO_3)_3.9H_2O$ reagent and 2 mL of $HgSCN_2$ reagent were added onto the sample and diluted to 25 mL with distilled deionized water. After 5 min reaction period, the absorbance was measured at 460 nm with Hach DR/2000 spectrophotometer. The chloride content was then determined by comparing the measured absorbance with the calibration curve prepared for the known concentrations of Cl^- by using NaCl.

(h) DO measurements: DO concentrations measured by WTW OxiLevel- 2 DO meter.

(i) pH measurements: pH values were measured by WTW Inolab-1 pH meter.

5.8. Compositions of Feed Solutions

5.8.1. Stock Synthetic Feed and Mineral Solutions

Compositions of the stock synthetic feed and mineral solutions used in both batch and continuous flow experiments are given in Table 5.9. The same stock solutions in batch experiments were also used in the enrichment period of nitrifiers. In both batch and continuous-flow experiments, the stock synthetic feed solution was diluted to maintain the desired ammonium nitrogen (NH_4-N) concentrations. In batch experiments, the stock mineral solution was diluted 40-folds. In continuous-flow experiments, the stock mineral solution was diluted 200-folds. All chemicals used in the preparation of stock synthetic feed and mineral solutions were supplied from Merck KGaA., Germany.

Table 5.9. Compositions of stock synthetic feed and mineral solutions

	BATCH EXPERIMENTS	CONTINUOUS-FLOW EXPERIMENTS
COMPOUNDS	Concentration (g/L)	Concentration (g/L)
Stock Synthetic Feed Solution		
$(NH_4)_2SO_4$	37.75	37.75
$NaHCO_3$	95	95
Na_2CO_3	-	28
Stock Mineral Solution		
$MgSO_4.7H_2O$	2.0	2.0
$CaCO_3$	0.1	0.1
$FeSO_4.7H_2O$	0.4	0.2
$MnSO_4.H_2O$	0.2	0.1
K_2HPO_4	0.3	0.3

5.8.2. Stock Trichloroethylene (TCE) Solution

A stock 500 mg/L TCE solution was prepared by the dissolution of 85 µL TCE (>99% pure, Merck KGaA.) in 250 mL deionized water. In the experiments, this stock solution was diluted to maintain the initial TCE concentration from 40 to 50000 µg/L.

5.8.3. Stock 1,2-Dichloroethane (1,2-DCA) Solution

The stock 1,2-DCA solution used in the batch experiments (1000 mg/L 1,2-DCA) was prepared by the dissolution of 203 µL 1,2-DCA (>99% pure, Merck KGaA.) in 250 mL deionized water. In batch experiments, this stock solution was diluted to maintain the initial 1,2-DCA concentration from 70 to 380000 µg/L. The stock 1,2-DCA solution used in the continuous-flow experiments (7380 mg/L) was prepared by dissolution of 1.5 mL 1,2-DCA (>99% pure, Merck KGaA.) in 250 mL deionized water. In continuous-flow experiments, this stock solution was diluted to the initial 1,2-DCA concentration from 1500 to 75000 µg/L.

6. RESULTS AND DISCUSSIONS

6.1. Enrichment of the Mixed Culture for Nitrifiers

The enrichment for nitrifiers was monitored through the increase in specific ammonium utilization rate (q_{NH4-N}). As seen from Figure 6.1, q_{NH4-N} showed an increase with enrichment time and reached a steady value of about 20-25 mg NH_4-N/gVSS.h at the end of 129 days. All subsequent experiments were then started using this enriched nitrifier culture.

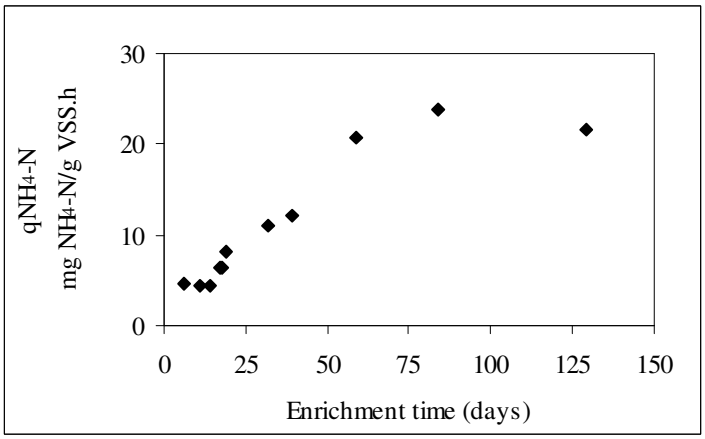

Figure 6.1. Specific ammonium utilization rates (q_{NH4-N}) during the enrichment period of nitrifiers

6.1.1. Evaluation of the Maximum Specific Ammonium Utilization Rate ($q_{max,NH4-N}$) and Half-Saturation Constant (K_s)

In order to find the maximum specific ammonium utilization rates ($q_{max,NH4-N}$) and half-saturation constants (K_s) of the enriched nitrifier culture (in the absence of TCE and 1,2-DCA) under diffused aeration conditions, the specific ammonium utilization rates (q_{NH4-N}) determined in batch kinetic experiments were evaluated with respect to the bulk NH_4-N concentrations as illustrated in Figure 6.2a.

In Figure 6.2a, the smooth transition of q_{NH4-N} from a first-order relation at low bulk NH_4-N concentrations to a zero-order relation at high bulk NH_4-N concentration can

mathematically be represented by the Monod model given in Eqn. 6.1.

$$q_{NH4-N} = q_{\max,NH4-N} \frac{S}{K_s + S} \quad (6.1)$$

where q_{NH4-N} is the specific ammonium utilization rate (mg/g.h), $q_{max,NH4-N}$ is the maximum specific ammonium utilization rate (mg/g.h), K_s is the half-saturation constant (mg/L) and S is the bulk substrate concentration (mg/L).

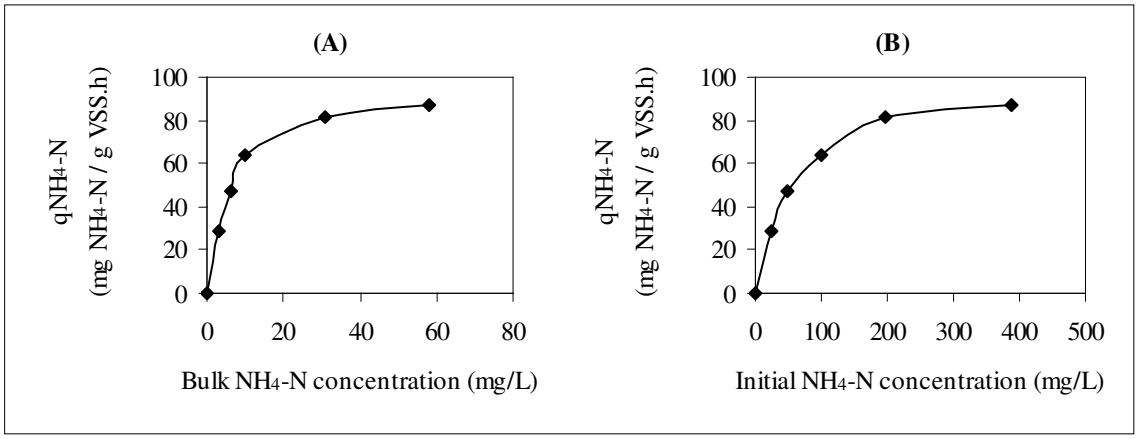

Figure 6.2. Specific ammonium utilization rates (q_{NH4-N}) of the enriched nitrifier culture with respect to (a) bulk NH_4-N concentrations (b) initial NH_4-N concentrations

For the estimation of the correct $q_{max,NH4-N}$ and K_s, the present bulk NH_4-N concentration should be taken. Otherwise, the use of the NH_4-N concentration at the start of each run, as in the case of later experiments (Sections 6.5 and 6.8), leads to an overestimation of these values. In order to see the differences between the exact and overestimated "apparent" $q_{max,NH4-N}$ and K_s values, q_{NH4-N} values were also evaluated with respect to the initial NH_4-N concentrations as illustrated in Figure 6.2b.

A common method presented in literature for estimation of the $q_{max,NH4-N}$ and K_s values is to transform the non-linear Monod equation into linearized forms by Lineweaver-Burk, Hanes-Woolf and Eadie-Hofstee plots (Table 6.1) and then to estimate the parameters using linear regression techniques. Although this approach is simple, the assumption of normally distributed errors inherent in linear regression may not be valid because the linearization alters the error distributions (Knightes and Peters, 2000).

Table 6.1. Linearized plots of Monod equation (Cornish-Bowden, 1995)

Name of Plotting	Linearized forms of Monod Equation	Plot	Slope of Plotting	Intercept of Plotting on X-axis	Intercept of Plotting on Y-axis
Lineweaver-Burk Plot	$\frac{1}{q_{NH_4-N}}\ versus\ \frac{1}{NH_4-N}$	$\frac{1}{q_{NH_4-N}}\ versus\ \frac{1}{NH_4-N}$	$\frac{K_s}{q_{\max,NH_4-N}}$	$-\frac{1}{K_s}$	$\frac{1}{q_{\max,NH_4-N}}$
Hanes-Woolf Plot	$\frac{NH_4-N}{q_{NH_4-N}}=\frac{K_s}{q_{\max,NH_4-N}}+\frac{NH_4-N}{q_{\max,NH_4-N}}$	$\frac{NH_4-N}{q_{NH_4-N}}\ versus\ NH_4-N$	$\frac{1}{q_{\max,NH_4-N}}$	$-K_s$	$\frac{K_s}{q_{\max,NH_4-N}}$
Eadie-Hofstee Plot	$q_{NH_4-N}=q_{\max,NH_4-N}-\frac{K_s}{NH_4-N}q_{NH_4-N}$	$q_{NH_4-N}\ versus\ \frac{q_{NH_4-N}}{NH_4-N}$	$-K_s$	$\frac{q_{\max,NH_4-N}}{K_s}$	$q_{\max,NH_4-N}$

Lineweaver–Burk plot, which is by far the most widely used plot in enzyme kinetics, gives a grossly misleading impression of the experimental error: for small values of specific substrate utilization rates (q) small errors in q lead to enormous errors in 1/q; but for large values of q the same small errors in q lead to barely noticeable errors in 1/q (Cornish-Bowden, 1995). Therefore, the error about the reciprocal of a data point is not symmetric and data points at low substrate concentration influence the slope and intercept more than those at high substrate concentrations (Shuler and Kargi, 2001).

In Hanes-Woolf plot, over a fair range of substrate concentration (S) the errors in s/q provide a faithful reflection of those in q. It is for this reason that Hanes-Woolf plot should be preferred over other straight-line plots for most purposes (Cornish-Bowden, 1995).

Eadie-Hofstee plot gives fairly good results in practice, though the fact that q appears in both coordinates means that errors in q affect both of them and cause deviations towards or away from the origin rather than parallel with the ordinate axis (Cornish-Bowden, 1995).

Another method is the nonlinear least square regression (NLSR) which has become more feasible with the recent advances in computing capabilities. Nowadays, several user-friendly computer programs for nonlinear fitting of equations to data are available, and therefore the difficulties in application of NLSR that existed in the past have been overcome (Smith et al., 1997). NLSR has been shown to be a better method for estimating the kinetic parameters than convenient linearized plots (Kim et al., 2002) because the data points are more likely to be normally distributed about a curve representing the model (Smith et al., 1997). However, distinguishing between inhibition models can be problematic when using NLSR (Kim et al., 2002) and hence the linearization methods are still a useful and common tool in the determination of the type of enzyme inhibition. Moreover, the problems with linearization are compounded when the rate data are obtained for only a small range of substrate concentrations or only at low substrate concentrations (similar to or less than K_s) (Smith et al., 1997).

The data shown in Figures 6.2a and 6.2b were analyzed by linearization (Table 6.1) and NLSR (using Ez-Fit5 package program by Perella Scientific Inc.) as illustrated in Figures 6.3 and 6.4, respectively. $q_{max,NH4\text{-}N}$ and K_s values determined from these analyses are summarized in Table 6.2.

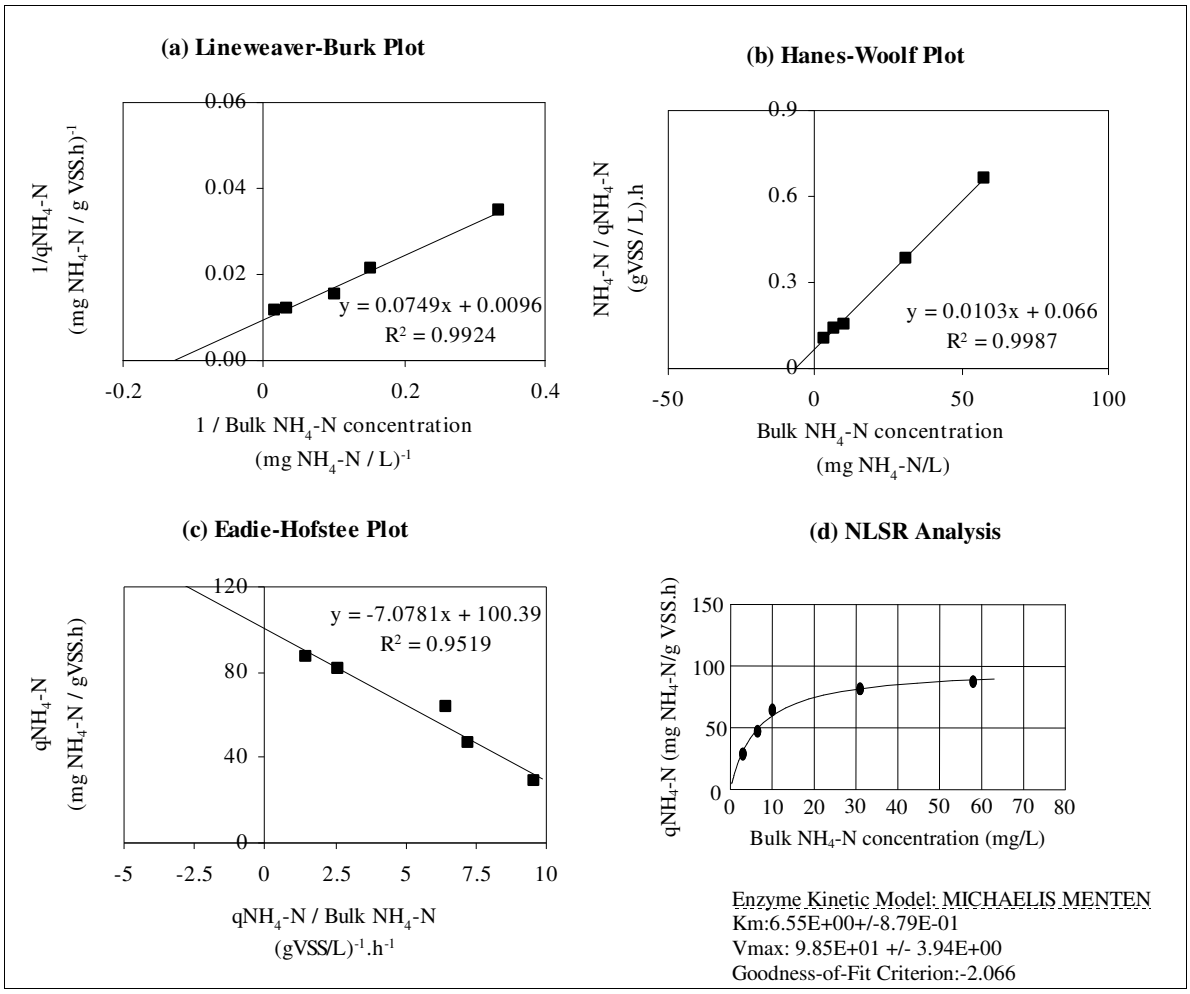

Figure 6.3. Determination of $q_{max,NH4\text{-}N}$ and K_s with respect to bulk NH_4-N concentrations using (a) Lineweaver-Burk plot, (b) Hanes-Woolf plot, (c) Eadie-Hofstee plot, and (d) NLSR analysis

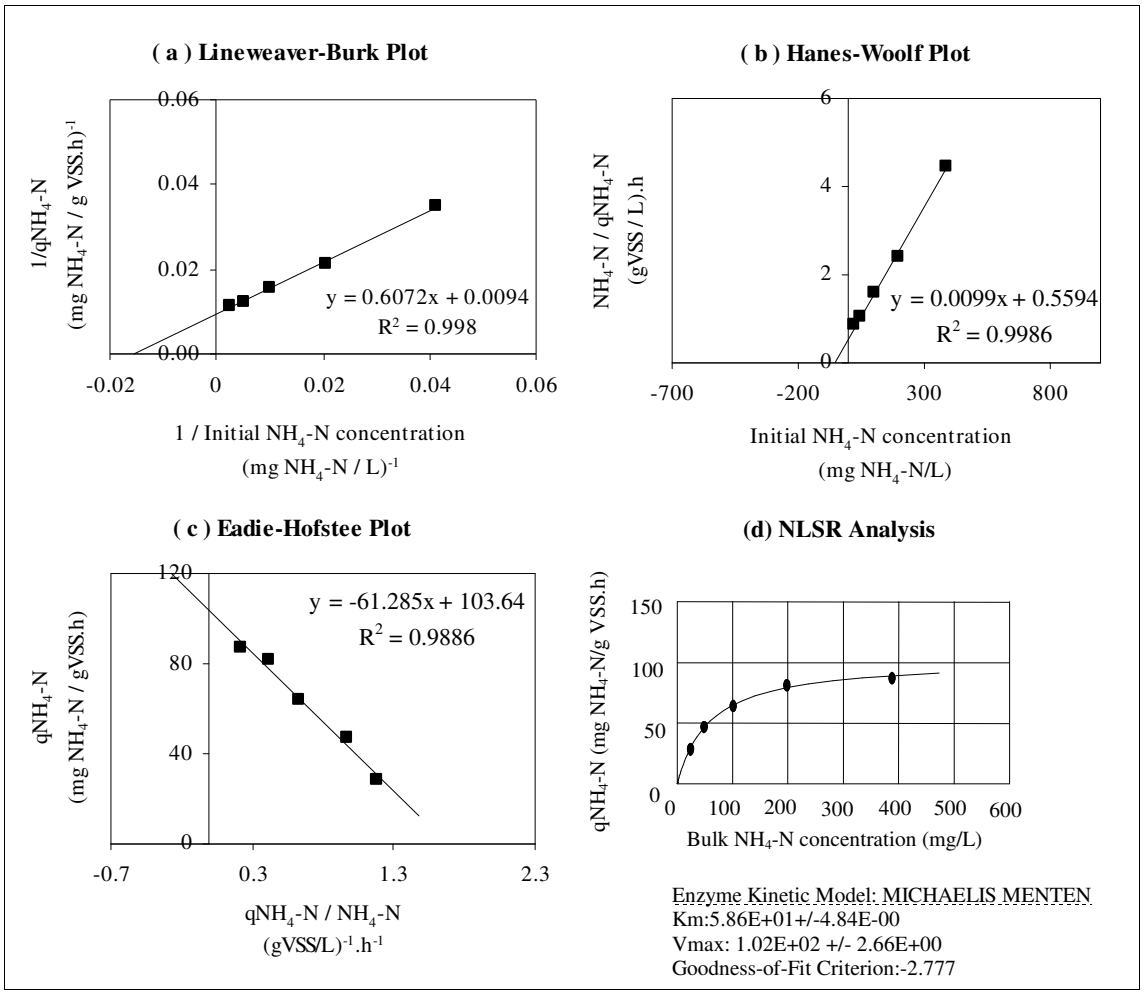

Figure 6.4. Determination of $q_{max,NH4-N}$ and K_s with respect to initial NH_4-N concentrations using (a) Lineweaver-Burk plot, (b) Hanes-Woolf plot, (c) Eadie-Hofstee plot, and (d) NLSR analysis

Table 6.2. $q_{max,NH4-N}$ and K_s values of the enriched nitrifier culture

Method	Values estimated with respect to bulk NH_4-N concentration		Values estimated with respect to initial NH_4-N concentration	
	$q_{max, NH4-N}$ mgNH_4-N/gVSS.h	K_s mg NH_4-N/L	$q_{max, NH4-N}$ mg NH_4-N/gVSS.h	K_s mg NH_4-N/L
Lineweaver-Burk	104.16	7.80	106.38	64.59
Hanes-Woolf	97.08	6.40	101.00	56.50
Eadie-Hofstee	100.39	7.07	103.64	61.28
NLSR analysis	98.47±3.94	6.55±0.87	102.28±2.66	58.57±4.84

As seen from Table 6.2, evaluation of the data with respect to the bulk NH_4-N concentrations resulted in $q_{max,NH4-N}$ and K_s values in the ranges of 97-104 mg NH_4-N/gVSS.h and 6.4-7.80 mg NH_4-N/L, respectively. In case of data evaluation with respect to the initial NH_4-N concentration, $q_{max, NH4-N}$ value was estimated in the range of 101-106 mg NH_4-N/gVSS.h which is very close to the value determined when the bulk NH_4-N concentration was used. However, the K_s value determined in the range of 57-65 mg NH_4-N/L was significantly higher than the value estimated when the bulk NH_4-N concentration was used. Therefore, these results clearly showed that K_s values estimated when the initial NH_4-N concentrations do not reflect the actual values and hence must be evaluated as "apparent" values.

6.1.1.1. Statistical Analysis of Kinetic Models. The kinetic models were developed by placing the $q_{max,NH4-N}$ and K_s values determined with linearization plots and NLSR analysis (Table 6.2) to the Eqn. 6.1. These models were analyzed statistically to evaluate the differences between model results and experimental data. For this purpose, initially, the residuals between experimental data and model results were examined. A few examples of these analyses are illustrated in Appendix T. Residuals appeared to be random and hence provided evidence that all models developed had no serious deficiencies. As a next step, analysis of variance (ANOVA) was performed at 95% confidence level (α= 0.05) using the MINITAB package program (Minitab Inc. U.S.). P-values resulting from these analyses (see Appendix T) were greater than α= 0.05 indicating that there are no significant differences among the models developed by linearization and NLSR

6.2. Evaluation of Various Oxygenation Methods

Prior to batch experiments, diffused aeration, hydrogen peroxide (H_2O_2) addition, oxygen releasing compound (ORC) addition and gas permeable membranes were evaluated to find the appropriate oxygenation method to satisfy the high oxygen requirement of nitrifiers without causing stripping of chlorinated organics (TCE or 1,2-DCA) in batch experiments.

The results of TCE measurements during fine-bubble diffused aeration and micro-bubble diffused aeration are shown in Figure 6.5 and 6.6, respectively. An air flow through

a fine bubble diffuser resulted in a sharp decrease of the initial TCE concentration of 1000 µg/L at both 0.75 L/min and 0.65 L/min air flowrates. The stripping rate of TCE at an air flow of 0.65 L/min was slower with respect to that observed at 0.75 L/min. 97% of the initially introduced TCE was stripped out from the system in 10 min and 15 min at air flowrates of 0.75 L/min and 0.65 L/min, respectively. Thus, fine bubble diffused aeration system was not an appropriate oxygenation method for batch experiments. In contrast to fine-bubble diffused aeration, micro bubble diffused aeration resulted in a more gradual stripping of TCE. The stripping rate of TCE at an air flow of 0.16 L/min was slower with respect to that observed at 0.75 L/min. 40-45% of the initially introduced TCE was stripped out from the system in 60 min and 120 min at pure oxygen gas flowrates of 0.65 L/min and 0.16 L/min, respectively. However, these observed stripping rates limited the use of this oxygenation system in batch experiments which were planned for a test period of 3- 4 h.

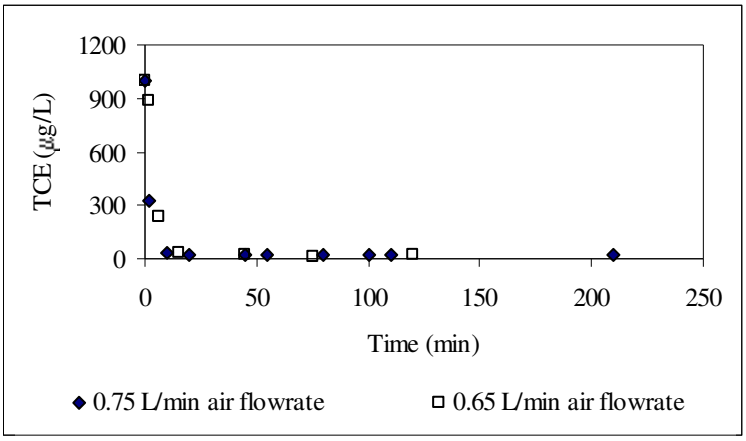

Figure 6.5. TCE stripping under fine- bubble diffused aeration

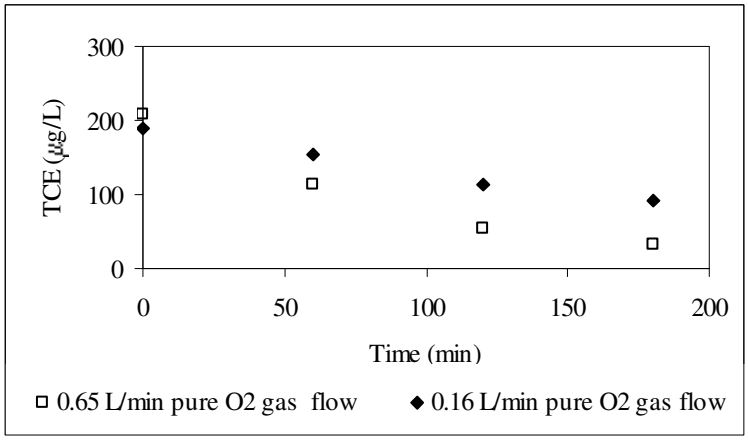

Figure 6.6. TCE stripping under micro-bubble diffused aeration with pure oxygen gas

Since dissociation of hydrogen peroxide (H_2O_2) results in formation of dissolved oxygen without the formation of air bubbles, H_2O_2 appears as an attractive oxygenation method when dealing with biodegradation of chlorinated organics under aerobic conditions. In literature, the use of H_2O_2 in the cometabolic degradation of chlorinated organics as an oxygen source (e.g., Guo et al., 2001) is mentioned. However, in our case, the sensitive characteristic of nitrifier species necessitated the investigation of the effect of H_2O_2 on nitrification efficiency. Figure 6.7 shows the specific ammonium utilization rates (q_{NH4-N}) observed in the case of diffused aeration condition and H_2O_2 addition. The q_{NH4-N} value observed in case of H_2O_2 addition was about one-half of the value observed in case of diffused air condition indicating about 50% inhibition of nitrification. Therefore, the option of H_2O_2 usage in batch experiments as an oxygen source was eliminated.

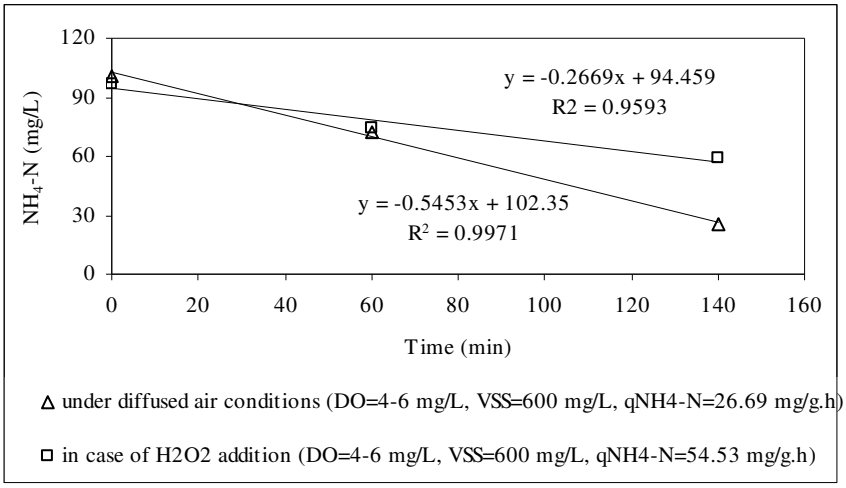

Figure 6.7. Inhibition of nitrification due to H_2O_2 addition as an oxygen source

Slow oxygen-releasing property of Oxygen Releasing Compound (ORC®) makes this compound unfavorable for high oxygen demanding nitrification process. Nevertheless, the oxygen release rate of this compound was investigated as shown in Figure 6.8. 0.5 g ORC® added into a 250 mL test bottle containing deionized water resulted in a very slow increase of DO concentration for the time period of 30 min. Thereafter, almost no change was observed in the DO concentration up to 90 min. These results clearly demonstrated that ORC® addition was not an appropriate oxygenation method for our experimental conditions. Moreover, the insoluble characteristic of ORC® resulted in the formation of chalk like slurry even at a small quantity of 0.5 g. This restricted the continuation of trials with greater amounts of ORC®.

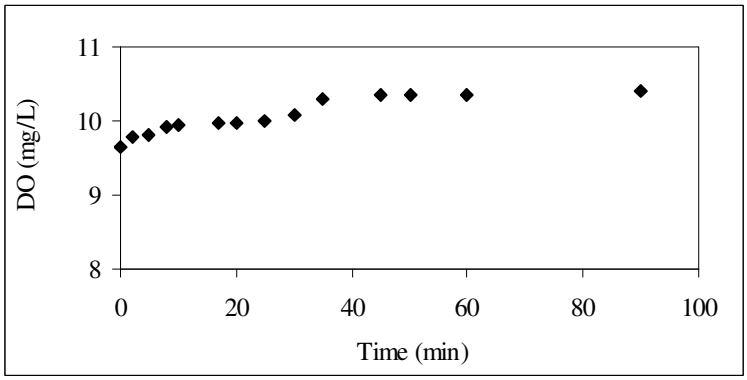

Figure 6.8. Oxygen release rate of ORC®

In literature, there are many studies evaluating bubble-free (bubbleless) oxygenation systems for different applications including bioreactors treating VOCs (Ahmed and Semmens, 1992; Brindle and Stephenson, 1996; Clapp et al., 1999, Gantzer, 1994; Dollerer and Wilderer, 1996). In our study, when the pure oxygen gas with an outlet pressure of < 0.1 bar was supplied through a 6 m long silicon gas permeable tubing, bubble formation could not be prevented. TCE measurements in a test period of 30 min (Figure 6.9) indicated that TCE stripped out from the system due to bubble formation. At the end of 30 min, about 93% of TCE was stripped from the system. In the case of gas permeable membrane module, the bubble formation was also observed. Therefore, this module was not evaluated further in terms of TCE stripping.

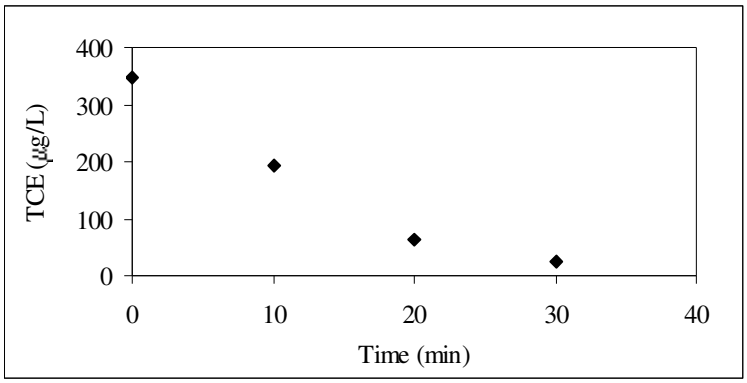

Figure 6.9. TCE stripping in case of pure oxygen supply through gas permeable silicon tubing

Since none of the oxygenation methods evaluated was found appropriate for our experimental studies, it was decided to perform all batch experiments under oxygen supersaturated conditions without air or pure oxygen supply throughout the experiments.

6.3. The Effect of TCE on the Specific Oxygen Uptake Rate (SOUR)

The immediate response of enriched nitrifier cultures to TCE concentration in an initial range of 50-50000 µg/L was assessed by SOUR as illustrated in Figure 6.10.

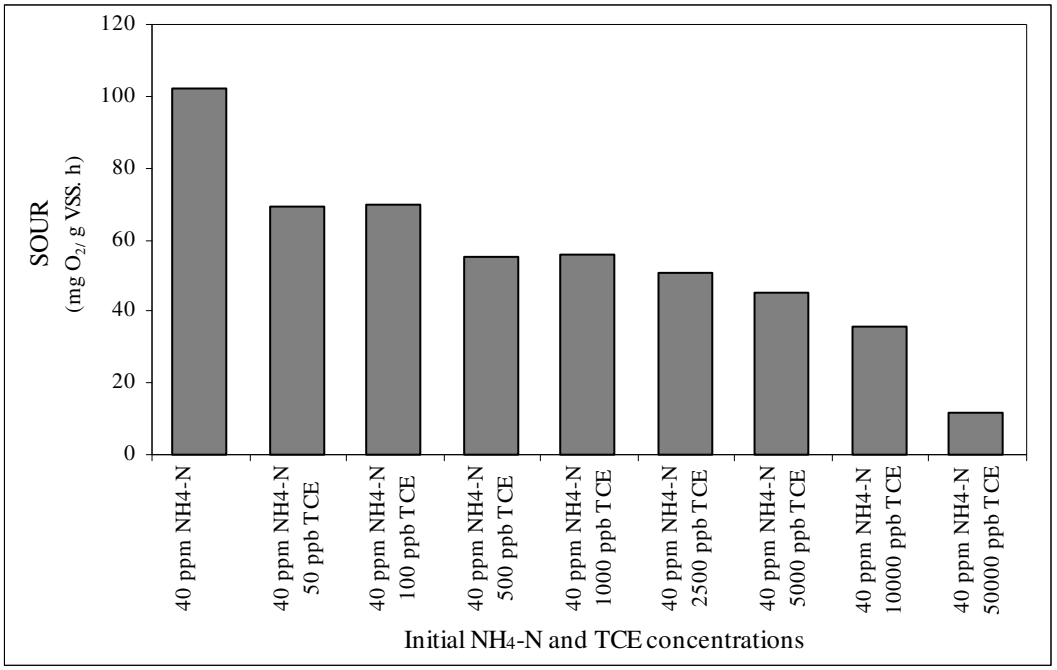

Figure 6.10. Decrease in the SOUR of an enriched nitrifier culture in the presence of TCE [Initial NH_4-N = 40 mg/L, Initial TCE = 0-50000 µg/L]

SOUR associated with ammonium oxidation decreased by about 30% at 50-100 µg/L TCE, 45% at 500 -1000 µg/L TCE, 50% at 2500 µg/L TCE, 56% at 5000 µg/L TCE, 65% at 10000 µg/L TCE and 88% at 50000 µg/L TCE. These results are consistent with the study of Hyman et al. (1995), which indicated that increasing TCE led to increased inhibition of O_2 uptake for pure *Nitrosomonas europaea* cells. The non-specific AMO enzyme, which serves as a catalyzer in the reduction and insertion of an oxygen atom from molecular oxygen into ammonia, is also able to catalyze the oxidation of TCE. In a previous study (Ely et al., 1995), TCE affinity for AMO was reported about four times greater than the NH_4-N affinity for AMO. Therefore, such decreases were observed in the SOUR due to the inhibition of the AMO enzyme by TCE.

6.4. Batch Experiments with TCE

6.4.1. Evaluation of Ammonium Removal in the Presence of TCE

Based on the results of preliminary OUR experiments, at a constant initial ammonium concentration of 40 mg/L NH_4-N, the specific ammonium utilization rates (q_{NH4-N}) and specific oxygen uptake rates (SOUR) were evaluated with respect to initial TCE concentrations in the range of 50-4500 µg/L as illustrated in Figure 6.11 and summarized in Table 6.3.

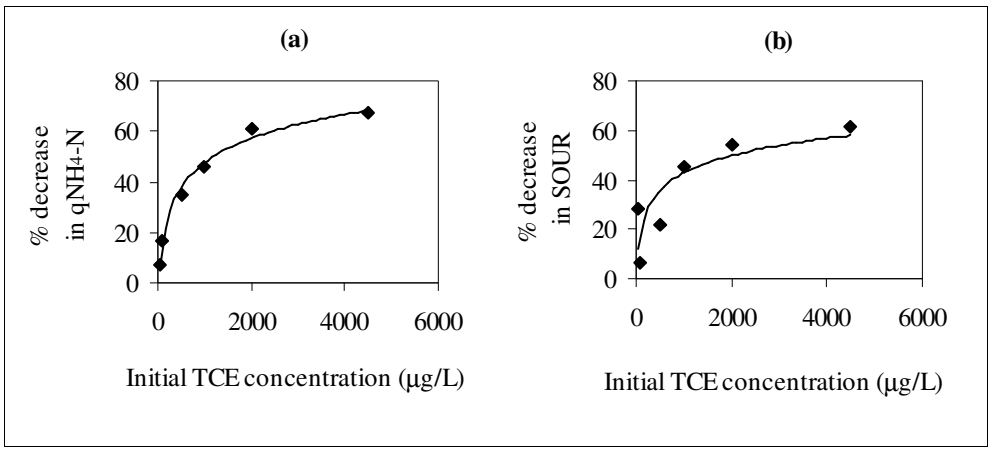

Figure 6.11. Effect of TCE on (a) specific ammonium utilization rate (q_{NH4-N}) and (b) specific oxygen uptake rate (SOUR)

In the presence of TCE (50-4500 µg/L), a relative decrease in q_{NH4-N} was observed with respect to the base q_{NH4-N}, which was 20-24 mg NH_4-N/gVSS.h in the absence of TCE. Figure 6.11a shows that the degree of inhibition increased with TCE concentration and reached 50% in the TCE concentration range of 1000-2000 µg/L.

As seen from Figure 6.11b, SOUR values showed a similar trend as in the case of q_{NH4-N} and a relative decrease was observed with respect to the base SOUR which was about 0.02-0.05 mg O_2/mg VSS.h. In terms of SOUR, a 50% decrease was observed in the TCE concentration range of 1000-2000 µg/L. This indicated that in these systems oxygen uptake and ammonium utilization were similarly affected by the presence of TCE. TCE may exert its effect in two basic ways. Either it may directly cause a toxic effect on the enzyme, or it may be degraded and its by-products may exert a toxicity. As discussed in

Section 6.4.3, TCE measurements clearly showed that TCE was cometabolically degraded. If the by-products formed during TCE degradation exerted a toxicity, a higher decrease would be expected in SOUR compared to those observed in 10-min preliminary SOUR experiments with negligible TCE degradation. However, the decreases observed in SOUR in 4 h tests were generally in accordance with those obtained from preliminary SOUR experiments having duration of only 10 min (Section 6.3). Therefore, it may be concluded that the toxic effect of TCE on ammonium oxidation was mainly attributable to the inhibition of AMO enzyme when the cells were exposed to TCE rather than the inhibition of the AMO enzyme by short-lived reactive intermediates produced during TCE oxidation. Even at a very high initial TCE concentration (4500 μg/L), ammonium oxidation was still possible and showed 68% decrease with respect to the control. This result is in contrast to a previous study (Yang, 1999) which indicated that in a system containing 4 mg/L NH_4-N and 4.8 mg/L enriched nitrifier culture, ammonium oxidation activity was completely halted when the initial TCE concentration was at 200 μg/L. The discrepancy between the results of the present study and those of Yang (1999) may be attributed to the differences in nitrifier concentrations. Moreover, the mixed culture used in this study and the culture in the study of Yang (1999) may contain different nitrifying strains.

6.4.2. Evaluation of TCE Volatilization in Batch Experiments

As seen from Figure 6.12, the volatilization rate of TCE from the liquid phase into the headspace of capped bottles increased linearly with TCE and the first-order rate constant was calculated as 0.0208 /h. The cometabolic degradation rates of TCE were calculated by considering these volatilized amounts.

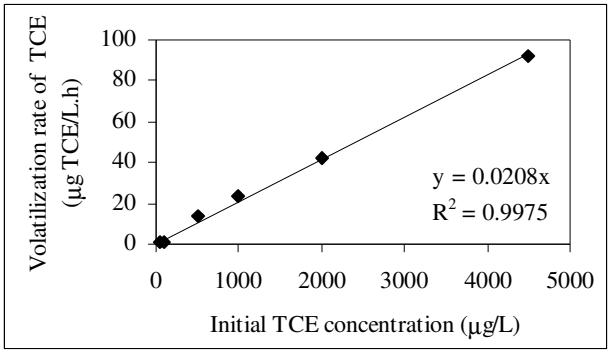

Figure 6.12. The volatilization rate of TCE with respect to the initial TCE concentration

6.4.3. Evaluation of Cometabolic Degradation of TCE

At a constant initial ammonium concentration of 40 mg/L NH_4-N, the specific cometabolic degradation rate of TCE (q_{TCE}) was evaluated with respect to the initial TCE concentration in the range of 50-4500 µg/L as illustrated in Figure 6.13 and summarized in Table 6.3.

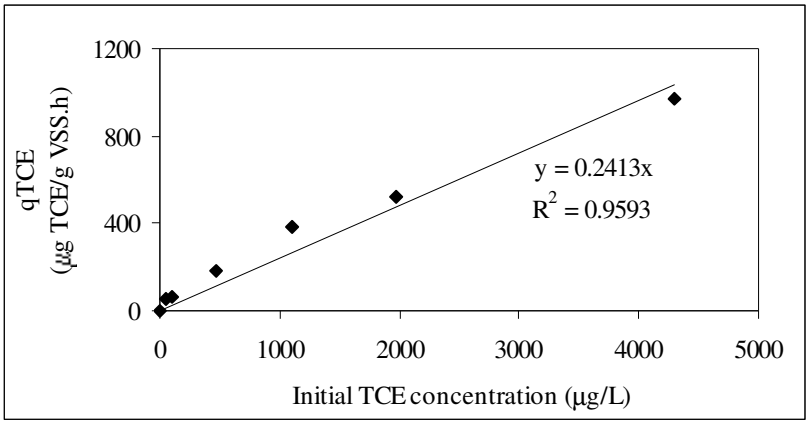

Figure 6.13. Effect of TCE concentration on the cometabolic degradation rate of TCE

As seen from Figure 6.13, the cometabolic degradation rate of TCE increased linearly with TCE concentration and a first-order rate constant of 0.24 L/gVSS.h (0.0057 L/mgVSS.d) was obtained. This value is considerably lower than the values (0.74 and 1.02 L/mgVSS.d) reported for pure *Nitrosomonas europaea* species (Alvarez-Cohen and Speitel, 2001). However, in the studies with pure *Nitrosomonas europaea* species, the biomass is reported in terms of protein. The reported values of 0.74 and 1.02 L/mgVSS.d are based on the assumption that the dry cell mass consists of 50% protein (Alvarez-Cohen and Speitel, 2001). Moreover, although the sludge used in the present study was enriched for nitrifiers, it certainly contained a high heterotrophic fraction since it originated from a sewage treatment plant. Therefore, in our system, the fraction of nitrifiers in the total VSS expression was much smaller than in pure culture studies and the cometabolic removal rates of TCE in our systems were quite low when the results were expressed on the basis of VSS.

The findings mentioned in Sections 6.3-6.4.3 were published in Journal of Hazardous Materials (Alpaslan-Kocamemi and Çeçen, 2005).

Table 6.3. Summary of the results of batch experiments with TCE

Experiment No	VSS	NH_4-N	TCE	Specific Ammonium Utilization Rate (q_{NH4-N})	% decrease in q_{NH4-N}	Specific Oxygen Uptake Rate (SOUR)	% decrease in SOUR	Volatilization Rate of TCE	Specific Cometabolic Degradation Rate of TCE (q_{TCE})
	mg/L	mg/L	µg/L	mg NH_4-N / gVSS.h	%	mg O_2 / mg VSS.h	%	µg TCE / L.h	µg TCE / gVSS.h
Exp. No:1									
1st Bottle	-	-	50	-	-	-	-	1.1	-
2nd Bottle	135	40	-	19.3	-	0.056	-	-	-
3rd Bottle	123	40	50	17.9	7.2	0.040	28.4	-	55.3
Exp. No:2									
1st Bottle	-	-	100	-	-	-	-	1.4	-
2nd Bottle	131	40	-	22.2	-	0.023	-	-	-
3rd Bottle	134	40	100	18.5	16.3	0.021	6.4	-	66.9
Exp. No:3									
1st Bottle	-	-	500	-	-	-	-	13.2	-
2nd Bottle	131	40	-	22.2	-	0.023	-	-	-
3rd Bottle	130	40	500	14.4	35.1	0.018	21.6	-	183.1
Exp. No:4									
1st Bottle	-	-	1000	-	-	-	-	23.0	-
2nd Bottle	131	40	-	22.2	-	0.023	-	-	-
3rd Bottle	137	40	1000	12.0	45.8	0.012	45.4	-	388.9
Exp. No:5									
1st Bottle	-	-	2000	-	-	-	-	42.1	-
2nd Bottle	135	40	-	24.3	-	0.030	-	-	-
3rd Bottle	133	40	2000	9.4	61.0	0.014	54.0	-	524.1
Exp. No:6									
1st Bottle	-	-	4500	-	-	-	-	92.4	-
2nd Bottle	135	40	-	24.3	-	0.030	-	-	-
3rd Bottle	144	40	4500	7.88	67.7	0.011	61.8	-	975.2

6.5. Batch Experiments with TCE Directed to Kinetic Modelling

6.5.1. Evaluation of Maximum Specific Ammonium Utilization Rate ($q_{max,NH4-N}$) and Half-Saturation Constant (K_s) in the Absence of TCE

The specific ammonium utilization rates (q_{NH4-N}) were first investigated at the initial NH_4-N concentrations of 25, 50, 100, 200 and 400 mg/L to determine the $q_{max,NH4-N}$ K_s in the absence of TCE under oxygen saturated conditions as illustrated in Figure 6.14. q_{NH4-N} values showed a smooth transition from a first- order relation at low initial NH_4-N concentrations to a zero-order relation at high initial NH_4-N concentrations, which can be mathematically represented by the Monod model (Eqn. 6.1). Therefore, the data were analyzed by linearization methods (Table 6.1) and nonlinear least square regression (NLSR) (using the Ez-Fit5 package program of Perella Scientific Inc.), which are explained in detail in Section 6.1.1 and illustrated in Figure 6.15. $q_{max,NH4-N}$ and K_s values estimated from the analysis of Figure 6.15 are summarized in Table 6.4.

As seen from the table, in the absence of TCE, the base constants, $q_{max,NH4-N}$ and K_s were found in the ranges of 86.2-87.8 mg NH_4-N/g VSS.h and 66.36-70.09 mg NH_4-N /L, respectively. This K_s value for ammonium is much higher than the common values reported in literature. This discrepancy can be explained as follows. As indicated in Eqn. 6.1, for the estimation of the correct K_s, the present bulk NH_4-N concentration should be taken. Otherwise, the use of the NH_4-N concentration at the start of each run leads to overestimation of this value. The experiments presented here were performed under oxygen saturated conditions. Since DO concentrations below 3-4 mg/L may become rate limiting for nitrification (see Section 3.3.1.5), experiments were ended in a maximum time of 2 hours when the bulk DO concentration reached about 4 mg/L. In such a short period, the differences between the initial and final NH_4-N concentrations were very small and hence in data analyses only the initial NH_4-N concentrations were considered as shown in Figure 6.14. Therefore, the reported K_s values (66.36-70.09 mg/L) must be considered as "apparent values". Similarly, K_s values estimated for the same culture under diffused air conditions (Table 6.2) using the initial NH_4-N concentrations ranged between 57-65 mg/L although the evaluation of the same data using the bulk NH_4-N concentration resulted in K_s values in the range of 6.4-7.8 mg/L.

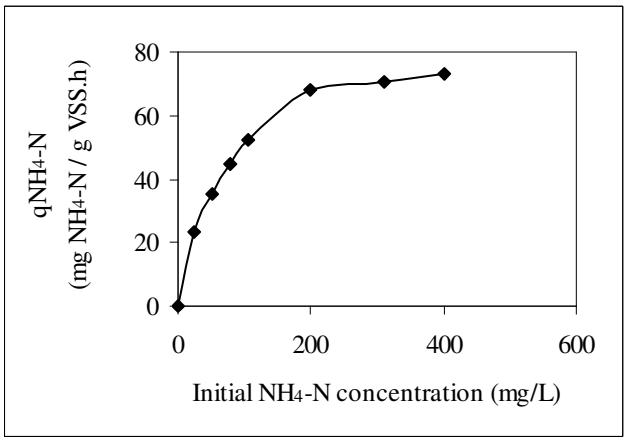

Figure 6.14. Specific ammonium utilization rates in dependence of initial ammonium concentrations

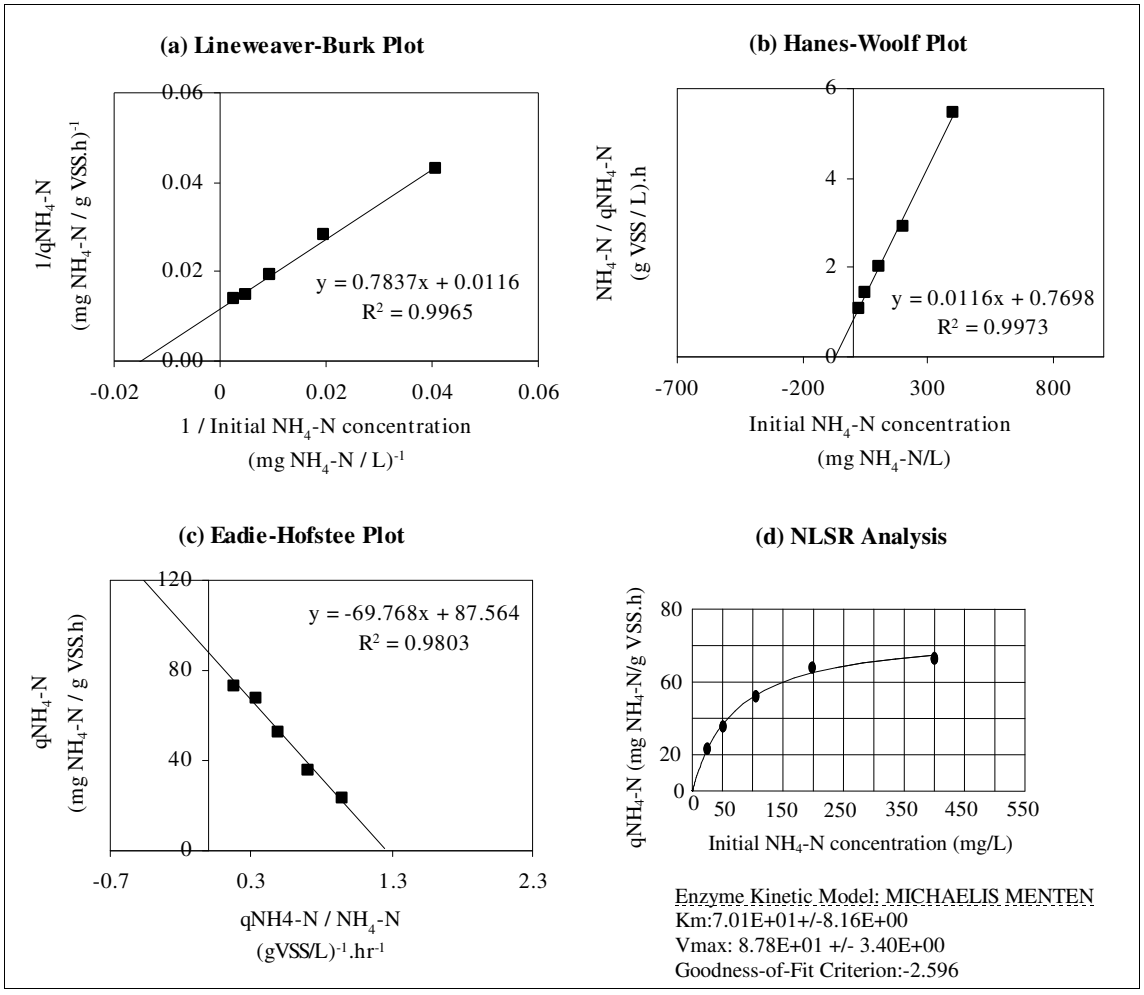

Figure 6.15. Determination of $q_{max,NH4-N}$ and K_s under oxygen saturated conditions using (a) Lineweaver-Burk plot, (b) Hanes-Woolf plot, (c) Eadie-Hofstee plot, and (d) NLSR analysis

6.5.2. The Effect of TCE on the Maximum Specific Ammonium Utilization Rate ($q_{max,NH4-N}$) and Half-Saturation Constant (K_s)

The effect of TCE on the maximum specific ammonium utilization rate ($q_{max,NH4-N}$) and half-saturation constant (K_s) were investigated in a TCE range of 40-845 µg/L and a NH_4-N range of 25-400 mg/L. The calculated specific ammonium utilization rates (q_{NH4-N}) are shown in Figure 6.16 which also shows the base q_{NH4-N} values.

At various TCE concentrations, q_{NH4-N} pattern still followed the Monod model (Eqn. 6.1). Increasing the TCE concentration resulted in a relative decrease in q_{NH4-N} with respect to the base q_{NH4-N}, indicating the inhibitory effect of TCE on nitrification. The analyses of the data in Figure 6.16 by linearization methods (Table 6.1) and nonlinear least square regression (NLSR) (Section 6.1.1) are illustrated in Figures 6.17-6.20. The apparent $q_{max,NH4-N}$ ($q^{app}_{max,NH4-N}$) and the apparent K_s (K^{app}_s) values determined from the analyses of Figures 6.17-6.19 are also summarized in Table 6.4. These estimated $q^{app}_{max,NH4-N}$ *and* K^{app}_s values at various TCE concentrations were further analyzed in Section 6.5.3 in order to evaluate the effect of TCE on ammonium utilization.

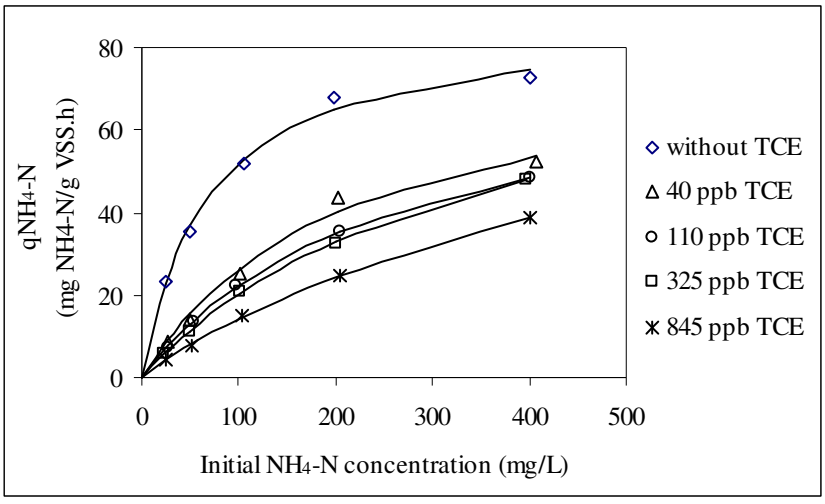

Figure 6.16. Specific ammonium utilization rates (q_{NH4-N}) in the presence of TCE

6.5.2.1. Statistical Analysis of Kinetic Models. The kinetic models were developed by placing the $q^{app}_{max,NH4-N}$ and K^{app}_s values determined with linearization plots and NLSR analysis (Table 6.4) to the Eqn. 6.1. These models were analyzed statistically to evaluate

the differences between model results and experimental data. For this purpose, initially, the residuals between experimental data and model results were examined. A few examples of these analyses are illustrated in Appendix T. Residuals appeared to be random and hence provided evidence that all models developed had no serious deficiencies. As a next step, analysis of variance (ANOVA) was performed at 95% confidence level (α= 0.05) using the MINITAB package program (Minitab Inc. U.S.). P-values resulting from these analyses (see Appendix T) were greater than α=0.05 indicating that there are no significant differences among the models developed by linearization and NLSR.

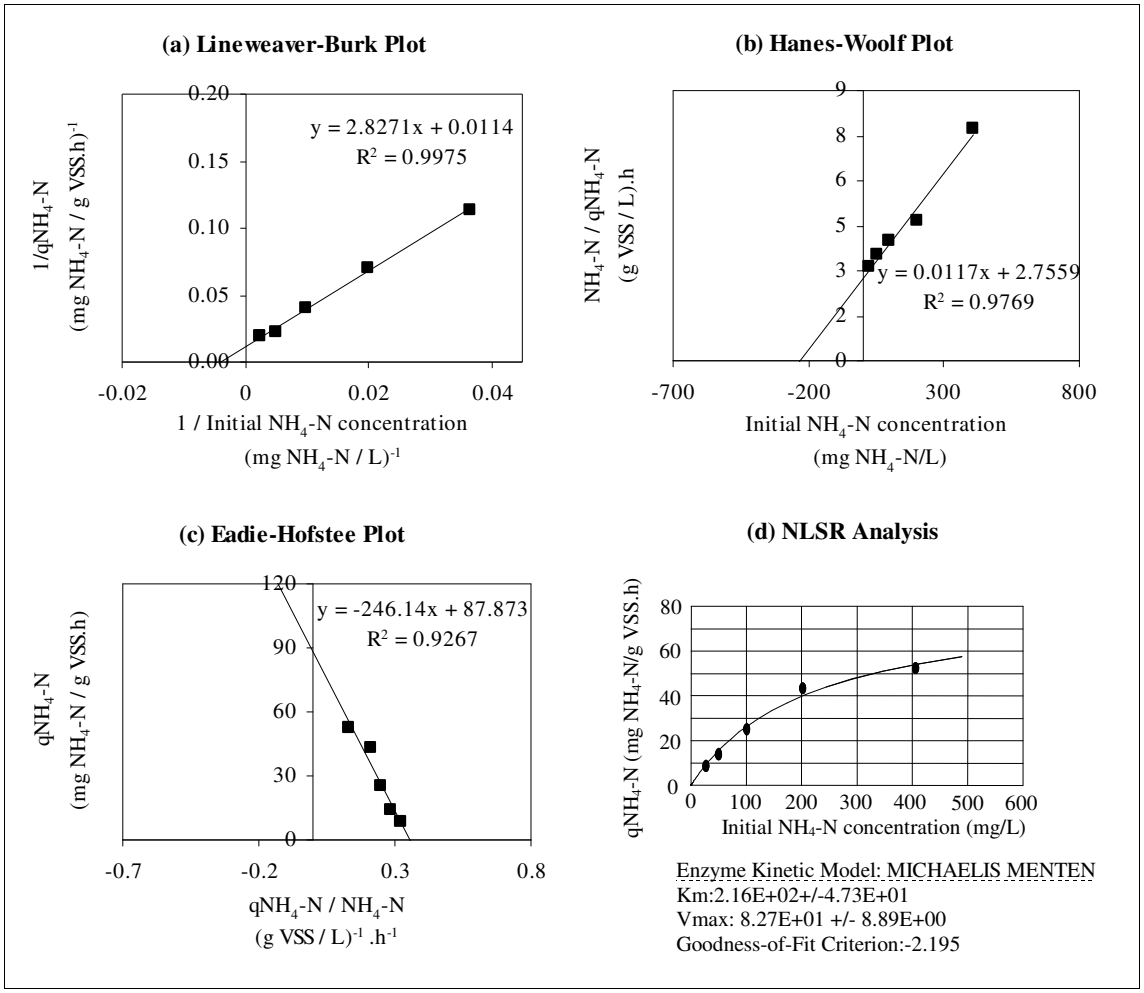

Figure 6.17. Determination of $q^{app}_{\max,NH\,4-N}$ *and* K^{app}_{s} at an initial TCE concentration of 40 µg/L using (a) Lineweaver-Burk plot, (b) Hanes-Woolf plot, (c) Eadie-Hofstee plot, and (d) NLSR analysis

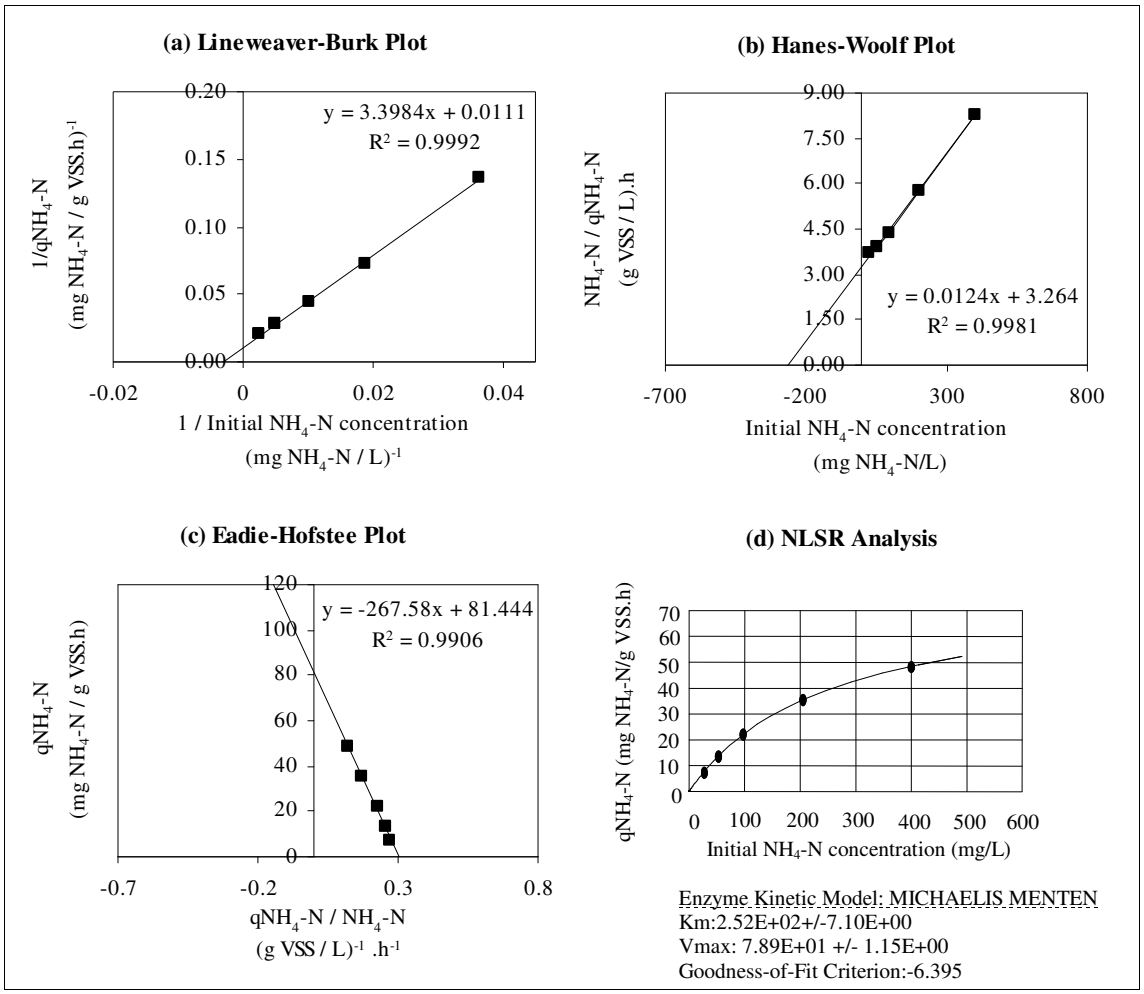

Figure 6.18. Determination of $q^{app}_{\max,NH4-N}$ *and* K^{app}_{s} at an initial TCE concentration of 110 µg/L using (a) Lineweaver-Burk plot, (b) Hanes-Woolf plot, (c) Eadie-Hofstee plot, and (d) NLSR analysis

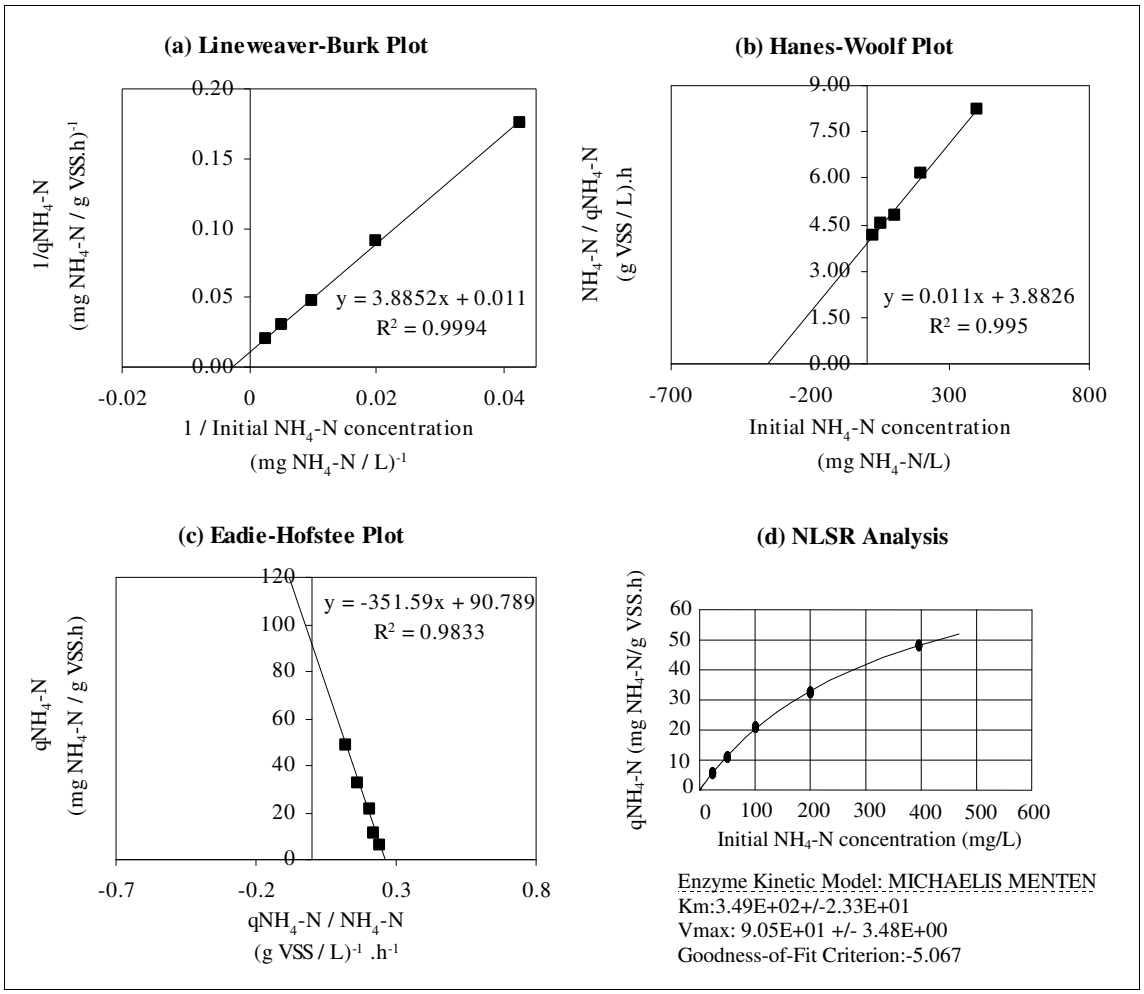

Figure 6.19. Determination of $q^{app}_{\max,NH4-N}$ *and* K^{app}_{s} at an initial TCE concentration of 325 µg/L using (a) Lineweaver-Burk plot, (b) Hanes-Woolf plot, (c) Eadie-Hofstee plot, and (d) NLSR analysis

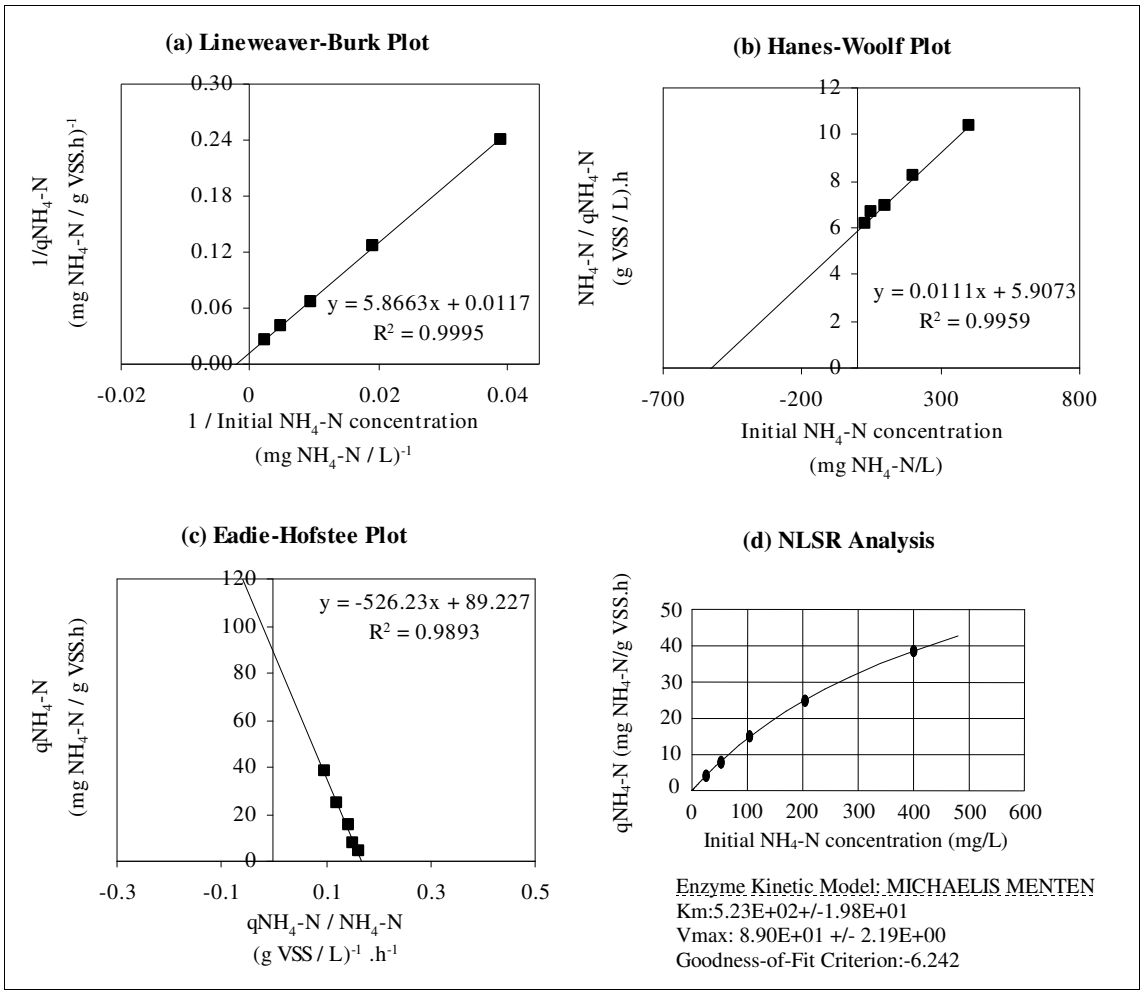

Figure 6.20. Determination of $q^{app}_{\max,NH4-N}$ *and* K^{app}_{s} at an initial TCE concentration of 845 µg/L using (a) Lineweaver-Burk plot, (b) Hanes-Woolf plot, (c) Eadie-Hofstee plot, and (d) NLSR analysis

Table 6.4. Apparent maximum specific ammonium utilization rates $(q_{\max,NH4-N}^{app})$ and apparent half-saturation constants (K_s^{app}) estimated by linearization methods and NLSR analysis at various TCE concentrations

Method	**in the absence of TCE**			**40 µg/L TCE**			**110 µg/L TCE**		
	R^2	$q_{\max,NH4-N}^{app}$ mgNH4-N/gVSS.h	K_s^{app} mg/L	R^2	$q_{\max,NH4-N}^{app}$ mgNH4-N/gVSS.h	K_s^{app} mg/L	R^2	$q_{\max,NH4-N}^{app}$ mgNH4-N/gVSS.h	K_s^{app} mg/L
Lineweaver-Burk (1/q vs. 1/S)	0.99	86.20	67.56	0.99	87.70	250.00	0.99	87.70	312.50
Hanes-Woolf (S/q vs. S)	0.99	86.20	66.36	0.97	85.40	235.54	0.99	80.60	263.20
Eadie-Hofstee (q vs. q/S)	0.98	87.56	69.76	0.92	87.87	246.14	0.99	81.44	267.58
NLSR analysis (Non-linear Least Square Regression)	0.97	87.80±3.4	70.09±8.16	0.95	82.73±8.89	215.59±47.3	0.99	78.87±1.15	251.85±7.1

Method	**325 µg/L TCE**			**845 µg/L TCE**		
	R^2	$q_{\max,NH4-N}^{app}$ mgNH4-N/gVSS.h	K_s^{app} mg/L	R^2	$q_{\max,NH4-N}^{app}$ mgNH4-N/gVSS.h	K_s^{app} mg/L
Lineweaver-Burk (1/q vs. 1/S)	0.99	90.9	353.20	0.99	85.47	501.39
Hanes-Woolf (S/q vs. S)	0.99	90.9	352.90	0.98	90.09	532.18
Eadie-Hofstee (q vs. q/S)	0.98	90.789	351.59	0.98	89.22	526.23
NLSR analysis (Non-linear Least Square Regression)	0.99	90.45±3.48	348.55±23.3	0.99	88.97±2.19	523.06±19.8

6.5.3. Inhibitory Characteristics of TCE on Ammonium Utilization

In order to understand the action of an inhibitor on substrate utilization, the first step is the identification of inhibition type. Once this is identified, kinetic constants can easily be estimated by the mathematical models described in Section 3.1.1.2.

The plottings shown in Figures 6.15, 6.17, 6.18, 6.19 and 6.20 were grouped together for each linearization method as illustrated in Figure 6.21. The inhibitory characteristics of TCE on ammonium utilization was initially evaluated by comparing Figure 6.21 with the Figure 6.22, which shows schematically how various types of inhibition influence various linearization plottings. The comparison of left hand quadrants in Figure 6.21 with Figure 6.22 clearly indicated a typical competitive inhibition characteristic.

As the next step, the data in Table 6.4 were evaluated to diagnose the type of TCE inhibition on nitrification. For this purpose, $q^{app}_{\max,NH4-N}$ and K_s^{app} values estimated in the presence of TCE were compared with the base $q^{app}_{\max,NH4-N}$ and K_s^{app}. As seen from the table, as the initial TCE concentration increased, K_s^{app} also increased, whereas $q^{app}_{\max,NH4-N}$ remained almost constant. These results exactly coincide with the characteristics of a competitive inhibitor, which is similar in structure to the normal enzyme substrate and competes with the substrate for the active site of the enzyme as explained in detail in Section 3.1.1.2.

In view of above-mentioned findings, TCE was found to be a competitive inhibitor of ammonia oxidation. This is in consistency with the results of Hyman et al. (1995) and Ely et al. (1995), who concluded that TCE was a competitive inhibitor by using a Dixon plot for the oxygen uptake rate measurements and a model solution, respectively**.** However, it should be noted that their results were obtained for pure *Nitrosomonas europaea* cultures as in many other studies.

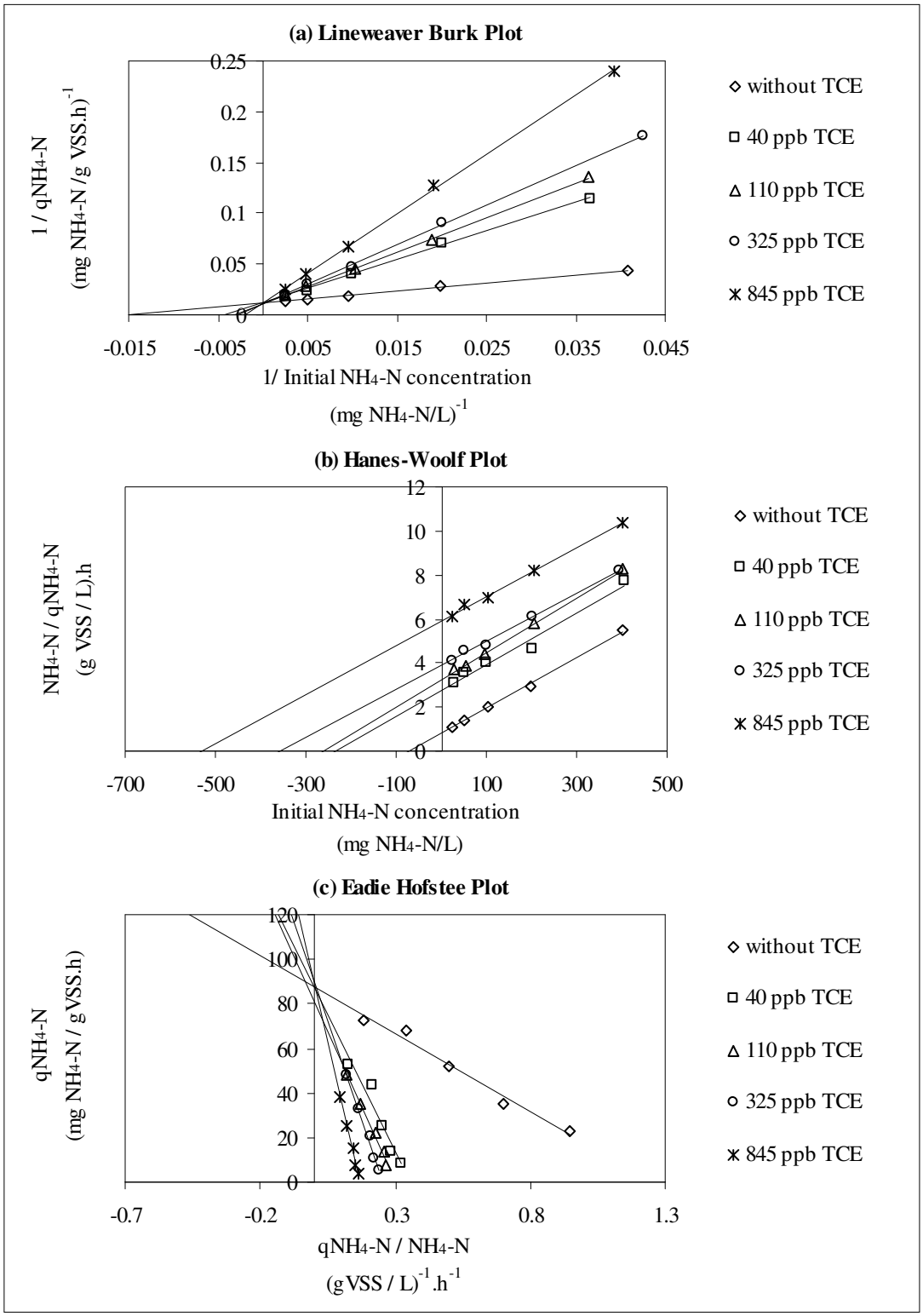

Figure 6.21. Effects of TCE on ammonium utilization rate as reflected by (a) Lineweaver-Burk plot, (b) Hanes-Woolf Plot and (c) Eadie-Hofstee Plot

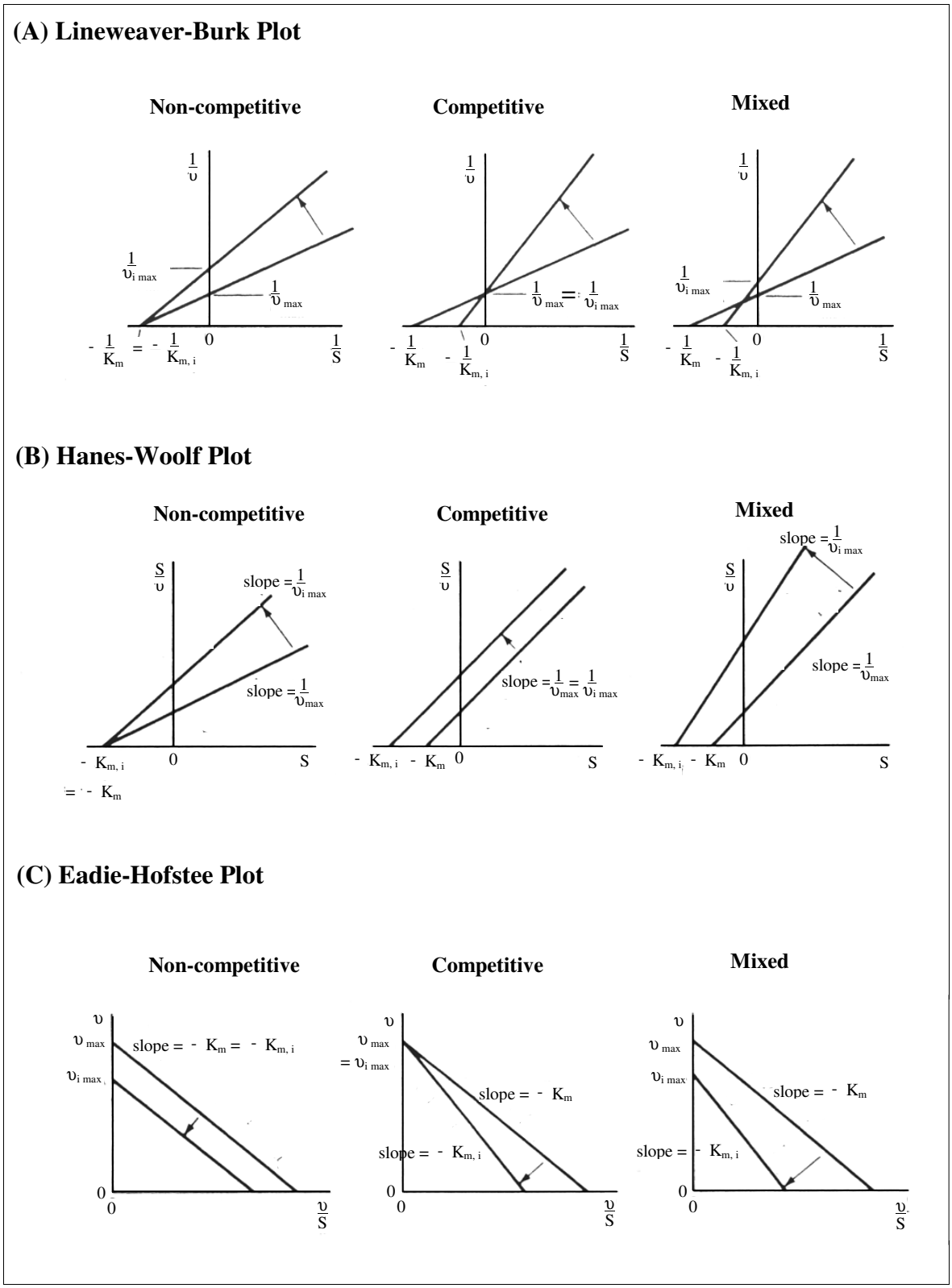

Figure 6.22. Effects of various types of inhibition as reflected in different linearized rate plots (subscript i denotes the presence of inhibitor) (Bailey and Ollis, 1986)

6.5.4. Determination of the Inhibition Coefficient (K_{ic}) of TCE

As described in Section 3.1.1.2, the net effect of a competitive inhibitor on substrate utilization is to increase K_s with a factor $(1+I/K_I)$ while leaving that of q_{max} unchanged as shown in Equation 6.2.

$$q = \frac{q_m^{app} S}{K_s^{app} + S} = \frac{q_m S}{K_s(1 + \frac{I}{K_{ic}}) + S} \tag{6.2}$$

The simplest approach to find the K_{ic} value in Eqn. 6.2 is to plot K_S^{app} values against the inhibitor concentrations [I]. However, since the K_S^{app} can never be estimated as accurately as $K_S^{app} / q_{max}^{app}$, the better approach to find the K_{ic} value is to plot $K_S^{app} / q_{max}^{app}$ against the inhibitor concentration [I] (Cornish-Bowden, 1995). The intercept of this plot on the x-axis will give the $-K_{ic}$ value. Plottings of the $K_S^{app} / q_{max}^{app}$ values reported in Table 6.4 against the initial TCE concentrations are shown in Figure 6.23. The K_{ic} values found from the x-axis intercepts of these linearized plottings are summarized in Table 6.5.

The K_{ic} value for TCE found in this study is low compared to K_{ic} values of 3942 µg/L (Hyman et al., 1995) and 1563 µg/L (Ely et al., 1997) determined with pure *Nitrosomonas europaea* cultures. The discrepancy between our results and those of Hyman et al. (1995) and Ely et al. (1997) may be attributed to different experimental conditions, such as temperature, nitrifier concentrations, and the use of an enriched culture instead of a pure culture.

K_s and K_{ic} are indicators of the affinity of the substrate and the inhibitory compound for the enzyme, respectively. The K_S^{app} values in the absence of TCE (Table 6.4) are in the range of 66-70 mg/L NH_4-N which corresponds to 4300-5000 µM. The comparison of this value with the K_{ic} value determined in the range of 5.07-6.11 µM (Table 6.5) clearly indicates that the affinity of the TCE for ammonia monooxygenase (AMO) enzyme was significantly higher than that of ammonium. As discussed in Section

6.1.1, the actual K_s value determined under diffused air conditions ranged between 6.4-7.8 mg/L NH_4-N which corresponded to 458-558 μM. Comparison of the K_{ic} value with the this actual K_s value also indicates the higher affinity of TCE for AMO enzyme with respect to ammonium.

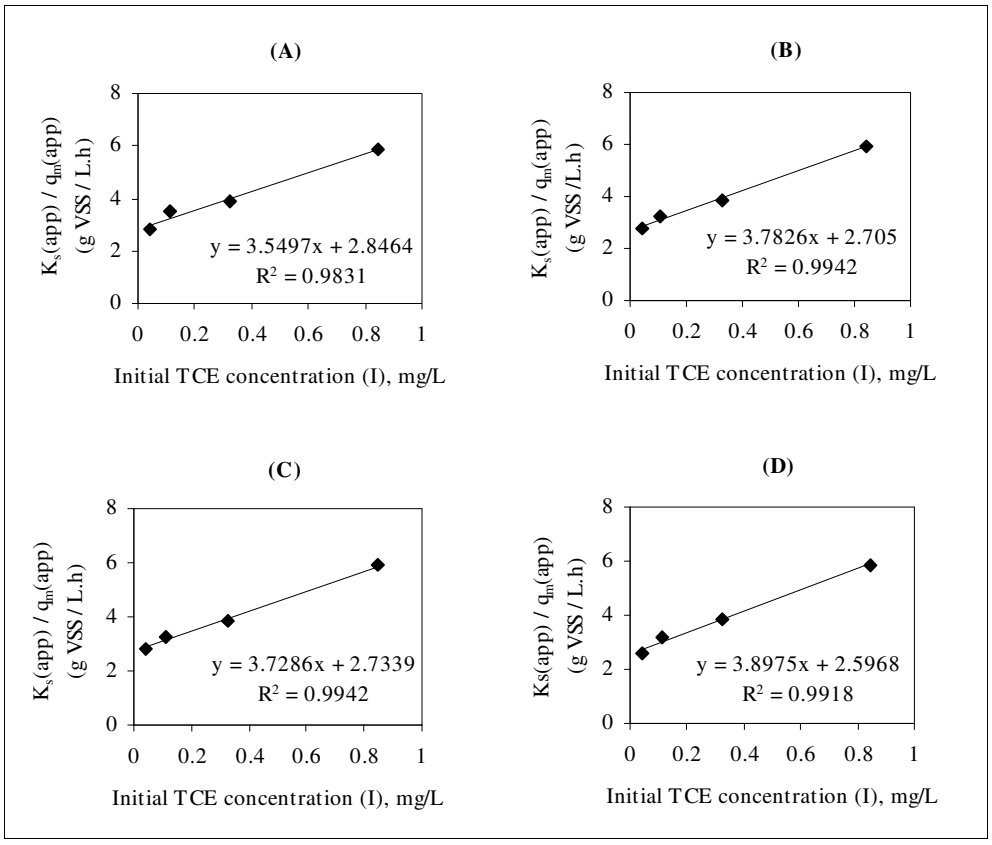

Figure 6.23. Estimation of TCE inhibition constant (K_{ic}) using the results of (a) Lineweaver-Burk plot, (b) Hanes-Woolf plot, (c) Eadie-Hofstee plot, and (d) non-linear regression analysis

Table 6.5. Estimation of TCE inhibition constant (K_{ic}) by several linearization methods and non-linear regression analysis

Source of Data	Estimated K_{ic} μg /L [μM]
Lineweaver-Burk Plot results	802 [6.11]
Hanes-Woolf Plot results	715 [5.44]
Eadie-Hofstee Plot results	733 [5.58]
NLSR analysis results	666 [5.07]

6.5.5. Evaluation of TCE Volatilization

As shown in Figure 6.24, the volatilization rate of TCE from the liquid phase into the headspace of capped bottles increased linearly with TCE and the first-order rate constant was calculated as 0.0028 /min (0.168 /h). The cometabolic degradation rates of TCE were calculated by considering these volatilized amounts.

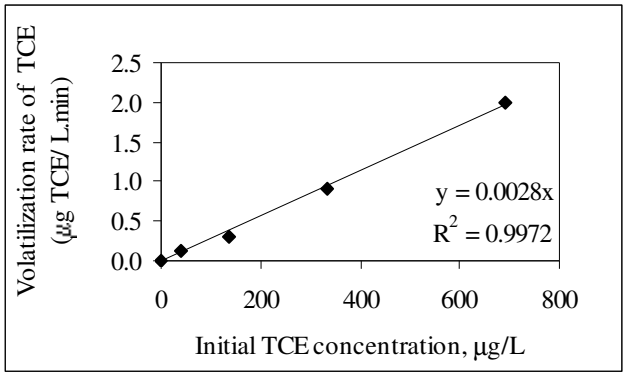

Figure 6.24. The volatilization rate of TCE with respect to the initial TCE concentration

6.5.6. Evaluation of Cometabolic TCE Degradation in Dependence of Ammonium Degradation

The specific cometabolic degradation rate of TCE (q_{TCE}) was evaluated at the initial NH_4-N concentrations of 25, 50, 100, 200 and 400 mg/L by keeping the initial TCE concentration constant.

At each initial NH_4-N concentration studied (Figure 6.25), the cometabolic degradation rates of TCE increased linearly with TCE. Linearization of the graphs in Figure 6.25 resulted in first-order cometabolic TCE degradation rate constants of 0.2657 L/g VSS.h at 25 mg/L NH_4-N, 0.3112 L/g VSS.h at 50 mg/L NH_4-N, 0.483 L/g VSS.h at 100 mg/L NH_4-N, 0.7321 L/g VSS.h at 200 mg/L NH_4-N and 1.0312 L/g VSS.h at 400 mg/L NH_4-N. These values are considerably lower than the values reported for pure *Nitrosomonas europaea* species as 30.8 L/gVSS.h and 42.5 L/gVSS.h for initial TCE concentrations of 0-3300 µg/L and 2100 µg/L, respectively (Alvarez-Cohen and Speitel, 2001). However, in those studies the reported values are based on the assumption that the dry cell mass consists of 50 % protein (Alvarez-Cohen and Speitel, 2001). On the other

hand, in our enriched nitrifier culture the fraction of nitrifiers in the total VSS expression was small. Therefore, q_{TCE} values were quite lower when the results were expressed on VSS basis. Also, the cometabolic TCE degradation followed first-order kinetics because the TCE concentrations (0-825 μg/L, Figure 6.25) were very small. If higher TCE concentrations were present, the TCE degradation rate would most probably reach saturation. However, it is very likely that also in real remediation systems, such as groundwater, TCE degradation follows first-order kinetics in the concentration ranges below 1000 μg/L.

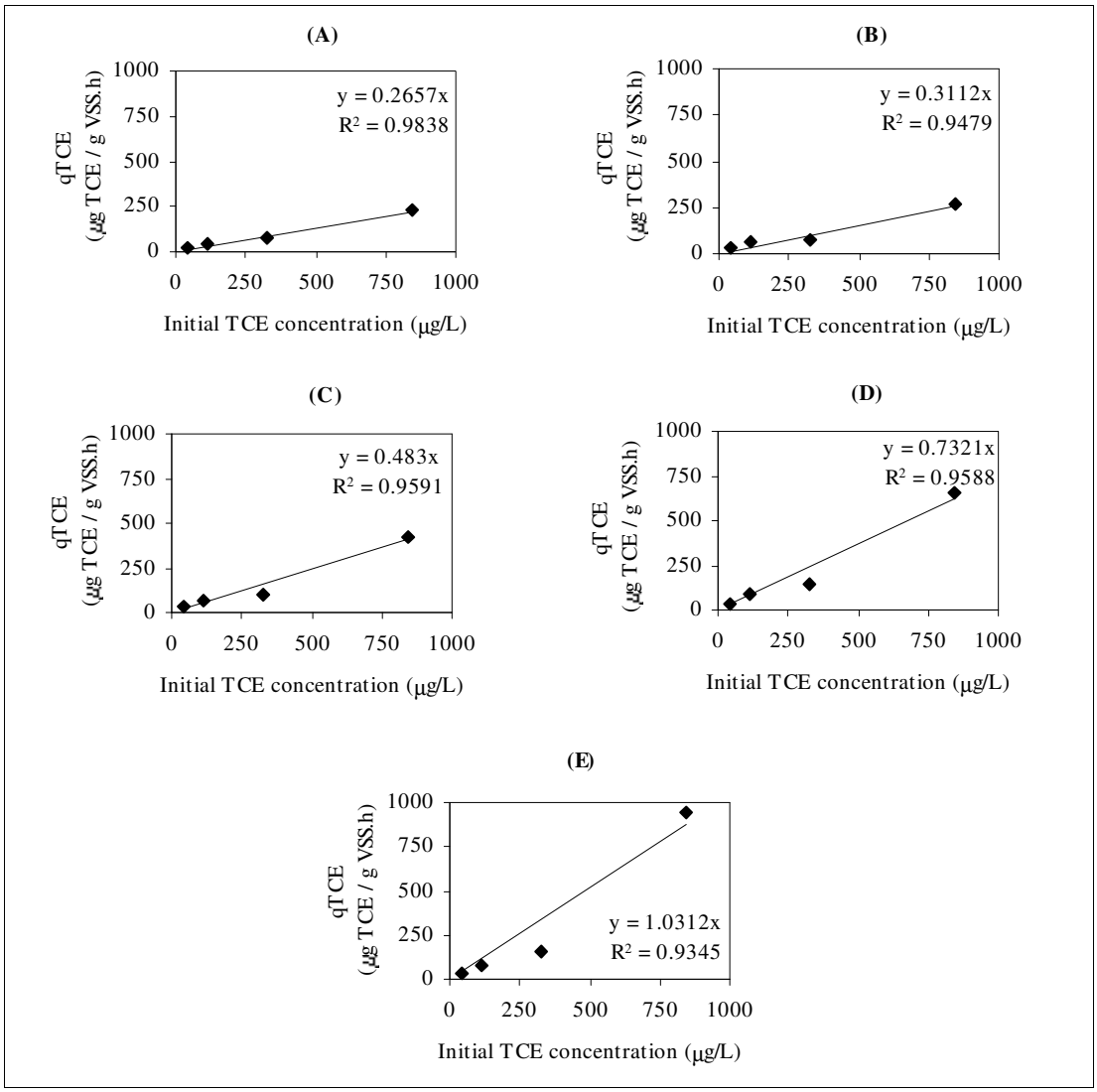

Figure 6.25. Cometabolic degradation rates of TCE (q_{TCE}) at initial NH_4-N concentrations of (a) 25 mg/L, (b) 50 mg/L, (c) 100 mg/L, (d) 200 mg/L and (e) 400 mg/L with respect to the initial TCE concentrations

Figure 6.26 illustrates the dependence of q_{TCE} values on ammonium utilization rates at each initial TCE concentration.

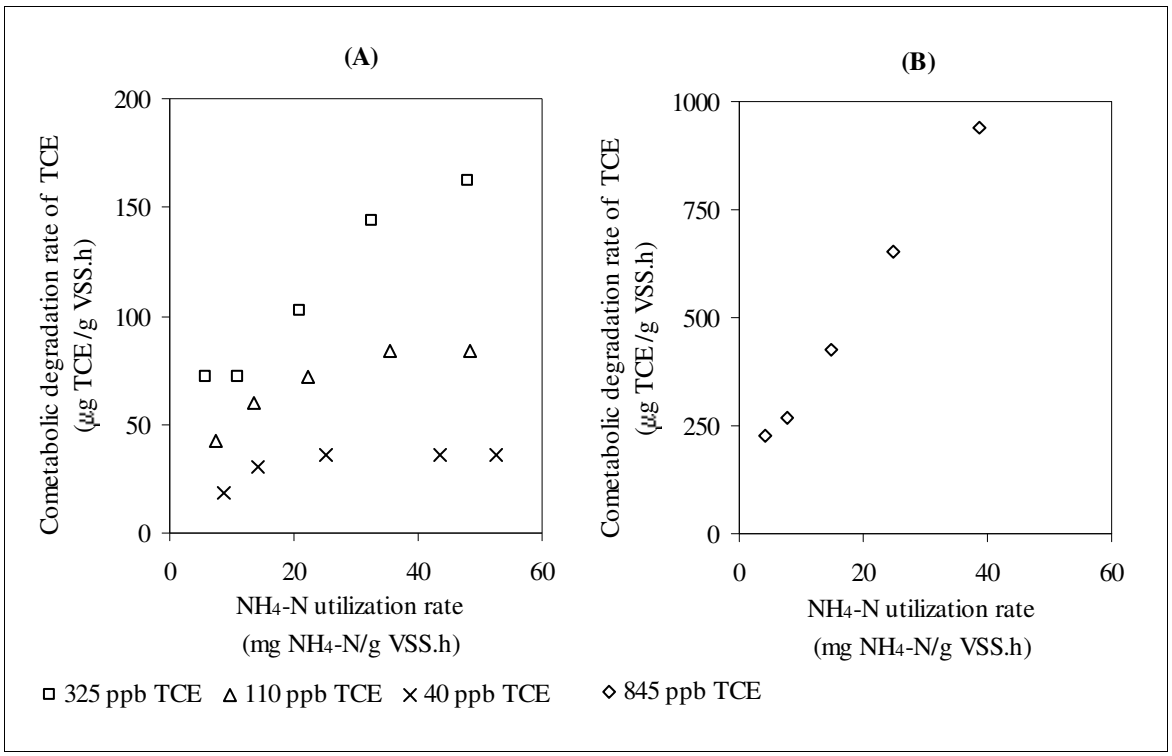

Figure 6.26. Cometabolic degradation rates of TCE (q_{TCE}) (a) at initial TCE concentrations of 40 μg/L, 110 μg/L, 325 μg/L (b) at an initial TCE concentration of 845 μg/L with respect to the ammonium utilization rates (q_{NH4-N})

The cometabolic degradation rates observed at each initial TCE concentration exhibited an increase with ammonium utilization rates (q_{NH4-N}), which is directly correlated with the initial NH_4-N concentration as shown in Figure 6.16. A saturation point was reached at high q_{NH4-N} values. It is well known that both the oxidation of growth- substrate and the cometabolic substrate by non-specific oxygenase enzymes consume reducing energy in the form of NAD(P)H as explained in Section 3.2.2. When the growth-substrate is oxidized by oxygenase enzymes, NAD(P)H is regenerated. However, when the cometabolic substrate is oxidized, NAD(P)H is not regenerated (Section 3.2.2). Therefore, reducing energy (NAD(P)H) is a potentially limiting reactant for cometabolic reactions. In this study, the increases in initial TCE degradation rates with an increase in growth substrate (NH_4-N) may be explained by the NAD(P)H (reductant) regeneration by the growth substrate. Since both TCE and NH_4-N compete for the same active site of the

enzyme ammonia monooxygenase (AMO), a decrease in TCE degradation rate may be expected at higher NH_4-N concentrations. However, the results of this study showed that NH_4-N had a positive effect on TCE degradation even at higher concentrations. This may be related to the considerably greater affinity of TCE for the enzyme AMO compared to ammonium as reported in Section 6.5.4. These results indirectly indicate that a system using ammonium as the primary substrate has a quite high TCE degradation capacity.

The cometabolic degradation potential of microorganisms is usually quantified by the transformation yield (T_y), which is defined as the mass of cometabolic substrate degraded per unit mass of growth substrate consumed (Ward et al., 1997). In the present study, the transformation yields were estimated by dividing the TCE degradation rates (q_{TCE}) shown in Figure 6.26 by the corresponding NH_4-N utilization rates ($q_{NH4\text{-}N}$). They were found to be variable depending on initial NH_4-N and TCE concentrations. Similarly, Ely et al. (1995b) reported that growth and non-growth substrate degradation are related to each other by a dimensionless constant (ε) unique to the particular enzyme/growth-substrate/non-growth substrate systems as shown in Equation 6.3.

$$\frac{dS/dt}{dI/dt} = \frac{k/K_s}{k_I/K_I}\frac{S}{I} \tag{6.3}$$

where $\frac{k/K_s}{k_I/K_I}$ =ε= ratio of the pseudo-first-order reaction rate constants for the growth substrate and non-growth substrate

Considering that the $q_{NH4\text{-}N}/q_{TCE}$ ratio equals $1/T_y$, a correlation between T_y and the initial TCE and NH_4-N concentrations can be found by rearranging Equation 6.3:

$$1/T_y = \varepsilon\ (NH_4\text{-}N / TCE) \tag{6.4}$$

The results of this study could also be roughly fitted into this model. In Figure 6.27, plotting $q_{NH4\text{-}N}/q_{TCE}$ against the initial NH_4-N/TCE showed that up to an NH_4-N/TCE ratio of 4800 a strong linear relationship exists between $q_{NH4\text{-}N}/q_{TCE}$ (1/Ty) and the initial NH_4-N/TCE ratio. The ε value was found as 0.253. However, beyond this ratio, increasing NH_4-N/TCE ratio will not result in a further increase in 1/Ty. In the application of this

model for practice, some safety factor should always be considered in order to avoid the overestimation of the transformation yield.

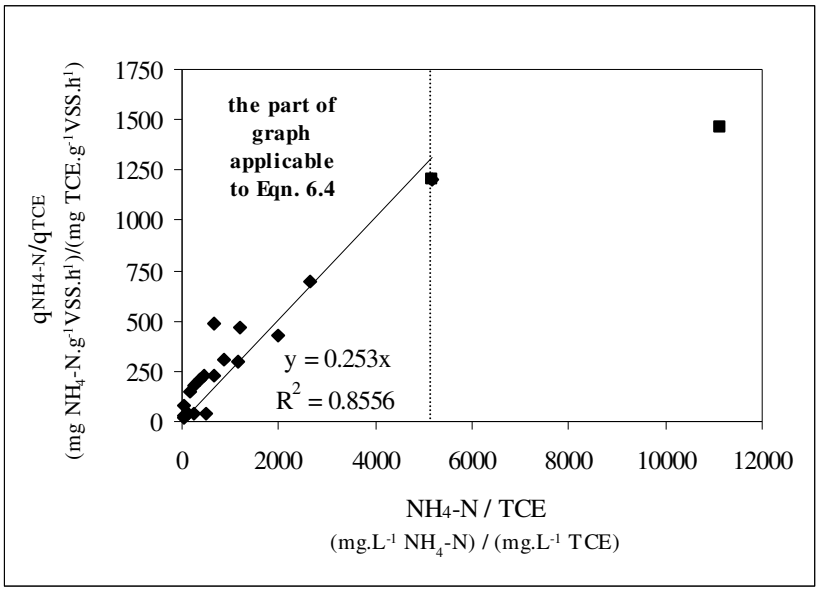

Figure 6.27. Relationship between the relative ratio of ammonium and TCE degradation rates and the relative ratio of ammonium and TCE concentrations

6.5.7. Implications for Engineering Applications

The findings of batch kinetic experiments with TCE have relevance for the improvement of engineered remediation/treatment systems for TCE removal from industrial effluents (such as discharges from dry-cleaning, textile manufacturing, automotive, metal and petroleum industries) and many groundwater systems. Although these findings determined under laboratory conditions are not directly representative of field conditions, they allow the estimation of growth substrate (ammonium) requirements for the reduction of TCE to a determined concentration. The implications of this research for real treatment systems can be presented by imagining the following scenario:

Consider that historic spillages of TCE at a dry-cleaning industrial plant has lead to pollution of the underlying aquifer. In the groundwater samples taken from the aquifer, the maximum TCE concentration was detected around 250 μg/L. The groundwater at that site can be treated in an ex-situ treatment system using a mixed culture enriched for nitrifiers. Here, the growth substrate NH_4-N will be added to the contaminated groundwater and the

process may proceed in a batch reactor until the desired level of treatment is achieved. In the design of this system, the amount of NH_4-N to be added to the system should be selected by considering that TCE will be removed with efficient use of NH_4-N. If two alternative initial NH_4-N concentrations of 50 and 100 mg/L are chosen, based upon Equation 6.4, transformation yield (T_y) of TCE, which is the amount of TCE that can be degraded per unit mass of ammonium**,** will be 0.019 and 0.0098, respectively. If 100% TCE removal takes place, based on the calculated T_y values, the decrease in ammonium concentration will be around 12.65 mg/L at 50 mg/L NH_4-N and 25.3 mg/L at 100 mg/L NH_4-N. Therefore, the effluent of the system will contain a significant amount of NH_4-N if 100 mg/L NH_4-N are added. However, as seen from Figures 6.25a and 6.25b, increasing NH_4-N concentration from 50 to 100 mg/L will not cause a significant change in TCE transformation rate indicating that the time necessary to achieve 100% TCE removal will be not much different for both ammonium concentrations. Thus, in that case the lower influent NH_4-N should be chosen.

Similarly, other scenarios can be imagined and the TCE removal and nitrification patterns can be predicted for different influent TCE and NH_4-N concentrations. These scenarios can also be applied to continuous-flow systems.

6.6. The Effect of 1,2-DCA on Specific Oxygen Uptake Rate (SOUR)

The immediate response of enriched nitrifier cultures to an initial 1,2-DCA concentration in the range of 70-380000 µg/L was assessed by specific oxygen uptake rate (SOUR) as illustrated in Figures 6.28-6.32.

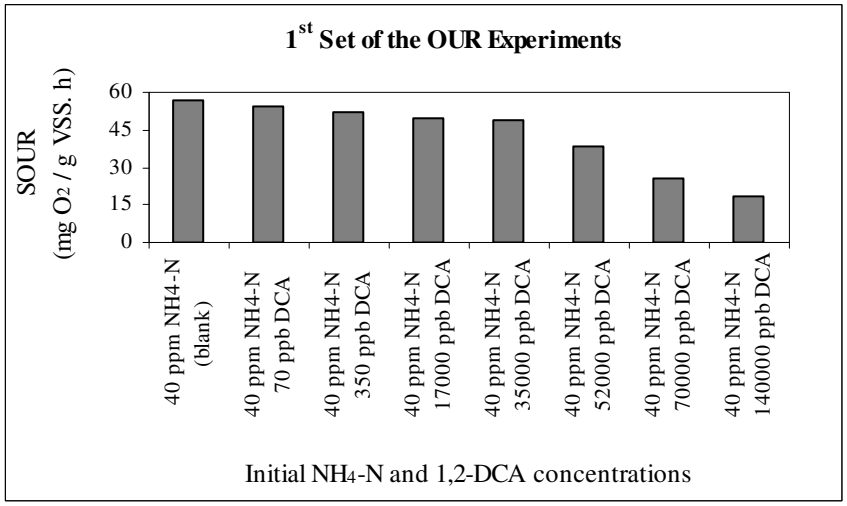

Figure 6.28. SOUR values observed in the 1st set OUR experiments with 1,2-DCA [Initial NH_4-N = 40 mg/L, Initial 1,2-DCA = 70-140000 µg/L]

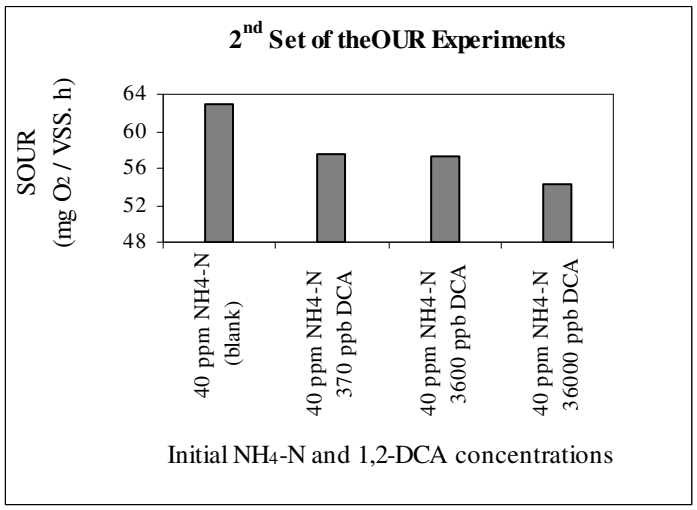

Figure 6.29. SOUR values observed in the 2nd set OUR experiments with 1,2-DCA [Initial NH_4-N = 40 mg/L, Initial 1,2-DCA = 370-36000 µg/L]

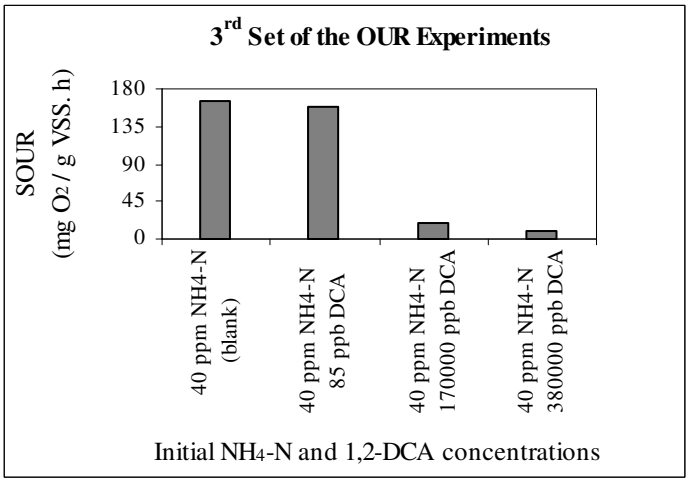

Figure 6.30. SOUR values observed in the 3rd set OUR experiments with 1,2-DCA [Initial NH_4-N = 40 mg/L, Initial 1,2-DCA = 85-380000 µg/L]

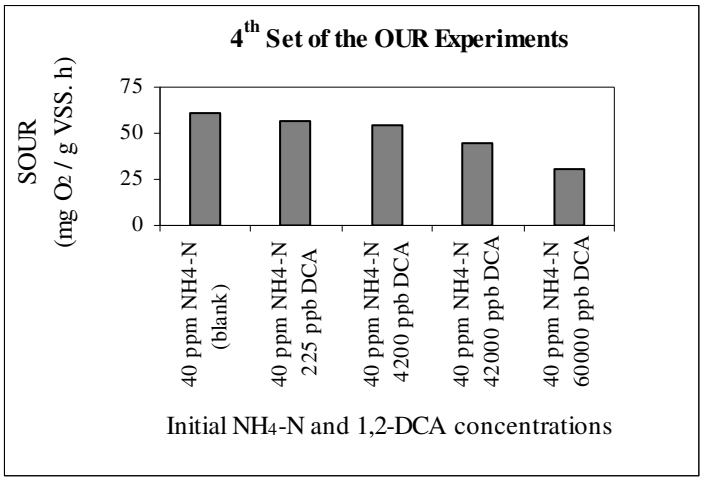

Figure 6.31. SOUR values observed in the 4th set OUR experiments with 1,2-DCA [Initial NH_4-N = 40 mg/L, Initial 1,2-DCA = 225-60000 µg/L]

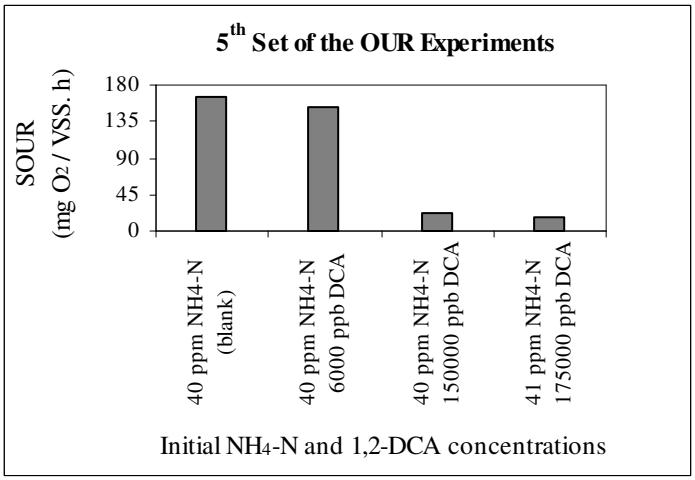

Figure 6.32. SOUR values observed in the 5th set OUR experiments with 1,2-DCA [Initial NH_4-N = 40 mg/L, Initial 1,2-DCA = 6000-175000 µg/L]

The relative percent decreases in SOUR values calculated with respect to the base SOUR value in each set of experiments (Figure 6.33) indicated that SOUR decreased slowly with an increase in 1,2-DCA. However, in the preliminary OUR experiments with TCE (Section 6.3), the SOUR of the same culture decreased more gradually with an increase in TCE and reached about 50% even at a much lower concentration (2500 µg/L TCE) compared to 1,2-DCA. This comparison indicates that the inhibitory effect of the chloroethene TCE on ammonia monooxygenase (AMO) enzyme is more significant than in the case of the chloroethane 1,2-DCA.

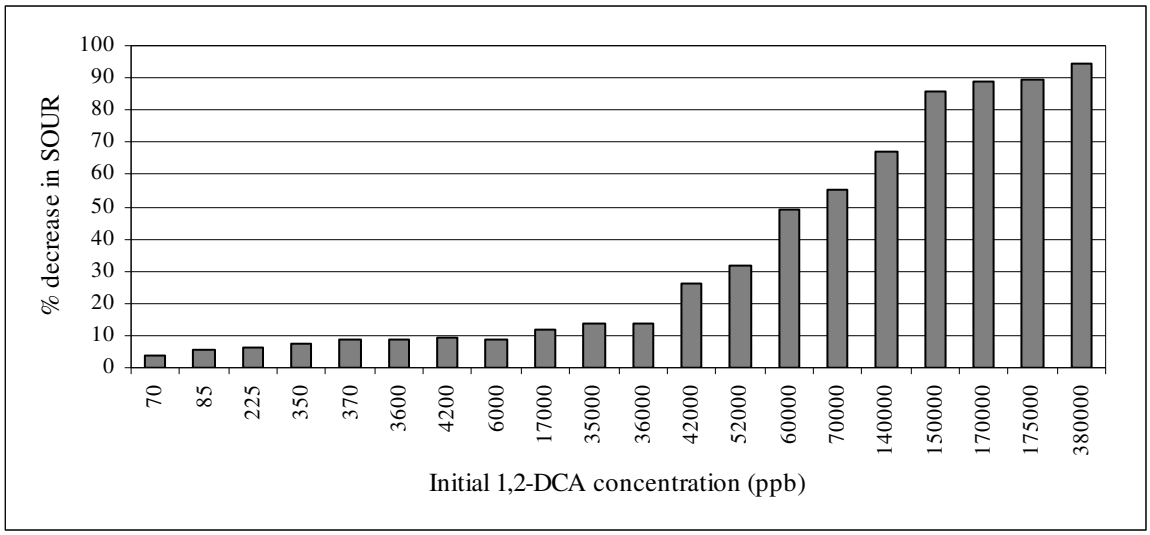

Figure 6.33. Decreases observed in SOUR at various 1,2-DCA concentrations [Initial NH_4-N = 40 mg/L, Initial 1,2-DCA = 70-380000 µg/L]

6.7. Batch Experiments with 1,2-DCA

6.7.1. Evaluation of Ammonium Removal in the Presence of 1,2-DCA

Based on the results of preliminary OUR experiments, at a constant initial ammonium concentration of 50 mg/L NH_4-N, the specific ammonium utilization rates ($q_{NH4\text{-}N}$) and specific oxygen uptake rates (SOUR) were evaluated at initial 1,2-DCA concentrations in the range of 1600-100000 µg/L as illustrated in Figure 6.34 and summarized in Table 6.6.

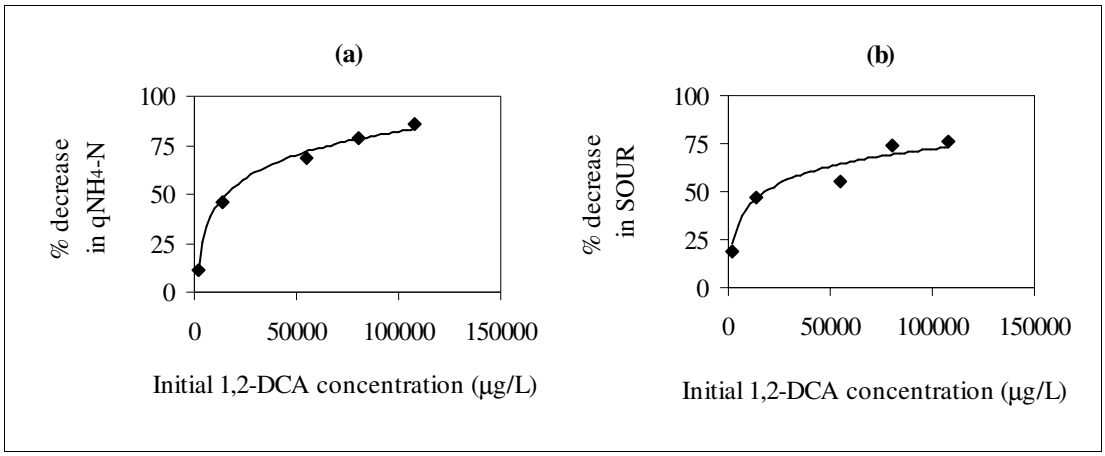

Figure 6.34. Effect of 1,2-DCA on (a) specific ammonium utilization rate (q_{NH4-N}) and (b) specific oxygen uptake rate (SOUR)

In the presence of 1,2-DCA (1600-100000 µg/L), both SOUR and q_{NH4-N} values showed gradual decreases with respect to base SOUR and q_{NH4-N} which were determined as 0.21 mg O_2/mgVSS.h and 59.52 mg NH_4-N/gVSS.h, respectively. Both SOUR and q_{NH4-N} were similarly affected by the presence of 1,2-DCA and indicated inhibition of ammonium utilization at increased 1,2-DCA. This inhibition degree measured in both parameters reached about 45-50% at 15000 µg/L 1,2-DCA. However, in preliminary OUR experiments (Section 6.6), inhibition had occurred at much higher concentrations and 50% decrease was observed in SOUR at a relatively high value of 60000 µg/L 1,2-DCA. The discrepancy between preliminary OUR and these batch experiments may be explained as follows. Preliminary OUR measurements were performed in a test period of 10 min. In such a short duration, degradation of 1,2-DCA was negligible and SOUR indicated mainly the inhibition of the AMO enzyme as a result of sudden exposure to 1,2-DCA. On the other hand, in batch experiments performed in a test period of 35-225 min, 1,2-DCA was cometabolically degraded by nitrifiers as discussed in Section 6.7.3. Therefore, the inhibition determined in terms of SOUR in these long-term experiments was not only due to exposure to this compound but possibly also due to inhibition of the AMO enzyme by short-lived reaction intermediates produced during degradation. Therefore, we may conclude that the inhibitory effect of 1,2-DCA on ammonium oxidation was mainly due to the inhibition of the AMO enzyme by short-lived reaction intermediates. In contrast to this, the results of batch experiments with TCE using the same culture (Section 6.4.1) indicated that the inhibitory effect of TCE on ammonium oxidation arose as a result of the inhibition

of AMO enzyme activity when the cells were exposed to this compound. Therefore, the inhibitory effects of TCE and 1,2-DCA should probably be explained by different mechanisms.

6.7.2. Evaluation of 1,2-DCA Volatilization in Batch Experiments

Figure 6.35 shows the volatilization rates of 1,2-DCA determined at various 1,2-DCA concentrations. The volatilization rate of 1,2-DCA showed a linear increase with increasing 1,2-DCA and the first-order rate constant was calculated as 0.0012 /min (0.072 /h). The cometabolic degradation rates of 1,2-DCA were calculated by considering the volatilization loss in each experiment.

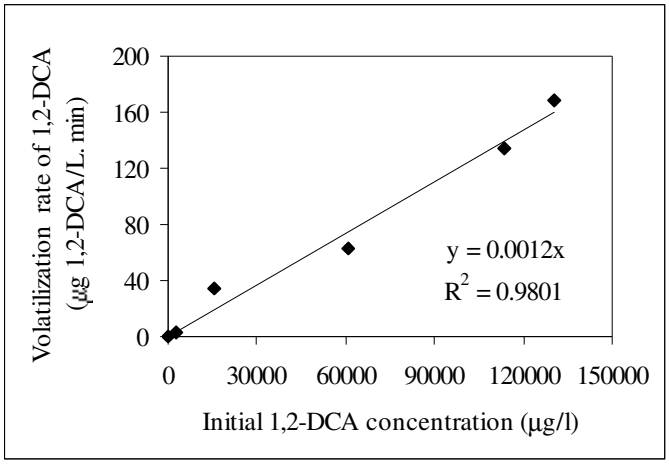

Figure 6.35. The volatilization rate of 1,2-DCA with respect to the initial 1,2-DCA concentration

6.7.3. Evaluation of Cometabolic Degradation of 1,2-DCA

At a constant initial NH_4-N concentration of 50 mg/L, the specific cometabolic degradation rate of 1,2-DCA (q_{DCA}) was evaluated with respect to the initial 1,2-DCA concentration in the range of 1600-100000 µg/L as illustrated in Figure 6.36 and summarized in Table 6.6.

The cometabolic degradation rate increased linearly with 1,2-DCA and the first-order cometabolic DCA degradation rate constant was determined as 0.4296 L/g VSS.h

(0.01031 L/mg.d). This value is considerably lower than the one (0.37 L/mg.d) reported for pure *Nitrosomonas europaea* species (Alvarez-Cohen and Speitel, 2001). But, in that study, the biomass was reported in terms of protein. The reported value of 0.37 L/mg.d is based on the assumption that the dry cell mass consists of 50% protein (Alvarez-Cohen and Speitel, 2001). This was also the case for the value reported in Section 6.4.3 where the reason of discrepancy between the values observed in the present study and reported in the literature was explained in detail. In batch experiments performed with TCE using the same enriched culture (Section 6.4.3), the first-order cometabolic TCE degradation rate constant was determined as 0.25 L/g VSS.h (0.0061 L/mgVSS.d) which was lower than that of 1,2-DCA.

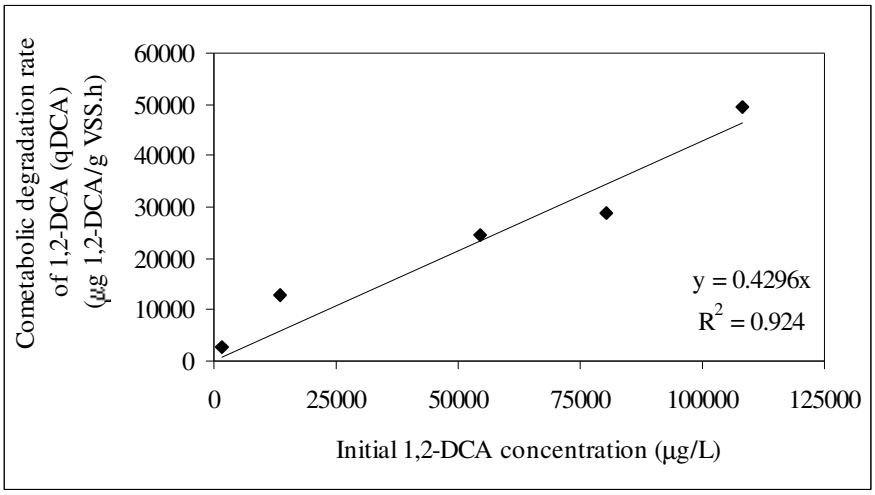

Figure 6.36. Effect of 1,2-DCA concentration on the cometabolic degradation rate of 1,2-DCA

Table 6.6. Summary of the results of batch experiments with 1,2-DCA

Exp. No.	VSS mg/L	NH_4-N mg/L	1,2-DCA µg/L	q_{NH4-N} mg NH_4-N / gVSS.h	% decrease in q_{NH4-N}	SOUR mg O_2 / mg VSS.h	% decrease in SOUR	q_{DCA} µg DCA / gVSS.h
1	214	50	-	59.52	-	0.219	-	-
2	247	50	1600	52.93	11	0.178	19	2742
3	160	50	15000	32.36	46	0.116	47	12726
4	176	50	50000	18.92	68	0.098	55	24468
5	340	50	75000	12.56	79	0.057	74	28770
6	256	50	100000	8.20	86	0.052	76	49314

6.8. Batch Experiments with 1,2-DCA Directed to Kinetic Modelling

6.8.1. Evaluation of Maximum Specific Ammonium Utilization Rate ($q_{max,NH4-N}$) and Half-Saturation Constant (K_s) in the Absence of 1,2-DCA

The specific ammonium utilization rates (q_{NH4-N}) were first investigated at the initial NH_4-N concentrations of 100, 200 and 400 mg/L to determine the maximum specific ammonium utilization rate ($q_{max,NH4-N}$) and half-saturation constant (K_s) in the absence of 1,2-DCA as illustrated in Figure 6.37. In batch experiments with 1,2-DCA (Table 6.6), q_{NH4-N} values were also estimated at initial NH_4-N concentration of 50 mg/L in the absence of 1,2-DCA (Exp. No:1). Since the experimental conditions in those experiments were the same as in the present batch kinetic experiments, these values were also used in data analysis as shown in Figure 6.37.

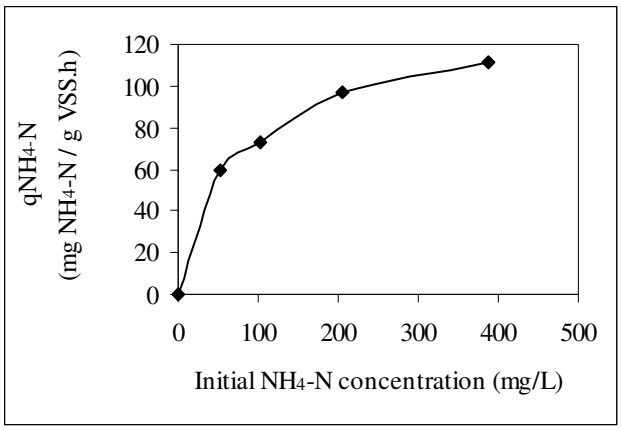

Figure 6.37. Specific ammonium utlization rates in the absence of 1,2-DCA

As done before (Section 6.5.1), the data shown in Figure 6.37 were analyzed by linearization methods (Table 6.1) and nonlinear least square regression (NLSR) (Section 6.1.1.) as illustrated in Figure 6.38. $q_{max,NH4-N}$ and K_s values determined from these analyses are given in Table 6.7. As seen from the table, in the absence of 1,2-DCA, the base constants, $q_{max,NH4-N}$ and K_s were found in the ranges of 121-131 mg NH_4-N/g VSS.h and 56-71 mg/L NH_4-N, respectively. It is clear that this K_s value for ammonium is much higher than the common values reported in the literature. The reason of this discrepancy was explained in detail in Section 6.5.1.

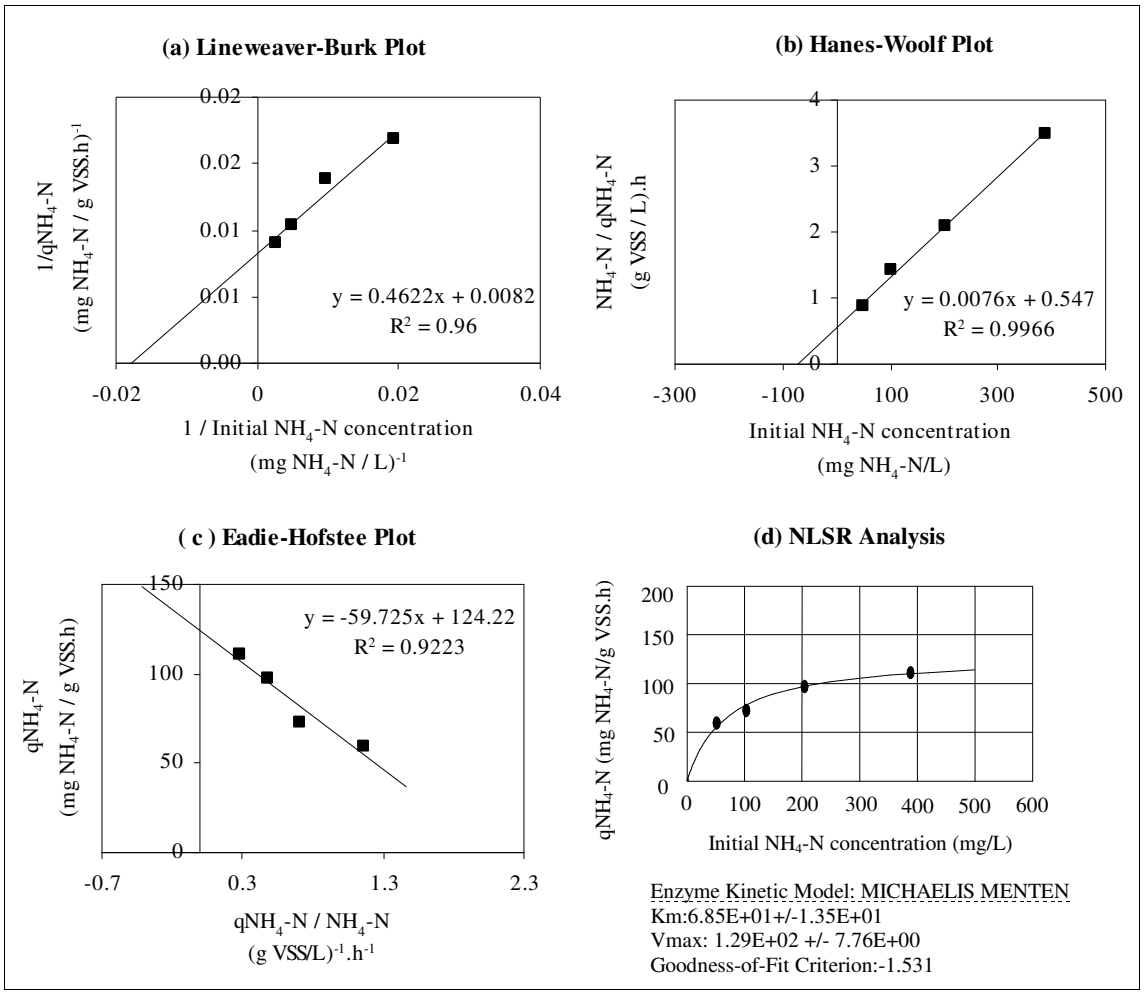

Figure 6.38. Determination of $q_{max,NH4-N}$ and K_s in the absence of 1,2-DCA under oxygen saturated conditions using (a) Lineweaver-Burk plot, (b) Hanes-Woolf plot, (c) Eadie-Hofstee plot, and (d) NLSR analysis

6.8.2. The Effect of 1,2-DCA on the Maximum Specific Ammonium Utilization Rate ($q_{max,NH4-N}$) and Half-Saturation Constant (K_s)

The effect of 1,2-DCA on $q_{max,NH4-N}$ and K_s were investigated in a 1,2-DCA range of 1600-100000 µg/L and a NH_4-N range of 100-400 mg/L as illustrated in Figure 6.39. In batch experiments with 1,2-DCA (Table 6.6), q_{NH4-N} values were also estimated at initial NH_4-N concentration of 50 mg/L for a 1,2-DCA range of 1600-100000 µg/L (Exp. No: 2-6). Since the experimental conditions in those experiments were the same as in present batch kinetic experiments, in data analysis, these values were also used as shown in Figure 6.39.

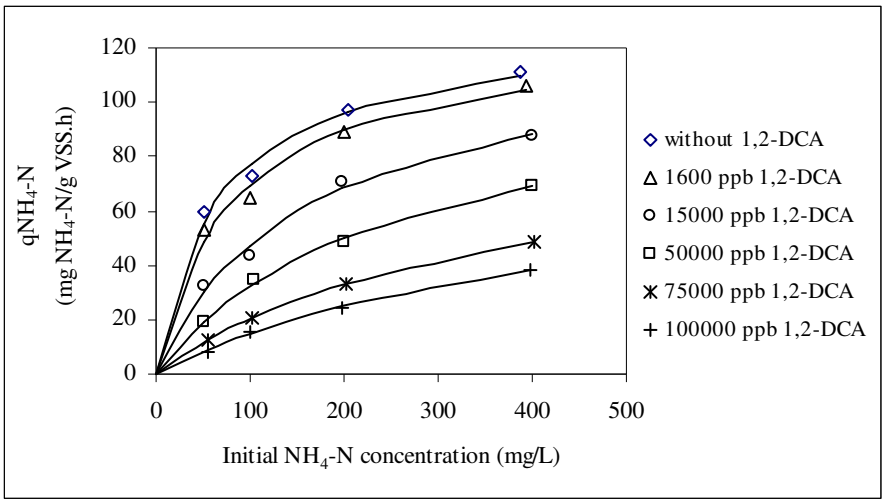

Figure 6.39. Specific ammonium utilization rates ($q_{NH4\text{-}N}$) in the presence of 1,2-DCA

At various 1,2-DCA concentrations, $q_{NH4\text{-}N}$ pattern still followed the Monod model (Eqn. 6.1). Increasing the 1,2-DCA concentration resulted in a relative decrease in $q_{NH4\text{-}N}$ with respect to the base $q_{NH4\text{-}N}$ in the absence of 1,2-DCA, indicating the inhibitory effect of 1,2-DCA on nitrification. However, in the study of Rasche et al. (1991), 1,2-DCA was classified as a compound having little or no toxic effect on pure *Nitrosomonas europaea* cells in terms of oxygen uptake activity of cells 1 h preincubated with NH_4-N and 1,2-DCA. In another study performed with pure *Nitrosomonas europaea* cells exposed to 0.4-0.58 mg/L NH_4-N and 2500-138000 µg/L 1,2-DCA (Ely et al., 1997) 1,2-DCA showed no deleterious effect on ammonia-oxidizing activity up to 138000 µg/L of 1,2-DCA.

The analyses of data in Figure 6.39 by linearization methods (Table 6.1) and nonlinear least square regression (NLSR) (Section 6.1.1) are illustrated in Figures 6.40-6.44. The apparent $q_{max,NH4\text{-}N}$ ($q^{app}_{max,NH4-N}$) and the apparent K_s (K^{app}_s) values determined from these analyses are summarized in Table 6.7. These estimated $q^{app}_{max,NH4-N}$ *and* K^{app}_s values at various 1,2-DCA concentrations were further analyzed in Section 6.8.3 in order to evaluate the effect of 1,2-DCA on ammonium utilization.

6.8.2.1. Statistical Analysis of Kinetic Models. The kinetic models were developed by placing the $q^{app}_{max,NH4-N}$ and K^{app}_s values determined with linearization plots and NLSR analysis (Table 6.7) to the Eqn. 6.1. These models were analyzed statistically to evaluate

the differences between model results and experimental data. For this purpose, initially, the residuals between experimental data and model results were examined. A few examples of these analyses are illustrated in Appendix T. Residuals appeared to be random and hence provided evidence that all models developed have no serious deficiencies. As a next step, analysis of variance (ANOVA) was performed at 95% confidence level (α= 0.05) using the MINITAB package program (Minitab Inc. U.S.). P-values resulting from these analyses (see Appendix T) were greater than α=0.05 indicating that there are no significant differences among the models developed by linearization and NLSR.

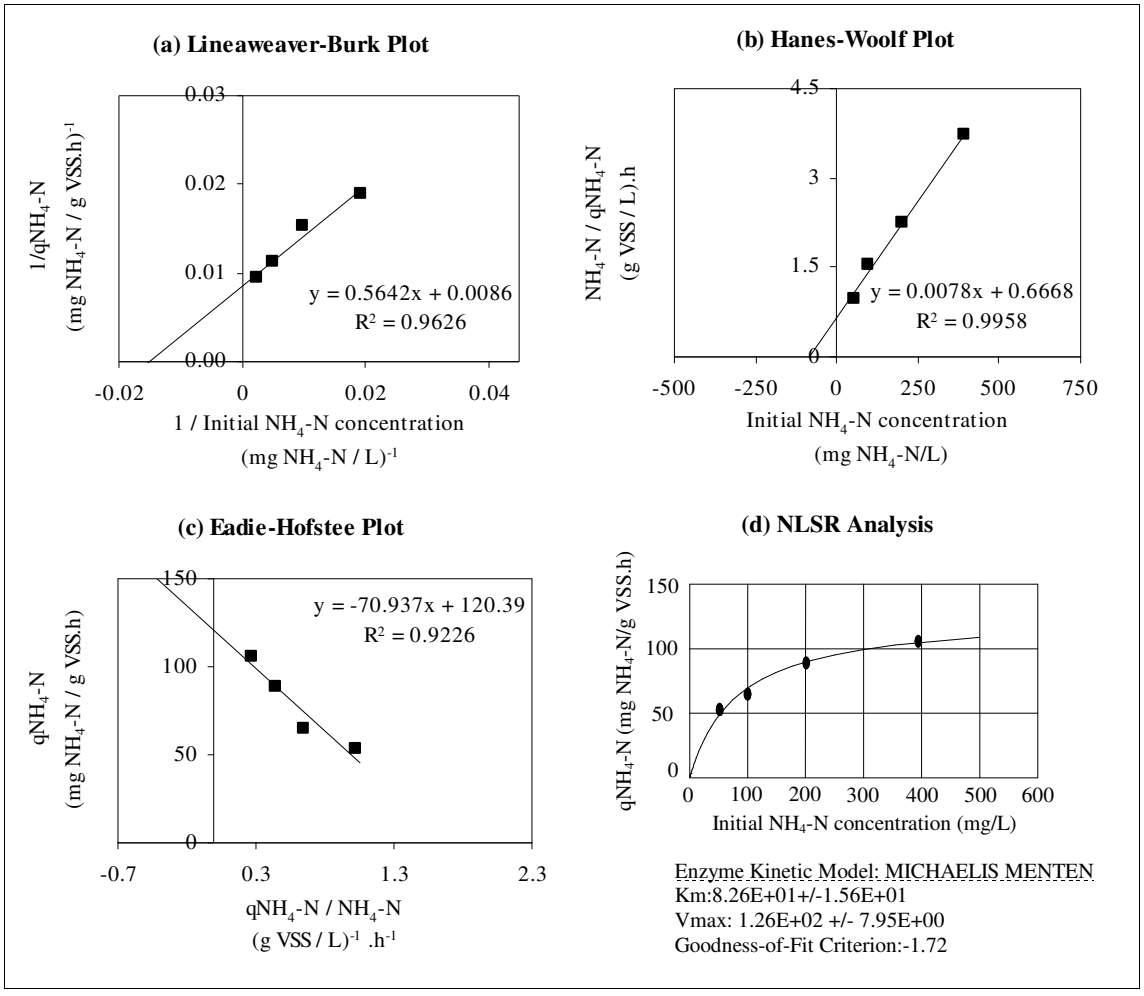

Figure 6.40. Determination of $q^{app}_{\max,NH\,4-N}$ *and* K^{app}_{s} at an initial 1,2-DCA concentration of 1600 µg/L using (a) Lineweaver-Burk plot, (b) Hanes-Woolf plot, (c) Eadie-Hofstee plot, and (d) NLSR analysis

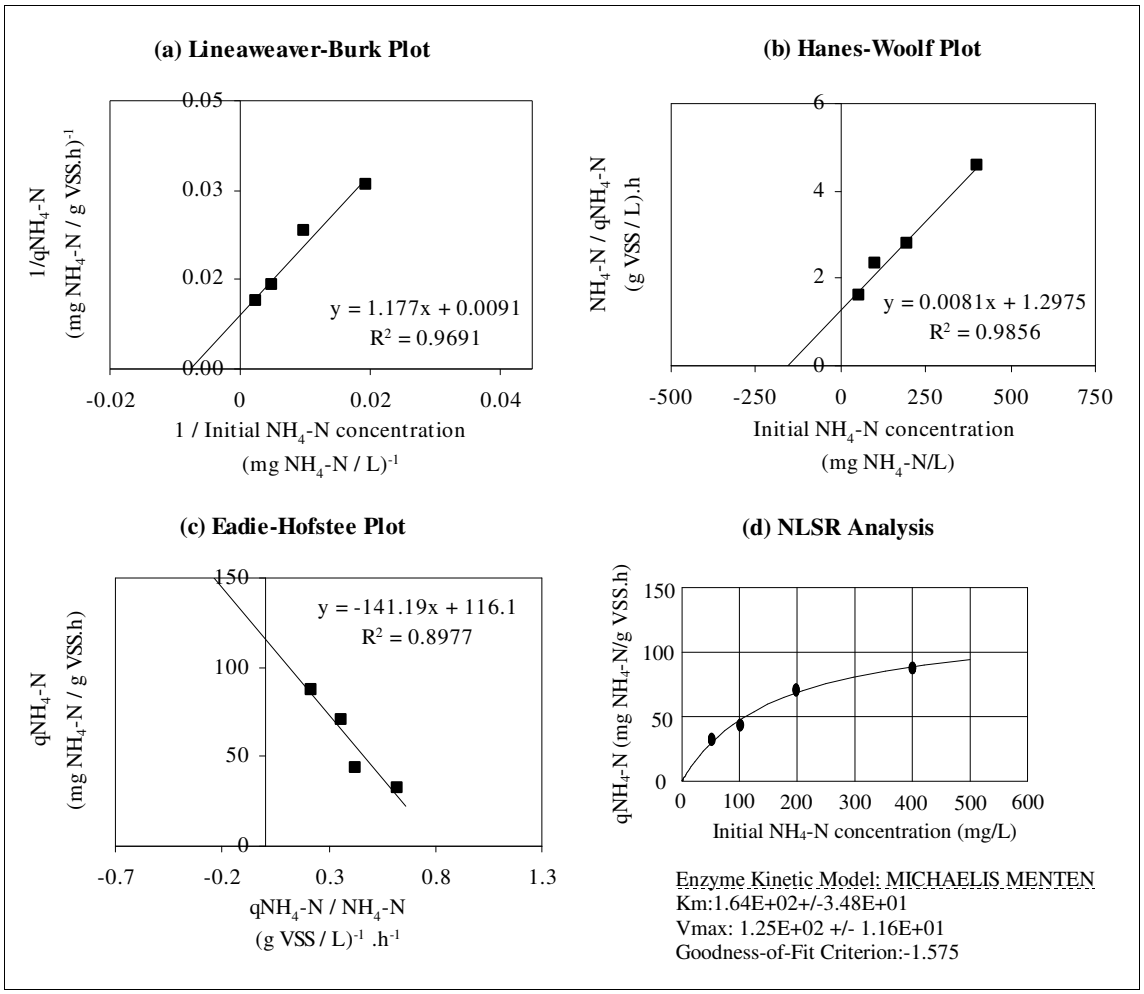

Figure 6.41. Determination of $q^{app}_{\max,NH\,4-N}$ *and* K^{app}_{s} at an initial 1,2-DCA concentration of 15000 µg/L using (a) Lineweaver-Burk plot, (b) Hanes-Woolf plot, (c) Eadie-Hofstee plot, and (d) NLSR analysis

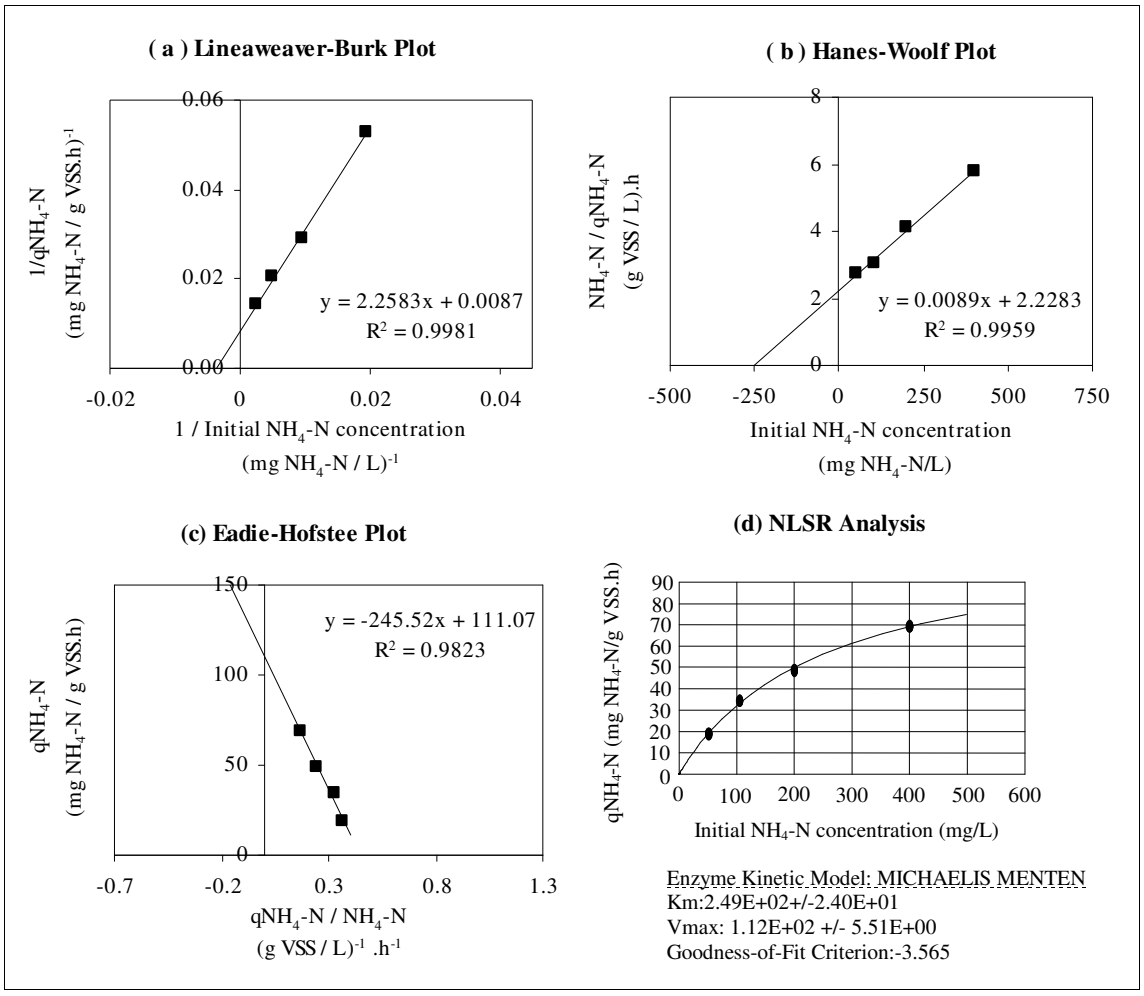

Figure 6.42. Determination of $q^{app}_{\max,NH\,4-N}$ *and* K^{app}_{s} at an initial 1,2-DCA concentration of 50000 µg/L using (a) Lineweaver-Burk plot, (b) Hanes-Woolf plot, (c) Eadie-Hofstee plot, and (d) NLSR analysis

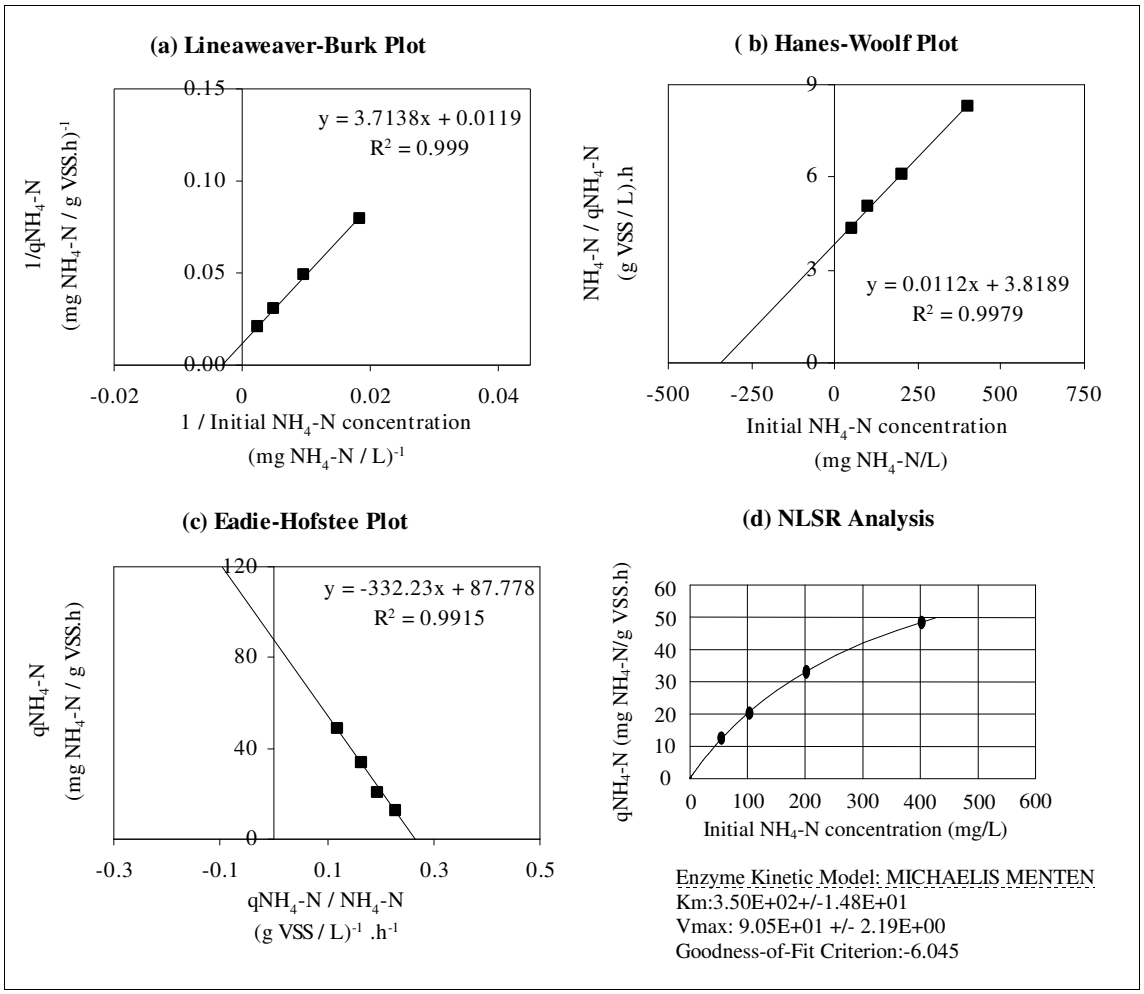

Figure 6.43. Determination of $q^{app}_{\max,NH\,4-N}$ *and* K^{app}_{s} at an initial 1,2-DCA concentration of 75000 µg/L using (a) Lineweaver-Burk plot, (b) Hanes-Woolf plot, (c) Eadie-Hofstee plot, and (d) NLSR analysis

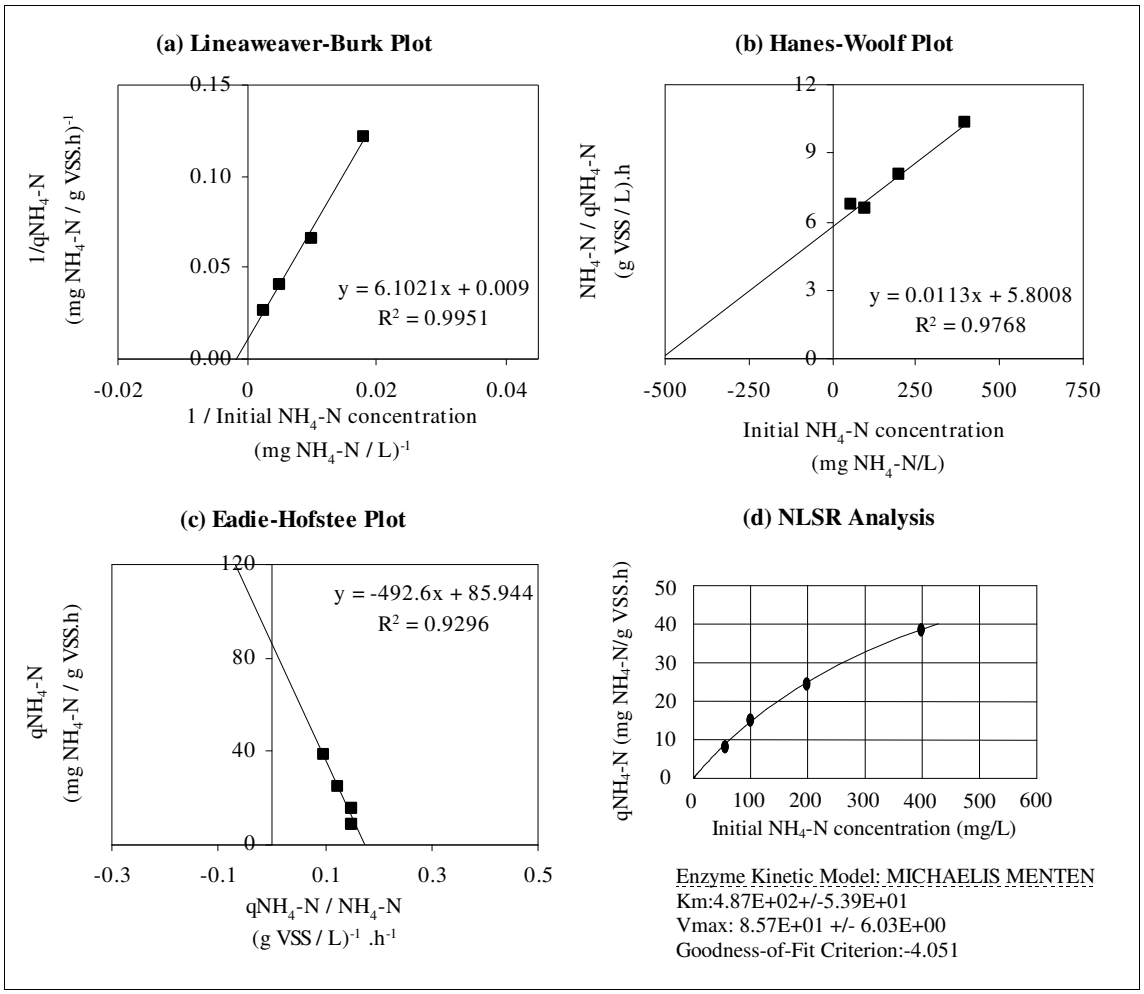

Figure 6.44. Determination of $q^{app}_{\max,NH\,4-N}$ *and* K^{app}_{s} at an initial 1,2-DCA concentration of 100000 µg/L using (a) Lineweaver-Burk plot, (b) Hanes-Woolf plot, (c) Eadie-Hofstee plot, and (d) NLSR analysis

Table 6.7. Apparent maximum specific ammonium utilization rates ($q_{\max,NH4-N}^{app}$) and apparent half-saturation constants (K_s^{app}) estimated by linearization methods and NLSR analysis at various 1,2-DCA concentrations

Method	in the absence of 1,2-DCA			1600 µg/L 1,2-DCA			15000 µg/L 1,2-DCA			50000 µg/L 1,2-DCA			75000 µg/L 1,2-DCA			100000 µg/L 1,2-DCA		
	R^2	$q_{\max,NH4-N}^{app}$ mgNH4-N / gVSS.h	K_s^{app} mg/L	R^2	$q_{\max,NH4-N}^{app}$ mgNH4-N / gVSS.h	K_s^{app} mg/L	R^2	$q_{\max,NH4-N}^{app}$ mgNH4-N / gVSS.h	K_s^{app} mg/L	R^2	$q_{\max,NH4-N}^{app}$ mgNH4-N / gVSS.h	K_s^{app} mg/L	R^2	$q_{\max,NH4-N}^{app}$ mgNH4-N / gVSS.h	K_s^{app} mg/L	R^2	$q_{\max,NH4-N}^{app}$ mgNH4-N / gVSS.h	K_s^{app} mg/L
Lineweaver-Burk (1/q vs. 1/S)	0.96	121.95	56.36	0.96	116.27	65.60	0.96	109.89	129.34	0.99	114.94	259.57	0.99	84.03	312.08	0.99	111.11	678.01
Hanes-Woolf (S/q vs. S)	0.99	131.57	71.97	0.99	128.20	85.48	0.98	123.45	160.18	0.99	112.35	250.37	0.99	89.28	340.97	0.94	88.49	513.34
Eadie-Hofstee (q vs. q/S)	0.92	124.22	59.72	0.92	120.39	70.93	0.89	116.10	141.19	0.98	111.07	245.52	0.99	87.77	332.23	0.85	85.94	492.6
NLSR analysis (Non-linear Least Square Regression)	0.92	129.26±7.7	68.54±13.5	0.93	126.41±7.9	82.61±15.6	0.95	124.5±11.5	163.99±34.8	0.99	112±5.5	249.16±24	0.99	90.50±2.1	349.66±14.8	0.99	85.68±6	486.52±53.8

6.8.3. Inhibitory Characteristics of 1,2-DCA on Ammonium Utilization

As done in TCE (Section 6.5.3), the inhibitory characteristics of 1,2-DCA on ammonium utilization was initially evaluated by comparing the Figure 6.45 (grouped plottings of Figures 6.38, 6.40-6.44) with the Figure 6.22. The comparison of left hand quadrants in Figure 6.45 with Figure 6.22 clearly indicated a typical mixed inhibition characteristic.

As the next step, the data in Table 6.7 were evaluated to diagnose the type of 1,2-DCA inhibition on nitrification. $q^{app}_{\max,NH4-N}$ and K^{app}_{s} values estimated at various 1,2-DCA concentrations were compared with the base $q^{app}_{\max,NH4-N}$ and K^{app}_{s}. As the initial 1,2-DCA concentration increased, K^{app}_{s} also increased, whereas $q^{app}_{\max,NH4-N}$ decreased. These results exactly coincide with the characteristics of a mixed inhibitor, which can bind both to the free enzyme (E) to build the enzyme-inhibitory substance (EI) complex with a dissociation constant K_{ic} and to the enzyme-substrate (ES) complex to build the enzyme-substrate-inhibitory substance (ESI) complex with a dissociation constant K_{iu} as explained in detail in Section 3.1.1.2. Hence, depending on the binding constants (K_{ic}, K_{iu}) of the inhibitor, both competitive and uncompetitive effects can be observed (Cornish-Bowden, 1995).

In view of the above-mentioned findings, 1,2-DCA was found to be a mixed inhibitor of ammonia oxidation. In a previous research performed with pure *Nitrosomonas europaea* species (Ely et al., 1997), the type of 1,2-DCA inhibition on nitrification was reported to be much more strongly competitive. However, in that study, the base data for competitive inhibition was not shown. Therefore, it is not possible to comment on why 1,2-DCA exhibited different inhibition characteristics in our study and that with pure *Nitrosomonas europaea* species (Ely et al., 1997).

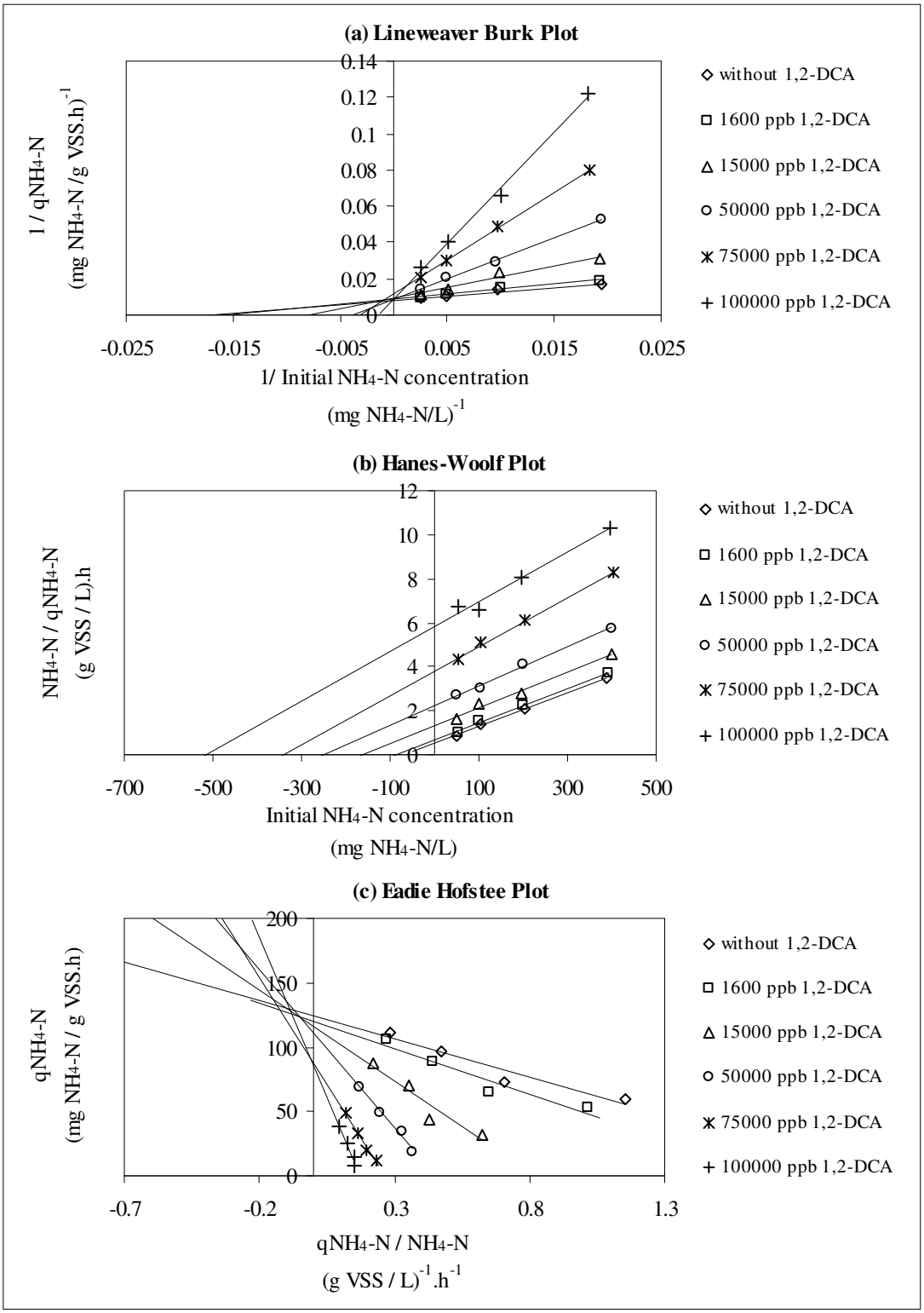

Figure 6.45. Effects of 1,2-DCA on ammonium utilization rate as reflected by (a) Lineweaver-Burk plot, (b) Hanes-Woolf Plot and (c) Eadie-Hofstee Plot

6.8.4. Determination of the Inhibition Coefficients (K_{ic} and K_{iu}) of 1,2-DCA

As described in Section 3.1.1.2, the net effect of a mixed inhibitor on substrate utilization (Eqn. 6.5) is to increase or decrease K_s by a factor $(1+I/K_{ic})/(1+I/K_{iu})$ while decreasing $q_{m\ by}$ a factor of $1/(1+I/K_{iu})$. Competitive inhibition is the limiting case of mixed inhibition in which K_{iu} approaches infinity, i.e. I/K_{iu} is negligible at all values of I and hence disappears from Eqn. 6.5. Similarly, uncompetitive inhibition is the other limiting case of mixed inhibition in which K_{ic} approaches infinity, i.e. I/K_{ic} is negligible at all values of I and hence disappears from Eqn. 6.5 (Cornish-Bowden, 1995).

$$q = \frac{q_m^{app} S}{K_s^{app} + S} = \frac{q_m \left[1/(1 + \frac{I}{K_{iu}}) \right] S}{K_s \left[(1 + \frac{I}{K_{ic}}) / (1 + \frac{I}{K_{iu}}) \right] + S} \qquad (6.5)$$

where K_{ic} is the dissociation constant of enzyme- inhibitory compound (EI) complex, K_{iu} is the dissociation constant of enzyme-substrate-inhibitory compound (EIS) complex.

The K_{ic} and K_{iu} values shown in Eqn. 6.5 can be found by plotting $K_S^{app} / q_{\max}^{app}$ and $1/q_{\max}^{app}$ values against the inhibitor concentrations [I], respectively. In each case, the result should be a straight line, with an intercept $-K_{ic}$ on the x-axis if $K_S^{app} / q_{\max}^{app}$ is plotted and intercept $-K_{iu}$ on the x-axis if $1/q_{\max}^{app}$ is plotted (Cornish–Bowden, 1995) To find the inhibition constants of 1,2-DCA, $K_S^{app} / q_{\max}^{app}$ and $1/q_{\max}^{app}$ values estimated with Hanes-Woolf, Eadie-Hofstee and NLSR methods (Table 6.7) were plotted against the initial 1,2-DCA concentrations as illustrated in Figures 6.46 and 6.47, respectively. In this analysis, Lineweaver-Burk plot results were disregarded due to fluctuations observed in either $q_{\max,NH4-N}^{app}$ *or* K_s^{app} as seen from Table 6.7.

The K_{ic} and K_{iu} values found from Figures 6.46 and 6.47 are summarized in Table 6.8. The K_{ic} values estimated by different methods was in the range of 6000-8000 µg/L 1,2-DCA, significantly lower than the range of K_{iu} (188000-200000 µg/L 1,2-DCA). This

indicated that 1,2-DCA had a greater affinity for the enzyme AMO (E) than the enzyme-substrate (ES) complex. In other words, at low 1,2-DCA concentrations (e.g < 25000 µg/L) the competitive characteristic of 1,2- DCA is stronger than its mixed characteristics, but still the mixed inhibition cannot be disregarded. In the study of Ely et al. (1997) performed with pure *Nitrosomonas europaea* cultures, 1,2-DCA inhibition on nitrification was reported to be much more strongly competitive and only the competitive inhibition constant K_{ic} was reported, and not the uncompetitive inhibition constant K_{iu}. Further, the K_{ic} value of 1000 ±360 µM (99000±3600 µg/L) reported in that study (Ely et al., 1997) is much higher than in the present study. The discrepancy between the result of the present study and that of Ely et al. (1997) may be attributed to different experimental conditions, such as temperature, nitrifier species, and the use of an enriched culture instead of a pure culture.

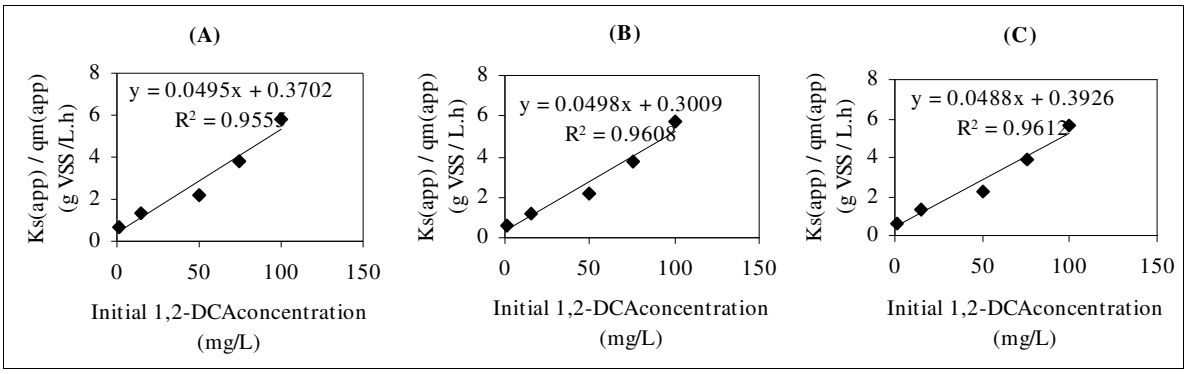

Figure 6.46. Estimation of the 1,2-DCA inhibition constant (K_{ic}) using the results of (a) Hanes-Woolf plot, (b) Eadie-Hofstee plot, and (c) non-linear regression analysis

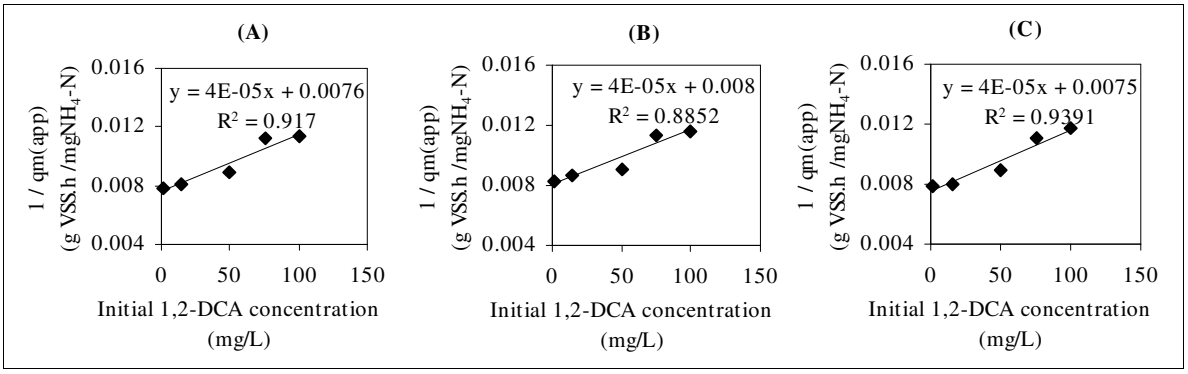

Figure 6.47. Estimation of the 1,2-DCA inhibition constant (K_{iu}) using the results of (a) Hanes-Woolf plot, (b) Eadie-Hofstee plot, and (c) non-linear regression analysis

Table 6.8. Estimation of the 1,2-DCA inhibition constant (K_{ic} and K_{iu}) by several linearization methods and non-linear regression analysis

Source of Data	Estimated K_{ic} µg /L [µM]	Estimated K_{iu} µg /L [µM]
Hanes-Woolf Plot results	7478 [75.57]	190000[1920]
Eadie-Hofstee Plot results	6042 [61.05]	200000[2021]
NLSR analysis results	8045 [81.30]	187500 [1895]

As reported in Section 6.8.1, K_S^{app} value in the absence of 1,2-DCA was in the range of 56-71 mg/L NH_4-N, which corresponds to 4000-5072 µM. The comparison of this value with the K_{ic} values reported in Table 6.8 clearly indicates that the affinity of 1,2-DCA for AMO enzyme is significantly higher than that of ammonium.

6.8.5. Evaluation of Cometabolic 1,2-DCA Degradation in Dependence of Ammonium Degradation

The specific cometabolic degradation rate of 1,2-DCA (q_{DCA}) was evaluated at the initial NH_4-N concentrations of 100, 200 and 400 mg/L by keeping the initial 1,2-DCA concentration constant. In batch experiments with 1,2-DCA (Section 6.7.3), q_{DCA} values were also estimated at initial NH_4-N concentration of 50 mg/L for a 1,2-DCA range of 1600-100000 µg/L (Exp. No: 2-6). Since the experimental conditions in those experiments were the same as in present batch kinetic experiments, these values were also used in data analysis, as shown in Figures 6.48 and 6.49.

At each initial NH_4-N concentration studied (Figure 6.48), the cometabolic degradation rate of 1,2-DCA increased linearly with 1,2-DCA. The first-order cometabolic degradation rate constants of 1,2-DCA were determined as 0.4296 L/g VSS.h at 50 mg/L NH_4-N, 0.6077 L/g VSS.h at 100 mg/L NH_4-N, 0.796 L/g VSS.h at 200 mg/L NH_4-N and 0.8741 L/g VSS.h at 400 mg/L NH_4-N. In a previous study performed with pure *Nitrosomonas europaea* species, this constant was reported as 0.37 L/mg.d (15.41 L/g VSS.h) for an initial 1,2-DCA range of 2500-140000 mg/L (Alvarez-Cohen and Speitel,

2001). This value is significantly higher than our values due to the reasons explained in detail in Section 6.5.6.

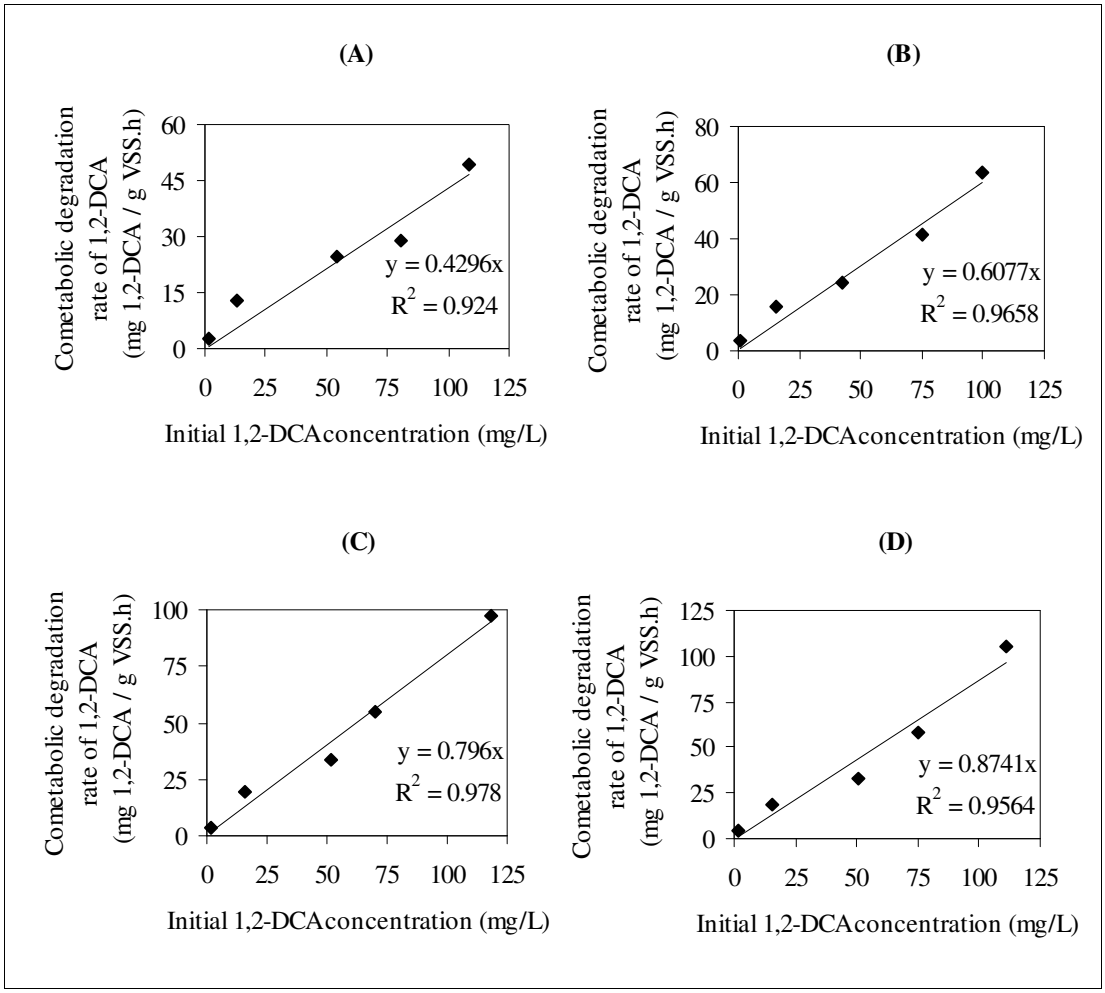

Figure 6.48. Cometabolic degradation rates of DCA (q_{DCA}) at initial NH_4-N concentrations of (a) 50 mg/L, (b) 100 mg/L, (c) 200 mg/L, (d) 400 mg/L with respect to the initial 1,2-DCA concentrations

Figure 6.49 illustrates the dependence of q_{DCA} values on ammonium utilization rates at each initial 1,2-DCA concentration. The q_{DCA} values observed at each 1,2-DCA concentration exhibited an increase with qNH_4-N and almost reached a saturation point at high q_{NH4-N} values. The increases in cometabolic 1,2-DCA degradation rates at increased ammonium utilization rates may be explained by NAD(P)H (reductant) regeneration by the growth substrate as discussed in Section 6.5.6. The nitrifying biomass had obviously a quite high capacity for cometabolic removal even at relatively high concentrations of 1,2-DCA.

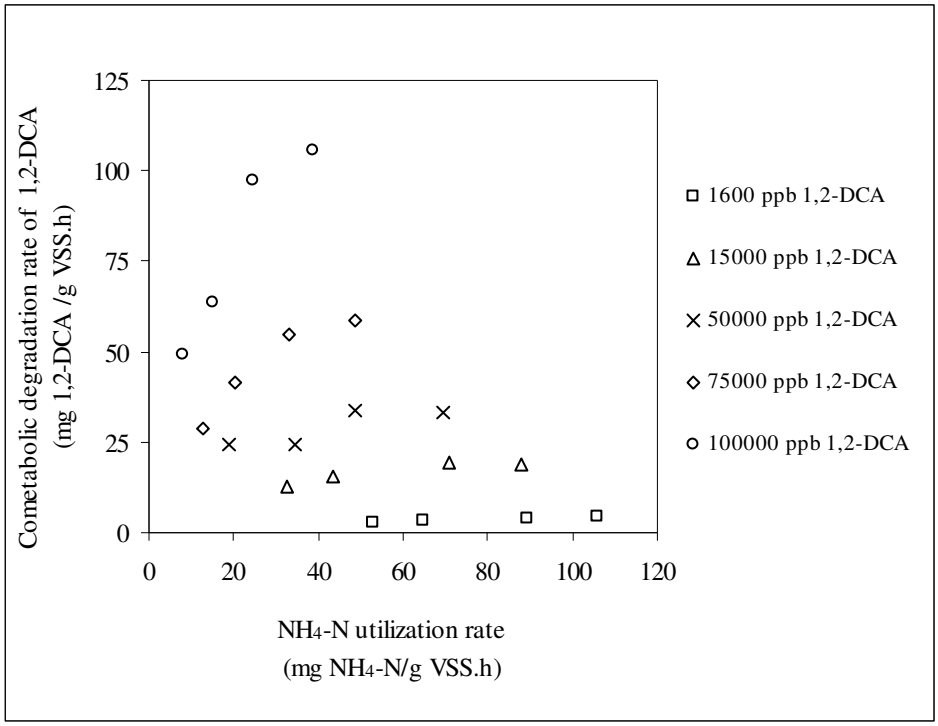

Figure 6.49. Dependence of cometabolic 1,2-DCA degradation rates (q_{DCA}) on ammonium utilization rates (q_{NH4-N}) at various 1,2-DCA levels

In the present study, the transformation yields were estimated by dividing the 1,2-DCA degradation rates (q_{DCA}) shown in Figure 6.49 by the corresponding NH_4-N utilization rates (q_{NH4-N}). As in the case of TCE (Section 6.5.6), considering that the q_{NH4-N}/q_{DCA} ratio equals $1/T_y$, a correlation between T_y and the initial 1,2-DCA and NH_4-N concentrations can be found by rearranging Eqn. 6.3:

$$1/T_y = \varepsilon \, (NH_4\text{-}N \, / \, 1,2\text{-}DCA) \qquad (6.7)$$

In Figure 6.50, plotting q_{NH4-N}/q_{DCA} against the initial NH_4-N/1,2-DCA showed that up to NH_4-N/1,2-DCA ratio of 110 a strong linear relationship exists between q_{NH4-N}/q_{DCA} ($1/T_y$) and initial NH_4-N/1,2-DCA ratio. The ε value was found as 0.2232. However, beyond this ratio, increasing NH_4-N/1,2-DCA ratio will not result in a further increase in $1/T_y$.

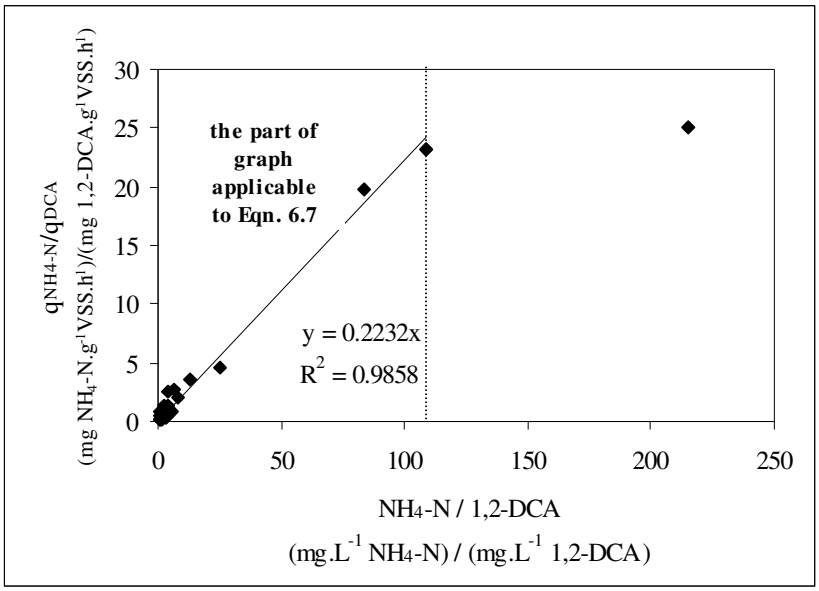

Figure 6.50. Relationship between the relative ratio of ammonium and 1,2-DCA degradation and the relative ratio of ammonium and 1,2-DCA concentrations

6.8.6. Implications for Engineering Applications

The findings of this research have relevance for the improvement of engineered remediation/treatment systems for 1,2-DCA removal from industrial effluents (such as discharges from vinyl chloride, organic solvents production industries) industries and many groundwater systems. The implications of this research for real treatment systems can be presented by imagining the following scenario:

Consider that historic spillages of 1,2-DCA at a vinyl chloride production plant has lead to pollution of the underlying aquifer. In the groundwater samples taken from the aquifer, the maximum 1,2-DCA concentration was detected around 1.6 mg/L. The groundwater at that site can be treated in an ex-situ treatment system using a mixed culture enriched for nitrifiers. Here, the growth substrate NH_4-N will be added to the contaminated groundwater and the process may proceed in a batch reactor until the desired level of treatment is achieved. In the design of this system, the amount of NH_4-N to be added to the system should be selected by considering that 1,2-DCA will be removed with efficient use of NH_4-N. If two alternative initial NH_4-N concentrations of 50 and 200 mg/L are chosen, based upon Equation 6.7, transformation yield (T_y) of 1,2-DCA, which is the amount of 1,2-DCA that can be degraded per unit mass of ammonium**,** will be 0.14 and 0.035,

respectively. If 100% 1,2-DCA removal takes place, based on the calculated T_y values, the decrease in ammonium concentration will be around 11 mg/L at 50 mg/L NH_4-N and 45 mg/L at 200 mg/L NH_4-N. Therefore, the effluent of the system will contain a significant amount of NH_4-N if 200 mg/L NH_4-N is added. However, as seen from Figure 6.48, increasing NH_4-N from 50 to 200 mg/L will not cause a significant change in 1,2-DCA transformation rate indicating that the time necessary to achieve 100% 1,2-DCA removal will be not much different for both ammonium concentrations. Thus, in that case the lower influent NH_4-N should be chosen.

Similarly, other scenarios can be imagined and the 1,2-DCA removal and nitrification patterns can be predicted for different influent 1,2-DCA and NH_4-N concentrations. These scenarios can also be applied to continuous-flow systems.

6.9. Continuous-Flow Experiments in a Nitrifying Biofilm Reactor

6.9.1. Evaluation of the Hydraulic Behavior in the Nitrifying Biofilm Reactor

The hydraulic behavior of the nitrifying biofilm reactor (Figure 5.5) was investigated during the continuous operation of the reactor for a month at an influent NH_4-N concentration of 35-55 mg/L. The NH_4-N measurements in the samples taken from various depths of the reactor (Port 0, Port 1, Port 2) are shown in Figure 6.51. During one-month operation, samples taken from various depths of the reactor showed negligible concentration gradients in NH_4-N. Regarding these results, the reactor was accepted as a completely stirred tank reactor (CSTR).

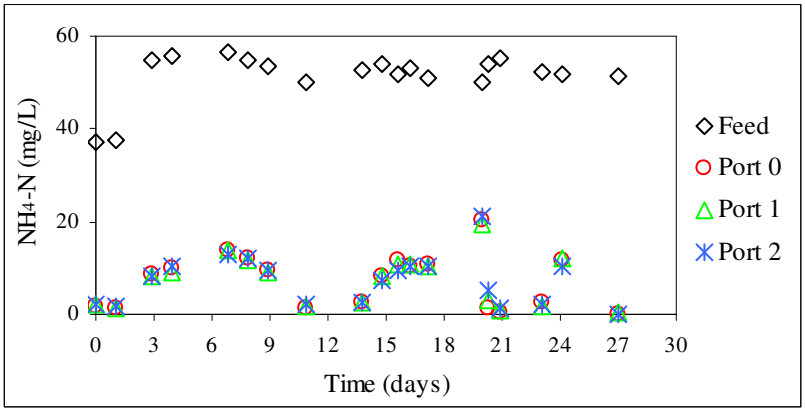

Figure 6.51. Daily NH_4-N measurements at various depths of the nitrifying biofilm reactor

6.9.2. Evaluation of the Nitrification Efficiency of the Nitrifying Biofilm Reactor Prior to Experiments with 1,2-DCA

Before starting the continuous-flow experiments with 1,2-DCA dosing, the nitrifying biofilm reactor, which was enriched for nitrifiers since 1994, was initially operated at various ammonium loading rates to investigate its nitrification efficiency in terms of ammonia removal, nitrite accumulation, nitrate formation.

NH_4-N loading and removal rate, nitrite accumulation rate, nitrate production rate and free ammonia (FA) concentration calculated from daily measurements at each ammonia loading are given in Table 6.9. The values presented in this table are steady–state

values. The achievement of steady-state conditions is shown in Figures R.1-R.2 in Appendix R. As seen from Table 6.9, except in Run 4, the bulk DO concentration ranged between 2.5 –3.5. The surface ammonium loading rate in the system, which is the removal rate per unit packing surface area, varied in the range of 2.05-11.97 $g/m^2.d$.

In a biofilm system, the reaction rate per unit biofilm area may be governed by liquid film diffusion, diffusional resistance to the penetration of the substrate, and/or by the intrinsic enzymatic reaction by some saturation expression such as Monod. It has been demonstrated that this leads to bulk first-order reactions because of either liquid film diffusion or first-order enzymatic reactions at low concentrations; to bulk half-order reactions at higher concentrations for biofilms that are only partly penetrated by the substrate. Finally, it may lead to bulk zero-order reactions at high concentrations when the biofilm is fully penetrated by the substrate (Çeçen and Gönenç, 1995). In order to illustrate the application of fundamental biofilm kinetics described above, the surface ammonium removal rates (Table 6.9) were plotted against the bulk NH_4-N concentrations as shown in Figure 6.52. In compliance with theoretical considerations, ammonium removal rate seems to be of first-order at low ammonium concentrations.

When the bulk NH_4-N concentration was in range of about 0.05-1.6 mg/L (Figure 6.52), nitrification followed half-order kinetics according to Eqn. 6.8. Half-order kinetics occurs when ammonium penetrates into the biofilm partially whereas dissolved oxygen penetrates fully into the film. Therefore, in that range, ammonium was the rate-limiting substrate. The half-order rate constant ($k_{1/2an}$) in this range was found as 0.86 $g^{1/2}/m^{1/2}.d$. Similarly, in a previous study (Çeçen and Gönenç, 1994) performed with a biofilm reactor with similar packing, the half-order reaction rate constant was reported as 0.9 $g^{1/2}/m^{1/2}.d$.

$$r_{an} = k_{1/2an} S_n^{*1/2} \tag{6.8}$$

where r_{an} is the ammonium removal rate, $g/m^2.d$; $k_{1/2an}$ is the half-order ammonium rate constant, $g^{1/2}/m^{1/2}.d$, and S_n^* is the bulk ammonium concentration, mg/L.

As seen from Figure 6.52, in a wide bulk ammonium range of 1.6-196 mg/L variations in bulk ammonia concentrations did not significantly affect the reaction rate indicating that nitrification became a zero-order reaction in ammonium according to Eqn. 6.9.

$$r_{an} = k_{0fn} L = k_{0an} \tag{6.9}$$

where k_{0fn}=intrinsic rate constant; L is the biofilm thickness; k_{0an} is the zero-order ammonium rate constant, g/m^2.d.

The observation of zero-order rate can be explained by oxygen limitation as also concluded in a number of researches (Çeçen and Gönenç, 1994; Çeçen and Gönenç, 1995; Çeçen, 1996; Çeçen and Orak, 1996). The concentration of the DO inside the biofilm is different from that in the bulk liquid and diminishes at some biofilm depth. Thus, although the full penetration of ammonium is no longer a problem at high concentrations, the DO concentration inside the filter limits the nitrification rate (Çeçen, 1996). In the present study, in the DO concentration range of 2.5-3.5 mg/L, the zero-order ammonium rate constant (k_{0an}) was found as 5.2±0.62 g/m^2.d. Similarly, in a previous study performed with the same biofilm reactor (Çeçen, 1996), k_{0an} was reported as 5.94 g/m^2.d in the DO concentration range of 2-3.5 mg/L.

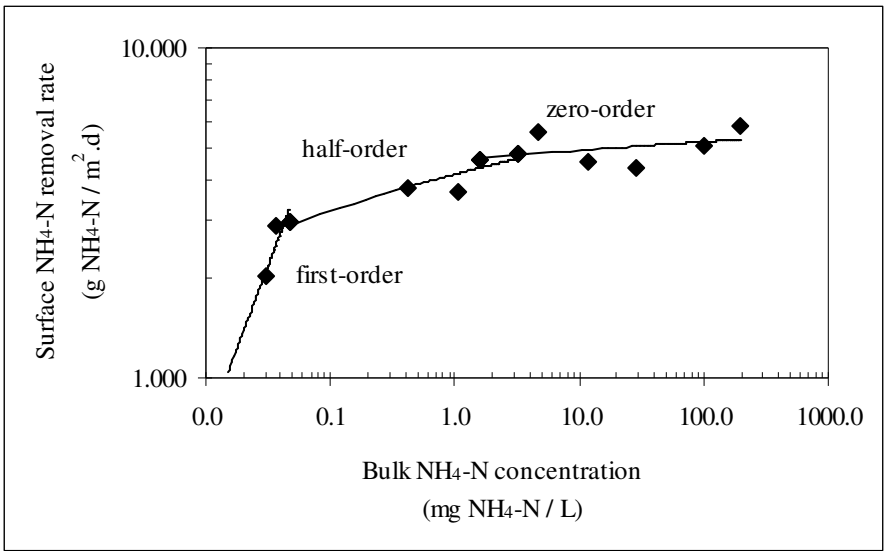

Figure 6.52. Dependence of ammonium removal rate on bulk ammonium concentration

In order to perform a further kinetic analysis in the nitrifying biofilm reactor, the variations in surface ammonium removal, nitrite accumulation, nitrate formation rates with the change in surface ammonium loading rates were illustrated in Figure 6.53. NH_4-N removal rate (r_{NH4-N}) showed an increase with NH_4-N loading rate and reached almost a saturation at a loading rate of 4.63 g/m^2.d. Beyond this point, the removal rate did not increase significantly with increased loading due to oxygen limitation. In the DO range of 2.5-3.5 mg/L, the system reached the maximum removal rate of 5.2±0.62 g/m^2.d. In previous studies performed with the same biofilm reactor, the maximum removal rates were observed as 3.5 g/m^2.d at a DO of 3.2-3.5 mg/L (Çeçen and Orak, 1996), 3.76 g/m^2.d at a DO of 3.2- 3.5 mg/L (Çeçen et al., 1995) and 5.94 g/m^2.d at a DO of 2-3.5 mg/L (Çeçen, 1996). The comparison of the value achieved in the present study with those reported in the past shows that better ammonia removal rates were achieved. This is most probably related with the enrichment of the reactor for nitrifiers due to the prolonged feeding with ammonium and mineral solutions only since 1994. However, the evaluation of the reactor in terms of nitrite accumulation and nitrate formation rates (Figure 6.53) clearly shows that increasing NH_4-N loading rates resulted in accumulation of NO_2-N and decrease in NO_3-N production rate (r_{NO3-N}) as shown also in other studies (Çeçen and Gönenç, 1994; Çeçen and Gönenç, 1995; Çeçen et al., 1995; Çeçen, 1996; Çeçen and Orak, 1996). At about 3.8 g/m^2.d and lower ammonium loading rates almost complete nitrification was achieved. Beyond this loading, nitrite accumulation started to increase with increasing ammonium loading rate.

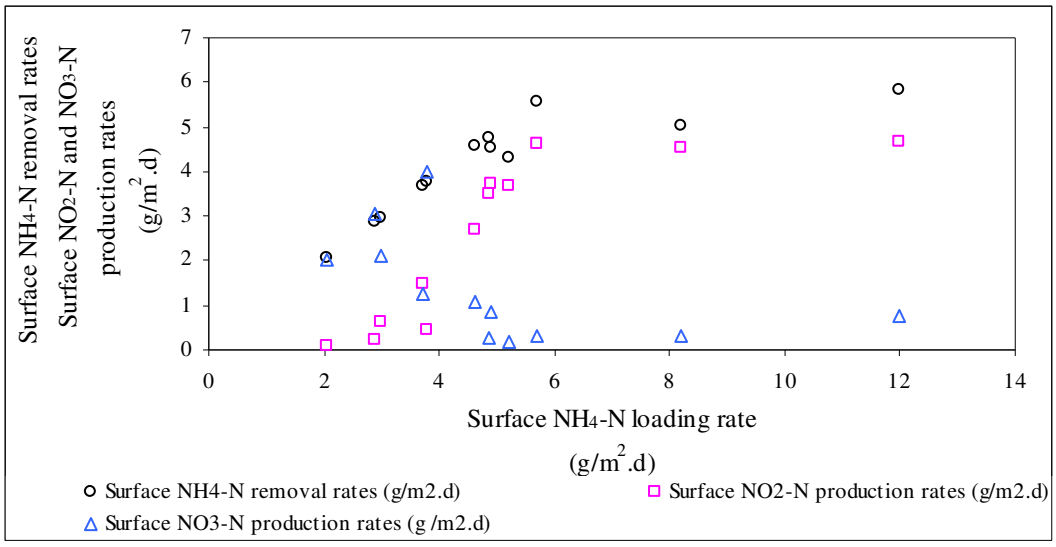

Figure 6.53. Dependence of ammonium removal, nitrite accumulation and nitrate formation rates on ammonium loading rates

NO_2-N accumulation observed at higher ammonia loading rates was further evaluated with respect to the bulk free ammonia (FA) concentrations and bulk DO concentrations reported in Table 6.9. During the runs, free nitrous acid (FNA) concentrations (0.00026-0.0079 mg/L) were much lower than the inhibitory levels reported in the literature (see Section 3.3.1.5) and hence disregarded in the data analysis. The percent inhibition of nitrite oxidation (I) was calculated as described in Eqn. 6.10.

$$I = \frac{r_{NO2-N}}{r_{NH4-N}} x\ 100 \tag{6.10}$$

Figure 6.54 illustrates the dependence of NO_2-N accumulation on free ammonia (FA) and bulk DO concentrations. The increase in FA (from 0.00033 to 21.52 mg/L) led to inhibition of nitrite oxidation due to inhibition of nitrite oxidizing species. However, the percent inhibition of NO_2-N oxidation in Experiments No:3 and No:4 clearly showed that the effect of low bulk DO concentration was more significant than the FA concentration as shown in other studies (Çeçen, 1996; Çeçen and Ipek, 1998).

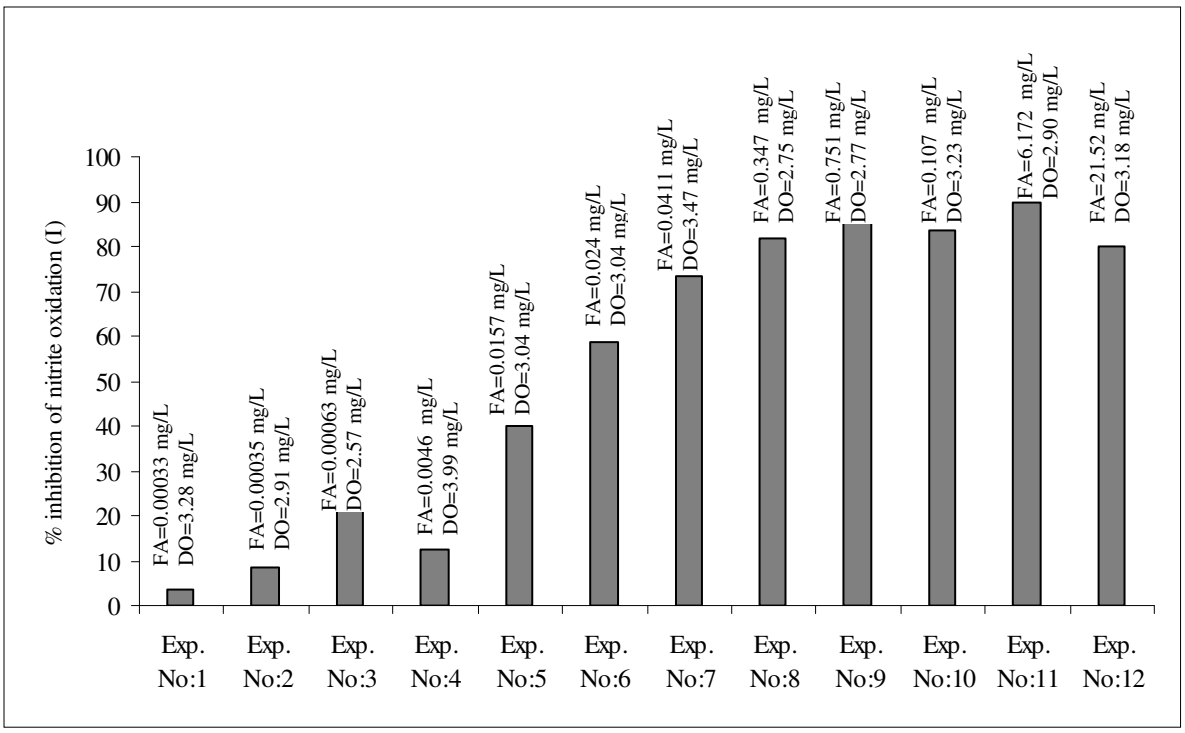

Figure 6.54. Dependence of NO_2-N accumulation on free ammonia (FA) and bulk DO concentrations

Figure 6.55 shows the effects of the C_{DO}/C_{NH4-N} and C_{DO}/C_{FA} ratios on nitrite accumulation. As seen from the figure, the percent inhibition of nitrite oxidation was decreased to very low levels (< 10 %) when the C_{DO}/C_{NH4-N} and C_{DO}/C_{FA} ratios were above 9 and 849, respectively.

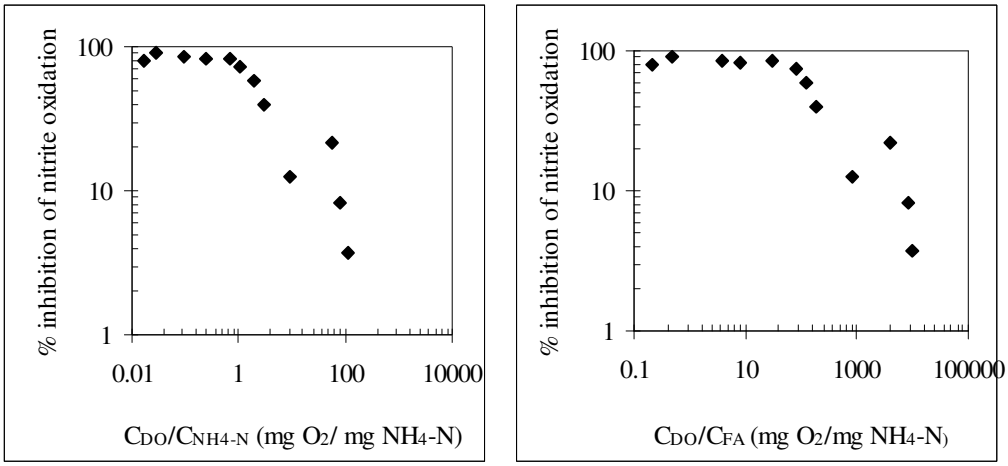

Figure 6.55. Dependence of nitrite accumulation on the ratio of (a) bulk dissolved oxygen to ammonium, (b) bulk dissolved oxygen to free ammonia

Table 6.9. Results of continuous-flow experiments in the nitrifying biofilm reactor under various NH_4-N loadings

Exp. No.	Feed Flowrate	Steady state ave. bulk T	Steady state ave. bulk DO	Steady state ave. bulk pH	Steady state feed NH_4-N	Steady state composite effluent NH_4-N	Free Ammonia Conc.	Steady-state composite effluent NO_2-N	Steady state composite effluent NO_3-N	Volumetric NH_4-N loading rate	Volumetric NH_4-N removal rate	Surface NH_4-N loading rate	Surface NH_4-N removal rate	Volumetric nitrite accumulation rate	Surface nitrite accumulation rate	Volumetric nitrate production rate	Surface nitrate production rate
	(L/day)	^{0}C	mg/L		mg/L	mg/L	mg/L	mg/L	mg/L	kg/m^3.d	kg/m^3.d	g/m^2.d	g/m^2.d	kg/m^3.d	g/m^2.d	kg/m^3.d	g/m^2.d
1	6	24	3.28	7.32	66	0.03	0.000332	2.41	64.65	0.0927	0.0927	2.052	2.051	0.003	0.075	0.091	2.020
2	6	24	2.91	7.27	93	0.04	0.000351	7.71	97.07	0.1306	0.1305	2.891	2.889	0.011	0.241	0.137	3.033
3	6	26	2.57	7.36	95	0.05	0.000637	20.70	67.37	0.1346	0.1345	2.979	2.978	0.029	0.647	0.095	2.105
4	6	23	3.99	7.37	122	0.43	0.004699	15.01	127.47	0.1718	0.1712	3.802	3.789	0.021	0.469	0.180	3.983
5	6	25	3.04	7.43	119	1.06	0.01572	47.07	40.39	0.1680	0.1665	3.719	3.686	0.066	1.471	0.057	1.262
6	6	26	3.04	7.39	148	1.59	0.024054	85.95	34.53	0.2095	0.2073	4.638	4.588	0.121	2.686	0.049	1.079
7	6	24	3.47	7.39	156	3.26	0.041129	112.23	8.01	0.2202	0.2156	4.875	4.773	0.158	3.507	0.011	0.250
8	6	24	2.75	7.77	157	11.75	0.347384	118.49	26.76	0.2216	0.2051	4.906	4.539	0.167	3.703	0.038	0.836
9	6	25	2.77	7.69	167	28.71	0.751424	117.70	5.05	0.2353	0.1948	5.208	4.311	0.166	3.678	0.007	0.158
10	6	25	3.23	7.63	182	4.75	0.107996	148.52	10.08	0.2575	0.2508	5.700	5.552	0.210	4.641	0.014	0.315
11	6	26	2.90	8.04	262	101.17	6.172927	144.48	9.41	0.3704	0.2275	8.198	5.036	0.204	4.515	0.013	0.294
12	6	26	3.18	8.15	383	196.25	21.52036	149.09	24.04	0.5409	0.2638	11.973	5.840	0.210	4.659	0.034	0.751

6.9.3. Continuous-Flow Experiments with 1,2-DCA

Continuous-flow experiments with 1,2-DCA were performed in two sets to investigate the cometabolic degradation, the inhibitory effect on nitrification and recovery of cells from 1,2-DCA inhibition. In the first set, 1,2-DCA concentrations varied between 1539-8087 μg/L (48-253 mg/m^2.d) for an average initial NH_4-N concentration of 152 mg/L (4.734 g/m^2.d). In the second set, 1,2-DCA concentrations varied between 1352-68087 μg/L(42-2128 mg/m^2.d) for an average initial NH_4-N concentration of 50 mg/L (1.566 g/m^2.d). NH_4-N loading and removal rates, nitrite accumulation rates (r_{NO2-N}), nitrate production rates (r_{NO3-N}), 1,2-DCA loading and removal rates and Cl^- production rates (calculated as described in Section 5.5.2) are given in Table 6.10. Stoichiometrically calculated Cl^- production rates in Table 6.10 were found by assuming as if all of the removed 1,2-DCA was fully degraded and converted to the end product Cl^-.

6.9.3.1. Effect of 1,2-DCA on Ammonium Utilization. The surface NH_4-N loading rates, steady-state surface NH_4-N removal rates (r_{NH4-N}) and percent ammonium removal efficiencies are shown in Figures 6.56, 6.57 and 6.58. As seen from Figure 6.56, in the 1st set experiments at high ammonium loadings (152 mg/L NH_4-N; 4.734 g/m^2.d), the influent 1,2-DCA concentration of 1539 μg/L (48 mg/m^2.d 1,2-DCA loading-Exp. No.2) caused almost no change in the ammonium removal efficiency with respect to the base value in Exp. No. 1. However, in the later runs (Exp. No.4 and Exp. No.6), the ammonium removal efficiency started to decrease with increasing influent 1,2-DCA and reached about 40% decrease at the influent 1,2-DCA concentration of 8087 μg/L (253 mg/m^2.d-Exp. No: 6). On the other hand, in the 2nd set of experiments (Figures 6.57 and 6.58) with low ammonium loadings (50 mg/L NH_4-N; 1.566 g/m^2.d), the influent 1,2-DCA concentrations up to 29116 μg/L (910 mg/m^2.d- Exp. No:18) caused almost no change in the ammonium removal efficiency with respect to the base value in Exp. No.8. In case of higher influent 1,2-DCA concentrations (Exp. No: 18 and 20), the ammonium removal efficiency decreased with increased 1,2-DCA loading and reached about 50% decrease at the influent 1,2-DCA concentration of 68087 μg/L (2128 mg/m^2.d-Exp. No: 20). These findings indicated that in case of higher ammonium loadings, the presence of 1,2-DCA inhibits ammonium utilization more severely than at lower ammonium loadings. These findings are not directly comparable with those obtained in batch kinetic experiments. In batch

experiments data interpretation was performed using the initial NH_4-N and 1,2-DCA concentrations rather than bulk concentrations. However, in view of the stronger competitive characteristic of 1,2-DCA observed at low 1,2-DCA concentrations (e.g < 25 mg/L) throughout batch kinetic experiments, it may be possible to conclude that there was also a competition between NH_4-N and 1,2-DCA for the active site of the AMO enzyme in continuous-flow experiments when the bulk 1,2-DCA ranged between 0.099-17.57 mg/L. In case of low ammonium loadings, since the active sites of the enzymes are not fully saturated with the substrate NH_4-N, there will be enough available sites for 1,2-DCA binding and hence the presence of 1,2-DCA will not severely inhibit the ammonium utilization rate. On the other hand, in case of high ammonium loadings, the active sites will begin to be saturated with NH_4-N and the presence of 1,2-DCA will cause severe inhibition of ammonium utilization due to its higher affinity (K_{ic} of 1,2-DCA << K_s of NH_4-N, see Section 6.8.4) for AMO with respect to NH_4-N.

Table 6.10. Results of continuous-flow experiments with 1,2-DCA in the nitrifying biofilm reactor

Exp. No.	Description of Experiment	Feed Flowrate	Steady-state ave. bulk T	Steady-state ave. bulk DO	Steady-state ave. bulk pH	Steady-state ave. feed NH_4-N	Steady-state composite effluent NH_4-N	Steady-state composite effluent NO_2-N	Steady-state composite effluent NO_3-N	Steady-state ave. feed 1,2-DCA	Steady-state composite effluent 1,2-DCA	Steady-state ave. feed Cl^-	Steady-state composite effluent Cl^-	Volumetric NH_4-N loading rate	Volumetric NH_4-N removal rate	Surface NH_4-N loading rate	Surface NH_4-N removal rate	Volumetric nitrite accumulation rate	Surface nnitrite accumulation rate	Volumetric nitrate production rate	Surface nitrate production rate	Surface 1,2-DCA loading rate	Surface 1,2-DCA removal rate	Stochiometrically calculated surface Cl^- production rate acc. to removed 1,2-DCA	Measured surface Cl^- production rate
		L/day	°C	mg/L		mg/L	mg/L	mg/L	mg/L	µg/L	µg/L	µg/L	µg/L	$kg/m^3.d$	$kg/m^3.d$	$g/m^2.d$	$g/m^2.d$	$kg/m^3.d$	$g/m^2.d$	$kg/m^3.d$	$g/m^2.d$	$mg/m^2.d$	$mg/m^2.d$	$mg/m^2.d$	$mg/m^2.d$
1	continuous feeding with only 156 mg/L NH_4-N	6	24	3.69	7.39	156	3.26	112.23	8.01	-	-	-	-	0.2202	0.2156	4.875	4.773	0.1584	3.507	0.0113	0.250	-	-	-	-
2	continuous feeding with 153 mg/L NH_4-N and 1539 ppb 1,2-DCA	6	24	4.40	7.30	153	0.48	77.61	29.39	1539	155	117	1008	0.2153	0.2146	4.766	4.751	0.1096	2.425	0.0415	0.918	48	43	31	28
3	continuous feeding with only 152 mg/L NH_4-N to investigate recovery	6	24	2.74	7.39	152	1.76	109.95	35.29	-	-	-	-	0.2139	0.2114	4.734	4.679	0.1552	3.436	0.0498	1.103	-	-	-	-
4	continuous feeding with 153 mg/L NH_4-N and 4728 ppb 1,2-DCA	6	23	3.65	7.61	153	24.75	86.43	40.73	4728	945	1294	2858	0.2160	0.1811	4.781	4.008	0.1220	2.701	0.0575	1.273	148	118	85	49
5	continuous feeding with only 151 mg/L NH_4-N to investigate recovery	6	25	2.95	7.59	151	16.09	95.11	19.45	-	-	-	-	0.2137	0.1910	4.730	4.228	0.1343	2.972	0.0275	0.608	-	-	-	-

Table 6.10. continued

Exp. No.	Description of Experiment	Feed Flowrate	Steady-state ave. bulk T	Steady-state ave. bulk DO	Steady-state ave. bulk pH	Steady-state ave. feed NH_4-N	Steady-state composite effluent NH_4-N	Steady-state composite effluent NO_2-N	Steady-state composite effluent NO_3-N	Steady-state ave. feed 1,2-DCA	Steady-state composite effluent 1,2-DCA	Steady-state ave. feed Cl^-	Steady-state composite effluent Cl^-	Volumetric NH_4-N loading rate	Volumetric NH_4-N removal rate	Surface NH_4-N loading rate	Surface NH_4-N removal rate	Volumetric nitrite accumulation rate	Surface nnitrite accumulation rate	Volumetric nitrate production rate	Surface nitrate production rate	Surface 1,2-DCA loading rate	Surface 1,2-DCA removal rate	Stochiometrically calculated surface Cl^- production rate acc. to removed 1,2-DCA	Measured surface Cl^- production rate
		L/day	^{0}C	mg/L		mg/L	mg/L	mg/L	mg/L	µg/L	µg/L	µg/L	µg/L	kg/m^3.d	kg/m^3.d	g/m^2.d	g/m^2.d	kg/m^3.d	g/m^2.d	kg/m^3.d	g/m^2.d	mg/m^2.d	mg/m^2.d	mg/m^2.d	mg/m^2.d
6	continuous feeding with 152 mg/L NH_4-N and 8087 ppb 1,2-DCA	6	25	3.80	7.92	152	61.20	54.48	36.72	8087	2436	300	3188	0.2149	0.1285	4.756	2.844	0.0769	1.702	0.0518	1.148	253	177	127	90
7	continuous feeding with only 149 mg/L NH_4-N to investigate recovery	6	25	3.74	7.73	149	15.33	72.54	58.96	-	-	-	-	0.2099	0.1882	4.646	4.167	0.1024	2.267	0.0832	1.843	-	-	-	-
8	continuous feeding with only 52 mg/L NH_4-N	6	26	2.84	7.19	52	0.52	1.37	52.29	-	-	-	-	0.0727	0.0720	1.609	1.593	0.0019	0.043	0.0738	1.634	-	-	-	-
9	continuous feeding with 53 mg/L NH_4-N and 1352 ppb 1,2-DCA	6	26	2.67	7.03	53	2.00	9.13	40.16	1352	298	129	686	0.0744	0.0716	1.647	1.585	0.0129	0.285	0.0567	1.255	42	33	24	17
10	continuous feeding with only 51 mg/L NH_4-N to investigate recovery	6	26	2.39	7.08	51	1.69	2.09	49.14	-	-	-	-	0.0724	0.0701	1.604	1.551	0.003	0.065	0.0694	1.536	-	-	-	-

Table 6.10. continued

Exp. No.	Description of Experiment	Feed Flowrate	Steady-state ave. bulk T	Steady-state ave. bulk DO	Steady-state ave. bulk pH	Steady-state ave. feed NH_4-N	Steady-state composite effluent NH_4-N	Steady-state composite effluent NO_2-N	Steady-state composite effluent NO_3-N	Steady-state ave. feed 1,2-DCA	Steady-state composite effluent 1,2-DCA	Steady-state ave. feed Cl^-	Steady-state composite effluent Cl^-	Volumetric NH_4-N loading rate	Volumetric NH_4-N removal rate	Surface NH_4-N loading rate	Surface NH_4-N removal rate	Volumetric nitrite accumulation rate	Surface nnitrite accumulation rate	Volumetric nitrate production rate	Surface nitrate production rate	Surface 1,2-DCA loading rate	Surface 1,2-DCA removal rate	Stochiometrically calculated surface Cl^- production rate acc. to removed 1,2-DCA	Measured surface Cl^- production rate
		L/day	^{0}C	mg/L		mg/L	mg/L	mg/L	mg/L	µg/L	µg/L	µg/L	µg/L	kg/m^3.d	kg/m^3.d	g/m^2.d	g/m^2.d	kg/m^3.d	g/m^2.d	kg/m^3.d	g/m^2.d	mg/m^2.d	mg/m^2.d	mg/m^2.d	mg/m^2.d
11	continuous feeding with 54 mg/L NH_4-N and 3844 ppb 1,2-DCA	6	26	2.64	7.34	54	0.83	4.57	46.10	3844	946	275	1171	0.0758	0.0746	1.677	1.651	0.0064	0.143	0.0651	1.441	120	91	65	28
12	continuous feeding with only 50 mg/L NH_4-N to investigate recovery	6	26	2.5	7.22	50	0.07	2.01	50.59	-	-	-	-	0.0707	0.0706	1.566	1.563	0.0028	0.063	0.0714	1.581	-	-	-	-
13	continuous feeding with 51 mg/L NH_4-N and 5891ppb 1,2-DCA	6	25	2.84	7.27	51	0.15	4.57	47.31	5891	1155	647	2631	0.0725	0.0723	1.605	1.601	0.0064	0.143	0.0668	1.478	184	148	106	62
14	continuous feeding with only 48 mg/L NH_4-N to investigate recovery	6	25	2.24	7.29	48	0.13	2.03	51.21	-	-	-	-	0.0678	0.0676	1.500	1.496	0.0029	0.063	0.0723	1.600	-	-	-	-

Table 6.10. continued

Exp. No.	Description of Experiment	Feed Flowrate	Steady-state ave. bulk T	Steady-state ave. bulk DO	Steady-state ave. bulk pH	Steady-state ave. feed NH_4-N	Steady-state composite effluent NH_4-N	Steady-state composite effluent NO_2-N	Steady-state composite effluent NO_3-N	Steady-state ave. feed 1,2-DCA	Steady-state composite effluent 1,2-DCA	Steady-state ave. feed Cl^-	Steady-state composite effluent Cl^-	Volumetric NH_4-N loading rate	Volumetric NH_4-N removal rate	Surface NH_4-N loading rate	Surface NH_4-N removal rate	Volumetric nitrite accumulation rate	Surface nnitrite accumulation rate	Volumetric nitrate production rate	Surface nitrate production rate	Surface 1,2-DCA loading rate	Surface 1,2-DCA removal rate	Stochiometrically calculated surface Cl^- production rate acc. to removed 1,2-DCA	Measured surface Cl^- production rate
		L/day	°C	mg/L		mg/L	mg/L	mg/L	mg/L	µg/L	µg/L	µg/L	µg/L	$kg/m^3.d$	$kg/m^3.d$	$g/m^2.d$	$g/m^2.d$	$kg/m^3.d$	$g/m^2.d$	$kg/m^3.d$	$g/m^2.d$	$mg/m^2.d$	$mg/m^2.d$	$mg/m^2.d$	$mg/m^2.d$
15	continuous feeding with 50 mg/L NH_4-N and 9791ppb 1,2-DCA	6	25	2.71	7.37	50	0.35	3.04	45.96	9791	1960	1994	4013	0.0699	0.0694	1.547	1.536	0.0043	0.095	0.0649	1.436	306	245	176	63
16	continuous feeding with only 46 mg/L NH_4-N to investigate recovery	6	26	3.02	7.28	46	0.15	1.22	48.28	-	-	-	-	0.0642	0.0640	1.422	1.417	0.0017	0.038	0.0682	1.509	-	-	-	-
17	continuous feeding with 51 mg/L NH_4-N and 14337 ppb 1,2-DCA	6	26	2.66	7.29	51	0.24	1.52	50.23	14337	2727	2409	7273	0.0716	0.0713	1.586	1.578	0.0021	0.048	0.0709	1.570	448	363	260	152
18	continuous feeding with 50 mg/L NH_4-N and 29116 ppb 1,2-DCA	6	27	4.12	7.38	51	3.88	1.52	55.35	29116	4801	414	10188	0.0716	0.0662	1.586	1.465	0.0021	0.048	0.0781	1.730	910	760	545	305

Table 6.10. continued

Exp. No.	Description of Experiment	Feed Flowrate	Steady-state ave. bulk T	Steady-state ave. bulk DO	Steady-state ave. bulk pH	Steady-state ave. feed NH_4-N	Steady-state composite effluent NH_4-N	Steady-state composite effluent NO_2-N	Steady-state composite effluent NO_3-N	Steady-state ave. feed 1,2-DCA	Steady-state composite effluent 1,2-DCA	Steady-state ave. feed Cl^-	Steady-state composite effluent Cl^-	Volumetric NH_4-N loading rate	Volumetric NH_4-N removal rate	Surface NH_4-N loading rate	Surface NH_4-N removal rate	Volumetric nitrite accumulation rate	Surface nnitrite accumulation rate	Volumetric nitrate production rate	Surface nitrate production rate	Surface 1,2-DCA loading rate	Surface 1,2-DCA removal rate	Stochiometrically calculated surface Cl^- production rate acc. to removed 1,2-DCA	Measured surface Cl^- production rate
		L/day	^0C	mg/L		mg/L	mg/L	mg/L	mg/L	µg/L	µg/L	µg/L	µg/L	$kg/m^3.d$	$kg/m^3.d$	$g/m^2.d$	$g/m^2.d$	$kg/m^3.d$	$g/m^2.d$	$kg/m^3.d$	$g/m^2.d$	$mg/m^2.d$	$mg/m^2.d$	$mg/m^2.d$	$mg/m^2.d$
19	continuous feeding with only 49 mg/L NH_4-N to investigate recovery	6	28	3.13	7.36	49	0.62	0.91	57.35	-	-	-	-	0.0688	0.0680	1.523	1.504	0.0013	0.029	0.0810	1.792	-	-	-	-
20	feeding with 53 mg/L NH_4-N and 68087 ppb 1,2-DCA	6	28	6.48	7.85	53	27	0.71	30.00	68087	17577	15229	27792	0.0744	0.0362	1.646	0.802	0.001	0.022	0.0424	0.938	2128	1578	1132	393
21	continuous feeding with only 42 mg/L NH_4-N to investigate recovery	6	28	2.00	7.62	42	0.23	2.43	48.97	-	-	-	-	0.0591	0.0587	1.307	1.300	0.0034	0.076	0.0691	1.530	-	-	-	-

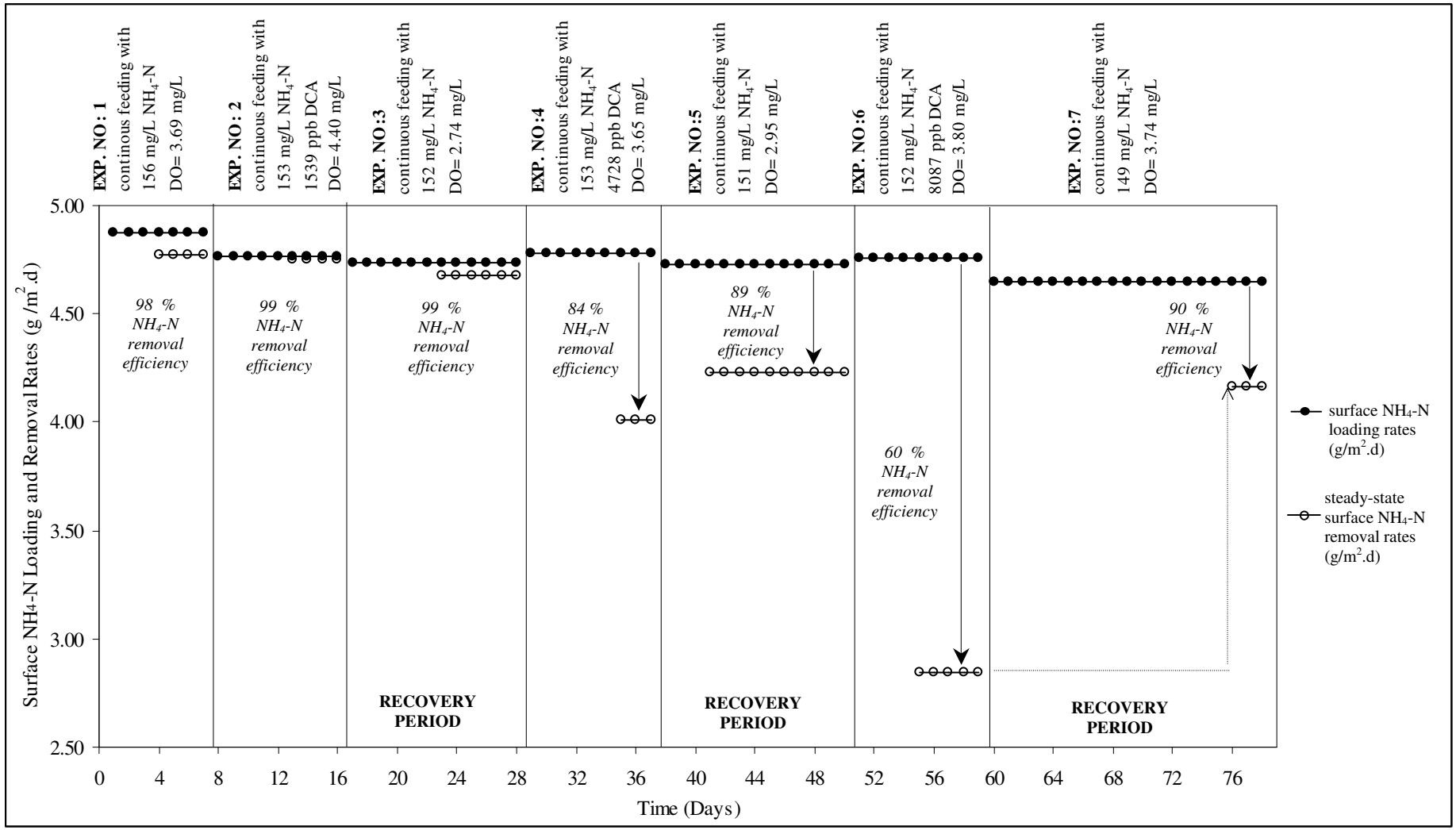

Figure 6.56. Chronological illustration of NH_4-N loading and removal rates in the 1st set of experiments [influent NH_4-N= 149-156 mg/L, influent 1,2-DCA=1539-8087 µg/L]

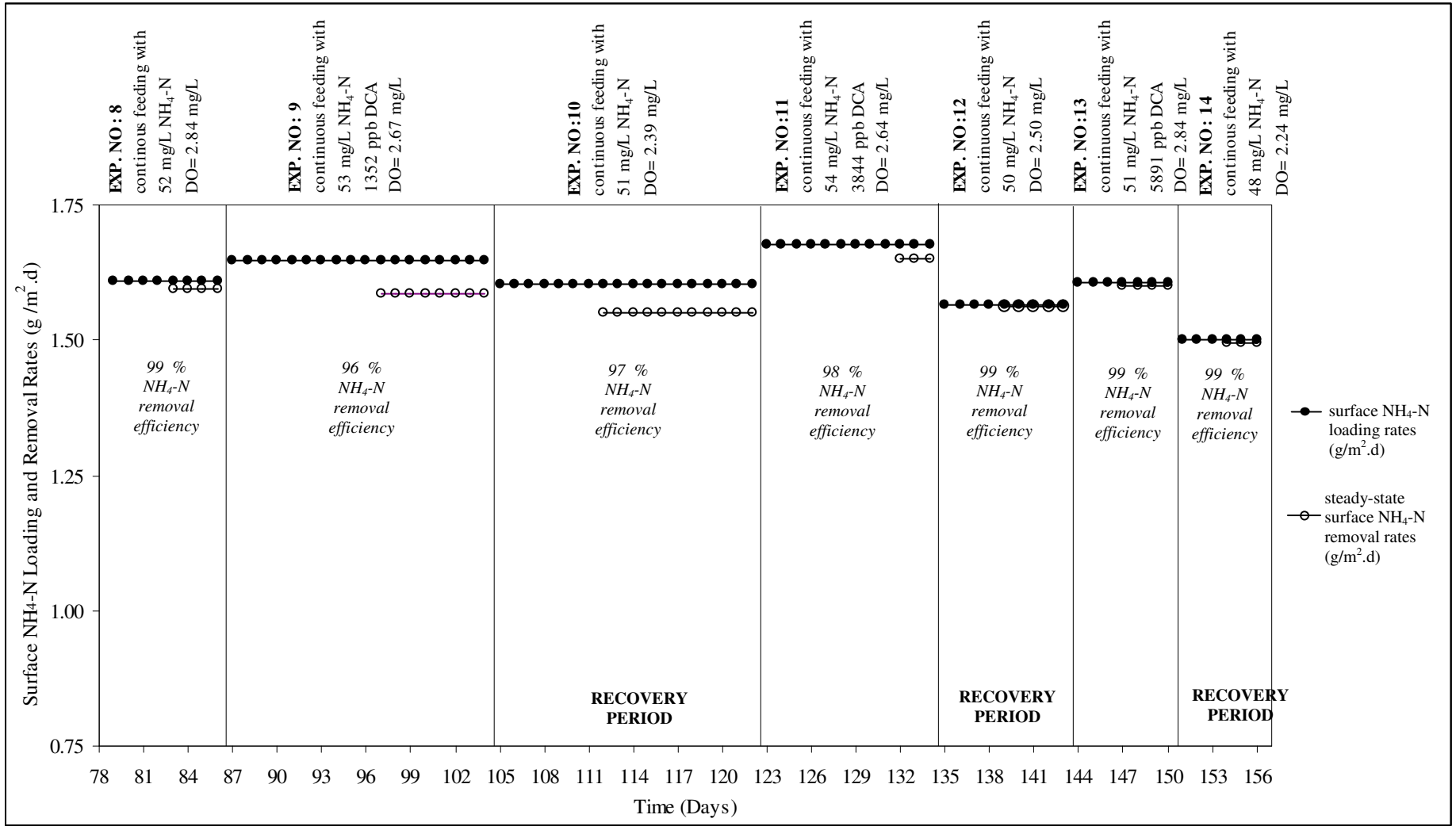

Figure 6.57. Chronological illustration of NH_4-N loading and removal rates in the 2nd set of experiments [influent NH_4-N= 48-54 mg/L , influent 1,2-DCA=1352-5891 µg/L]

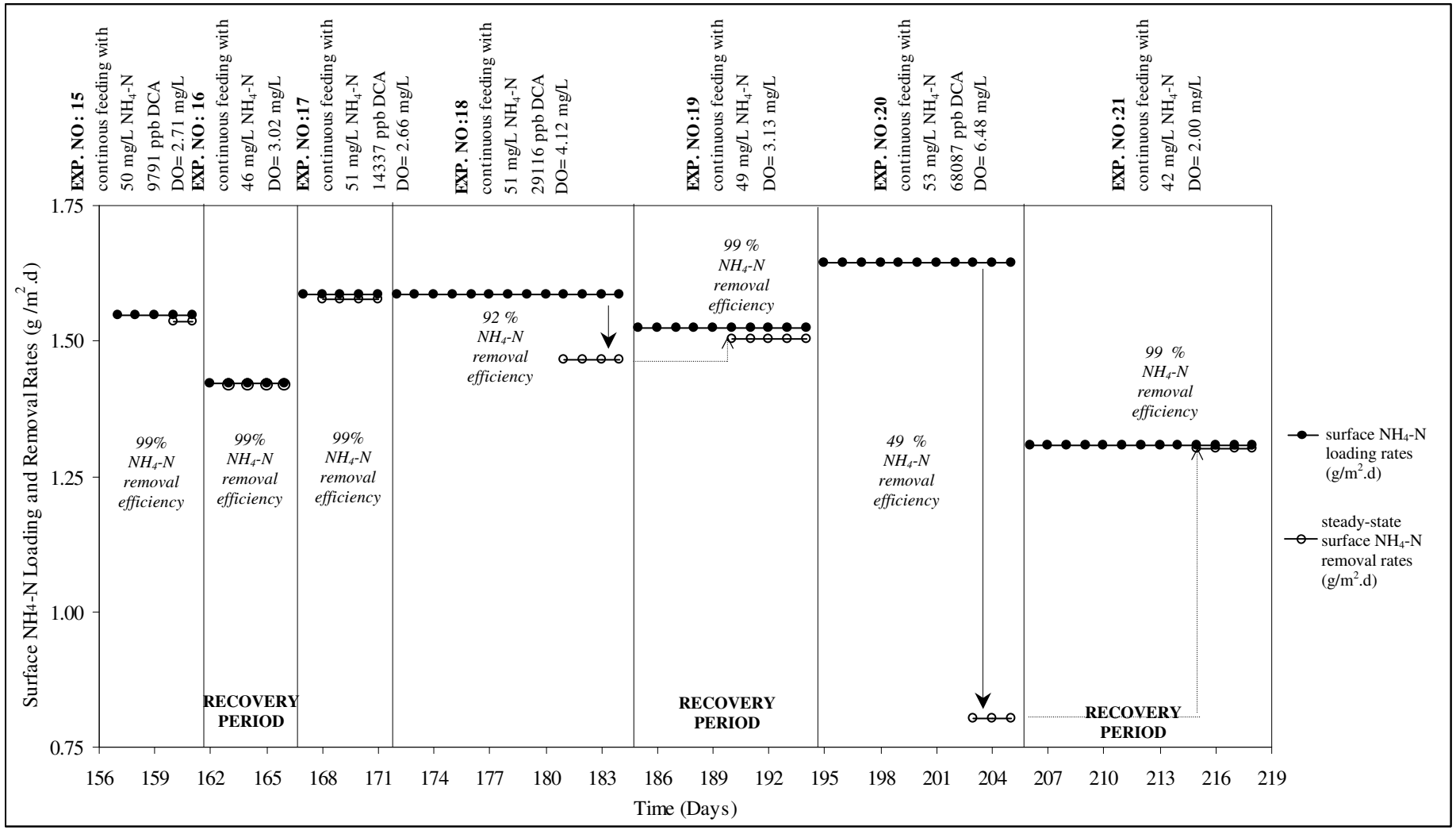

Figure 6.58. Chronological illustration of NH_4-N loading and removal rates in the 2nd set of experiments [influent NH_4-N= 42-53 mg/L , influent 1,2-DCA=9791-68087 µg/L]

In Figure 6.59, the surface ammonium removal rates observed with respect to the bulk NH_4-N concentrations were transferred into Figure 6.52 showing dependence of ammonium utilization rate on bulk ammonium concentration during preliminary experiments.

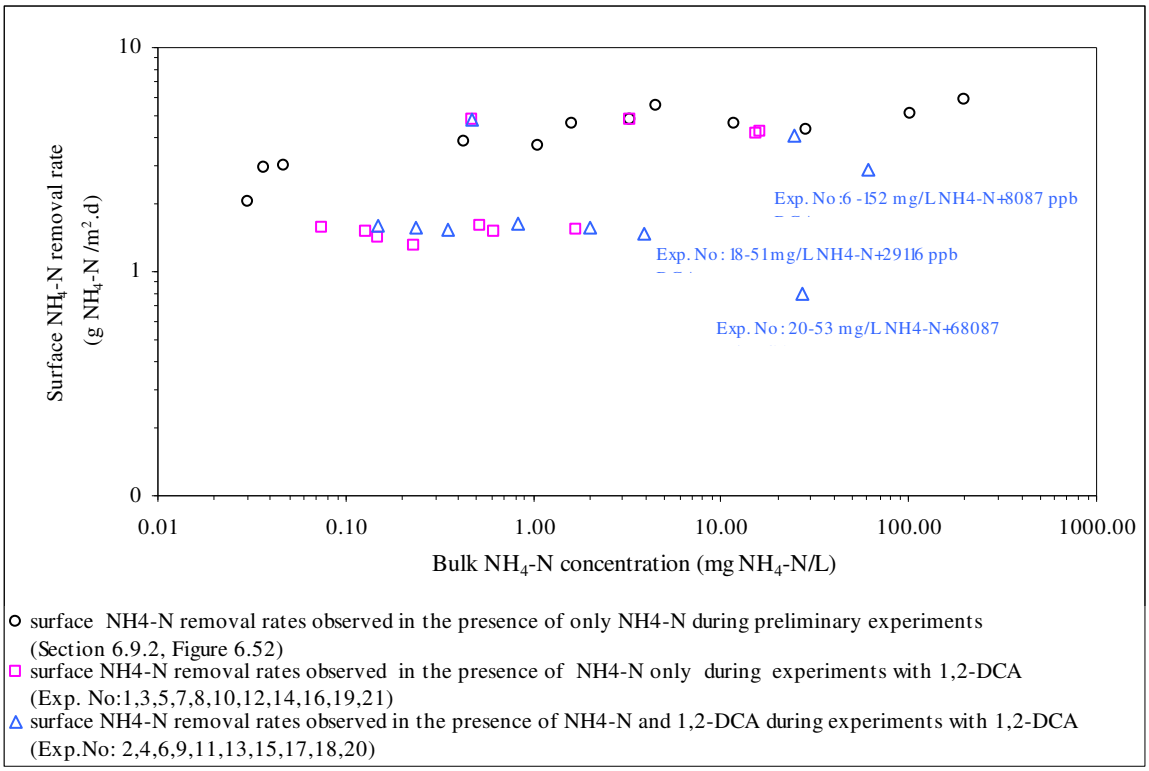

Figure 6.59. Surface NH_4-N removal rates during preliminary experiments with ammonium only and during experiments with 1,2-DCA

The decreases observed in surface ammonium removal rates at increased 1,2-DCA loadings (Exp.No: 6 and 20) are apparent in Figure 6.59. These decreases resulted in significant increases in bulk NH_4-N concentrations. At both high ammonium (152 mg/L NH_4-N; 4.734 g/m^2.d) and low ammonium loadings (50 mg/L; 1.566 g/m^2.d), the steady-state surface NH_4-N removal rates during recovery (in the presence of NH_4-N only) were in compliance with those observed through preliminary experiments. These results clearly indicated that 1,2-DCA inhibition on ammonium utilization was reversible due to the ability of cells to recover from inhibitory effects. Similarly, in previous studies with TCE (Rasche, 1991; Hyman et al., 1995; Ely et al., 1995b) *Nitrosomonas europaea* cells were found to be able to recover from the inhibitory effects of TCE. The recovery periods shown in Figures 6.56, 6.57 and 6.58 indicated that when inhibition of ammonia oxidizing activity

was greater, a longer recovery phase was needed as also observed in a previous study with TCE (Hyman et al., 1995). Since the slot-blot analyses performed throughout continuous flow experiments (Section 6.10.2) indicated no significant changes in the quantity of *Nitrosomonas* species, the recovery of cells from the inhibitory effects of 1,2-DCA was most probably due to the resynthesis of new proteins within preexisting cells rather than the growth of new cells as also indicated by other researchers (Hyman et al., 1995).

The inhibitory effect of 1,2-DCA on nitrification was further evaluated in terms of nitrite accumulation and nitrate production rates as illustrated in Figure 6.60. This figure shows the $r_{NH4-N,}$ r_{NO2-N} and r_{NO3-N} values observed during experiments with DCA (including recovery experiments with NH_4-N only) and those observed during preliminary experiments (Section 6.9.2) with increasing NH_4-N loading rates. The above-discussed decreases observed in surface ammonium removal rates at increased 1,2-DCA loadings (Exp.No: 6 and 20) are also apparent in Figure 6.60. As discussed above, r_{NH4-N} values observed during recovery experiments with only NH_4-N (152 and 50 mg/L) were in consistency with those in preliminary experiments (Section 6.9.2) indicating the reversibility of 1,2-DCA inhibition. The r_{NO2-N} values observed during recovery experiments were slightly different from those observed in preliminary experiments (Section 6.9.2) due to the differences in bulk DO concentrations. As discussed in Section 6.9.2, the effect of low bulk DO concentration on NO_2-N accumulation is very significant. The slight differences observed between the r_{NO3-N} values in recovery and preliminary experiments are directly related with the changes observed in r_{NO2-N} values. The decreases in r_{NH4-N} values due to 1,2-DCA inhibition resulted in proportional decreases in the r_{NO3-N} values indicating no inhibitory effect of 1,2-DCA on the conversion of nitrite to nitrate. Additionally, the nitrite accumulation rates observed especially at high ammonium loadings at various concentrations of 1,2-DCA (e.g. Exp. No: 4 and 6) were in good agreement with those observed during preliminary experiments. As discussed in Section 3.3.1.3, conversion of ammonium to nitrite occurs in two steps: conversion of ammonium to hydroxylamine through the catalysis of AMO enzyme, conversion of hydroxylamine to nitrite through the catalysis of HAO enzyme. Therefore, nitrite accumulations under ammonium utilization inhibited conditions indicated that 1,2-DCA inhibits primarily the conversion of ammonium to hydroxylamine by binding to the AMO enzyme. Similarly, in studies of Ely et al. (1995b, 1997), hydrazine (alternative substrate of HAO enzyme)

dependent activity tests of *Nitrosomonas europaea* cells showed that inactivating injuries of 1,2-DCA and other chlorinated organic compounds (e.g., TCE, 1,1-DCE) appeared limited primarily to AMO due to undiminished hydrazine-dependent activities. In contrast, Rasche et al. (1991) reported the partial inactivation of hydrazine-dependent activity of *Nitrosomonas europaea* cells preincubated for 1 h with 1,2-DCA.

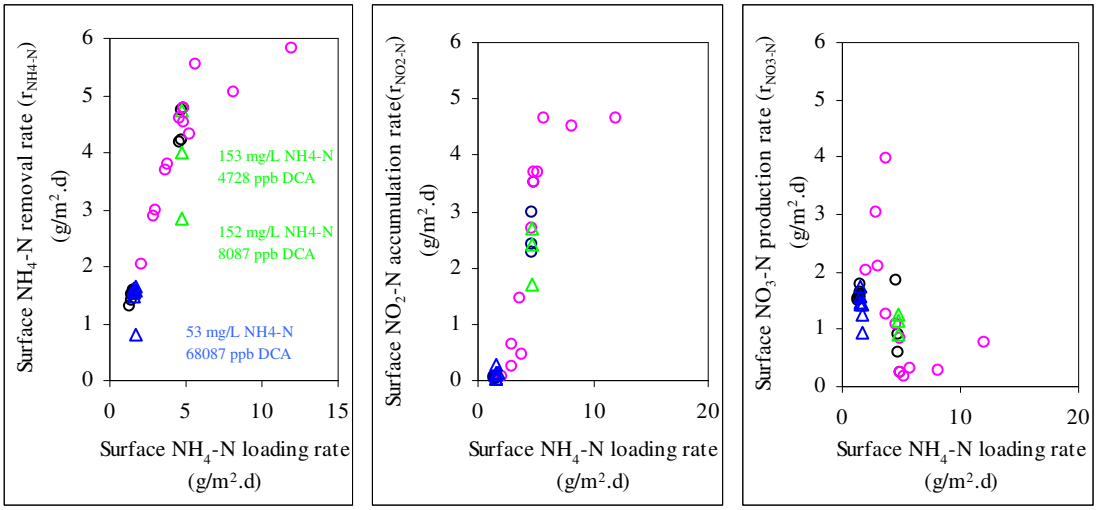

Figure 6.60. Dependence of ammonium removal, nitrite accumulation and nitrate formation rates on ammonium loading rates in preliminary experiments and experiments with 1,2-DCA [r_{NH4-N}, r_{NO2-N} and r_{NO3-N} values in the presence of o only NH_4-N during preliminary experiments (Section 6.9.2), o only NH_4-N during experiments with 1,2-DCA (recovery experiments), Δ initial average NH_4-N concentration of 152 mg/L and various 1,2-DCA concentrations, Δ initial average NH_4-N concentration of 50 mg/L and various 1,2-DCA concentrations]

6.9.3.2. Cometabolic Degradation of 1,2-DCA. The surface 1,2-DCA loading rates, steady-state surface 1,2-DCA removal rates and percent 1,2-DCA total removal efficiencies are also shown in Figures 6.61, 6.62 and 6.63. The observed removals in 1,2-DCA may be due to biological degradation, volatilization or another unknown mechanism. In general, cometabolic degradation of chlorinated organics under aerobic conditions occurs through oxidative dechlorination. Oxidative dechlorination is thought to result from spontaneous elimination of chloride ion from an unstable chlorinated organic epoxide, which is generated in the monooxygenation of a chlorinated organic (Fetzner, 1998). Therefore, in these experiments, the measurements of chloride (Cl^-) releases were used as

an indicator for the initiation of cometabolic degradation through dechlorination. Stoichiometrically, the complete mineralization of each 1,2-DCA molecule results in the release of two chloride ions. The calculated chloride production rates shown in Figures 6.61, 6.62 and 6.63 were obtained by applying this stoichiometric relationship. The percentages of measured and stoichiometrically calculated Cl^- production rates (Figures 6.61, 6.62 and 6.63) were used in the evaluation of the extent of 1,2-DCA degradation.

As seen from Figures 6.61, 6.62 and 6.63, at both high ammonium loadings (152 mg/L NH_4-N; 4.734 g/m^2.d) and low ammonium loadings (50 mg/L; 1.566 g/m^2.d), a significant portion of the initially introduced 1,2-DCA was removed from the system. The total 1,2-DCA removal efficiencies ranged between 70-90 %. In compliance with the results of batch kinetic experiments with 1,2-DCA, for similar 1,2-DCA loadings (e.g., Exp. No: 2 and 9; Exp. No: 4 and 11) 1,2-DCA removal rates exhibited an increase with increasing ammonium utilization rates. In all experiments, the measured Cl^- production rates were found lower than the stoichiometrically calculated ones. This indicated that some portion of the removed 1,2-DCA was either incompletely dechlorinated into by-products [e.g., chloroacetaldehyde ($ClCH_2CHO$)] or volatilized from the system. The detection of high bulk 1,2-DCA concentrations throughout the experiments eliminates the possibility of 1,2-DCA volatilization from the system. A previous work (Rasche et al., 1991) also showed that the cometabolic degradation of 1,2-DCA by *Nitrosomonas europaea* cells resulted in the formation of chloroacetaldehyde ($ClCH_2CHO$), consistent with the oxidative dechlorination mechanism of the monochlorinated carbon.

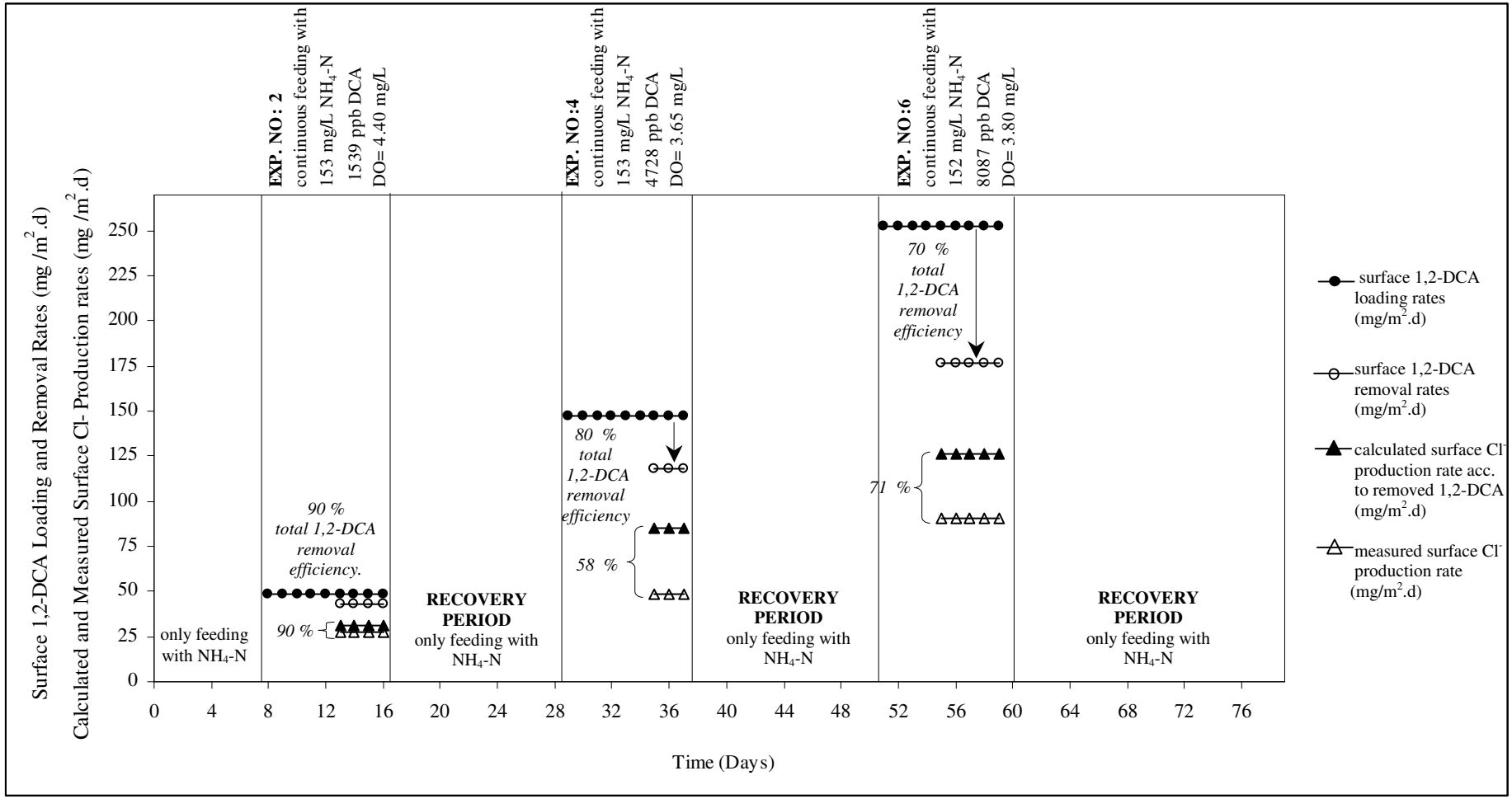

Figure 6.61. Chronological illustration of 1,2-DCA loading and removal rates, calculated and measured surface Cl^- production rates in the 1st set of experiments [initial NH_4-N= 149-156 mg/L, initial 1,2-DCA=1539-8087 µg/L]

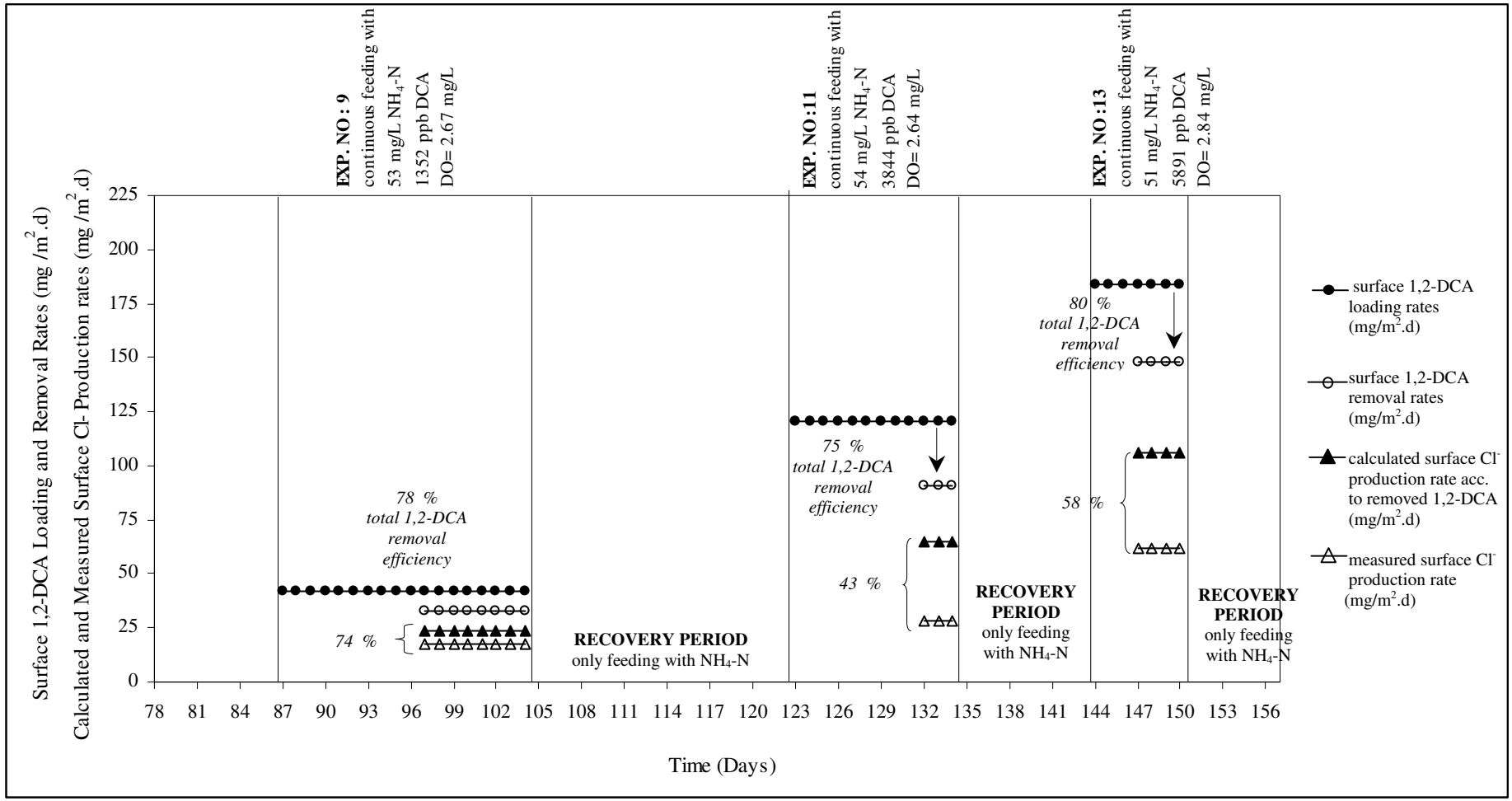

Figure 6.62. Chronological illustration of 1,2-DCA loading and removal rates, calculated and measured surface Cl^- production rates in the 2nd set of experiments [initial NH_4-N= 48-54 mg/L , initial 1,2-DCA=1352-5891 µg/L]

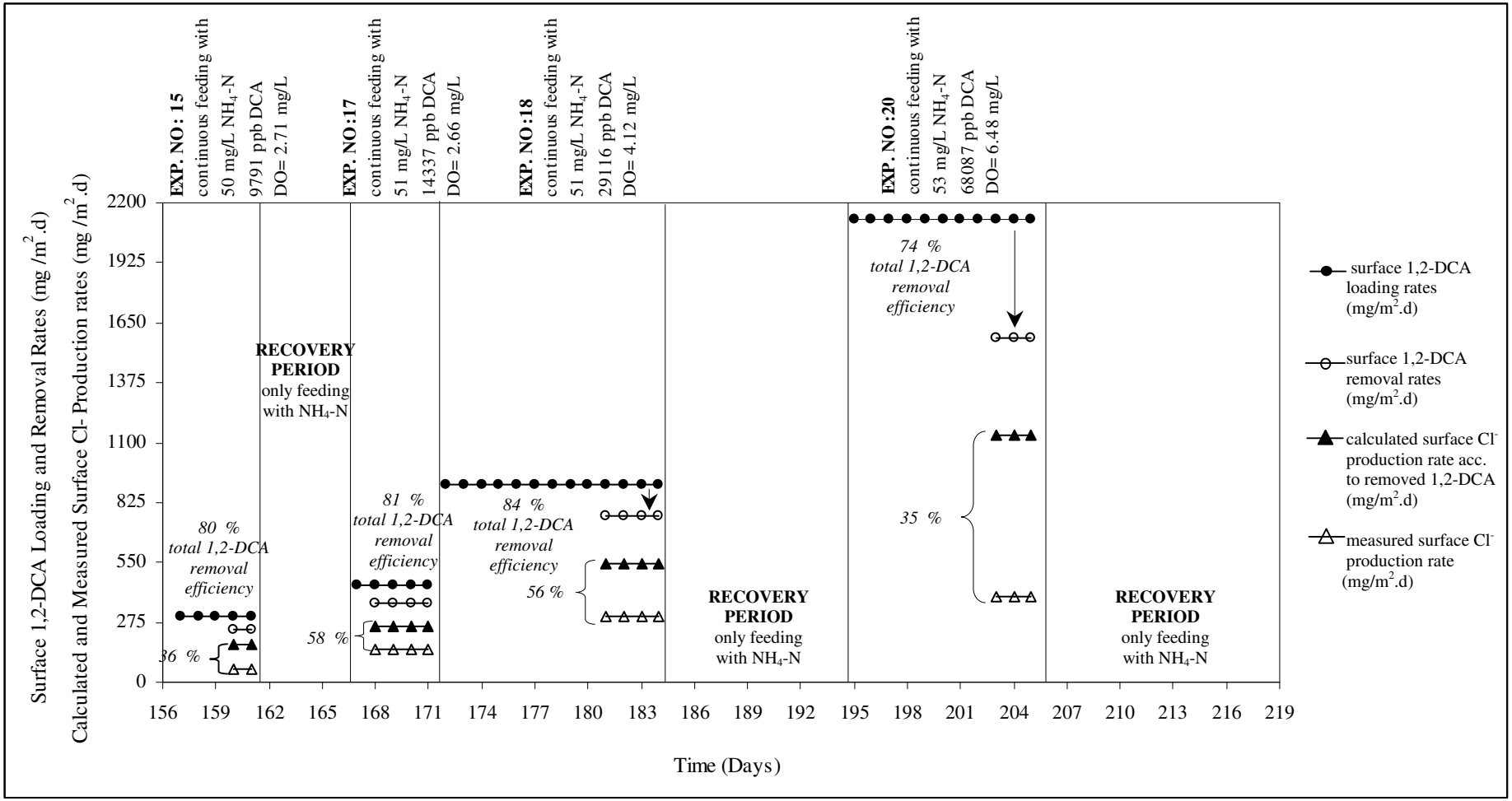

Figure 6.63. Chronological illustration of 1,2-DCA loading and removal rates, calculated and measured surface Cl^- production rates in the 2nd set of experiments [initial NH_4-N= 42-53 mg/L, initial 1,2-DCA=9791-68087 µg/L]

Figure 6.64 illustrates the dependence of 1,2-DCA removal rates on bulk 1,2-DCA concentrations. In the studied 1,2-DCA range, 1,2-DCA-removal rate increased with 1,2-DCA concentration. This indicated the quite high 1,2-DCA-removal capacity of the system. In literature, for several bench-scale packed bed bioreactors inoculated with the *Xanthobacter autotrophicus GJ10* bacterium which utilizes 1,2-DCA as sole carbon source 1,2-DCA removal rates were observed in the range of 0.6-120 g/m^3.d at the influent 1,2-DCA concentrations ranging between 0.6 to 25 mg/L (Field and Alvarez, 2004). In the present study, the 1,2-DCA removal rates observed in the range of 33-1578 mg/m^2.d (1.487-71.309 g/m^3.d) at influent concentrations ranging from 1.3-68 mg/L 1,2-DCA are comparable with those reported in literature. By considering the fact that cometabolic degradation rates are usually slower than the metabolic ones, the closeness of our cometabolic 1,2-DCA removal rates with those observed during metabolic degradation of 1,2-DCA by *Xanthobacter autotrophicus GJ10* bacterium indicates the quite high 1,2-DCA cometabolic degradation capacity of nitrifiers.

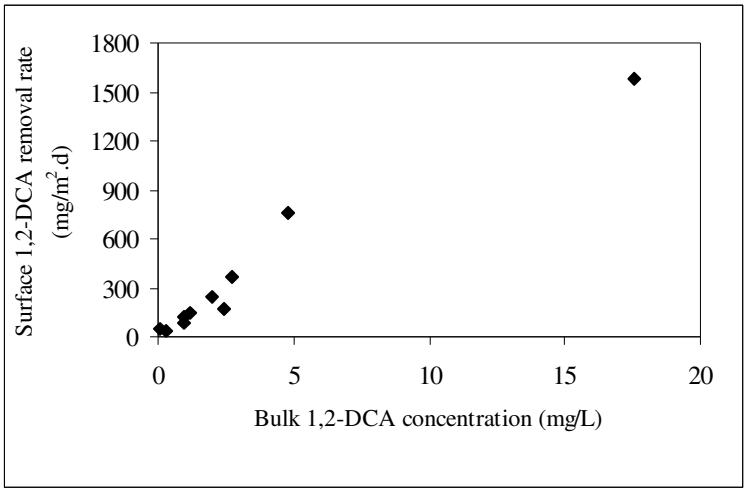

Figure 6.64. Dependence of total 1,2-DCA removal rates on bulk 1,2-DCA concentration

The relationship between 1,2-DCA removal rates and measured Cl^- production rates was shown in Figure 6.65. Cl^- production rate increased with increasing 1,2-DCA removal rates and reached almost saturation at an 1,2-DCA removal rate of 1588 mg/m^2.d. This increase in Cl^- production with increasing 1,2-DCA removal rates ensures that chloride ion release was associated with oxidative dechlorination of 1,2-DCA. Since the oxidative dechlorination of 1,2-DCA is heavily dependent on the reducing energy in the form of NAD(P)H, which can only be regenerated by growth-substrate oxidation, inhibition of

ammonium oxidation results in the regeneration of less NAD(P)H. This indirectly diminishes the chloride ion elimination from the unstable 1,2-DCA epoxide generated in the monooxygenation of 1,2-DCA. Therefore, saturation of Cl^- release at high 1,2-DCA removal rates was most probably related to inhibition of ammonium oxidation activity. Similarly, in the study of Hyman et al. (1995) performed with pure *Nitrosomonas europaea* species, chloride ion release from TCE oxidation was found as a saturable process, which was closely associated with TCE-dependent inactivation of ammonia oxidation.

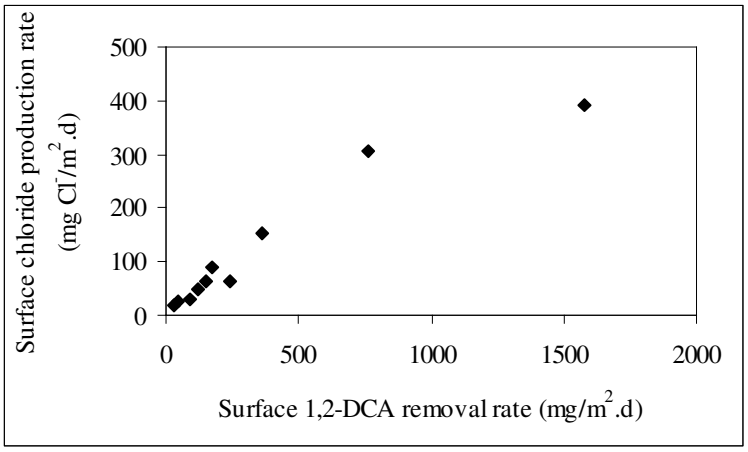

Figure 6.65. Dependence of chloride production rate on 1,2-DCA removal rate

6.9.3.3. Relationship between Ammonium Utilization Rate and 1,2-DCA Cometabolic Degradation Rate. As mentioned in batch experiments, the cometabolic degradation potential of microorganisms is usually defined by the transformation yield (T_y). The transformation yields estimated by dividing the 1,2-DCA removal rates (r_{DCA}) to the corresponding NH_4-N removal rates (r_{NH4-N}) were found to be dependent on NH_4-N and 1,2-DCA loading rates. Figure 6.66 shows r_{NH4-N}/r_{DCA} against NH_4-N loading rate/1,2-DCA loading rate. A strong linear relationship exists between r_{NH4-N}/r_{DCA} and NH_4-N /1,2-DCA loading rates. By considering that the r_{NH4-N}/r_{DCA} equals $1/T_y$, a correlation between $1/T_y$ and NH_4-N and 1,2-DCA loading rates can be written as follows:

$$\frac{1}{T_y} = \frac{r_{NH4-N}}{r_{DCA}} = 1.12 \frac{NH_4 - N \ loading \ \ rate}{1{,}2 - DCA \ loading \ \ rate} \qquad (6.9)$$

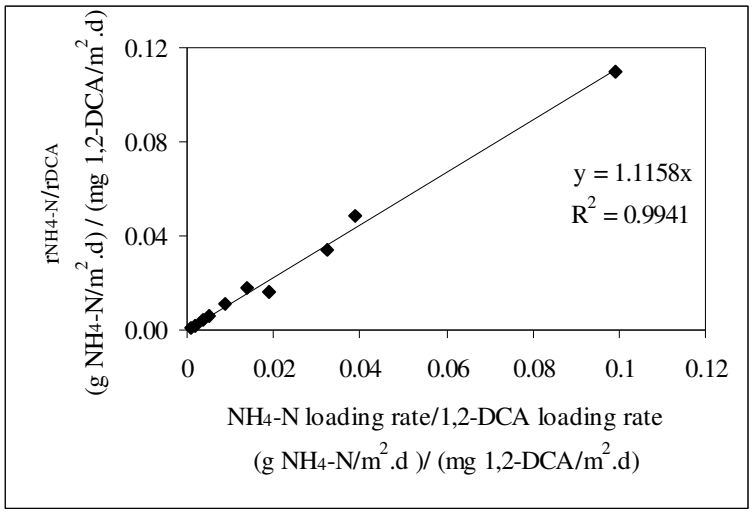

Figure 6.66**.** Relationship between the relative ratio of $r_{NH4\text{-}N}$ and r_{DCA} and the relative ratio of NH_4-N loading and 1,2-DCA loading rates

6.9.4. Implications for Engineering Applications

.

The findings of continuous-flow experiments can be implemented for engineering applications in many different ways. Two examples are given below:

Initially, the findings of preliminary continuous-flow experiments performed to investigate the nitrification kinetics of the biofilm reactor allow the estimation of optimum surface loading rates for a specific NH_4-N discharge criterion. This can be presented by imagining the following scenario:

Consider that a high-strength wastewater with 200 mg/L NH_4-N concentration will be treated in the upflow biofilm reactor to meet the effluent discharge criterion of 50 mg/L NH_4-N. In view of the findings of this study, if the system is operated in a DO concentration of 2.5-3.5 mg/L, the maximum achievable ammonium utilization rate will be 5.2 g/m^2.d. This means that the decrease of 200 mg/L influent NH_4-N concentration to 50 mg/L in the effluent requires the hydraulic loading rate of 34.66 L/m^2.d. Therefore, the surface loading to the system must be 6.93 g/m^2.d.

Secondly, the findings of the continuous-flow experiments with 1,2-DCA allow the estimation of the optimum influent concentration of the growth-substrate (ammonium)

necessary for the reduction of 1,2-DCA to a specific discharge concentration. Although these findings determined under laboratory conditions are not directly representative of field conditions, they will be helpful for the improvement of packed bed submerged biofilm reactors for 1,2-DCA removal from industrial effluents (such as vinyl chloride production plant) and many groundwater systems. The implications of these findings for real treatment systems can be presented by imagining the following scenario:

Consider that leachate generated from a hazardous waste landfill site has led to the contamination of the underlying aquifer with 1,2-DCA at a concentration of 2000 μg/L. The groundwater at that site can be pumped and treated in a continuous-flow ex-situ packed bed submerged biofilm reactor containing a mixed culture enriched for nitrifiers. In the design of such a system, the influent NH_4-N concentration should be selected by considering that 1,2-DCA will be removed with efficient use of NH_4-N. If two alternative influent NH_4-N concentrations of 50 and 100 mg/L are chosen, based on Eqn 6.9, transformation yield (T_y) of 1,2-DCA, which is the amount of 1,2-DCA that can be degraded per unit mass of ammonium, will be 0.028 and 0.056, respectively. If 80% 1,2-DCA removal takes place, based on the calculated T_y values, the ammonium removal rates will be around 0.0448 and 0.0896 $g/m^2.d$. It means that the effluent will contain 5.2 mg/L and 10.4 mg/L NH_4-N at 50 and 100 mg/L influent NH_4-N concentrations, respectively. This clearly shows that increasing influent NH_4-N concentration will result in an increase in effluent NH_4-N concentration without causing a significant increase in 1,2-DCA removal rate. Therefore, in that case the lower influent NH_4-N should be chosen.

Similarly, other scenarios can be imagined and the 1,2-DCA removal and nitrification patterns can be predicted for different influent 1,2-DCA and NH_4-N concentrations.

6.10. Characterization of the Microbial Community in the Nitrifying Biofilm Reactor by Molecular Biology Techniques

6.10.1. FISH (Fluorescence In-Situ Hybridization) Results

In order to detect, identify and characterize the microbial community in the nitrifying biofilm reactor, FISH technique was applied to the biofilm samples taken at regular time intervals in continuous-flow experiments (Section 6.9). A few of the photomicrographs belonging to these analyses are illustrated in Figure 6.67. In this figure, each photomicrograph couple represents the same field of the microscopic view and hence they are directly comparable with each other.

As seen from Figure 6.67, the dominant organisms in the biofilm were in the Bacteria domain. Due to the hybridization signals detected with the NSO190 probe, the dominant species in the Bacteria domain were found to be the members of the genus *Nitrosomonas*. As seen from the figure, *Nitrosomonas* species spherically formed dense microcolonies. Hybridization signals detected for Bacteria and *Nitrosomonas* species were quite comparable indicating the low quantities of other bacterial species. This is most probably related with the enrichment of the reactor for nitrifiers due to the prolonged feeding since 1994 with ammonia and mineral solutions only.

In this study, no hybridization signals could be observed when *Nitrobacter* and *Nitrospira* specific probes (NIT3 and NTSPA662) were used in the case of any biofilm sample. There may be several possible reasons for the failure of FISH to identify *Nitrospira* and *Nitrobacter* species as also indicated in other studies (e.g., Jang et al., 2002). As a first possibility, unknown nitrite oxidizing bacteria other than *Nitrobacter* and *Nitrospira* species could be present in high numbers. However, since the slot-blot analysis results given in Section 6.10.2 clearly demonstrated the presence of *Nitrobacter* and *Nitrospira* species in biofilm samples, this possibility was disregarded. Another possibility may be that the cellular rRNA content of the active cells in the sample was too low for in-situ identification or there was insufficient *Nitrobacter* and *Nitrospira* cell impermeabilization (Mertoğlu, 2005b).

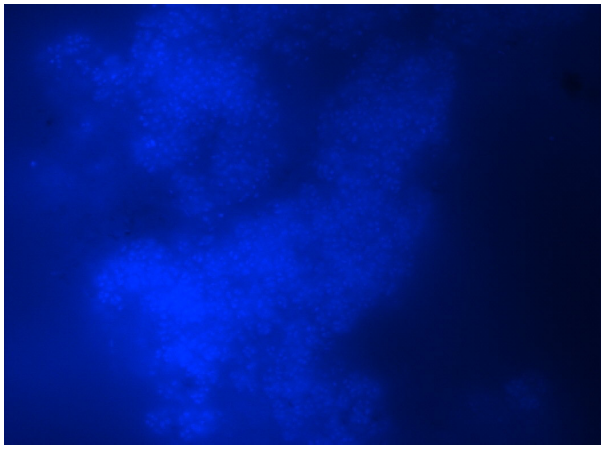

All microorganisms (DAPI)
01.10.04 – Run No:3 in Section 6.9.2

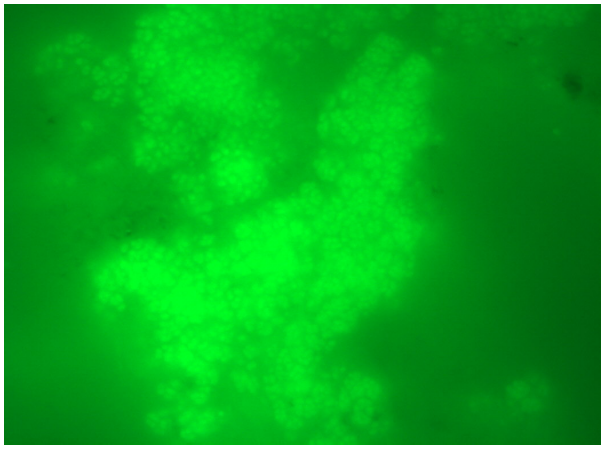

Bacteria (EUB 338)
01.10.04 – Run No:3 in Section 6.9.2

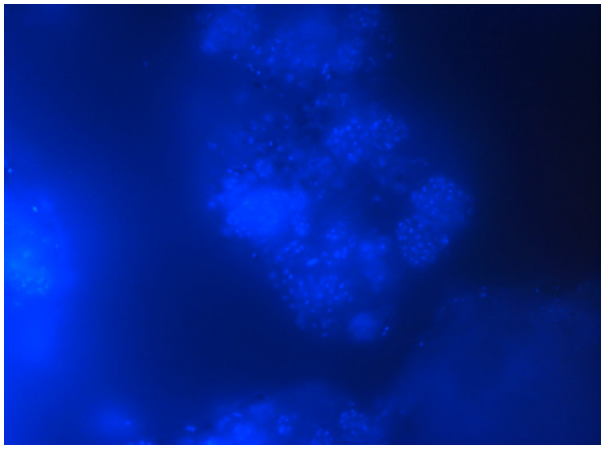

All microorganisms (DAPI)
25.04.05- Run No:10 in Section 6.9.3

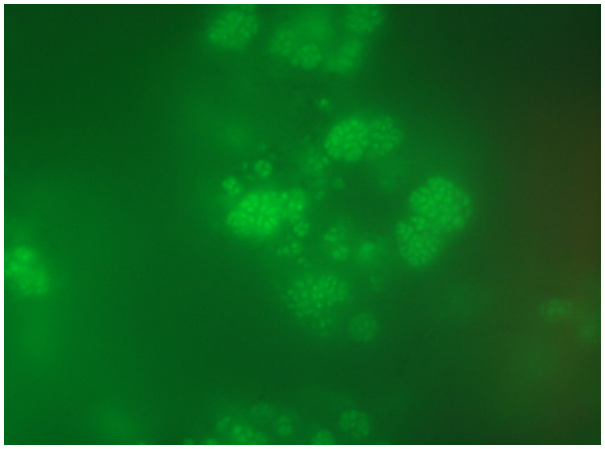

Bacteria (EUB338)
25.04.05-Run No:10 in Section 6.9.3

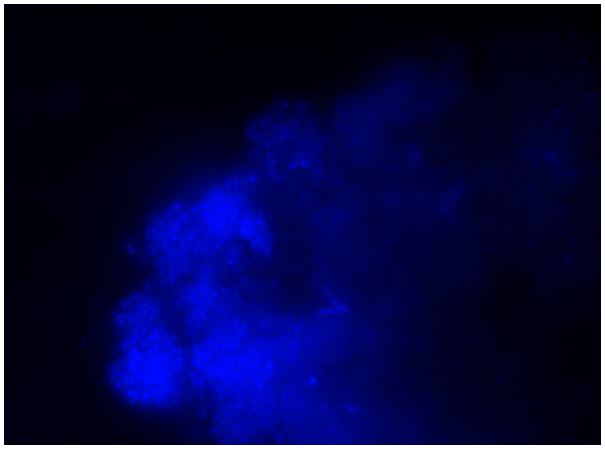

All microorganisms (DAPI)
06.01.05-Run No:7 in Section 6.9.2

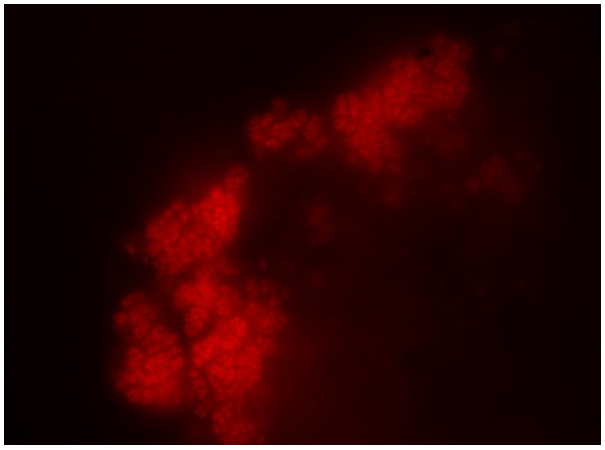

Nitrosomonas species (NSO 190)
06.01.05-Run No:7 in Section 6.9.2

Figure 6.67. Photomicrographs of FISH with oligonucleotide probes EUB338 (green) for bacteria domain, NSO190 (red) for *Nitrosomonas* species. All microorganisms were visualized by DAPI staining (blue).

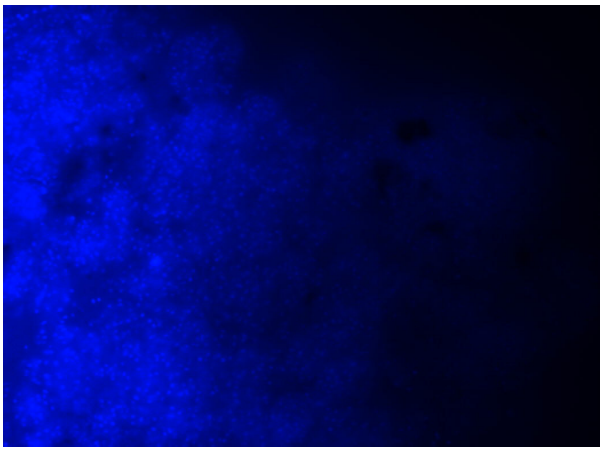

All microorganisms (DAPI)
04.03.05– Run No:6 in Section 6.9.3

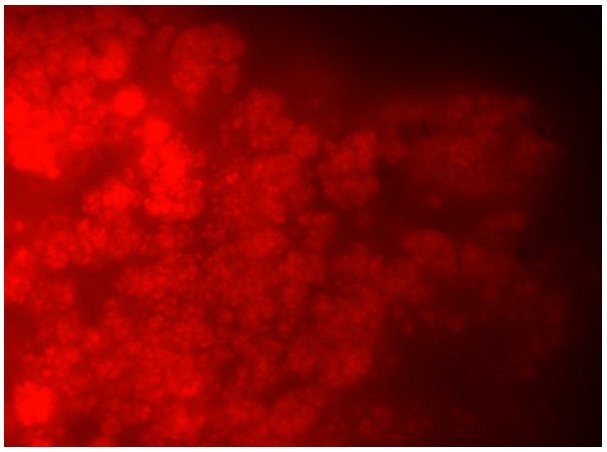

Nitrosomonas species (NSO 190)
04.03.05 – Run No:6 in Section 6.9.3

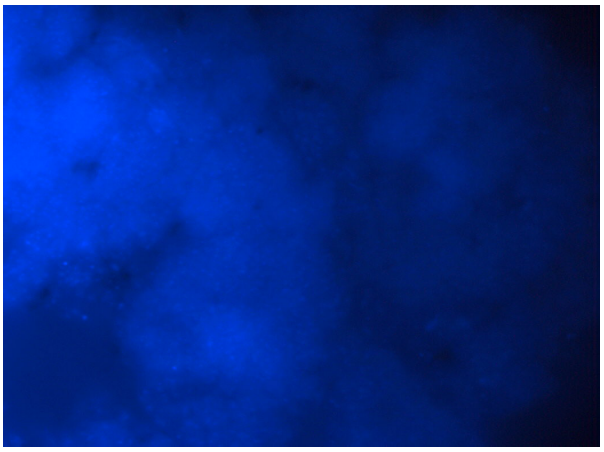

All microorganisms (DAPI)
25.04.05- Run No:10 in Section 6.9.3

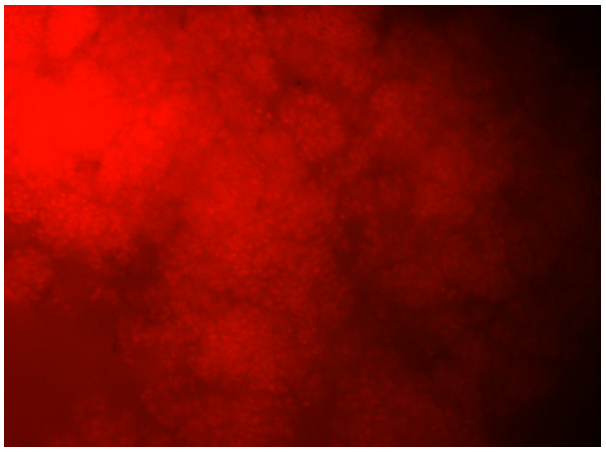

Nitrosomonas species (NSO190)
25.04.05-Run No:10 in Section 6.9.3

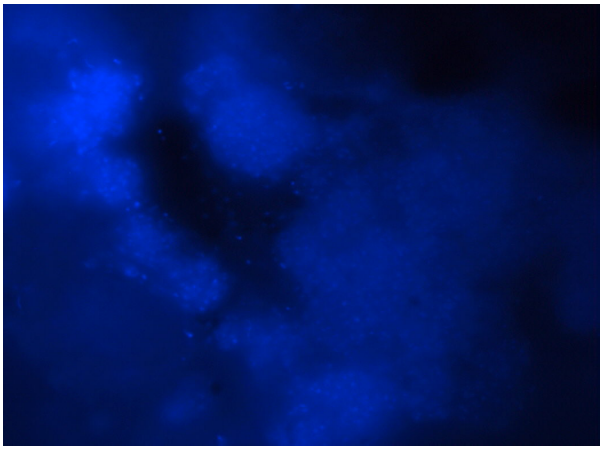

All microorganisms (DAPI)
18.05.05-Run No:11 in Section 6.9.3

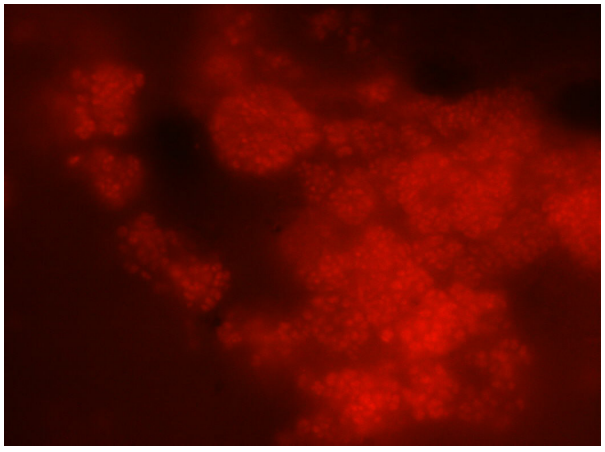

Nitrosomonas species (NSO190)
18.05.05-Run No:11 in Section 6.9.3

Figure 6.67. continued

6.10.2. Slot-Blot Hybridization Results

Slot-blot hybridization was performed with DNA isolates of biofilm samples taken at regular time intervals in continuous-flow experiments (Section 6.9). This was done to investigate the variations and activity of all microbial populations and also to quantify the relative abundance of microbial species. The results of these analyses are shown in Figure 6.68.

In contrast to FISH results (Section 6.10.1), hybridization signals were observed not only for Bacteria domain and *Nitrosomonas* species, but also *Nitrobacte*r and *Nitrospira* species. In Figure 6.68, the thickness of each band is directly proportional to the target DNA quantity. However, since the DNA isolates used in these analyses were not PCR amplified, the band thicknesses observed for each species may provide an insight for the quantity changes with respect to time. In this respect, it may be concluded that no significant changes occurred in the quantity of Bacteria domain, *Nitrosomonas*, *Nitrobacter* and *Nitrospira* species during the operation of the nitrifying biofilm reactor at various ammonium and 1,2-DCA loadings for a time period of about one year from 01.06.04 to 11.08.05. The comparison of band thicknesses detected for Bacteria domain with those for *Nitrosomonas* species indicated that *Nitrosomonas* species were the dominant species in the biofilm. On the other hand, *Nitrobacter* and *Nitrospira* species comprised a small fraction in the total Bacteria domain. The band thicknesses detected for *Nitrobacter* and *Nitrospira* species indicated that the quantity of these species were almost equal to each other. This finding was in contrast with recent researches (Daims et al., 2000; Daims et al., 2001; Schramm et al., 1998) indicating that *Nitrospira* is the primary nitrite oxidizer in nitrifying biofilm reactors. This discrepancy may be related with the differences in operating conditions, especially influent ammonium loadings (Mertoğlu, 2005b).

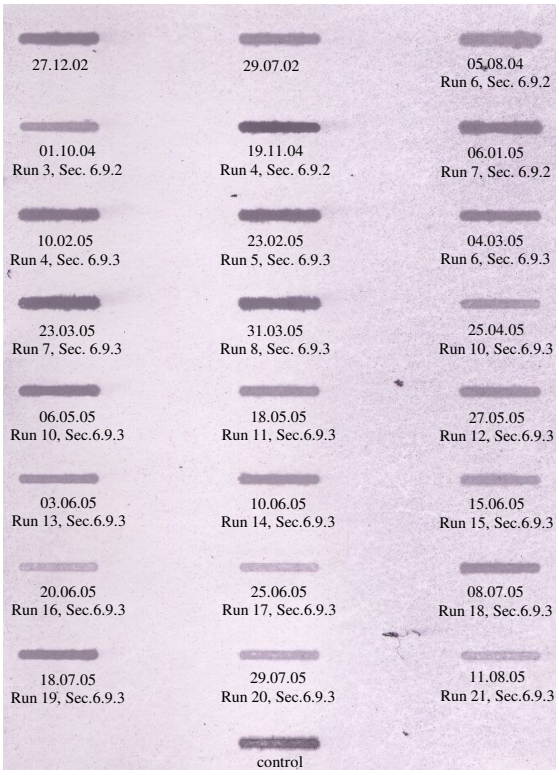

Bacteria (EUB338)

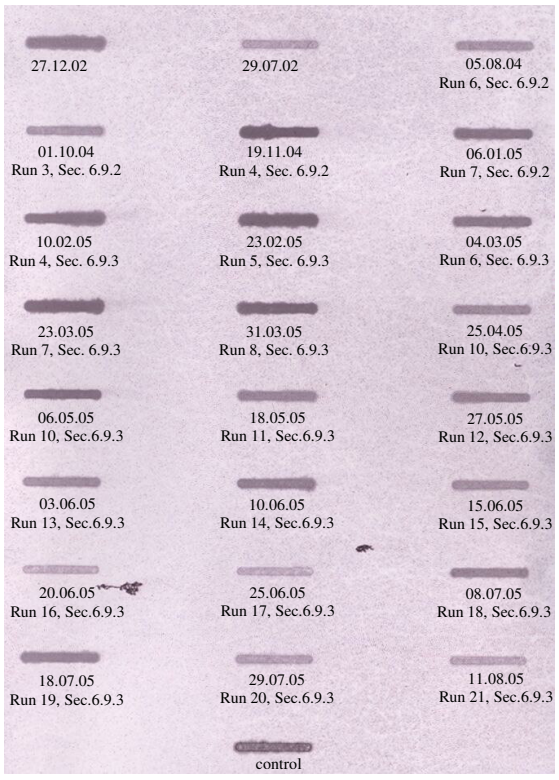

Nitrosomonas species (NSO190)

Nitrobacter species (NIT3)

Nitrospira species (NTSPA662)

Figure 6.68. Results of slot-blot analyses with oligonucleotide probes of EUB338 for Bacteria domain, NSO190 for *Nitrosomonas* species, NIT3 for *Nitrobacter* species, and NTSPA662 for *Nitrospira* species

6.10.3. DGGE (Denaturing Gradient Gel Electrophoresis) Results

DGGE analysis was initially performed to screen whether any changes occurred in the diversity of Bacteria population during continuous-flow experiments (Section 6.9) in the nitrifying biofilm reactor. The DNA sequence differences in the PCR amplified bacterial 16S rRNA genes of the DNA isolates of the biofilm samples are shown in Figure 6.69. DGGE profiles of bacterial 16S rRNA genes in all samples were very similar indicating no shift in the diversity of Bacteria population (Mertoğlu, 2005b).

As a next step, DNA sequence differences in the PCR amplified amoA genes of the DNA isolates were evaluated in order to screen the changes occurred in the diversity of ammonia oxidizers. As seen from Figure 6.69, similar to DGGE profiles of bacterial 16S rRNA, banding patterns and intensities of amoA genes of the DNA isolates were found very similar indicating that no shift had occurred in the diversity of ammonia oxidizers during the operation of the nitrifying biofilm reactor at various ammonium and 1,2-DCA loadings for a time period of about one year.

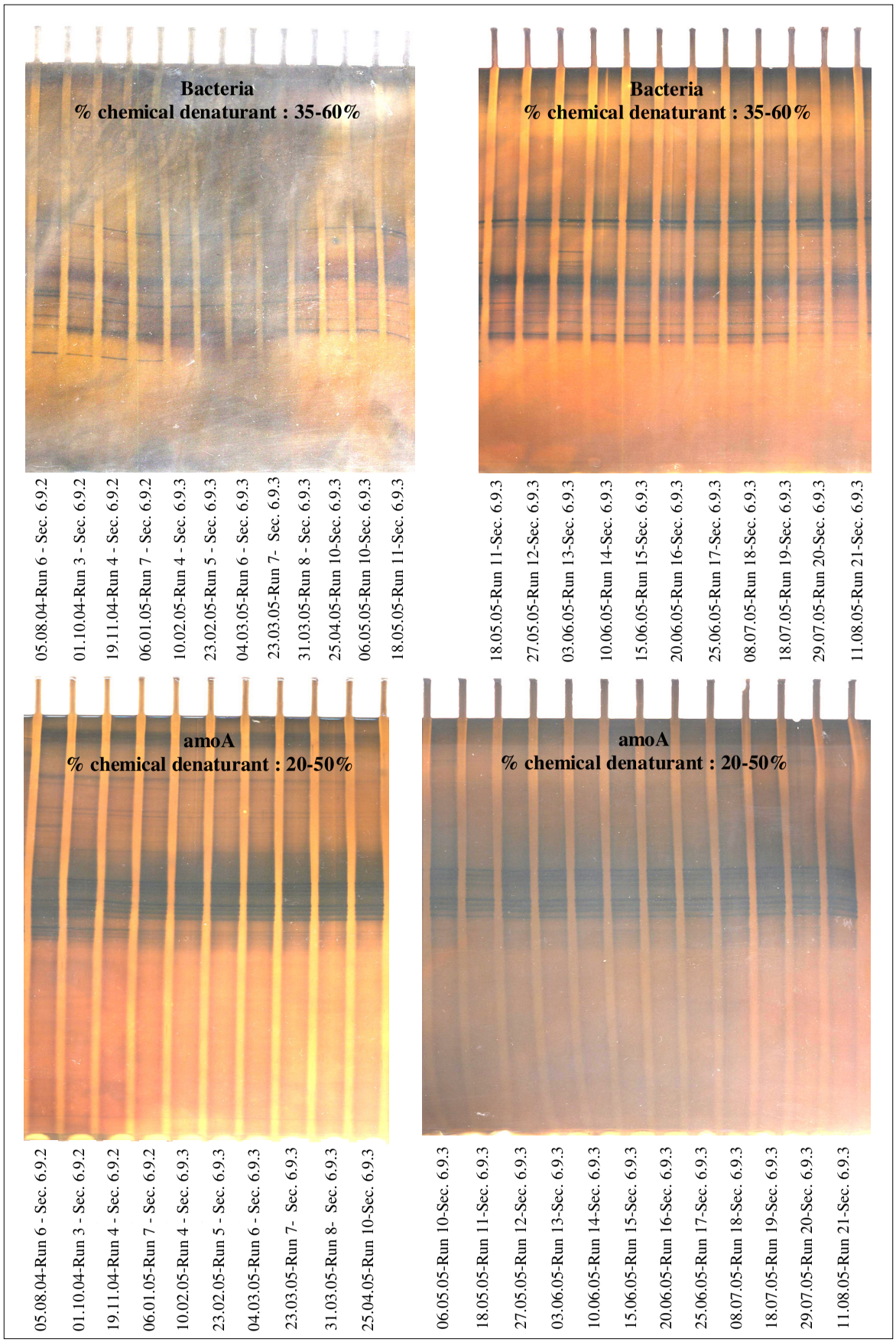

Figure 6.69. DGGE results of PCR amplified bacterial 16S rRNA and amoA genes

7. CONCLUSIONS AND RECOMMENDATIONS

Within the scope of this study, the cometabolic removals of TCE and 1,2-DCA were investigated and their inhibitory effects on nitrification were assessed through batch suspended-growth and continuous-flow biofilm experiments using enriched nitrifying cultures for a time period of about 3.5 years. The major conclusions obtained from these experiments are as follows:

1) In suspended-growth enriched nitrifying batch systems, the presence of TCE (or 1,2-DCA) resulted in both the inhibition of oxygen uptake and ammonium utilization rates. The inhibitory levels of the chloroethane 1,2-DCA were found to be much higher than those of the chloroethene TCE.

2) The inhibitory effect of chloroethene TCE on ammonium oxidation was mainly attributable to the inhibition of ammonia monooxygenase (AMO) enzyme when the cells were exposed to TCE rather than the inhibition of the AMO enzyme by short-lived reactive intermediates produced during TCE oxidation. In contrast to this, the inhibitory effect of the chloroethane 1,2-DCA arose due to the inhibition of the AMO enzyme in nitrifiers by short-lived reaction intermediates produced during 1,2-DCA oxidation.

3) Both TCE and 1,2-DCA were found to be cometabolically degradable by enriched nitrifier cultures using ammonium as the primary substrate. The cometabolic degradation rate of the chloroethane 1,2-DCA was found to be higher than that of the chloroethene TCE.

4) TCE was found to be a competitive inhibitor on ammonia oxidation, which is similar in structure to the normal enzyme substrate and competes with the substrate for the active site of the enzyme. However, the affinity of the TCE for AMO enzyme was found to be significantly higher than that of ammonium.

5) 1,2-DCA was identified as a mixed inhibitor on ammonia oxidation, which can bind both to the free enzyme (E) to build the enzyme-inhibitory substance (EI) complex

and to the enzyme-substrate (ES) complex to build the enzyme-substrate-inhibitory substance (ESI) complex. However, the affinity 1,2-DCA for AMO enzyme was found to be significantly higher than its affinity for enzyme (AMO)-substrate (ammonium) complex. This indicated that at low 1,2-DCA concentrations the competitive characteristic of 1,2- DCA is stronger than its mixed characteristics, but still the mixed inhibition cannot be disregarded. Additionally, the affinity of the 1,2-DCA for AMO enzyme was found to be significantly higher than that of ammonium.

6) The significantly greater affinities of TCE and 1,2-DCA for the AMO enzyme and also NAD(P)H (reductant) regeneration by ammonium resulted in an increase of first-order TCE (or 1,2-DCA) degradation rate constants with increasing ammonium. This indicated that a system using ammonium as the primary substrate has a quite high TCE (or 1,2-DCA) degradation capacity.

7) Ammonium and TCE (or 1,2-DCA) degradation rates were found to be strongly dependent on the initial ammonium and TCE (or 1,2-DCA) concentrations. A strong linear relationship was found between the relative ratio of ammonium and TCE (or 1,2-DCA) degradations and the relative ratio of ammonium and TCE (or 1,2-DCA) concentrations. This relationship allows the estimation of growth substrate (ammonium) requirements for the reduction of TCE (or 1,2-DCA) to a determined concentration and has relevance for the improvement of engineered remediation/treatment systems for TCE (or 1,2-DCA) removal from industrial effluents and many groundwater systems.

8) Statistical analyses of the kinetic models developed by linearized plots of Monod equation (e.g., Lineweaver-Burk, Hanes-Woolf and Eadie-Hofstee plots) and non-linear least square regression (NLSR) resulted in no significant differences among the models. Regarding this finding, it may be concluded that problems with linearization, which are commonly reported in literature, can be compounded when the rate data are obtained for a wide range of substrate concentrations or at substrate concentrations greater than K_s as in the case of present study.

9) In preliminary continuous-flow experiments performed at various ammonium loadings, fundamental biofilm kinetics was found to be applicable to the nitrifying biofilm

reactor. In other words, in nitrification, three kinetic regions, first-, half-, and zero-order could be differentiated. The estimated half-order and zero-order ammonium rate constants were in consistency with those reported in literature for biofilm reactors with similar packings. These kinetic findings are of high importance since they allow the estimation of optimum surface loading rates for a specific NH_4-N discharge criterion.

10) Nitrite accumulation in the biofilm reactor was found to be dependent on both bulk DO concentration and free ammonia (FA) concentration in the reactor. However, the effect of low bulk DO concentration on nitrite accumulation was more significant than bulk FA concentration. Also, the level of nitrite accumulation was shown to be relevant with $C_{DO}/C_{NH4\text{-}N}$ and C_{DO}/C_{FA} ratios.

11) In continuous-flow experiments in the biofilm reactor with 1,2-DCA, 1,2-DCA had no inhibitory effect on the conversion of nitrite to nitrate. It inhibited primarily the conversion of ammonium to hydroxylamine by binding to the AMO enzyme. In case of higher ammonium loadings, the presence of 1,2-DCA inhibited ammonium utilization more severely than at lower ammonium loadings due to stronger competitive inhibition characteristics of 1,2-DCA at bulk 1,2-DCA concentrations present in the reactor and the higher affinity of 1,2-DCA for AMO enzyme with respect to NH_4-N (see Item 5). In case of low ammonium loadings, the competition between 1,2-DCA and NH_4-N for the active site of AMO enzyme resulted in no severe inhibition of ammonium utilization since the active sites of AMO enzymes were probably not fully saturated with the substrate NH_4-N. Hence, there were probably enough available sites for binding of 1,2-DCA. However, in case of higher ammonium loadings, the active sites of AMO enzymes were almost saturated with the NH_4-N. Hence, the presence of 1,2-DCA caused severe inhibition of ammonium utilization due to the higher affinity of 1,2-DCA for AMO enzyme with respect to NH_4-N as mentioned in Item 5.

12) 1,2-DCA inhibition on ammonium utilization in the biofilm reactor was found to be reversible due to the ability of cells to recover from inhibitory effects. When inhibition of ammonia oxidizing activity was greater, a longer recovery phase was needed. Since the results of slot-blot analyses (see Item 18) indicated no significant changes in the quantity of *Nitrosomonas* species throughout the experiments, the recovery of cells from the

inhibitory effects of 1,2-DCA was most probably due to the resynthesis of new proteins within preexisting cells rather than the growth of new cells.

13) At both low ammonium loadings and high ammonium loadings in the biofilm reactor, a great portion (70-90 %) of the initially introduced 1,2-DCA was successfully removed from the system. However, the measured Cl^- production rates were found lower than the stoichiometrically calculated ones. This indicated that some portion of the removed 1,2-DCA was either incompletely dechlorinated into by-products [e.g., chloroacetaldehyde ($ClCH_2CHO$)] or volatilized from the system. However, the detection of high bulk 1,2-DCA concentrations throughout experiments eliminates the possibility of 1,2-DCA volatilization from the system. Moreover, the possibility of formation of incompletely dechlorinated by-products, such as chloroacetaldehyde ($ClCH_2CHO$), is consistent with the oxidative dechlorination mechanism of the monochlorinated carbon.

14) In the biofilm reactor, the increase in Cl^- production with increasing 1,2-DCA removal rates ensured that Cl^- ion release was associated with oxidative dechlorination of 1,2-DCA. Saturation of Cl^- release at high 1,2-DCA removal rates was most probably related to the extent of 1,2-DCA dependent inhibition of ammonium oxidation activity.

15) In the 1,2-DCA concentration range studied in the biofilm reactor, 1,2-DCA removal rate increased with 1,2-DCA concentration as in the case of suspended-growth batch experiments using an enriched nitrifying culture. This indicated the high 1,2-DCA removal capacity of the nitrifying biofilm reactor. Moreover, cometabolic 1,2-DCA degradation rates observed in the present study were found to be quite comparable with metabolic 1,2-DCA degradation rates observed in other studies by pure cultures (e.g., *Xanthobacter autotrophicus* GJ10) which are able to utilize 1,2-DCA as sole carbon and energy source. By considering the fact that the cometabolic degradation rates are usually slower than the metabolic ones, this finding also indicated the quite high 1,2-DCA cometabolic degradation capacity of nitrifiers.

16) As in the case of suspended-growth batch experiments, in continuous-flow experiments with 1,2-DCA in the biofilm reactor, ammonium and 1,2-DCA degradation rates were found to be dependent on NH_4-N and 1,2-DCA loading rates. A linear

relationship was found between the relative ratio of ammonium and 1,2-DCA degradation rates ($r_{NH4\text{-}N}$ /r_{DCA}) and the relative ratio of ammonium and 1,2-DCA loading rates (NH_4-N/DCA). This relationship allows the estimation of growth substrate (ammonium) requirements for the reduction of 1,2-DCA to a specific discharge concentration. This finding will be helpful for the improvement of packed bed submerged biofilm reactor systems for 1,2-DCA removal from industrial effluents and many groundwater systems.

17) FISH analyses of the biofilm samples taken at regular time intervals in continuous-flow experiments indicated that the dominant organisms in the nitrifying biofilm were in the Bacteria domain. The hybridization signals detected for Bacteria and *Nitrosomonas* species were quite comparable indicating the low quantities of other bacterial species. This finding ensured the enrichment of the biofilm reactor for nitrifiers.

18) In slot-blot analyses, in contrast to FISH results, hybridization signals were observed not only for Bacteria domain and *Nitrosomonas* species, but also for *Nitrobacte*r and *Nitrospira* species. No significant changes were observed in the quantity of species in the Bacteria domain, *Nitrosomonas*, *Nitrobacter* and *Nitrospira* species during the operation of the nitrifying biofilm reactor at various ammonium and 1,2-DCA loadings for a time period of about one year. *Nitrosomonas* species were found to be the dominant species in the biofilm. On the other hand, *Nitrobacter* and *Nitrospira* species comprised a small fraction in the total Bacteria domain. The quantitities of *Nitrobacter* and *Nitrospira* species were found to be almost equal to each other. This finding was in contrast to the findings of other researches indicating that *Nitrospira* is the primary nitrite oxidizer in nitrifying biofilm reactors. This discrepancy may be related to the differences in operating conditions, especially in influent ammonium loadings.

19) DGGE profiles of the PCR amplified bacterial 16S rRNA and amoA genes indicated that no shift had occurred in the diversities of Bacteria population and ammonia oxidizers species during the operation of the nitrifying biofilm reactor at various ammonium and 1,2-DCA loadings for a time period of about one year.

The findings of this study provided information to understand the limits of cometabolic degradation of TCE and 1,2-DCA in nitrifying systems. In literature, there is

no such detailed study demonstrating the cometabolism of TCE and 1,2-DCA with a nitrifying culture and dependence of the process on various factors. Therefore, this research could fill a gap in literature and be useful in the design of engineered TCE or 1,2-DCA remediation/treatment systems. In view of the findings of this study, followings are the recommendations for future researches:

1) In the present study, none of the oxygenation methods evaluated (e.g., diffused aeration, H_2O_2 addition, ORC® addition, gas permeable membranes) was found to be appropriate to satisfy the high oxygen requirement of nitrifiers without causing stripping of TCE or 1,2-DCA. Regarding the literature review, bubble-free (or bubbleless) oxygenation via gas permeable membranes may be an attractive solution if the operational conditions are adjusted properly. Therefore, much research must be devoted to this issue.

2) Regarding the widespread occurrence of either TCE or 1,2-DCA in subsurface media in which nitrifying bacteria are ubiquitously present, bioremediation of these compounds in groundwater or soil media is another area requiring additional research.

3) Additional research must be devoted to the identification of chlorinated by-products, especially in the case of cometabolic 1,2-DCA degradation.

4) In the present study, continuous-flow experiments in a nitrifying biofilm reactor could only be carried out with 1,2-DCA because of the high volatility of TCE even at very low rates of pure oxygen supply. The evaluation of cometabolic TCE degradation in a continuous-flow nitrifying biofilm reactor involving an appropriate bubble-free oxygenation system would provide better insight into the applicability of this process under field conditions.

5) TCE or 1,2-DCA contaminated subsurface media usually involves other chlorinated organics formed as a result of natural degradation of these compounds. Therefore, cometabolic degradation of TCE or 1,2-DCA must also be studied in the presence of other chlorinated organic compounds that may coexist with TCE (or 1,2-DCA) in the subsurface media.

REFERENCES

Ahmed, T., Semmens, M., 1992. Use of sealed end hollow fibers for bubbleless membrane aeration: experimental studies. Journal of Membrane Science, 69 (1-2), 1-10.

Alpaslan Kocamemi, B., Çeçen, F., 2005. Cometabolic degradation of TCE in enriched nitrifying batch systems. Journal of Hazardous Materials, B125, 260-265.

Alvarez-Cohen, L., Speitel Jr., G.E., 2001. Kinetics of aerobic cometabolism of chlorinated solvents. Biodegradation, 12, 105-126.

Anderson, J.E., McCarty, P.L., 1997. Transformation yields of chlorinated ethenes by a methanotrophic mixed culture expressing particulate methane monooxygenase. Applied and Environmental Microbiology, 63(2), 687-693.

APHA, AWWA, WEF, 1998. Standard Methods for the Examination of Water and Wastewater. 20th ed., American Public Heath Association, Washington DC, USA.

Arciero, D., Vannelli, T., Logan, M., Hooper, A.B., 1989. Degradation of trichloroethylene by ammonia-oxidizing bacterium *Nitrosomonas europaea*. Biochemical and Biophysical Research Communications, 159(2), 640-643.

Arp, D.J., Yeager, C.M., Hyman, M.R., 2001. Molecular and cellular fundamentals of aerobic cometabolism of trichloroethylene. Biodegradation, 12, 81-103.

Arvin, E., Harremoes, P., 1990. Concepts and models for biofilm reactor performance. Water Science and Technology, 22, 171-192.

ATSDR (Agency for Toxic Substances and Disease Registry), 1997. Toxicological profile for Trichloroethylene, U.S. Department of Health and Human Services, Public Health Service, Agency for Toxic Substances and Disease Registry, Atlanta, Georgia. http://www.atsdr.cdc.gov/toxprofiles/tp19.pdf, 2004.

ATSDR (Agency for Toxic Substances and Disease Registry), 2001a. Toxicological profile for 1,2-Dichloroethane, U.S. Department of Health and Human Services, Public Health Service, Agency for Toxic Substances and Disease Registry, Atlanta, Georgia. http://www.atsdr.cdc.gov/toxprofiles/tp38.pdf, 2004.

ATSDR(Agency for Toxic Substances and Disease Registry), 2001b. ToxFAQs for 1,2-Dichloroethane http://www.atsdr.cdc.gov/tfacts38.html, 2004.

ATSDR(Agency for Toxic Substances and Disease Registry), 2003. ToxFAQs for Trichloroethylene (TCE) http://www.atsdr.cdc.gov/tfacts19.html, 2004.

Bailey, J.E., Ollis, D.F., 1986. Biochemical Engineering Fundamentals. Mc-Graw Hill, Singapore.

Boller, M., Gujer, W., Tschui, M., 1994. Parameters affecting nitrifying biofilm reactors. Water Science and Technology, 29(10-11), 1-11.

Bradley, P.M., 2003. History and ecology of chloroethene biodegradation: A review. Bioremediation Journal, 7(2), 81-109.

Brindle, K., Stephenson, T., 1996. Nitrification in a bubbleless oxygen mass transfer membrane bioreactor. Water Science and Technology, 34(9), 261-267.

CEPA (Canadian Environmental Protection Act), 1993. Priority substances list assessment report: Trichloroetylene, En40-215/27E, Government of Canada, Environment Canada, Health Canada, Ottawa, Canada.
http://www.hc-sc.gc.ca/hecs-sesc/exsd/pdf/trichloroethylene.pdf, 2005.

CEPA (Canadian Environmental Protection Act), 1994. Priority substances list assessment report: 1,2-Dichloroethane, En40-215/38E, Government of Canada, Environment Canada, Health Canada, Canada.
http://www.hc-sc.gc.ca/hecs-sesc/exsd/pdf/1_2_dichloroethane.pdf, 2005.

Chang, H., Alvarez-Cohen, L, 1995a. Transformation capacities of chlorinated organics by mixed cultures enriched on methane, propane, toluene, or phenol. Biotechnology and Bioengineering, 45, 440-449.

Chang, H., Alvarez-Cohen, L, 1995b. Model for the cometabolic biodegradation of chlorinated organics. Environmental Science and Technology, 29(9), 2357-2367.

Chang, H., Alvarez-Cohen, L, 1996. Biodegradation of individual and multiple chlorinated aliphatic hydrocarbons by methane-oxidizing cultures. Applied and Environmental Microbiology, 62(9), 3371-3377.

Chu, K.-H., Alvarez-Cohen, L., 2000. Treatment of chlorinated solvents by nitrogen-fixing and nitrate-supplied methane oxidizers in column packed with unsaturated porous media. Environmental Science and Technology, 34(9),1784-1793.

Clapp, L.W., Reagan, J.M., Ali, F., Newman, J.D., Park, J.K., Noguera, D.R., 1999. Activity, structure, and stratification of membrane-attached methanotrophic biofilms cometabolically degrading trichloroethylene, Water Science and Technology, 39(7), 153-161.

Cornish-Bowden, A., 1995. Fundamentals of Enzyme Kinetics. Portland Press Ltd, London.

Criddle, C.S., 1993. The kinetics of cometabolism. Biotechnology and Bioengineering, 41 (11), 1048-1056.

Çeçen, F., Gönenç, I.E., 1994. Nitrogen removal characteristics of nitrification and denitrification filters. Water Science and Technology, 29(10-11), 409-416.

Çeçen, F., Gönenç, I.E., 1995. Criteria for nitrification and denitrification of high-strength wastes in two upflow submerged filters. Water Environment Research, 67(2), 132-142.

Çeçen F., Orak E., Gökçin P., 1995. Nitrification studies on fertilizer wastewaters in activated sludge and biofilm reactors. Water Science and Technology, 32 (12), 141-148.

Çeçen F., 1996. Investigation of partial and full nitrification characteristics of fertilizer wastewaters in a submerged biofilm reactor. Water Science and Technology, 34 (11), 77-85.

Çeçen, F., Orak, E., 1996. Nitrification of fertilizer wastewaters in a biofilm reactor. Journal of Chemical Technology and Biotechnology, 65, 229-238.

Çeçen F., Ipek S., 1998. Determination of the inhibition of ammonia-N and urea-N oxidation by the fed-batch reactor (FBR) technique. Wat. Sci. Tech., 38 (1), 141-148.

Daims, H., Nielsen, P.H., Nielsen, J.L., Juretschko, S., Wagner, M., 2000. Novel *Nitrospira*-like bacteria as dominant nitrite-oxidizers in biofilms from wastewater treatment plants: diversity and *in situ* physiology. Water Science and Technology, 41(4), 85-90.

Daims, H., Purkhold, U., Bjerrum, L., Arnold, E., Wilderer, P.A., Wagner, M., 2001. Nitrification in sequencing biofilm batch reactor: lessons from molecular approaches. Water Science and Technology, 43(3), 9-18.

Dollerer, J., Wilderer, P.A., 1996. Biological treatment of leachates from hazardous waste landfills using SBBR technology. Water Science and Technology, 34(7-8), 437-444.

Dyer, M., Van Heiningen, E., Gerritse, J., 2000. In situ bioremediation of 1,2-dichloroethane under anaerobic conditions. Geotechnical and Geological Engineering, 18, 313-334.

Ely, R.L., Williamson, K.J., Guenther, R.B., Hyman, M.R., Arp, D.J., 1995a. A cometabolic kinetics model incorporating enzyme inhibition, inactivation, and recovery: I. Model development, analysis, and testing. Biotechnology and Bioengineering, 46(3), 218-231.

Ely, R.L., Hyman, M.R., Arp, D.J., Guenther, R.B., Williamson, K.J., 1995b. A cometabolic kinetics model incorporating enzyme inhibition, inactivation, and recovery: II. Trichloroethylene degradation experiments. Biotechnology and Bioengineering, 46(3), 232-245.

Ely, R.L., Williamson, K.J., Hyman, M.R., Arp, D.J., 1997. Cometabolism of chlorinated solvents by nitrifying bacteria: kinetics, substrate, interactions, toxicity effects, and bacterial response. Biotechnology and Bioengineering, 54(6), 520-534.

EPA (United States Environmental Protection Agency), 1992. TCE removal from contaminated soil and groundwater, EPA/540/S-92/002, Office of Solid Waste and Emergency Response, US EPA, Washington, D.C. http://www.epa.gov/tio/tsp/download/tce.pdf, 2004.

EPA (United States Environmental Protection Agency), 1993a. Emerging technology summary: Pilot-Scale demonstration of a two-stage methanotrophic bioreactor for biodegradation of trichloroethylene in groundwater, EPA/540/S-93/505, Superfund Innovative Technology Evaluation, US EPA, Washington, D.C. http://www.epa.gov/ORD/SITE/reports/540s93505/540s93505.pdf, 2004.

EPA (United States Environmental Protection Agency), 1993b. Nitrogen Removal, EPA/625/R-93/010, Office of Research and Development, Office of Water, Washington, DC 20460.

EPA (United States Environmental Protection Agency) , 2000. Treatment Experiences at RCRA Corrective Actions , EPA 542-F-00-020, Solid Waste and Emergency Response (5102G), US EPA, Washington, D.C. http://clu-in.org/download/remed/rcraexp.pdf, 2004.

Fetzner, S., 1998. Bacterial dehalogenation. Applied Microbiology and Biotechnology, 50, 633-657.

Field, J.A., Sierra-Alvarez, R., 2004. Biodegradability of chlorinated solvents and related chlorinated aliphatic compounds. Reviews in Environmental Science & Bio/Technology, 3, 185-254.

Florence, T.M., Farrar, Y.J., 1971. Spectrophotometric determination of chloride at the parts-per-billion level by the mercury(II) thiocyanate method. Analytica Chimica Acta, 54, 373-377.

Gaudy, F.A., Gaudy, E.T., 1980. Microbiology for Environmental Scientists and Engineers. McGraw-Hill Inc., U.S.A.

Gantzer, C.J., 1994. Bubbleless oxygen dissolution for reducing VOC emissions from wastewater treatment plants. U.S. Environmental Protection Agency, National Center for Environmental Research, EPA Contract Number: 68D40037. http://cfpub.epa.gov/ncer_abstracts/index.cfm/fuseaction/display.abstractDetail/abstract/1479, 2004.

Ginestet, P., Audic, J.M., Block, J.C., 2001. Chlorinated solvents cometabolism by an enriched nitrifying bacterial consortium. Water Science and Technology, 1 (4), 95-102.

Guo, G-L., Tseng, D-H., Huang, S-L., 2001. Co-metabolic degradation of trichloroethylene by *Pseudomonas putida* in a fibrous bed bioreactor. Biotechnology Letters, 23, 1653-1657.

Hage, J.C., Hartmans, S., 1999. Monooxygenase-mediated 1,2-dichloroethane degradation by *Pseudomonas sp.* strain DCA1. Applied and Environmental Microbiology, 65 (6), 2466-2470.

http://www.azdeq.gov/environ/waste/sps/download/phoenix/wcpnpb.pdf, 2005: Registry Report-West Central Phoenix-North Plume

http://www.braytonlaw.com/news/mednews/070204_bery_fl.htm, 2005: Groundwater Near Former Florida Plant Contaminated.

http://www.costperformance.org/search.cfm, 2005: FRTR (Federal Remediation Technologies Roundtable)- Pump and Treat of Contaminated Groundwater at the OTT/Story/Cordova Superfund Site, North Muskegon, Michigan (2001)

http://www.costperformance.org/search.cfm, 2005: FRTR (Federal Remediation Technologies Roundtable)- Pump and Treat of Contaminated Groundwater at the U.S. Aviex Superfund Site, Niles, Michigan (1998)

http://www.costperformance.org/search.cfm, 2005: FRTR (Federal Remediation Technologies Roundtable)- Pump and Treat and In Situ Bioremediation of Contaminated Groundwater at the French Ltd. Superfund Site, Crosby, Texas (1998)

http://clu-in.org/contaminantfocus/default.focus/sec/Trichloroethylene_(TCE)/cat/Overview/: Contaminant Focus- Trichloroethylene (TCE), 2004.

http://www.drycleancoalition.org/profiles, 2005: State Coalition for Remediation of Drycleaners- Site Profiles-View-Butler Cleaners Site (#2), Jacksonville, Florida, U.S.

http://www.drycleancoalition.org/profiles, 2005: State Coalition for Remediation of Drycleaners- Site Profiles-View-Denver Colarado Dry Cleaner, Denver, Colorado, U.S.

http://www.lanl.gov/orgs/d/d4/enviro/etcap/bio_soil.html, 2005: ETCAP (Environmental Technology Cost-savings Analysis Project) –Soil, Sediment & Sludge: Biological treatments- Jasco Chemical Superfund Site, Mountain View, California (1992)

http://www.regenesis.com/products/orc/, 2004: ORC (Oxygen Release Compound) Overview

http://www.synthetech.com/download/wastewater.pdf, 2005: Sythetech Inc., Albany, Oregon, U.S., The use of evaporation and biological treatment to meet pharmaceutical pretreatment standards.

http://www.toronto.ca/health/pdf/cr_appendix_b_trichloroethylene.pdf, 2005: Tox-Probe Inc., Ten Carcinogens in Toronto-Trichloroethylene.

Hyman, M.R., Russell, S.A., Ely, R.L., Williamson, K.J., Arp, D.J., 1995. Inhibition, inactivation, and recovery of ammonia-oxidizing activity in cometabolism of trichloroethylene by *Nitrosomonas europaea*. Applied and Environmental Microbiology, 61(4), 1480-1487.

Inguva, S., Shreve, G.S., 1999. Biodegradation kinetics of trichloroethylene and 1,2-dichloroethane by *Burkholderia (Pseudomonas) cepacia* $PR1_{31}$ and *Xanthobacter autotrophicus* GJ10. International Biodeterioration and Biodegradation, 43: 57-61

Janssen, D.B., Scheper, A., Dijkhuizen, L., Witholt, B., 1985. Degradation of halogenated aliphatic compounds by *Xanthobacter autotrophicus GJ10*. Applied and Environmental Microbiology, 49(3), 673-677.

Juliastuti, S.R., Baeyens, J., Creemers, C., Bixio, D., Lodewyckx, E., 2003. The inhibitory effect of heavy metals and organic compounds on the net maximum specific growth rate of the autotrophic biomass in activated sludge. Journal of Hazardous Materials, 2003 (1-3), 271-283.

Klecka, G.M., Carpenter, C.L., Gonsior, S.J., 1998. Biological transformations of 1,2-dichloroethane in subsurface soils and groundwater. Journal of Contaminant Hydrology, 34, 139-154.

Knightes, C.D., Peters, C.A., 2000. Statistical analysis of nonlinear parameter estimation for Monod biodegradation kinetics using bivariate data. Biotechnology and Bioengineering, 69 (2),160-170.

Mader, Sylvia S., 1990. Biology. Wm. C. Brown Publishers, U.S.A.

Magnuson, J.K., Stern, R.V., Gossett, J.M., Zinder, S.H., Burris, D.R., 1998. Reductive dechlorination of tetrachloroethene to ethene by a two-component enzyme pathway. Applied and Environmental Microbiology, 64(4), 1270-1275.

McCarty, P.L., 2000. Novel biological removal of hazardous chemicals at trace levels. Water Science and Technology, 42(12), 49-60.

Mertoğlu, B., 2005a. Monitoring of Microorganisms in Aerobic and Anaerobic Landfill Bioreactors by Using Molecular Techniques, Ph.D. Thesis, Marmara University, Institute of Graduate Studies in Pure and Applied Sciences.

Mertoğlu, B., 2005b. Cooperative work of the candidate with Bülent Mertoğlu at Marmara University, Department of Environmental Engineering.

Metcalf and Eddy, Inc., 2003. Wastewater Engineering Treatment and Reuse. McGraw Hill Inc., 4th Edition, New York.

Moran, L., Scrimgeour, K., Horton, H., Oehs, R., Rawn, J., 1994. Biochemistry, Prentice Hall, 2nd Edition, New Jersey, USA.

Oldenhius, R., Vink, R.L.J.M., Janssen, D.B., Witholt, B., 1989. Degradation of chlorinated aliphatic hydrocarbons by *Methylosinus trichosporium* OB3b expressing soluble methane monooxygenase. Applied and Environmental Microbiology, 55, 2819-2826.

Orak, Elvan, 1994. Start-up and Operation of a Nitrifying Biofilm Reactor, M.S. Thesis, Bogazici University, Institute of Environmental Sciences.

Racsche, M.E., Hyman, M.R., Arp, D.J., 1991. Factors limiting aliphatic chlorocarbon degradation by *Nitrosomonas europaea*: Cometabolic inactivation of ammonia monooxygenase and substrate specificity. Applied and Environmental Microbiology, 57(10), 2986-2994.

Papp, R., 1996. Organochlorine waste management. Pure &Applied Chemistry, 68 (9), 1801-1808.

Rittmann, B.E, McCarty, P.L., 2001. Environmental Biotechnology: Principles and Applications. McGraw Hill, New York.

Schramm, A., Beer, D., Wagner, M., Amann, R., 1998. Identification and activities in situ of *Nitrosospira* and *Nitrospira* spp. as dominant populations in a nitrifying fluidized bed reactor. Applied and Environmental Microbiology, 64(9), 3480-3485.

Shuler, M.L., Kargi, F., 2001. Bioprocess Engineering Basic Concepts, Prentice Hall, International Series in the Physical and Chemical Engineering Sciences.

Singleton, I., 1994. Microbial metabolism of Xenobiotics: Fundamental and applied research. Journal of Chemical Technology and Biotechnology, 59, 9-23.

Smith, L.H., Kitanidis, P.K., McCarty, P.L., 1997. Numerical modelling and uncertainties in rate coefficients for methane utilization and TCE cometabolism by a methane-oxidizing mixed culture. Biotechnology and Bioengineering, 53 (3), 320-331.

Speitel, G.E., Segar, R.L., 1995. Cometabolism in biofilm reactors. Water Science and Technology, 31(1), 215-225.

Van Hylckama Vlieg, J.E.T., Janssen, D.B., 2001. Formation and detoxification of reactive intermediates in the metabolism of chlorinated ethenes. Journal of Biotechnology, 85, 81-102.

Vannelli, T., Logan, M., Arciero, D., Hooper, A.B., 1990. Degradation of halogenated aliphatic compounds by the ammonia-oxidizing bacterium *Nitrosomonas europaea.* Applied and Environmental Microbiology, 56(4), 1169-1171.

Ward, C.H., Cherry, J.A., Scalf, M.R., 1997. Subsurface restoration. Ann Arbor Press Inc., Michigan, USA.

Yang, L., 1997. Metabolism dechlorination of trichloroethylene by nitrifying bacteria in an enriched batch culture, 52nd Purdue Industrial Waste Conference Proceedings May 5-7, 1997, Purdue University, West Lafayette, Indiana, 105-114.

Yang, L., Chang, Y.-F., Chou, M.-S., 1999. Feasibility of bioremediation of trichloroethylene contaminated sites by nitrifying bacteria through cometabolism with ammonia. Journal of Hazardous Materials, B69, 111-126.

Yeager, C.M., Arthur, K.M., Bottomley, P.J., Arp, D.J., 2004. Trichloroethylene degradation by toluene-oxidizing bacteria grown on non-aromatic substrates. Biodegradation, 15, 19-28.

APPENDIX A: NH_4-N, NO_2-N and NO_3-N MEASUREMENTS DURING THE ENRICHMENT PERIOD FOR NITRIFIERS

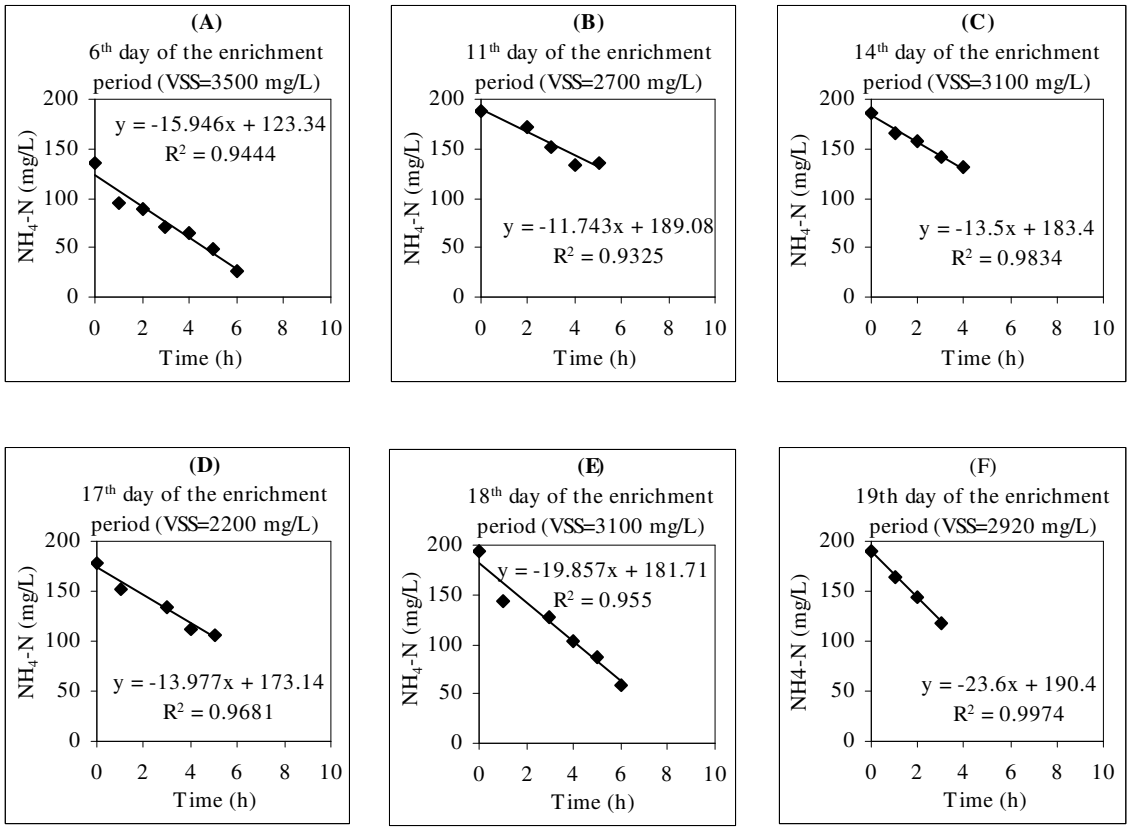

Figure A.1. Ammonium (NH_4-N) utilization at the (a) 6th day, (b) 11th day, (c) 14th day, (d) 17th day, (e) 18th day and (f) 19th day of the enrichment period

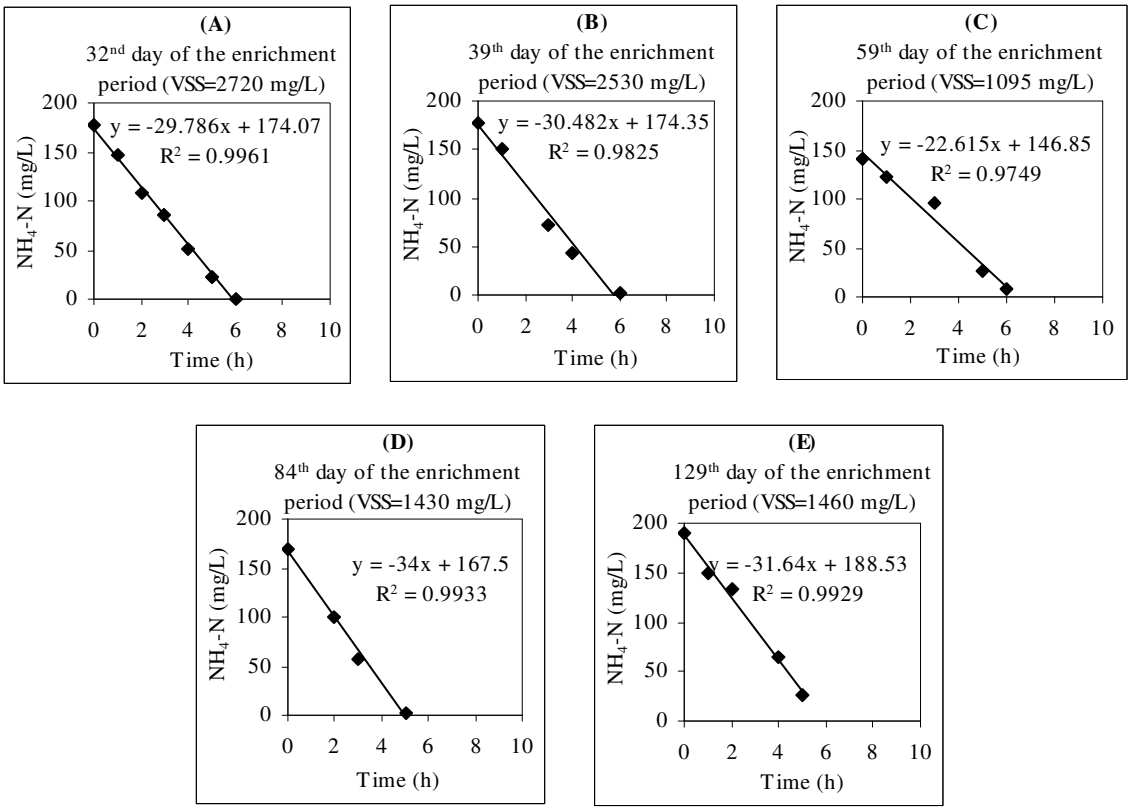

Figure A.2. Ammonium (NH_4-N) utilization at the (a) 32nd day, (b) 39th day, (c) 59th day, (d) 84th day, (e) 129th day of the enrichment period

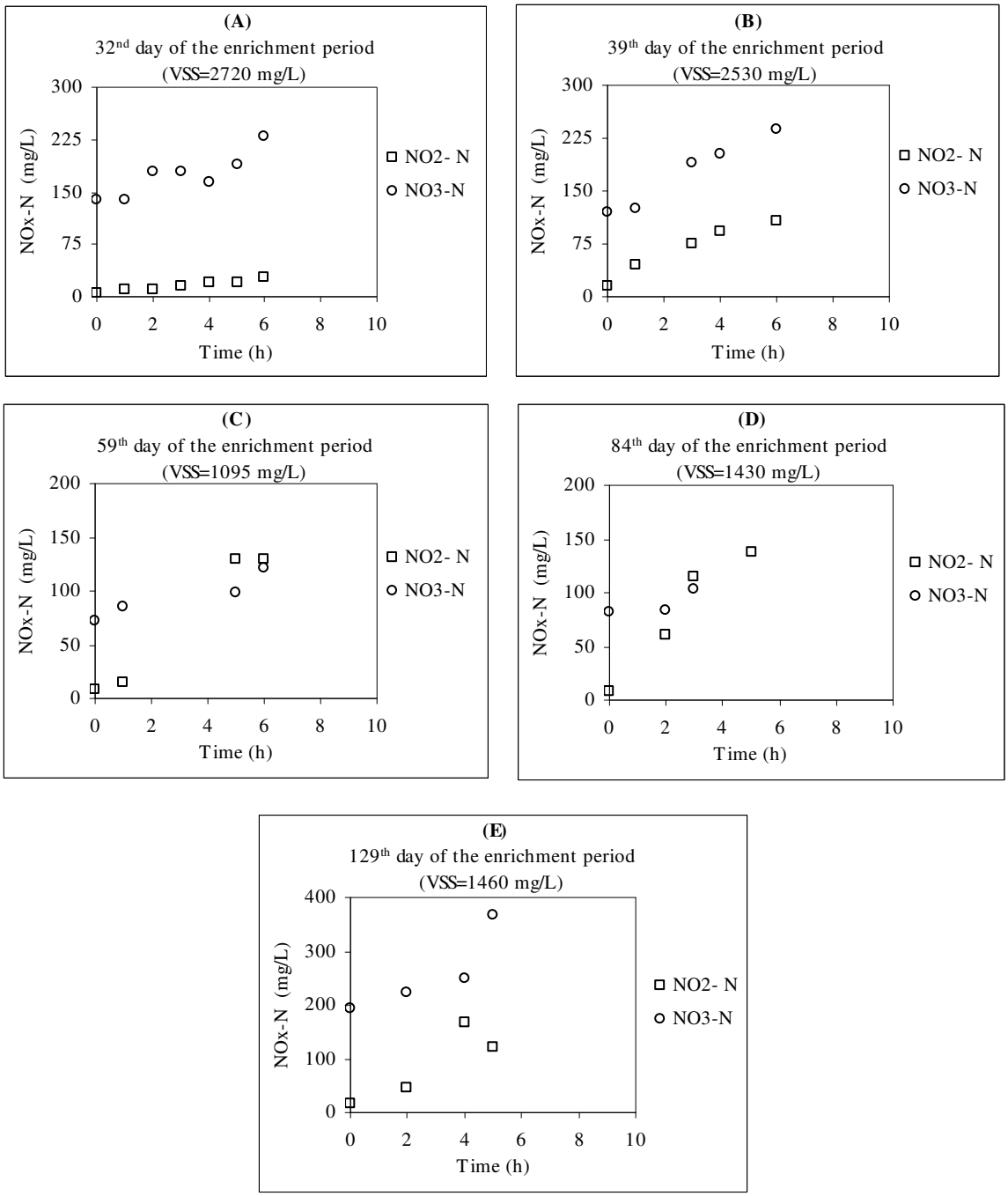

Figure A.3. Nitrite (NO_2-N) and nitrate (NO_3-N) measurements at the (a) 32nd day, (b) 39th day, (c) 59th day, (d) 84th day, (e) 129th day of the enrichment period

APPENDIX B: DETERMINATION OF SPECIFIC AMMONIUM UTILIZATION RATES (qNH_4-N) UNDER DIFFUSED AIR CONDITIONS

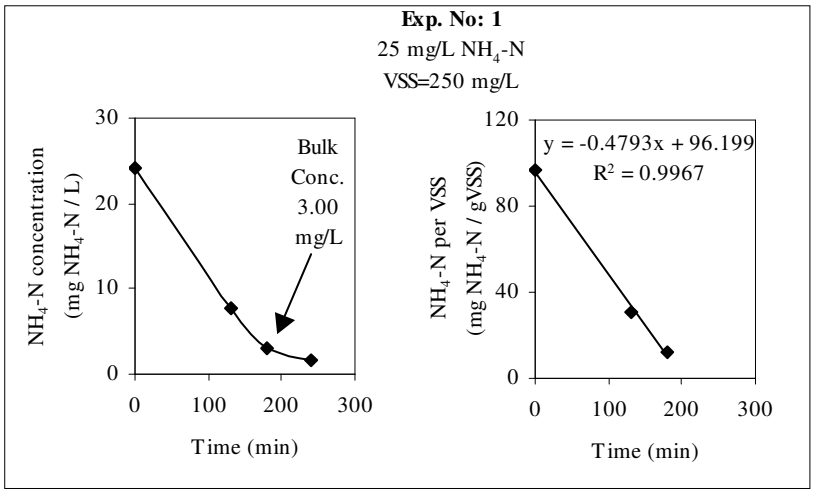

Figure B.1. Ammonium (NH_4-N) utilization under diffused air condition in Exp. No.1

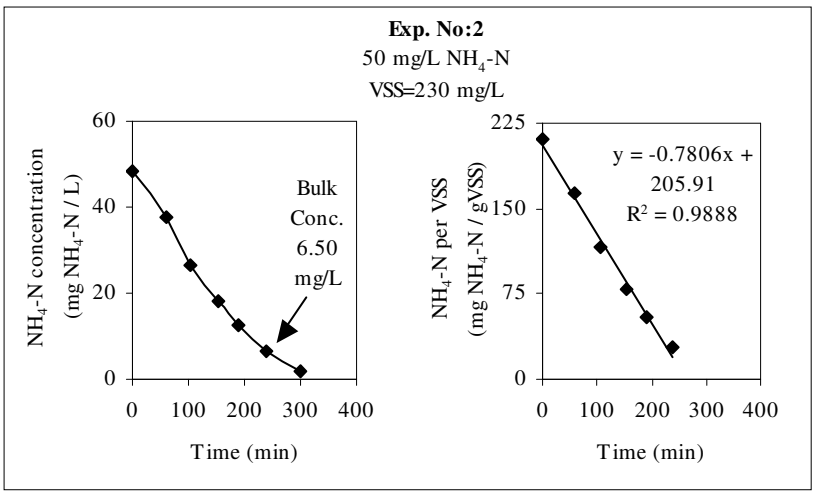

Figure B.2. Ammonium (NH_4-N) utilization under diffused air condition in Exp. No.2

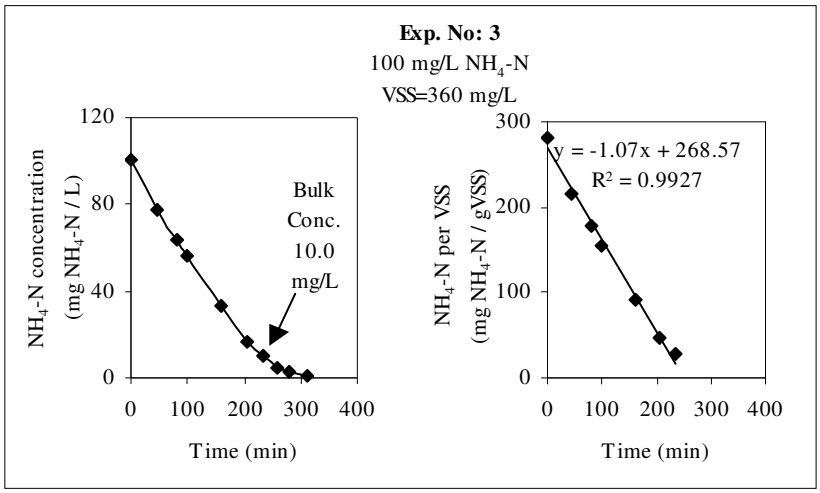

Figure B.3. Ammonium (NH_4-N) utilization under diffused air condition in Exp. No.3

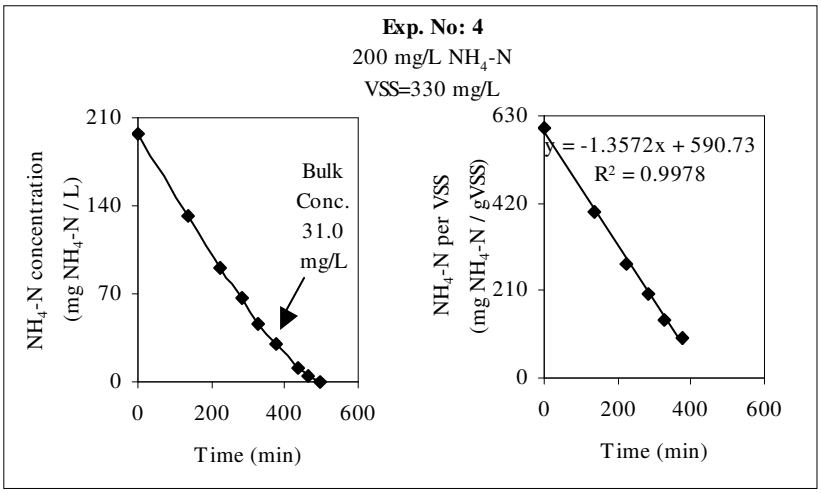

Figure B.4. Ammonium (NH_4-N) utilization under diffused air condition in Exp. No.4

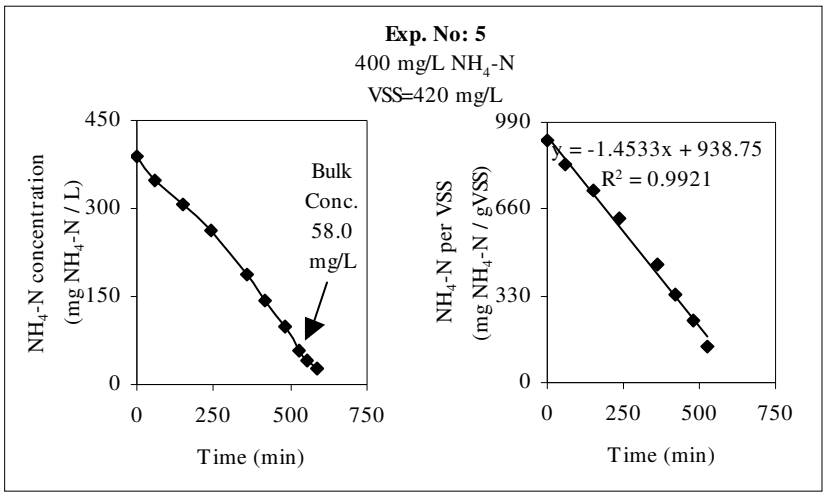

Figure B.5. Ammonium (NH_4-N) utilization under diffused air condition in Exp. No.5

APPENDIX C: DETERMINATION OF SPECIFIC OXYGEN UPTAKE RATES (SOUR) IN PRELIMINARY OXYGEN UPTAKE RATE (OUR) EXPERIMENTS WITH TCE

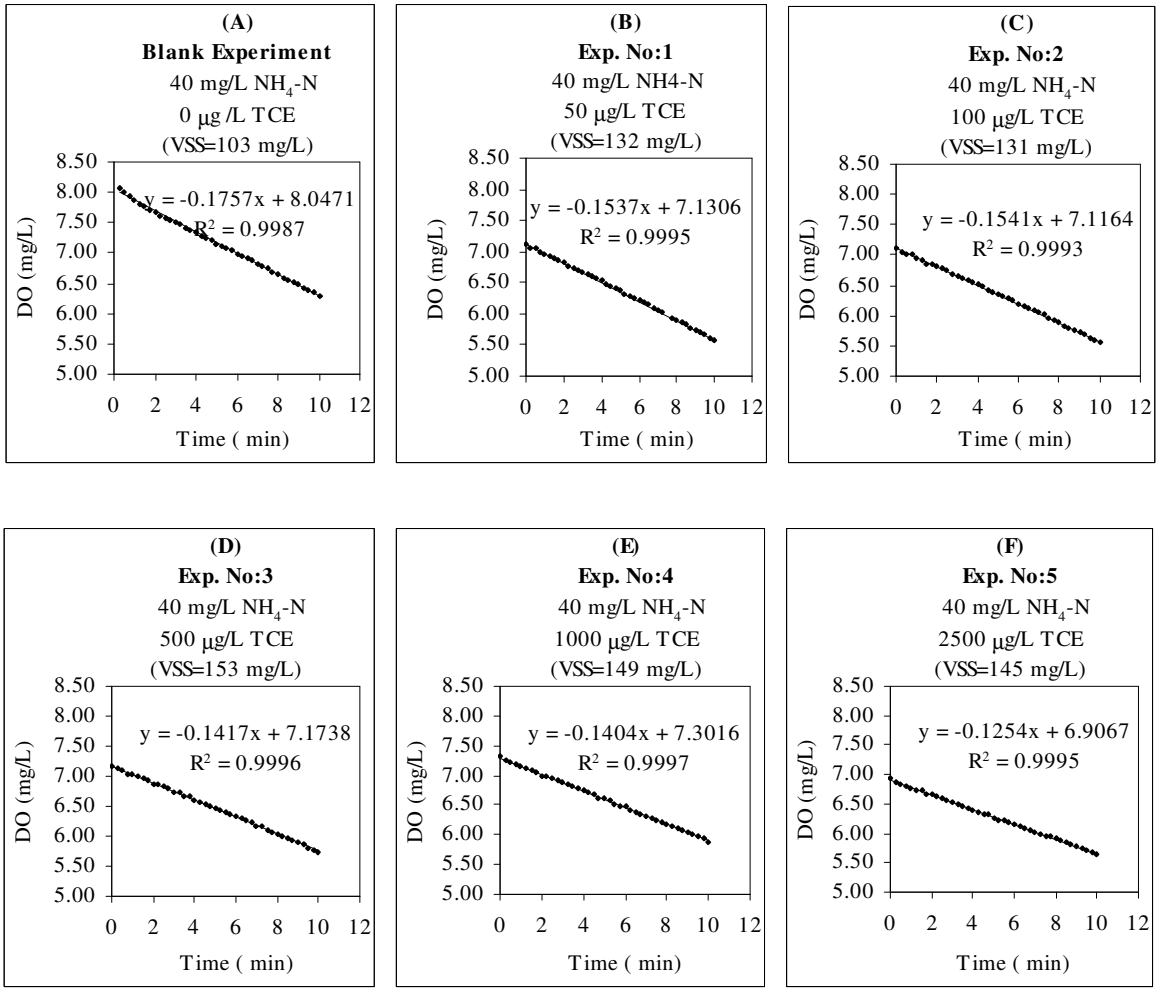

Figure C.1. Preliminary oxygen uptake with TCE (a) in the blank experiment (b) in Exp. No.1 (c) in Exp. No.2 (d) in Exp. No.3 (e) in Exp. No.4 and (f) in Exp. No.5

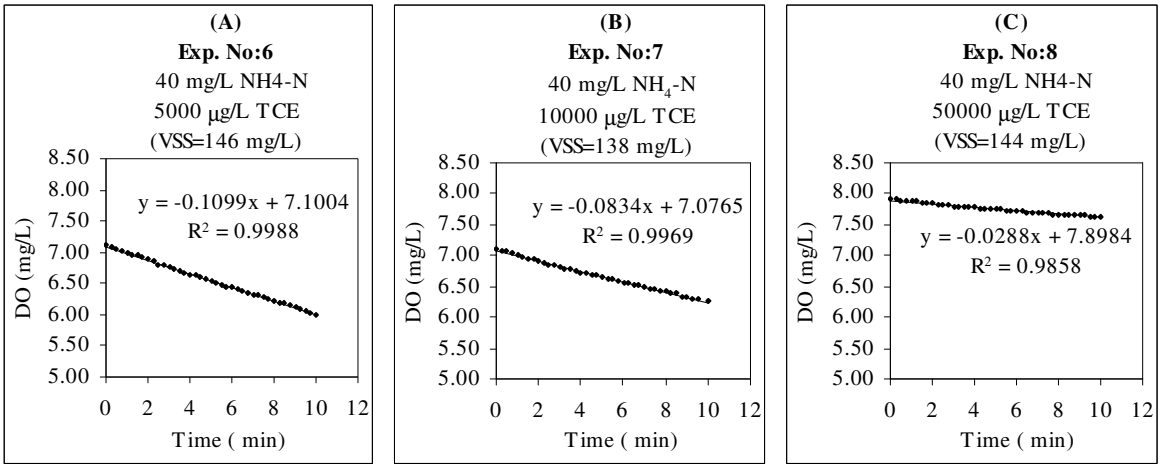

Figure C.2. Preliminary oxygen uptake with TCE (a) in Exp. No.6, (b) in Exp. No.7, (c) in Exp. No.8

APPENDIX D: DETERMINATION OF SPECIFIC AMMONIUM UTILIZATION RATES (qNH4-N) IN BATCH EXPERIMENTS WITH TCE

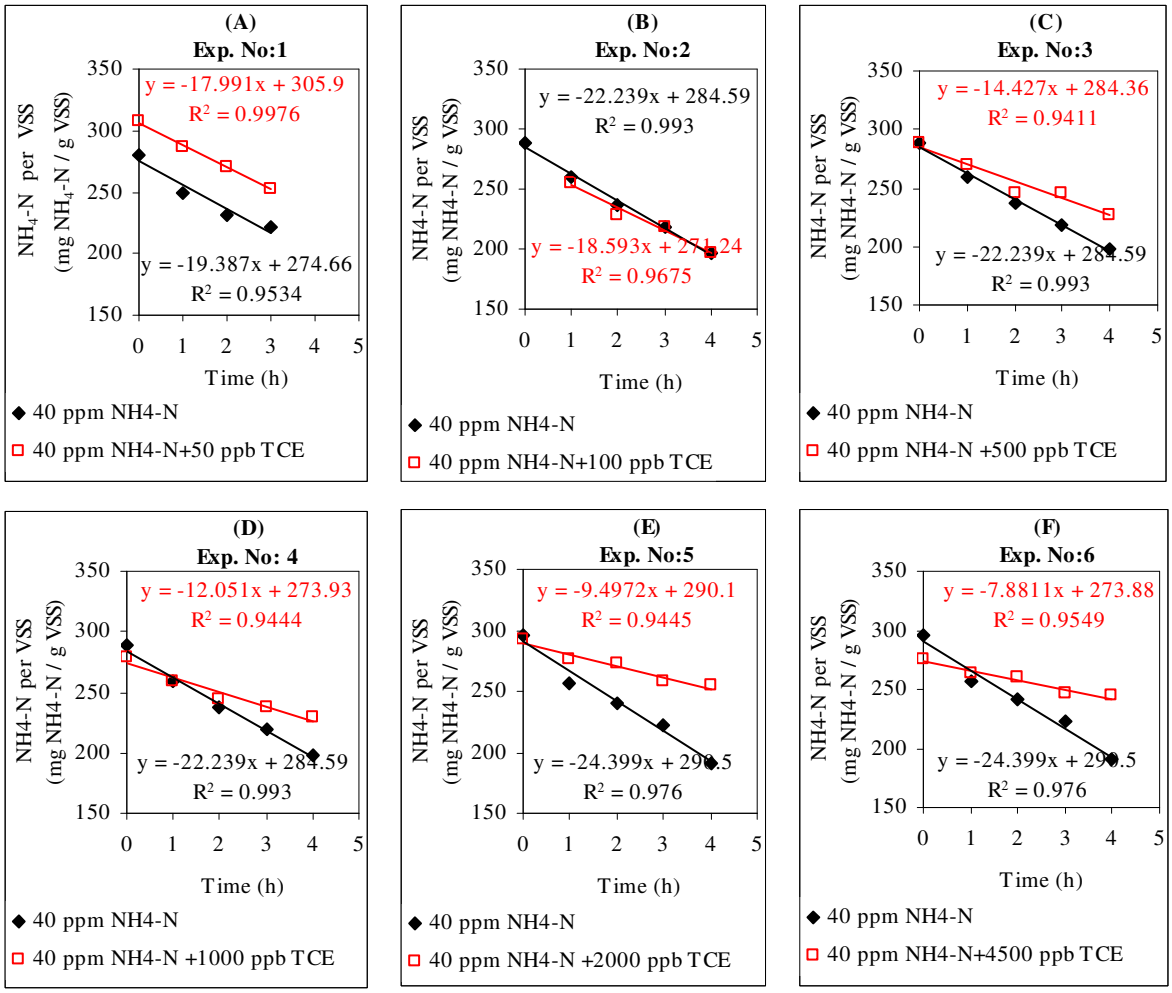

Figure D.1. Specific ammonium utilization in batch experiments with TCE (a) in Exp. No.1, (b) in Exp. No.2, (c) in Exp. No.3, (d) in Exp. No.4, (e) in Exp. No.5, and (f) in Exp. No.6

APPENDIX E: DETERMINATION OF SPECIFIC OXYGEN UPTAKE RATES (SOUR) IN BATCH EXPERIMENTS WITH TCE

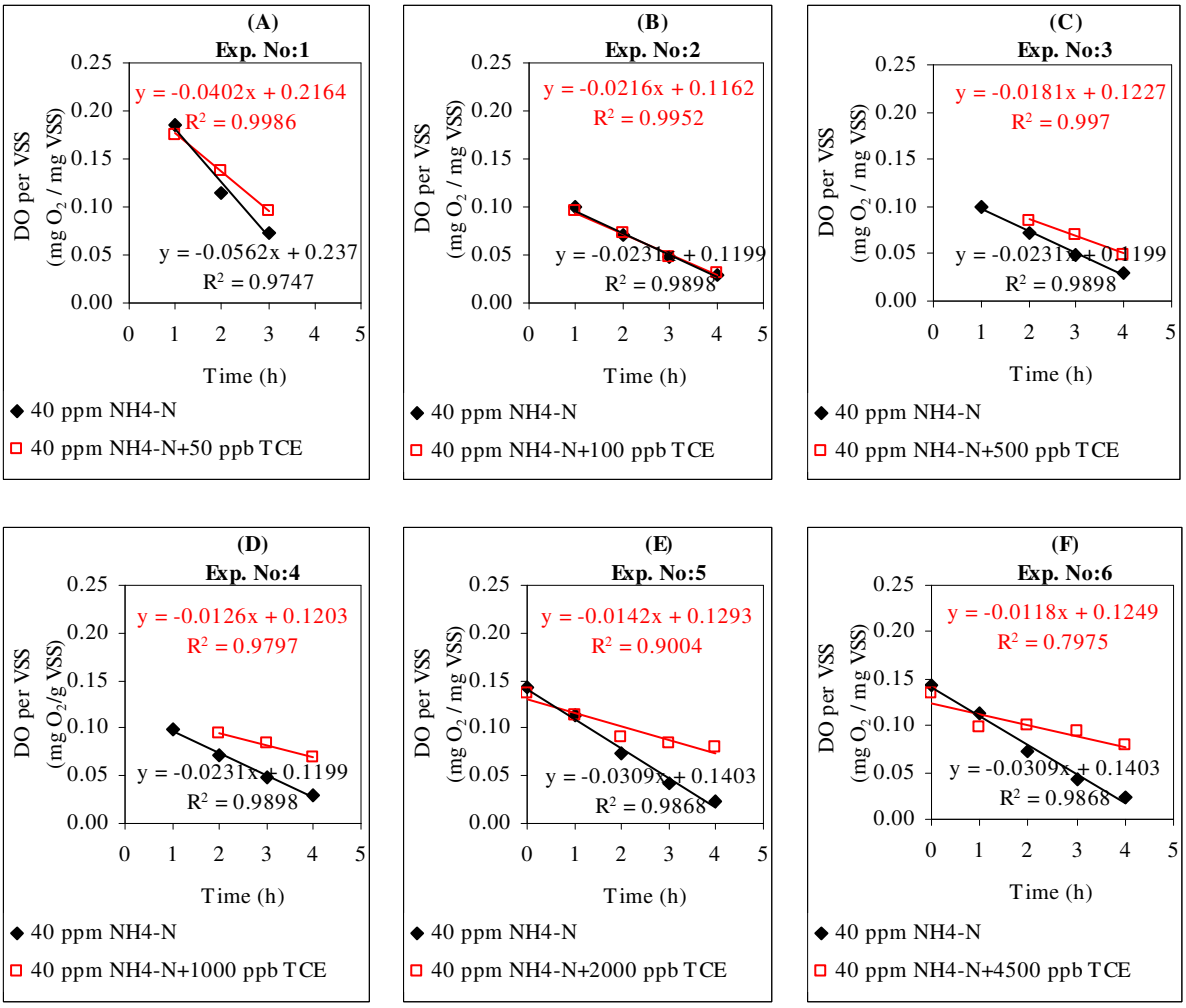

Figure E.1. Specific oxygen uptake in batch experiments with TCE (a) in Exp. No.1, (b) in Exp. No.2, (c) in Exp. No.3, (d) in Exp. No.4, (e) in Exp. No.5, and (f) in Exp. No.6

APPENDIX F: DETERMINATION OF TCE VOLATILIZATION RATES IN BATCH EXPERIMENTS

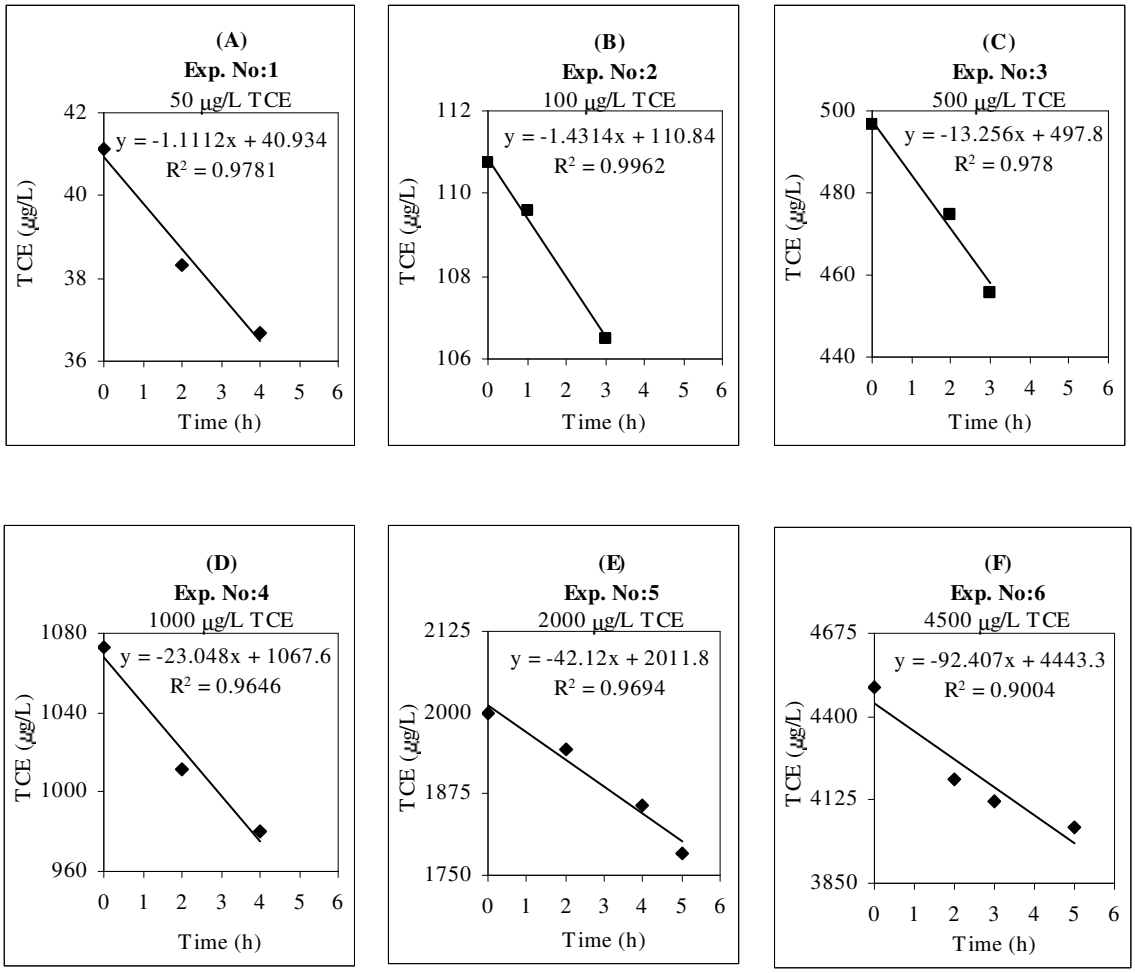

Figure F.1. Volatilization rates of TCE for the initial TCE concentration of (a) 50 µg/L, (b) 100 µg/L, (c) 500 µg/L, (d) 1000 µg/L, (e) 2000 µg/L, (f) 4500 µg/L

APPENDIX G: DETERMINATION OF SPECIFIC COMETABOLIC TCE DEGRADATION RATES (qTCE) IN BATCH EXPERIMENTS

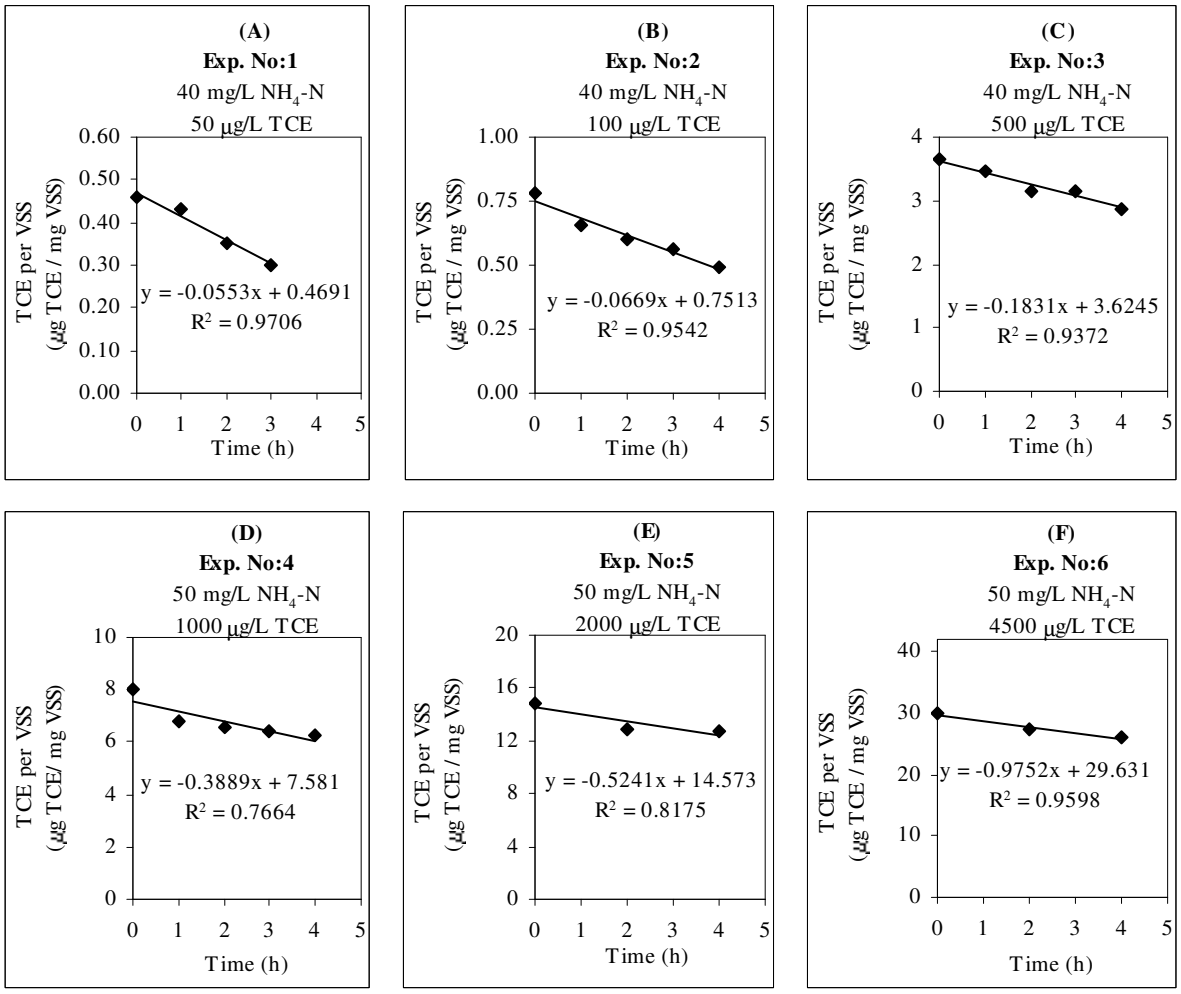

Figure G.1. Specific cometabolic degradation of TCE in batch experiments (a) in Exp. No.1, (b) in Exp. No.2, (c) in Exp. No.3, (d) in Exp. No.4, (e) in Exp. No.5, (f) in Exp. No.6

APPENDIX H: DETERMINATION OF SPECIFIC AMMONIUM UTILIZATION RATES (qNH_4-N) IN BATCH EXPERIMENTS WITH TCE DIRECTED TO KINETIC MODELLING

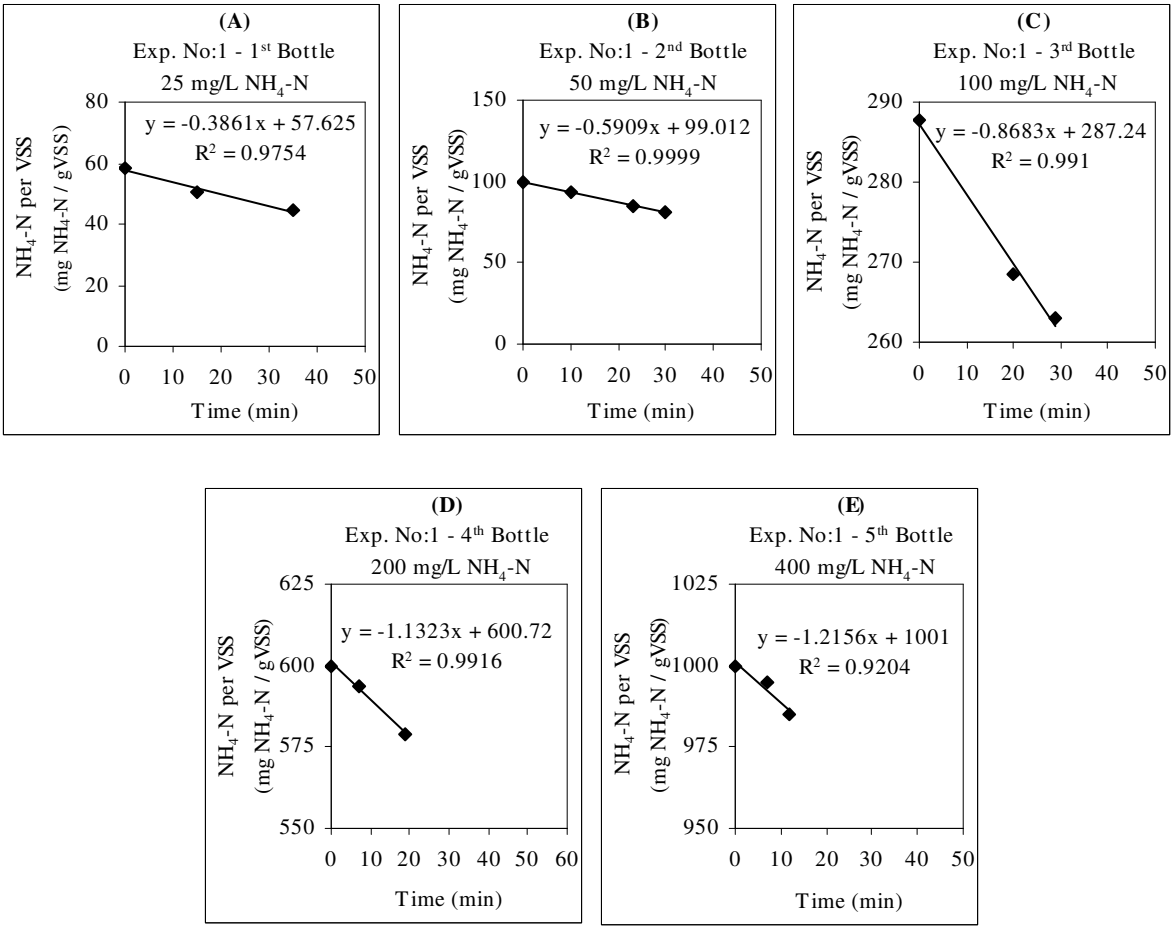

Figure H.1. Specific ammonium utilization in batch experiments with TCE directed to kinetic modelling No.1 (a) 1st bottle, (b) 2nd bottle, (c) 3rd bottle, (d) 4th bottle, (e) 5th bottle

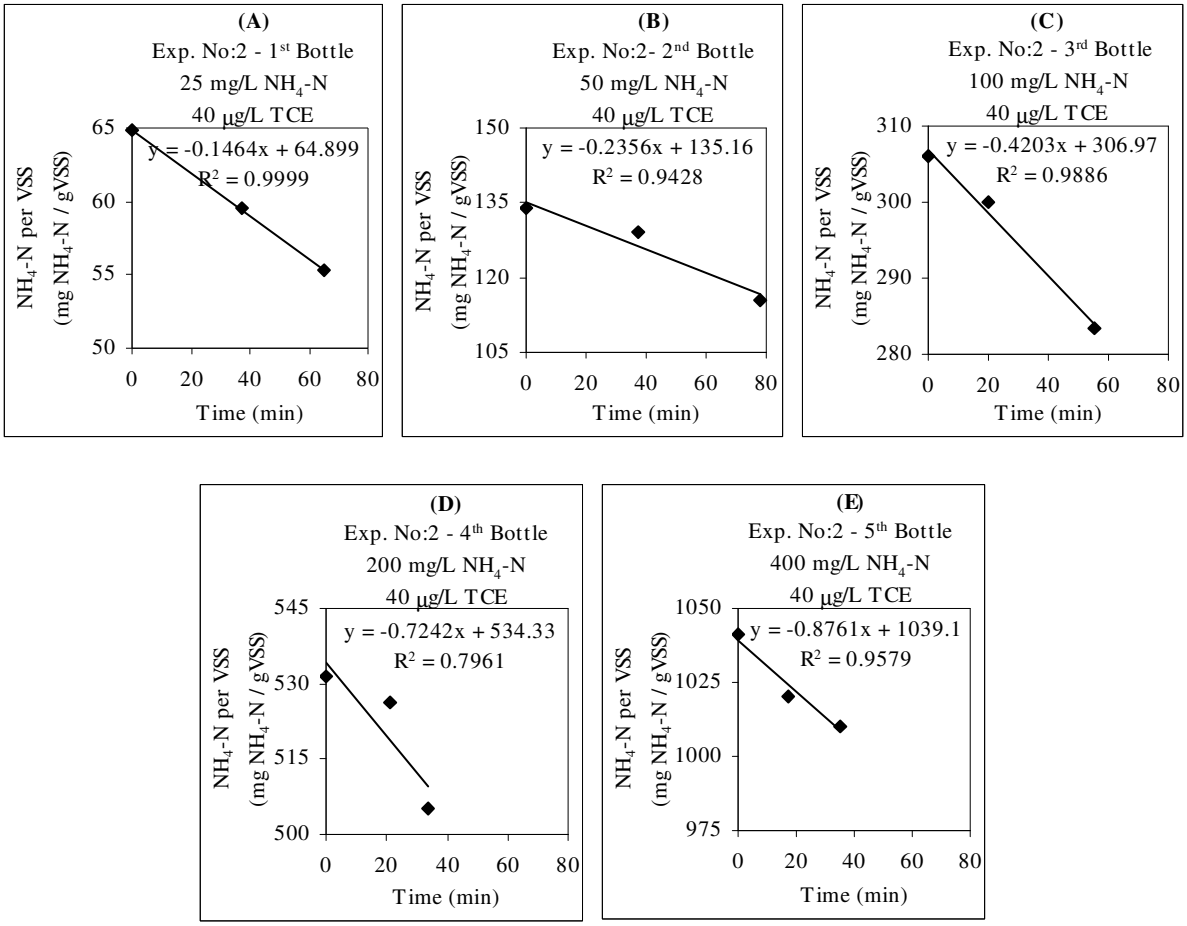

Figure H.2. Specific ammonium utilization in batch experiments with TCE directed to kinetic modelling No.2 (a) 1st bottle, (b) 2nd bottle, (c) 3rd bottle, (d) 4th bottle, (e) 5th bottle

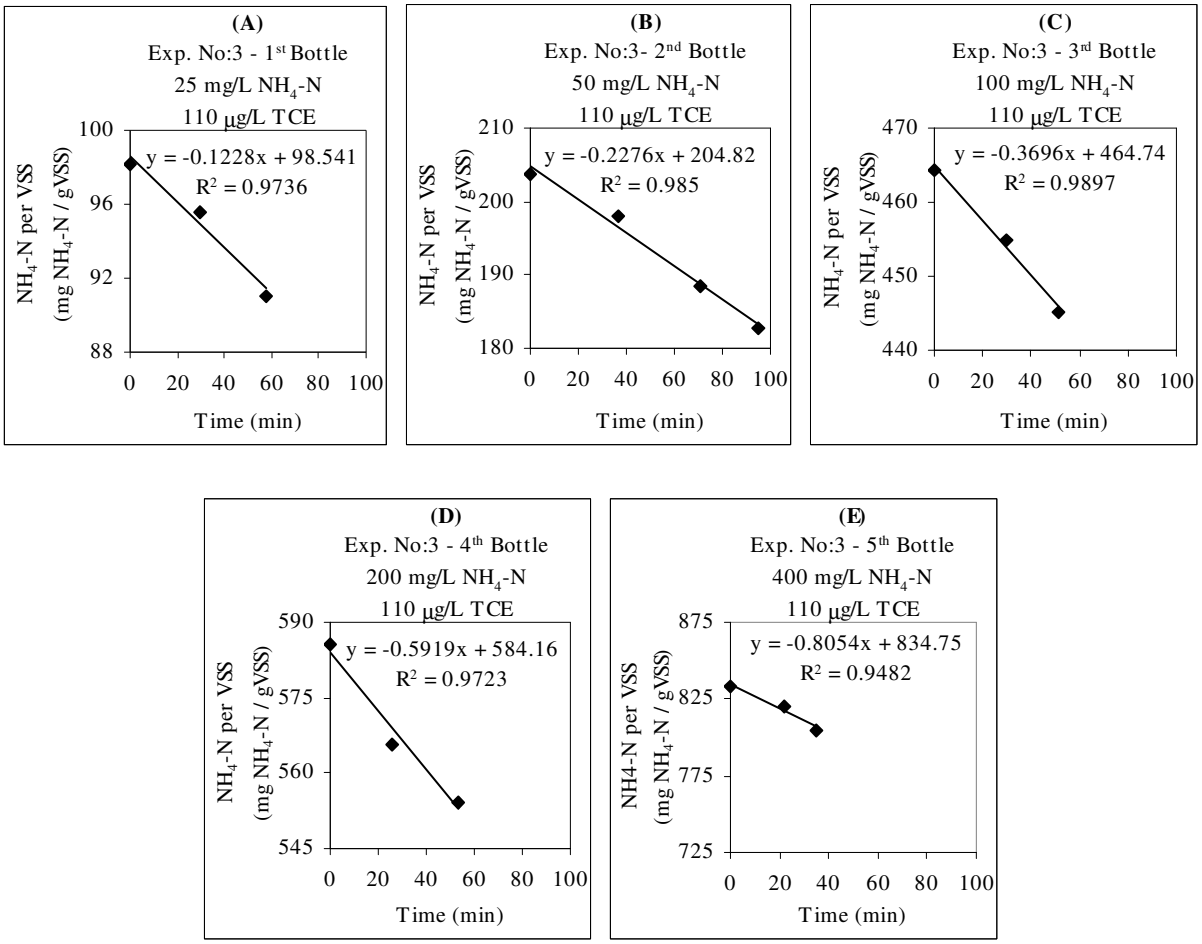

Figure H.3. Specific ammonium utilization in batch experiments with TCE directed to kinetic modelling No.3 (a) 1st bottle, (b) 2nd bottle, (c) 3rd bottle, (d) 4th bottle, (e) 5th bottle

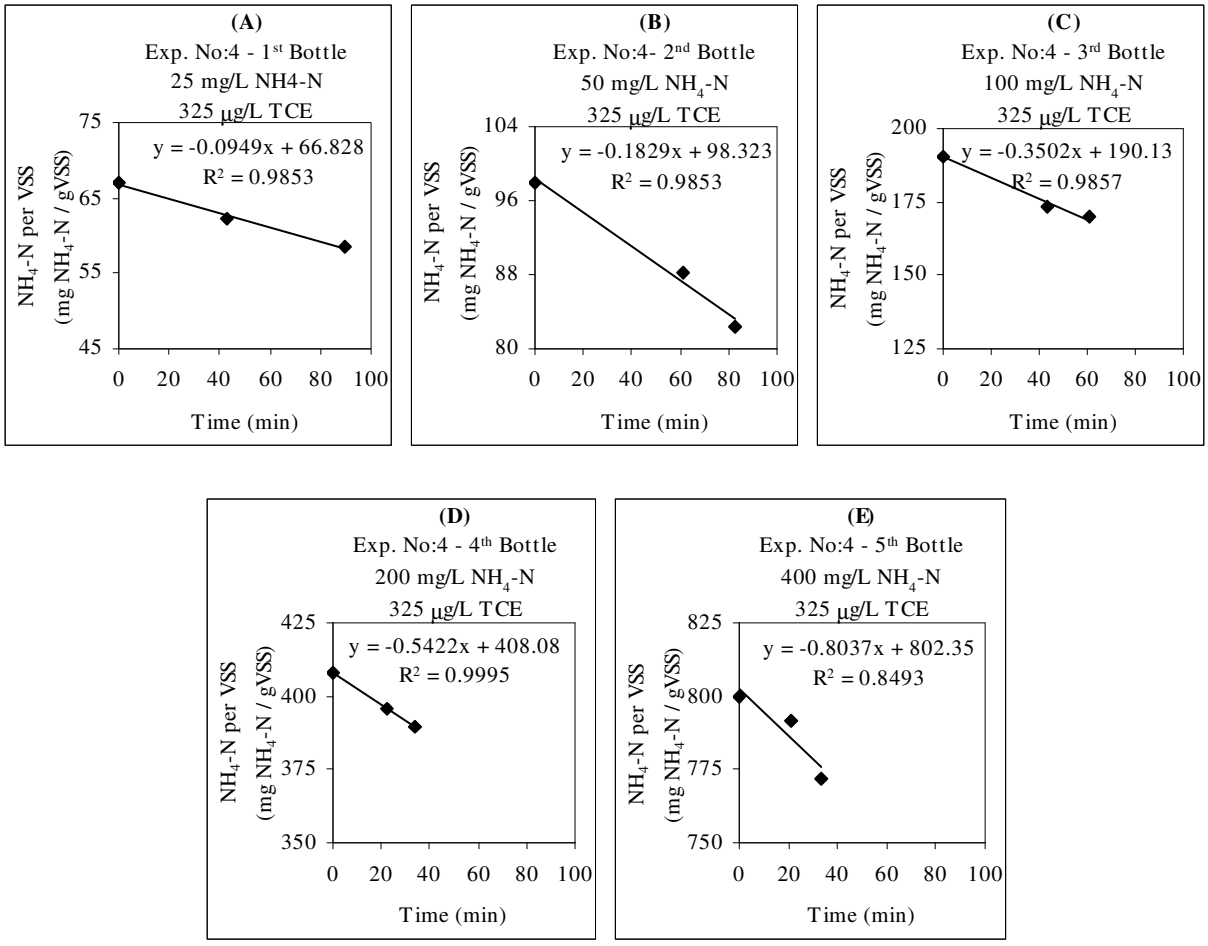

Figure H.4. Specific ammonium utilization in batch experiments with TCE directed to kinetic modelling No.4 (a) 1st bottle, (b) 2nd bottle, (c) 3rd bottle, (d) 4th bottle, (e) 5th bottle

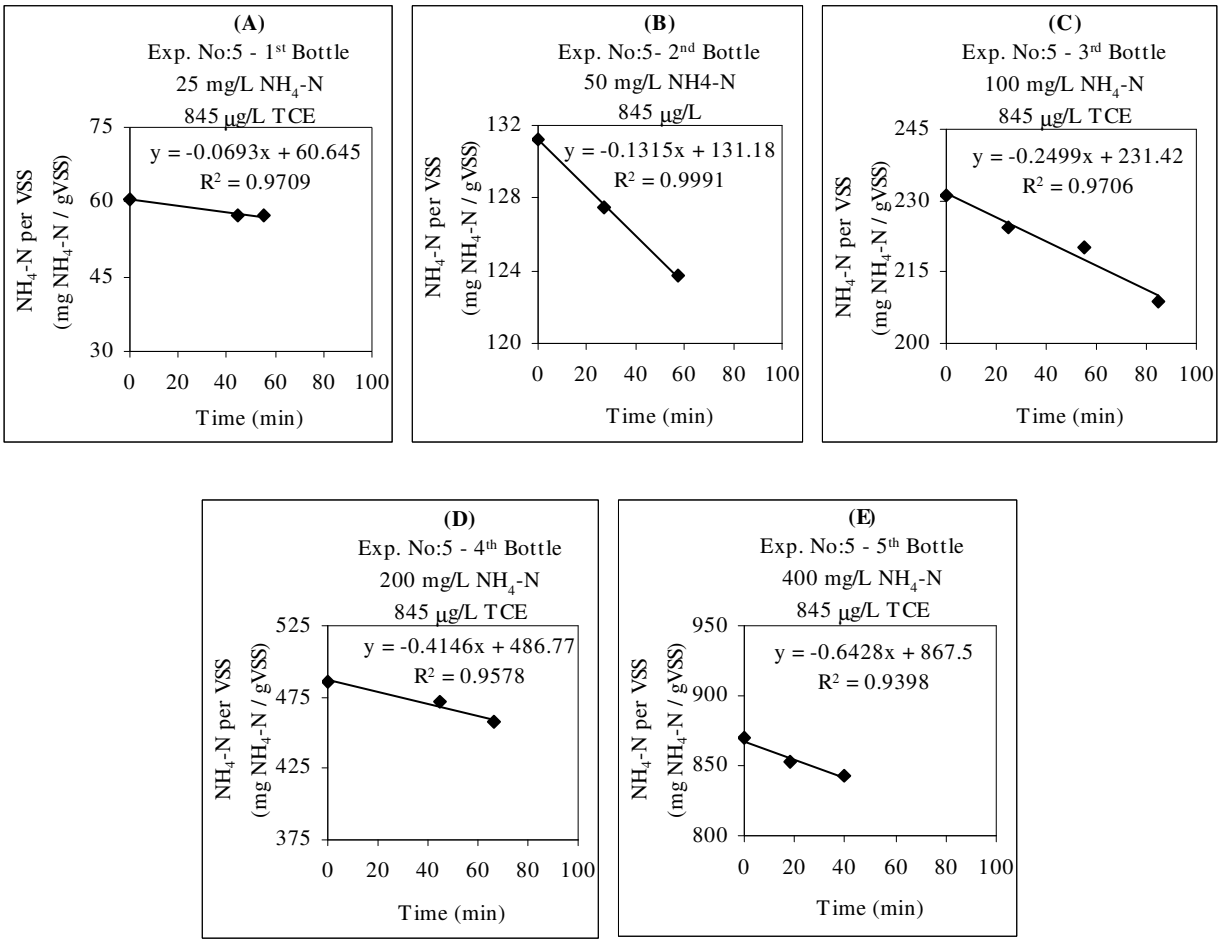

Figure H.5. Specific ammonium utilization in batch experiments with TCE directed to kinetic modelling No.5 (a) 1st bottle, (b) 2nd bottle, (c) 3rd bottle, (d) 4th bottle, (e) 5th bottle

APPENDIX I: DETERMINATION OF TCE VOLATILIZATION RATES IN BATCH EXPERIMENTS WITH TCE DIRECTED TO KINETIC MODELLING

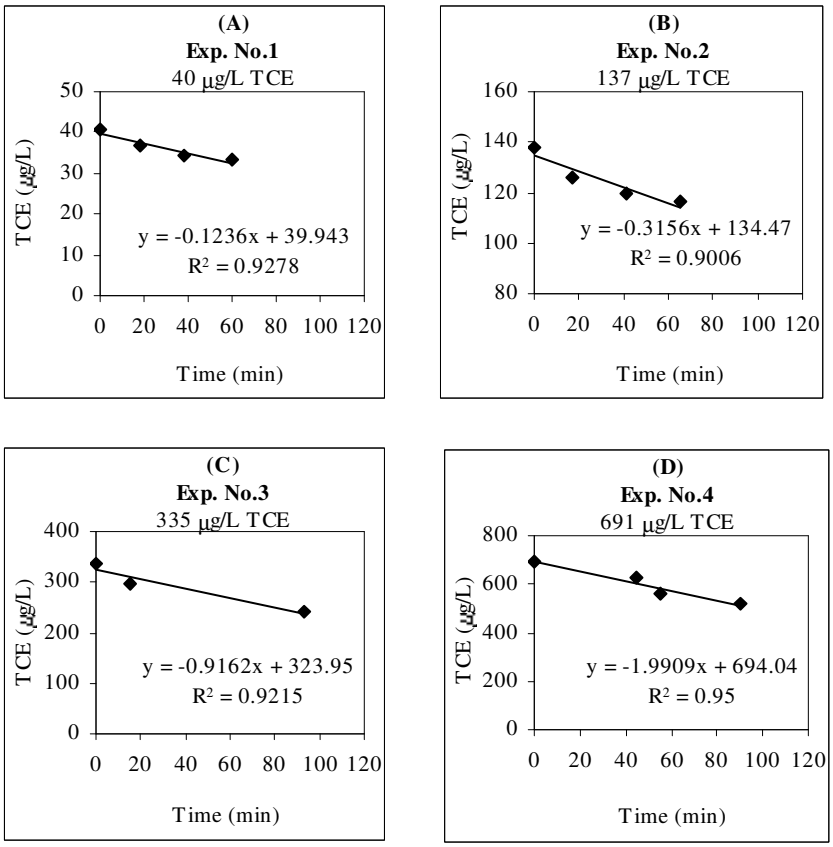

Figure I.1. Volatilization of TCE for the initial TCE concentration of (a) 40 µg/L, (b) 137 µg/L, (c) 335 µg/L, (d) 691 µg/L

APPENDIX J: DETERMINATION OF SPECIFIC COMETABOLIC TCE DEGRADATION RATES (qTCE) IN BATCH EXPERIMENTS DIRECTED TO KINETIC MODELLING

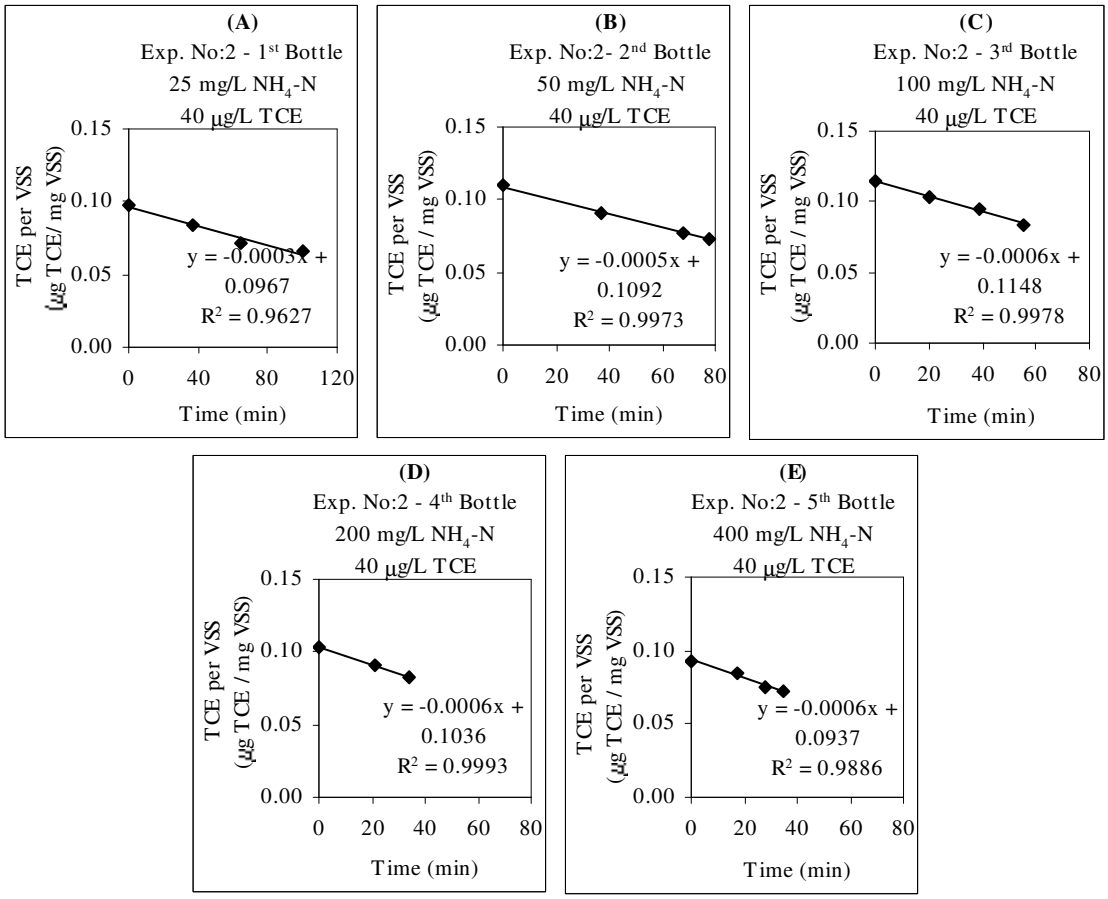

Figure J.1. Specific cometabolic TCE degradation in batch experiments directed to kinetic modelling No.2 (a) 1st bottle, (b) 2nd bottle, (c) 3rd bottle, (d) 4th bottle, (e) 5th bottle

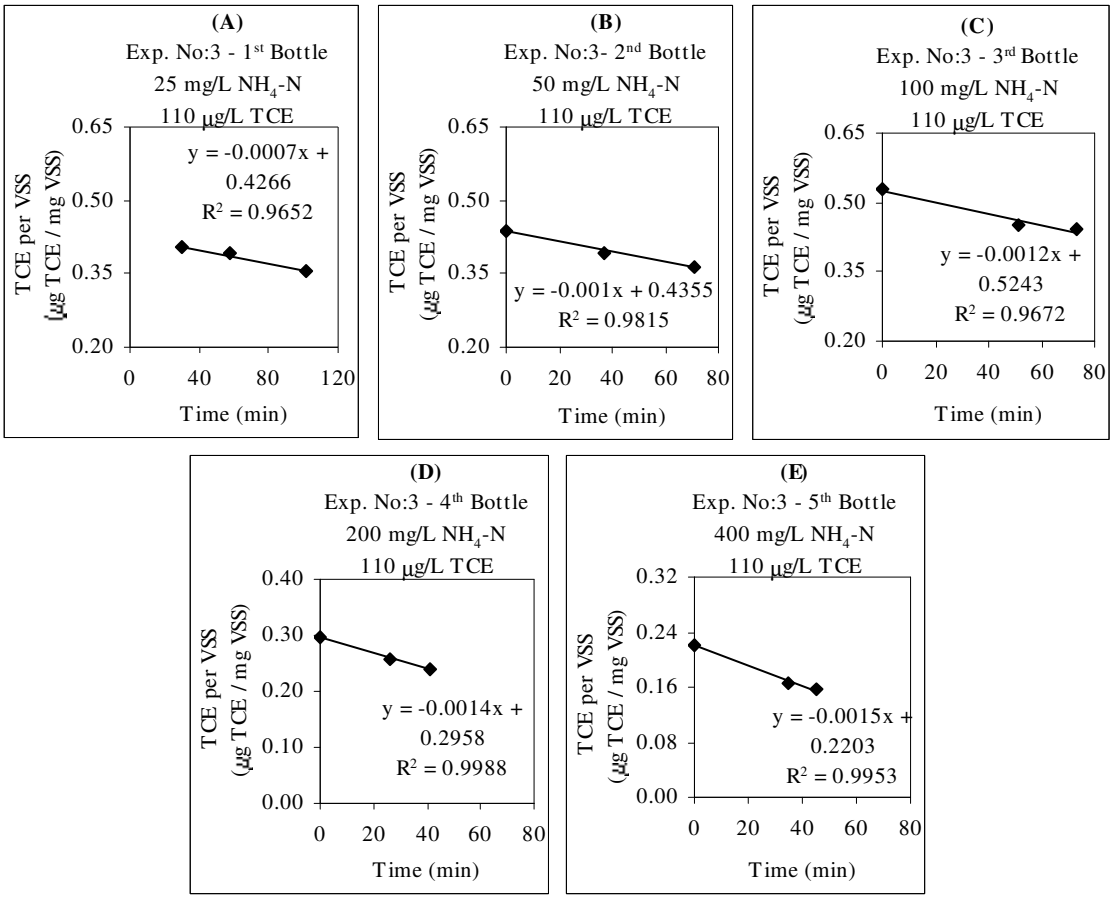

Figure J.2. Specific cometabolic TCE degradation in batch experiments directed to kinetic modelling No.3 (a) 1st bottle, (b) 2nd bottle, (c) 3rd bottle, (d) 4th bottle, (e) 5th bottle

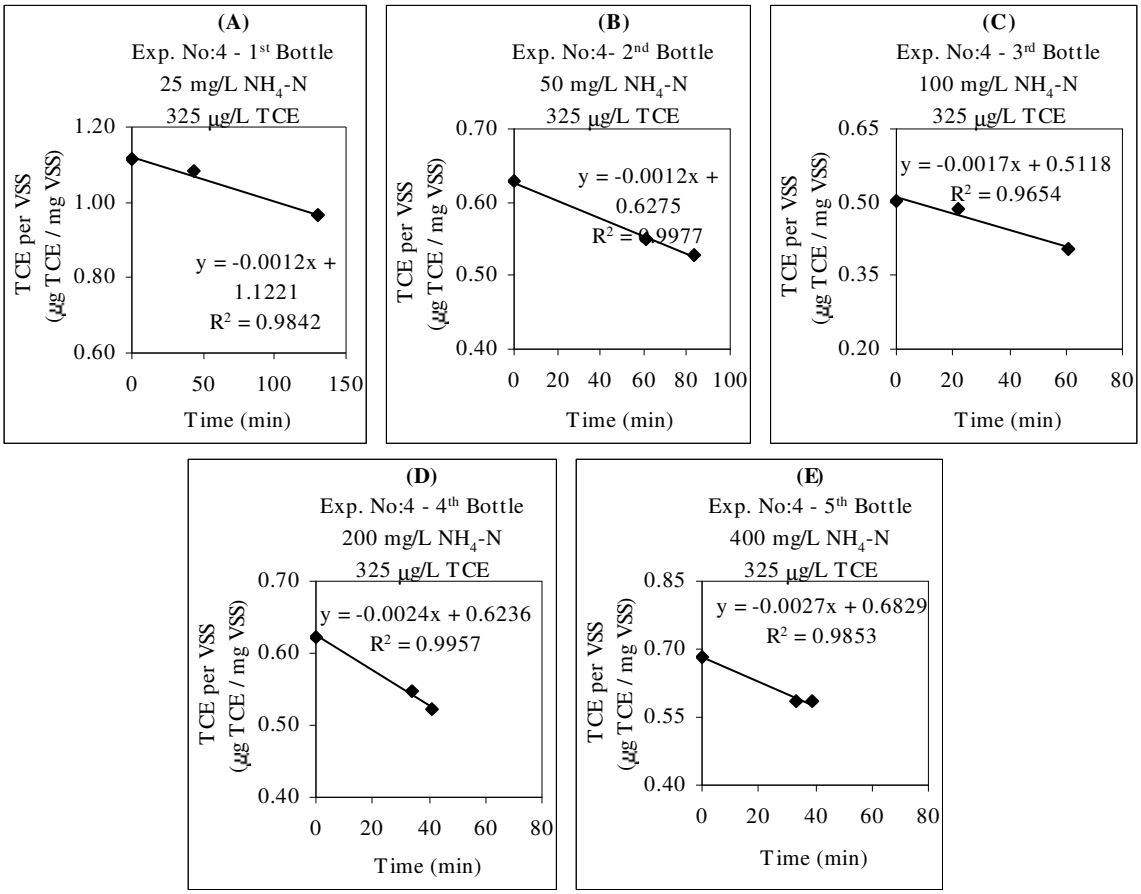

Figure J.3. Specific cometabolic TCE degradation in batch experiments directed to kinetic modelling No.4 (a) 1st bottle, (b) 2nd bottle, (c) 3rd bottle, (d) 4th bottle, (e) 5th bottle

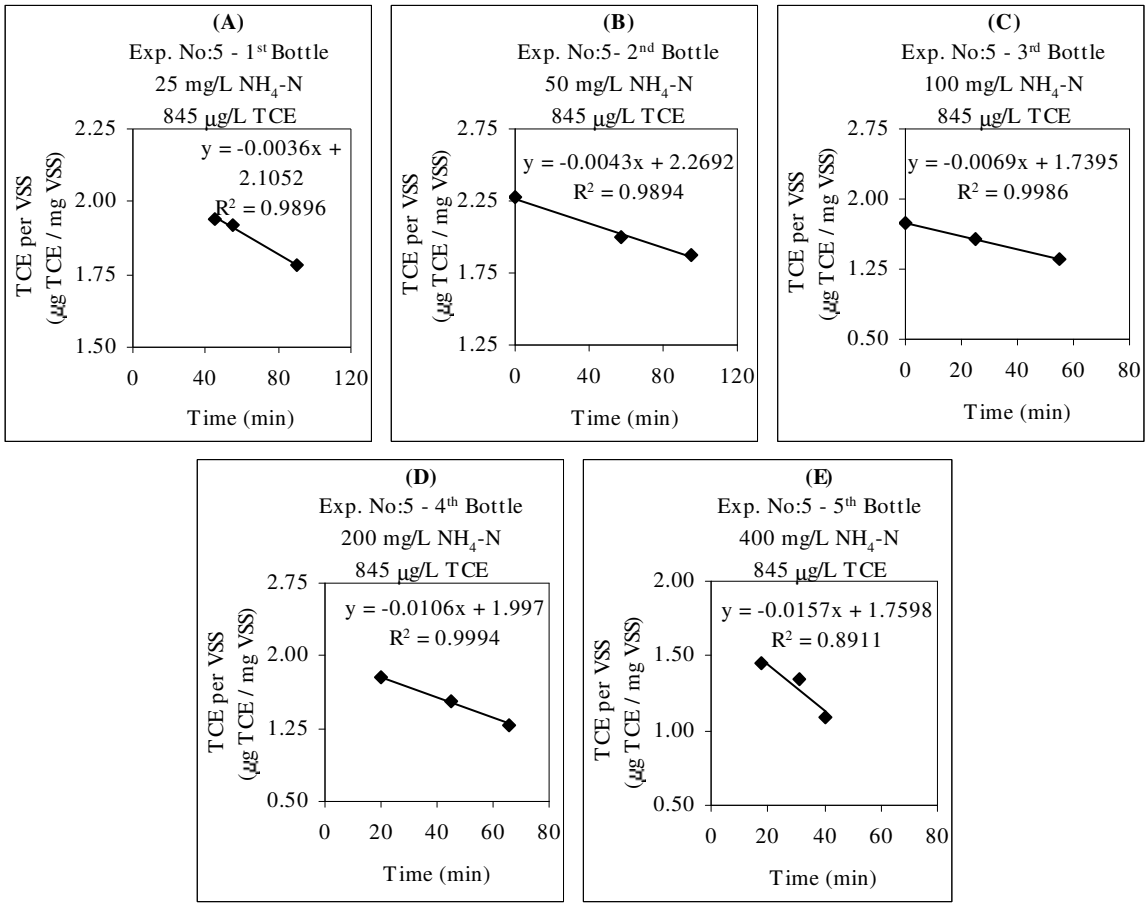

Figure J.4. Specific cometabolic TCE degradation in batch experiments directed to kinetic modelling No.5 (a) 1st bottle, (b) 2nd bottle, (c) 3rd bottle, (d) 4th bottle, (e) 5th bottle

APPENDIX K: DETERMINATION OF SPECIFIC OXYGEN UPTAKE RATES (SOUR) IN PRELIMINARY OXYGEN UPTAKE RATE (OUR) EXPERIMENTS WITH 1,2-DCA

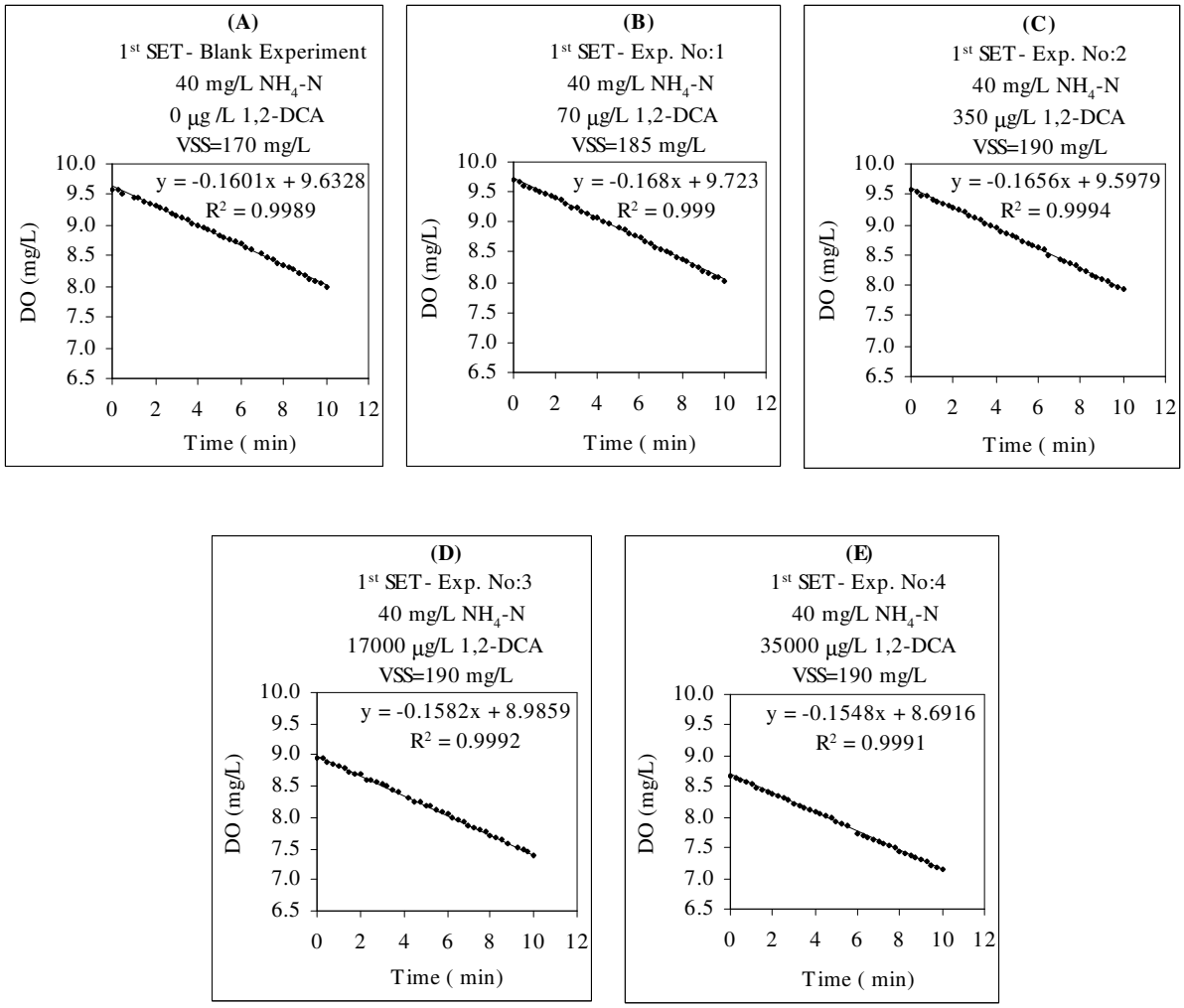

Figure K.1. Preliminary oxygen uptake with 1,2-DCA (a) 1st Set-Blank, (b) 1st Set-Exp.No.1, (c) 1st Set-Exp. No.2, (d) 1st Set-Exp. No.3, (e) 1st Set-Exp. No.4

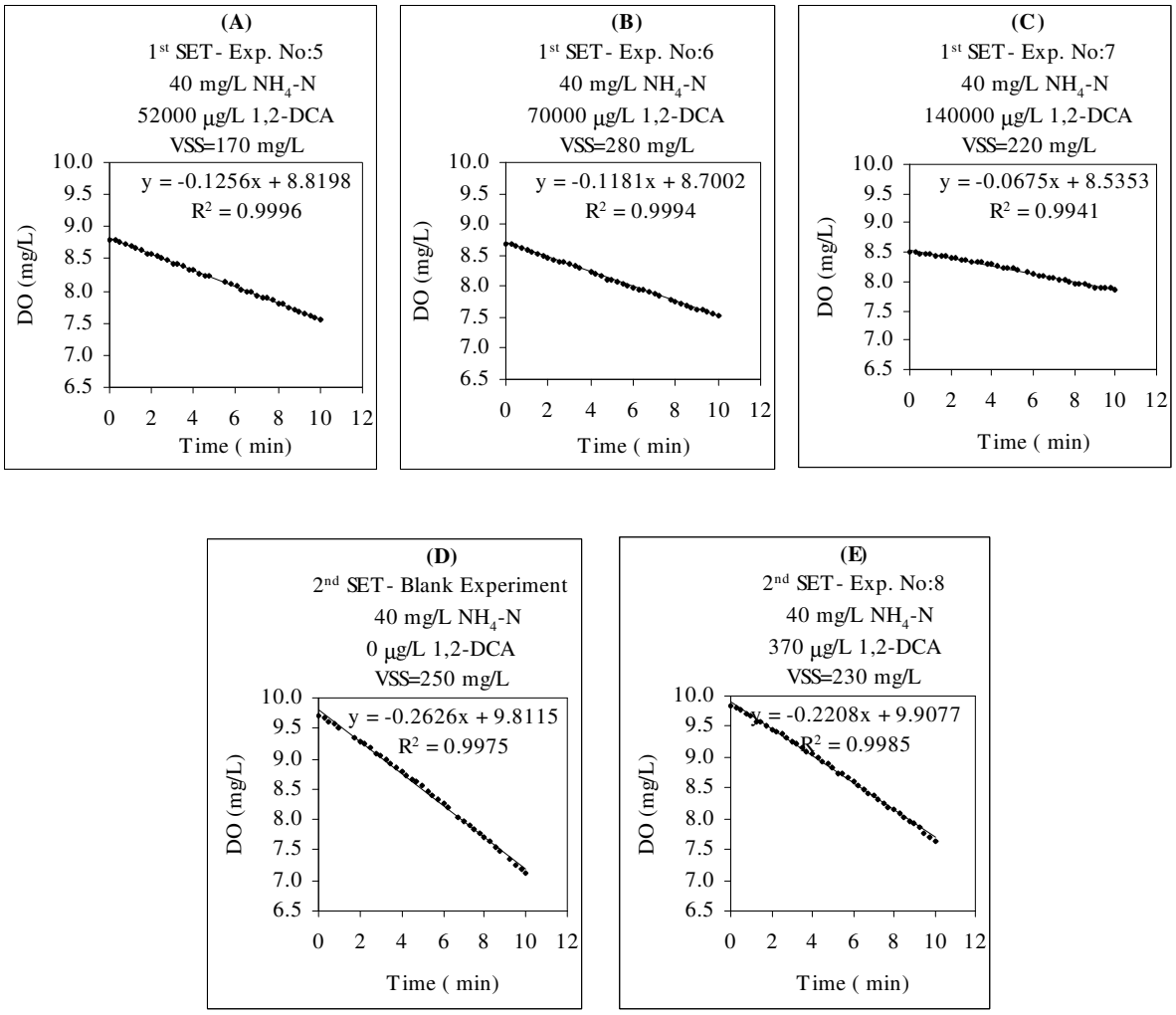

Figure K.2. Preliminary oxygen uptake with 1,2-DCA (a) 1st Set-Exp. No.5, (b) 1st Set-Exp. No.6, (c) 1st Set-Exp. No.7, (d) 2nd Set-Blank, (e) 2nd Set-Exp. No.8

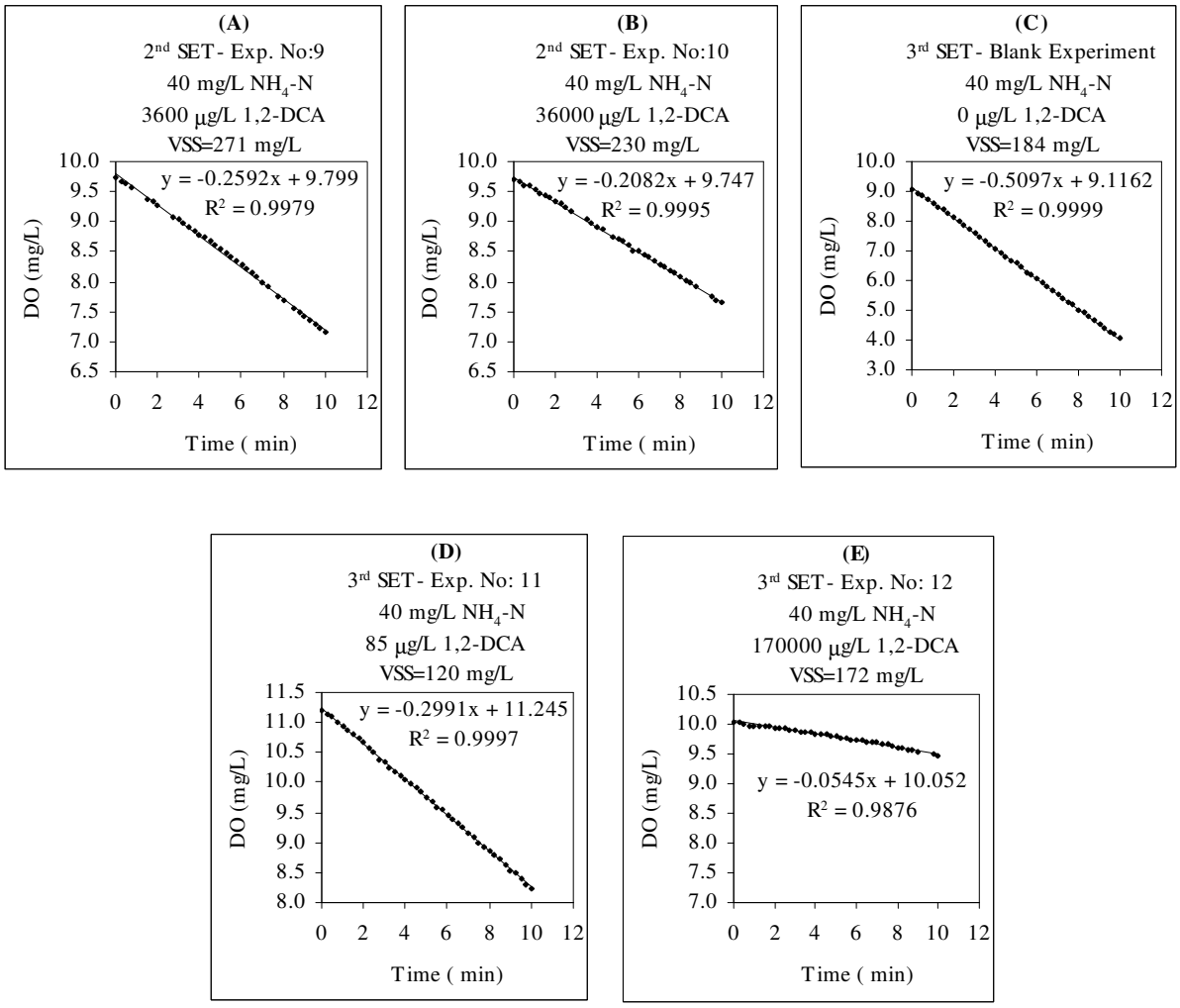

Figure K.3. Preliminary oxygen uptake with 1,2-DCA (a) 2nd Set-Exp. No.9, (b) 2nd Set-Exp. No.10, (c) 3rd Set-Blank, (d) 3rd Set-Exp. No.11, (e) 3rd Set-Exp. No. 12

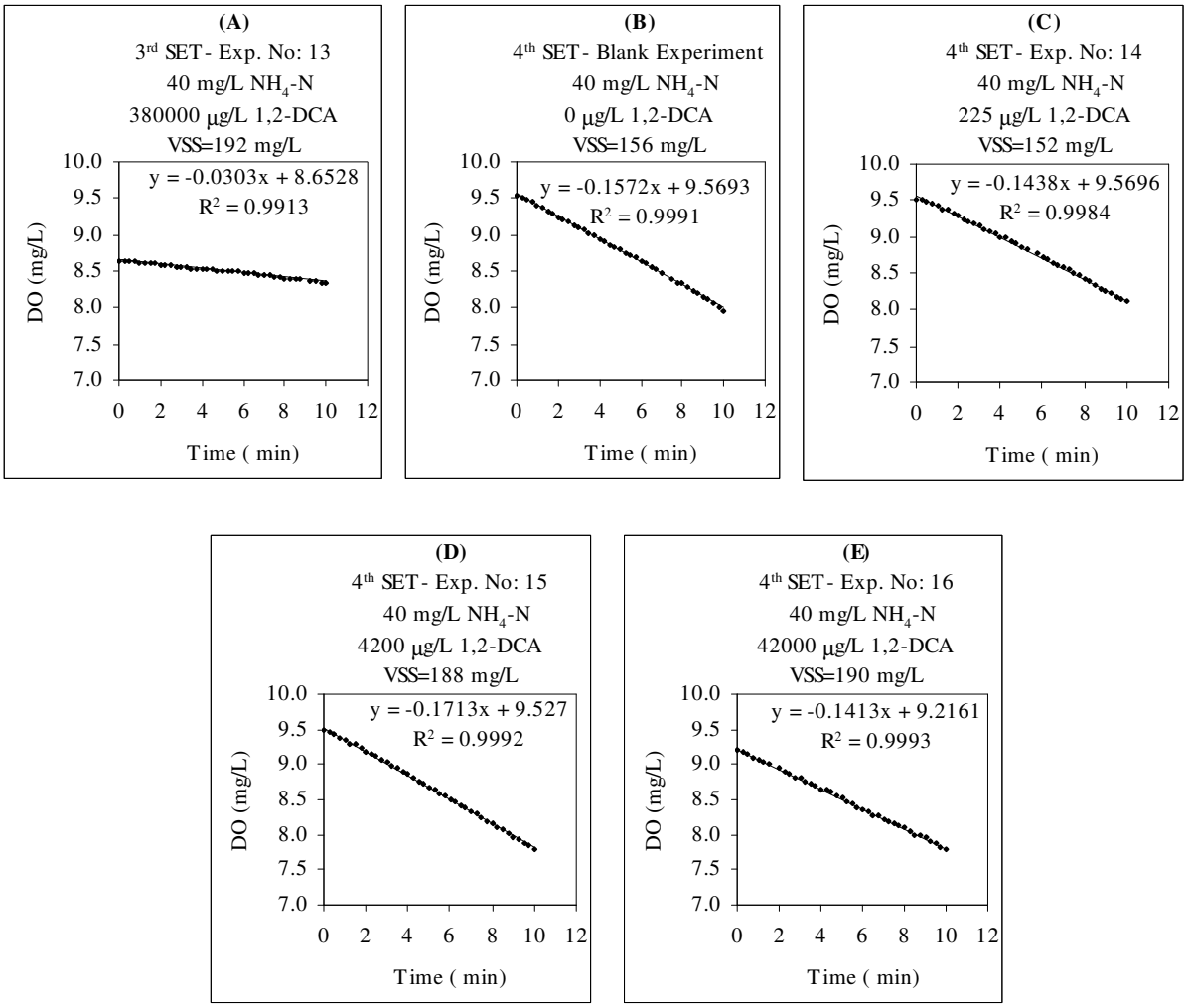

Figure K.4. Preliminary oxygen uptake with 1,2-DCA (a) 3rd Set-Exp. No.13, (b) 4th Set-Blank, (c) 4th Set-Exp. No.14, (d) 4th Set-Exp. No.15, (e) 4th Set-Exp. No.16

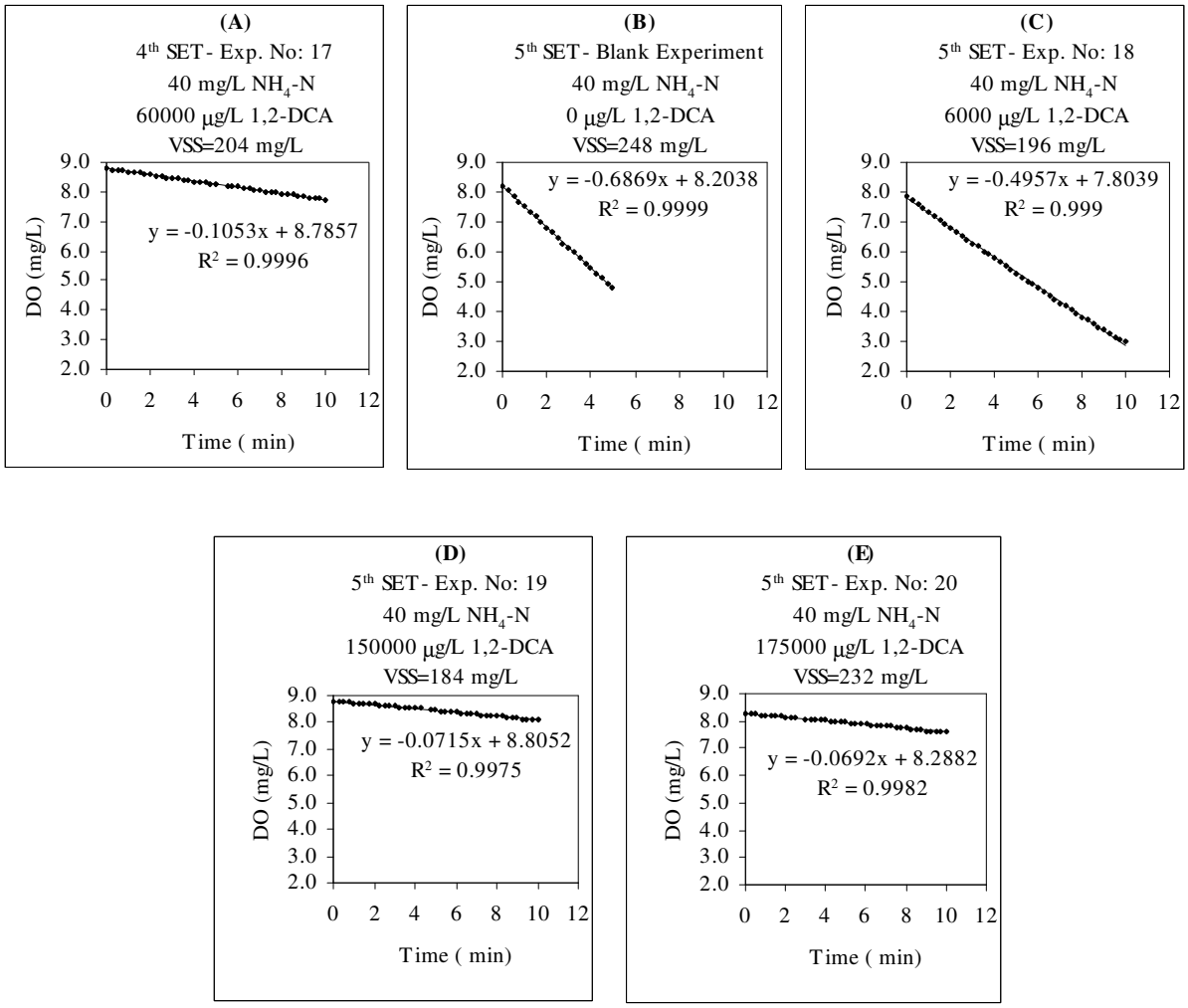

Figure K.5. Preliminary oxygen uptake with 1,2-DCA (a) 4th Set-Exp. No.17, (b) 5th Set-Blank, (c) 5th Set-Exp. No. 18, (d) 5th Set-Exp. No.19, (e) 5th Set-Exp. No.20

APPENDIX L: DETERMINATION OF SPECIFIC AMMONIUM UTILIZATION RATES (qNH_4-N) DURING BATCH EXPERIMENTS WITH 1,2-DCA

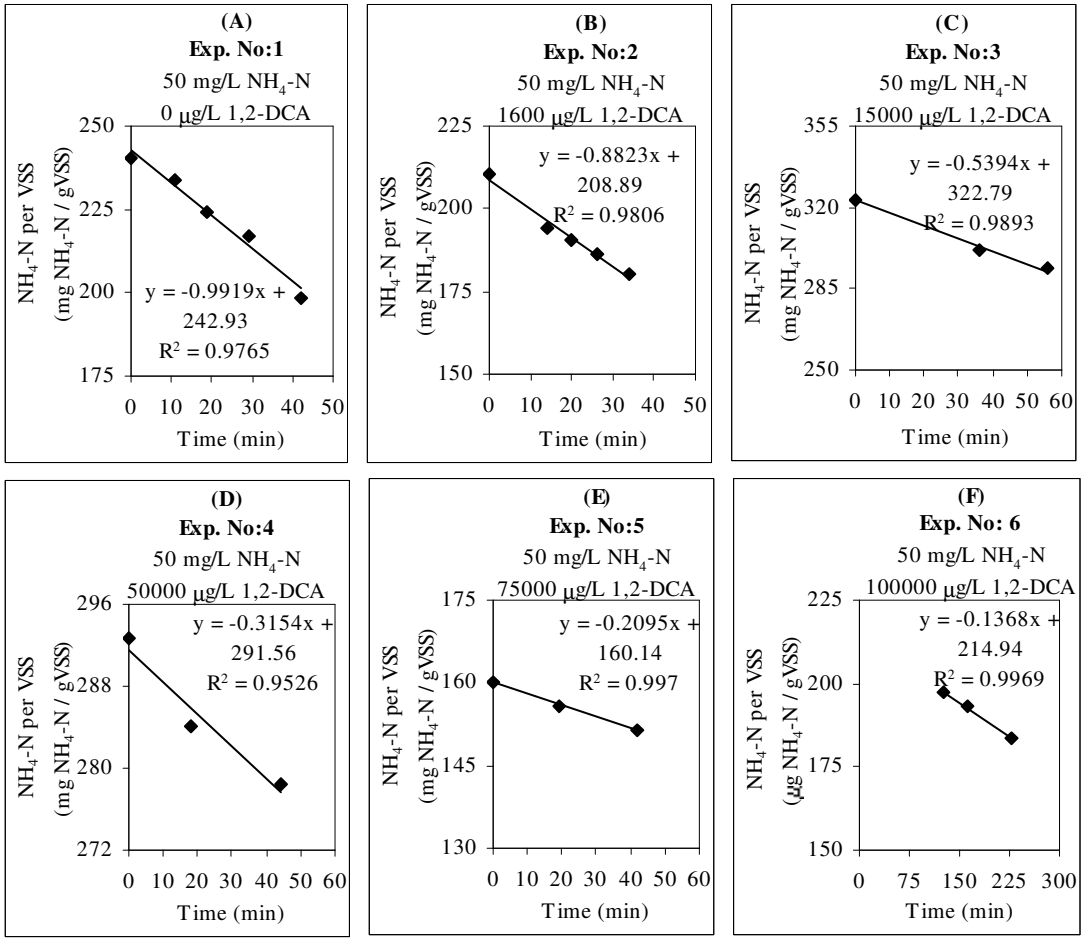

Figure L.1. Specific ammonium utilization in batch experiments with 1,2-DCA (a) in Exp. No.1, (b) in Exp. No.2, (c) in Exp. No.3, (d) in Exp. No.4, (e) in Exp. No.5, and (f) in Exp. No.6

APPENDIX M: DETERMINATION OF SPECIFIC OXYGEN UPTAKE RATES (SOUR) IN BATCH EXPERIMENTS WITH 1,2-DCA

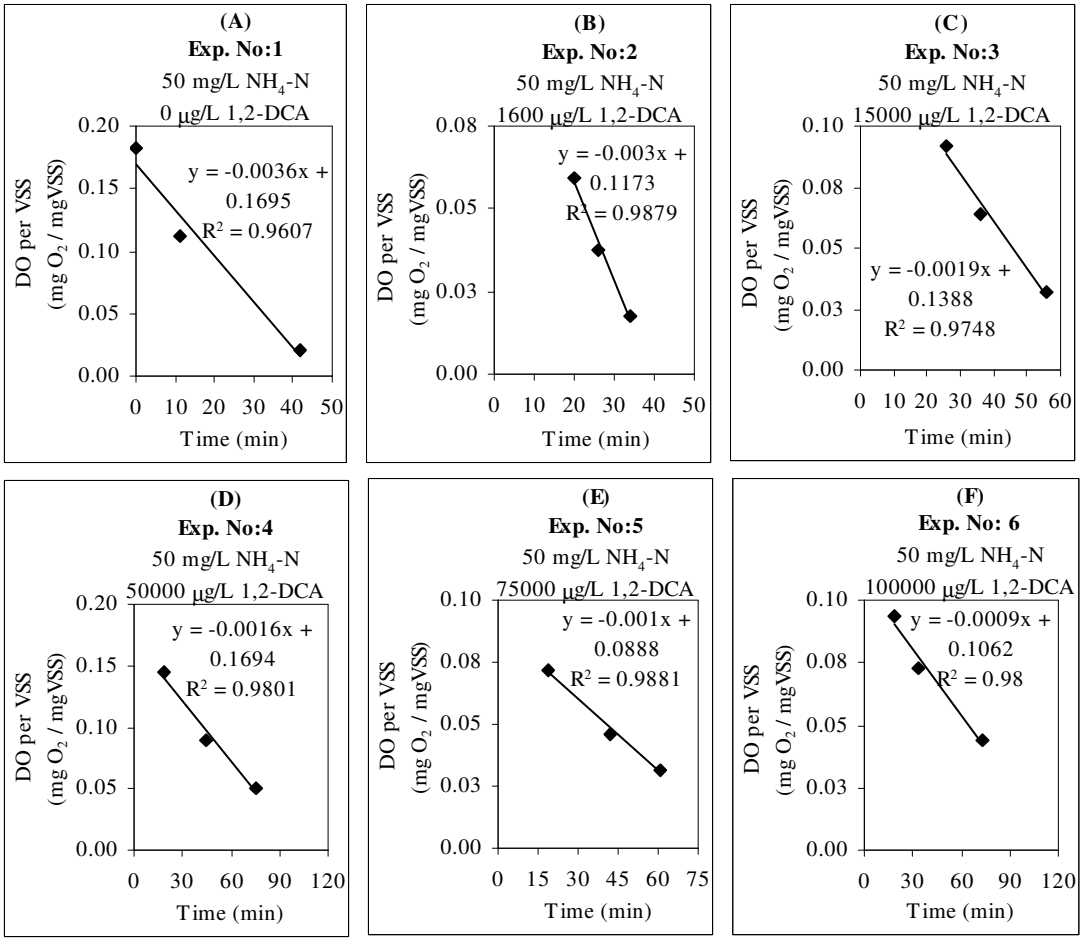

Figure M.1. Specific oxygen uptake in batch experiments with 1,2-DCA (a) in Exp. No.1, (b) in Exp. No.2, (c) in Exp. No.3, (d) in Exp. No.4, (e) in Exp. No.5, and (f) in Exp. No.6

APPENDIX N: DETERMINATION OF 1,2-DCA VOLATILIZATION RATES IN BATCH EXPERIMENTS

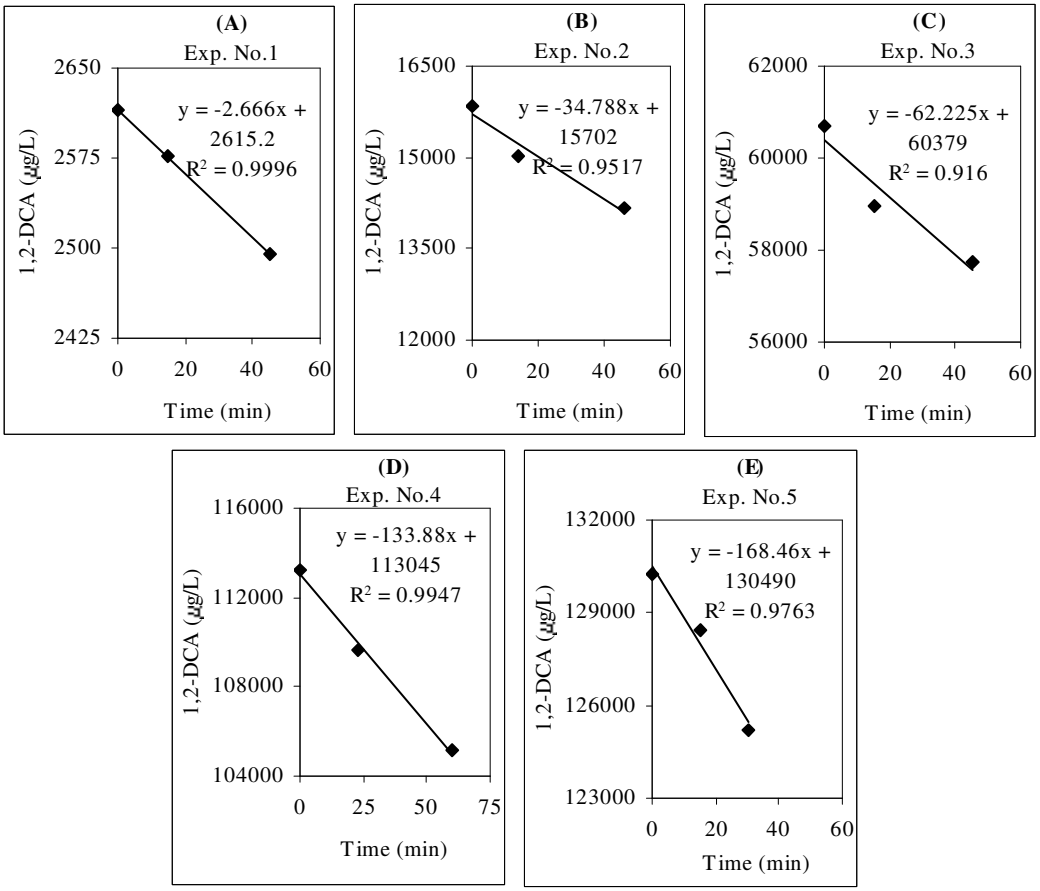

Figure N.1. Volatilization of 1,2-DCA for the initial concentration of (a) 2614 µg/L (b) 15847 µg/L, (c) 60705 µg/L, (d) 113254 µg/L, (e) 130262 µg/L

APPENDIX O: DETERMINATION OF SPECIFIC COMETABOLIC 1,2-DCA DEGRADATION RATES (qDCA) IN BATCH EXPERIMENTS

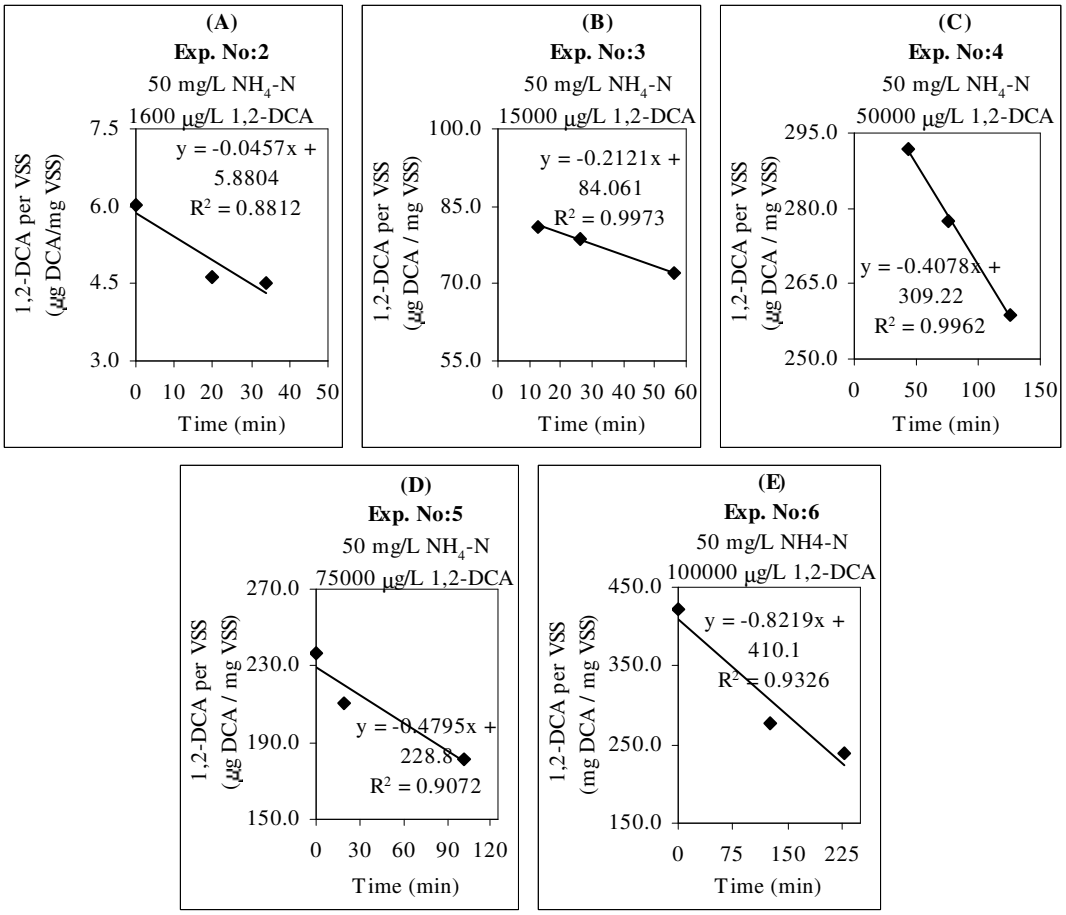

Figure O.1. Specific cometabolic 1,2-DCA degradation in batch experiments (a) Exp. No.1, (b) Exp. No.2, (c) Exp. No.3, (d) Exp. No.5, and (e) Exp. No.6

APPENDIX P: DETERMINATION OF SPECIFIC AMMONIUM UTILIZATION RATES (qNH_4-N) DURING BATCH EXPERIMENTS WITH 1,2-DCA DIRECTED TO KINETIC MODELLING

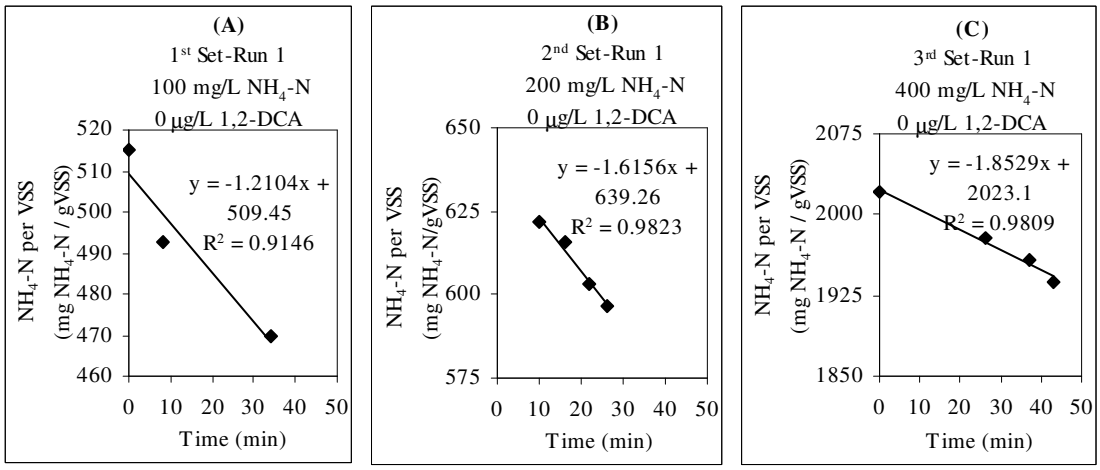

Figure P.1. Specific ammonium utilization in batch experiments with 1,2-DCA directed to kinetic modelling (a) 1st Set-Run 1, (b)2nd Set-Run 1, (c) 3rd Set- Run 1

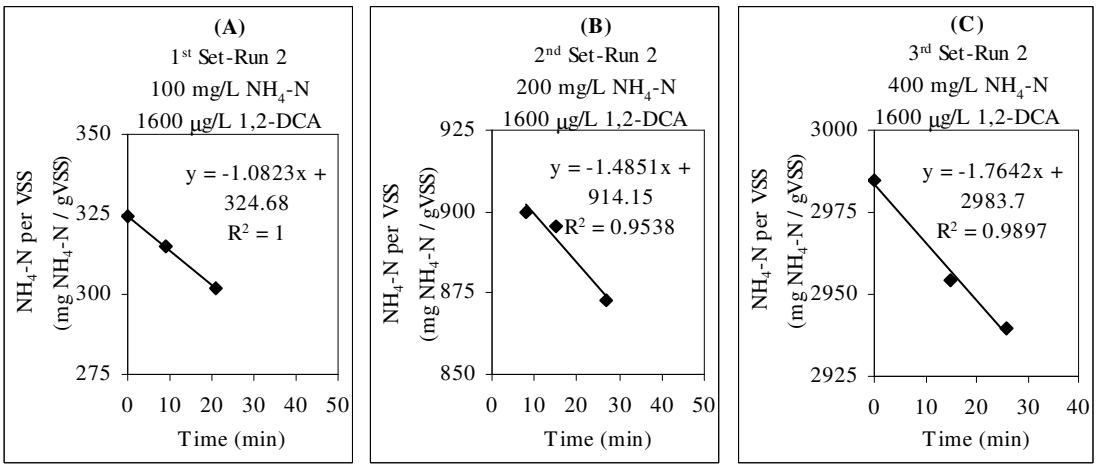

Figure P.2. Specific ammonium utilization in batch experiments with 1,2-DCA directed to kinetic modelling (a) 1st Set-Run 2, (b) 2nd Set-Run 2, (c) 3rd Set- Run 2

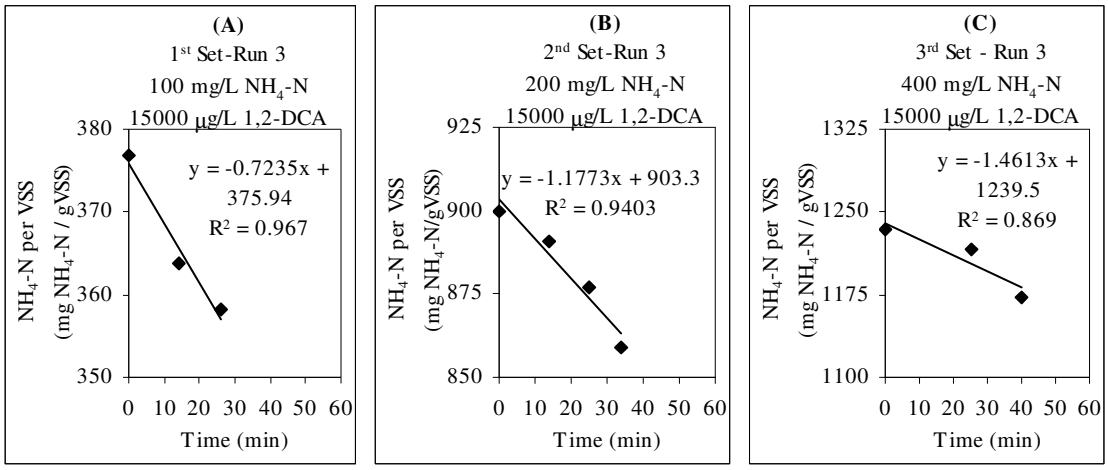

Figure P.3. Specific ammonium utilization rates in the batch kinetic experiments with 1,2-DCA (a) 1st Set-Run 3, (b) 2nd Set-Run 3, (c) 3rd Set- Run 3

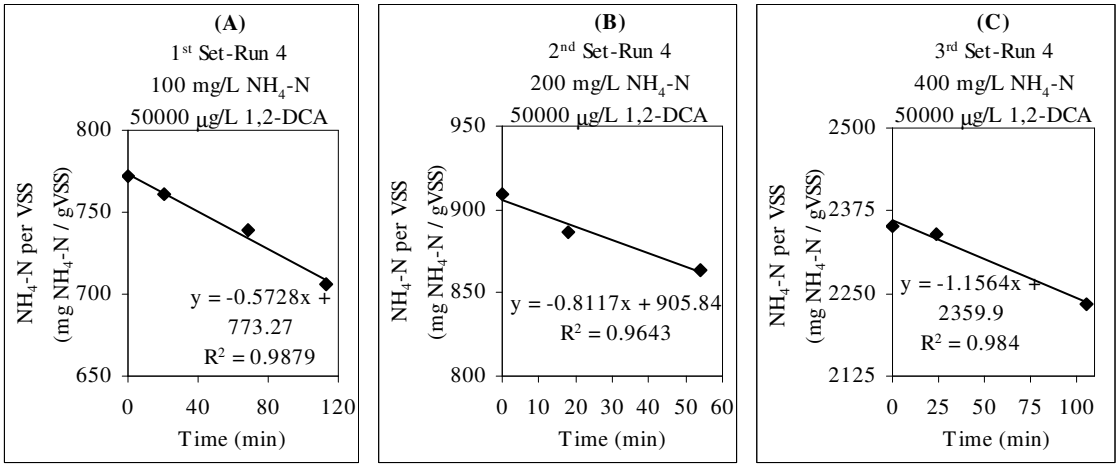

Figure P.4. Specific ammonium utilization in batch experiments with 1,2-DCA directed to kinetic modelling (a) 1st Set-Run 4, (b) 2nd Set-Run 4, (c) 3rd Set- Run 4

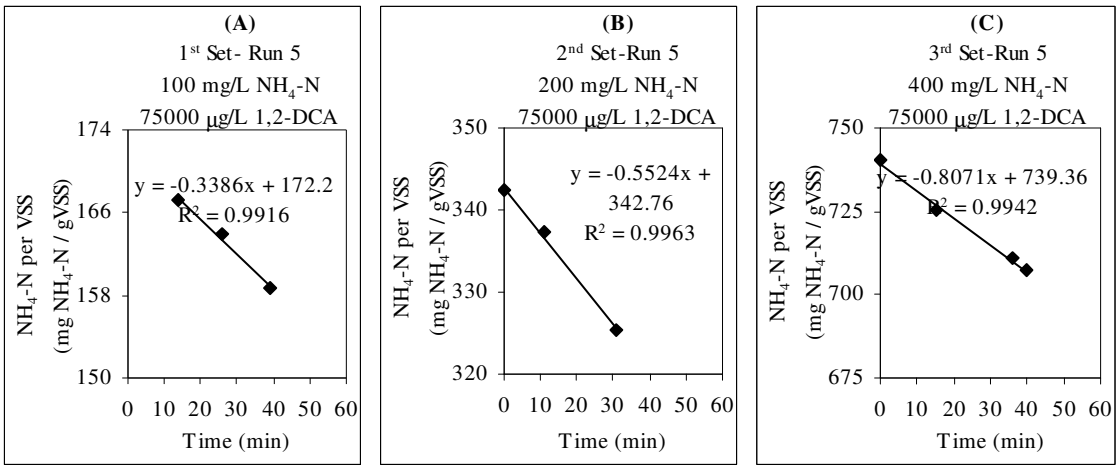

Figure P.5. Specific ammonium utilization in batch experiments with 1,2-DCA directed to kinetic modelling (a) 1st Set-Run 5, (b) 2nd Set-Run 5, (c) 3rd Set- Run 5

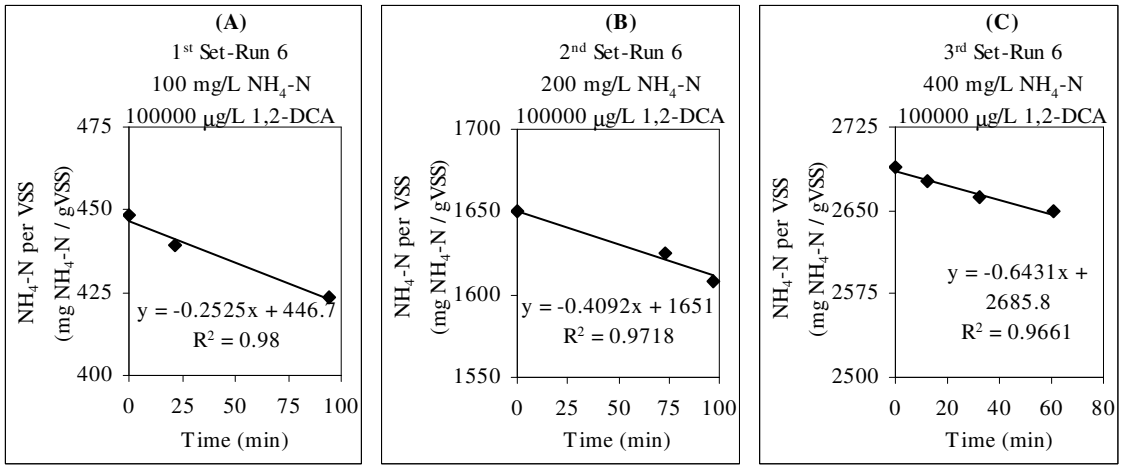

Figure P.6. Specific ammonium utilization in batch experiments with 1,2-DCA directed to kinetic modelling (a) 1st Set-Run 6, (b) 2nd Set-Run 6, (c) 3rd Set- Run 6

APPENDIX Q: DETERMINATION OF SPECIFIC COMETABOLIC 1,2-DCA DEGRADATION RATES (qDCA) IN BATCH EXPERIMENTS DIRECTED TO KINETIC MODELLING

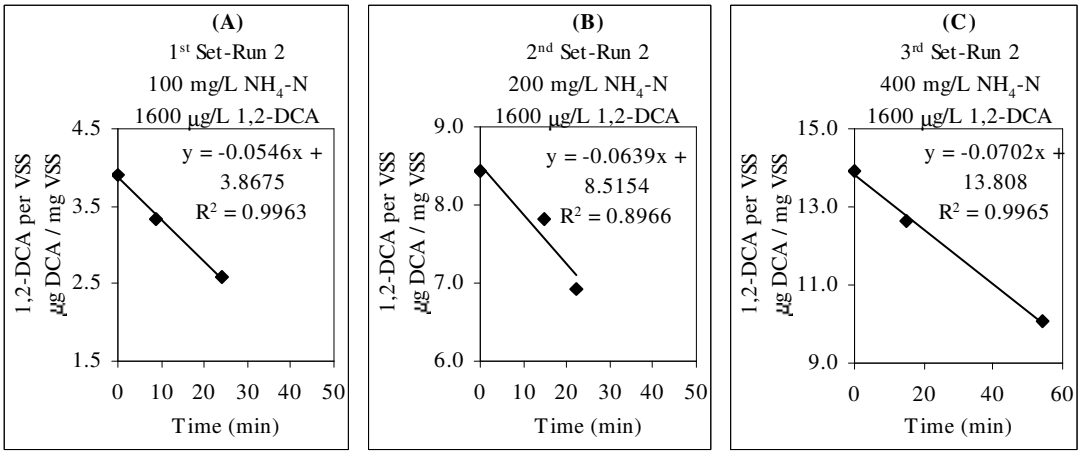

Figure Q.1. Specific cometabolic 1,2-DCA degradation in batch experiments directed to kinetic modelling (a) 1st Set-Run 2, (b) 2nd Set-Run 2, (c) 3rd Set- Run 2

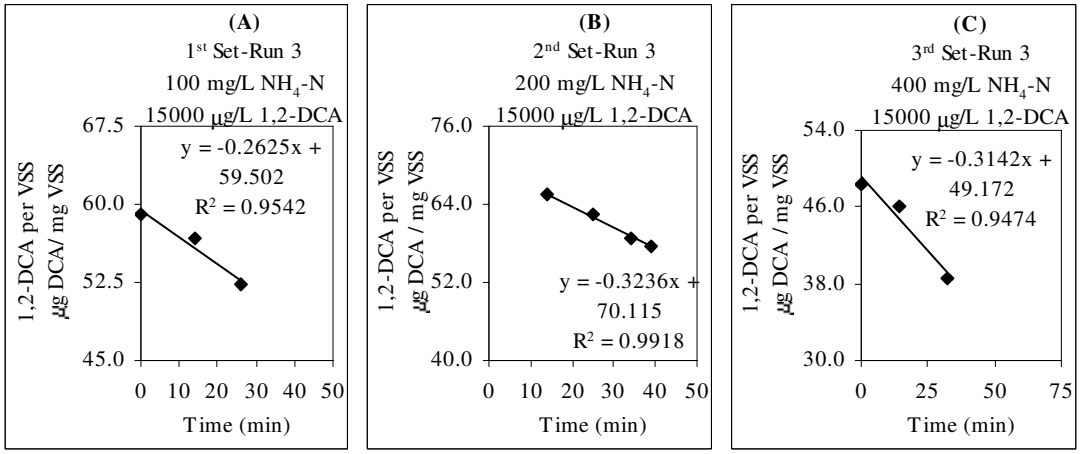

Figure Q.2. Specific cometabolic 1,2-DCA degradation in batch experiments directed to kinetic modelling (a) 1st Set-Run 3, (b) 2nd Set-Run 3, (c) 3rd Set- Run 3

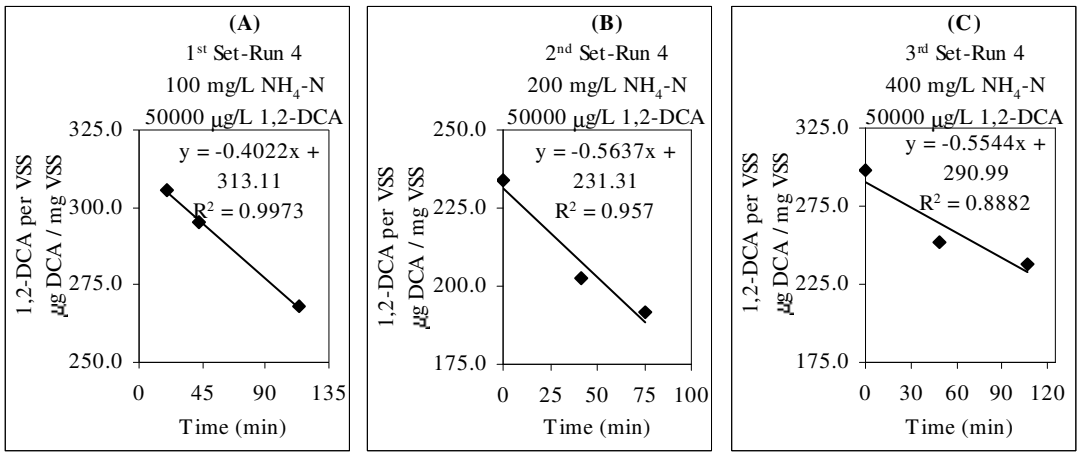

Figure Q.3. Specific cometabolic 1,2-DCA degradation in batch experiments directed to kinetic modelling (a) 1st Set-Run 4, (b) 2nd Set-Run 4, (c) 3rd Set- Run 4

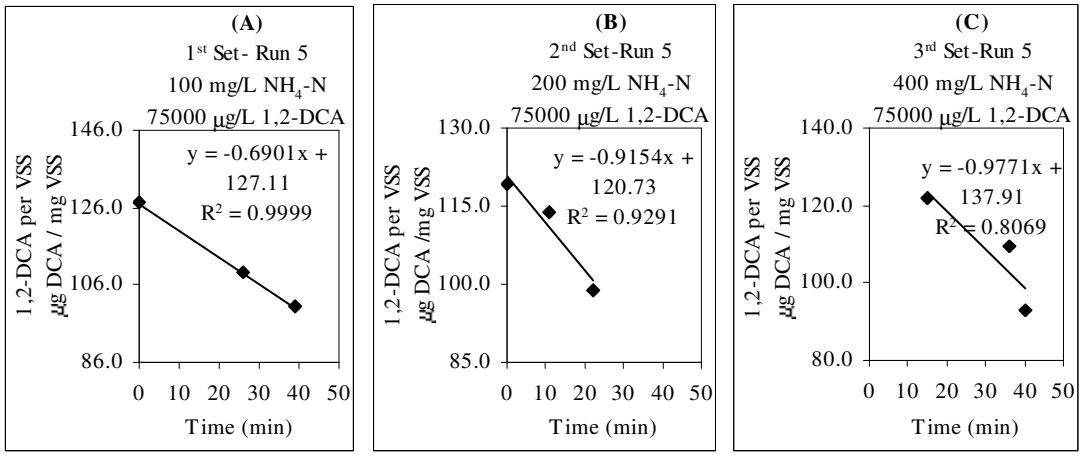

Figure Q.4. Specific cometabolic 1,2-DCA degradation in batch experiments directed to kinetic modelling (a) 1st Set-Run 5, (b) 2nd Set-Run 5, (c) 3rd Set- Run 5

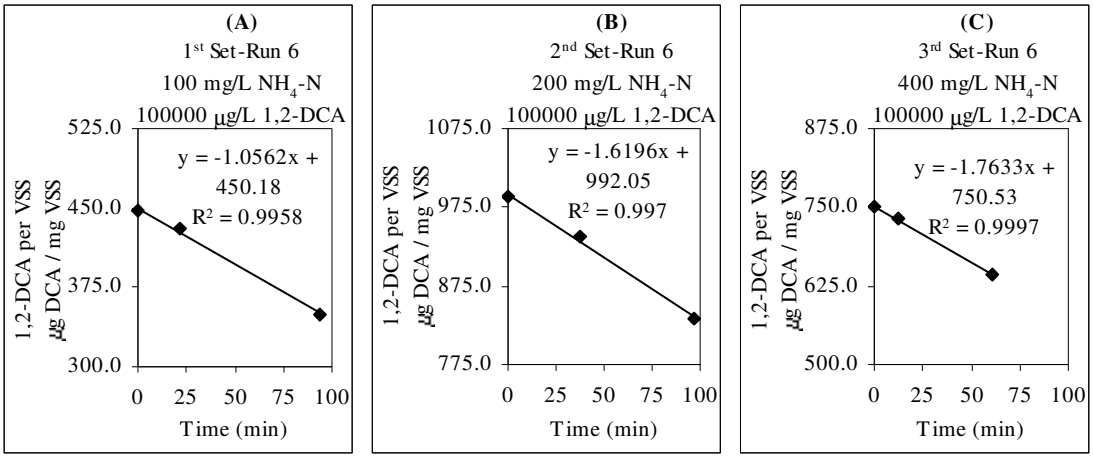

Figure Q.5. Specific cometabolic 1,2-DCA degradation in batch experiments directed to kinetic modelling (a) 1st Set-Run 6, (b) 2nd Set-Run 6, (c) 3rd Set- Run 6

APPENDIX R: DAILY MEASUREMENTS IN PRELIMINARY CONTINUOUS-FLOW BIOFILM EXPERIMENTS AT VARIOUS AMMONIUM LOADS

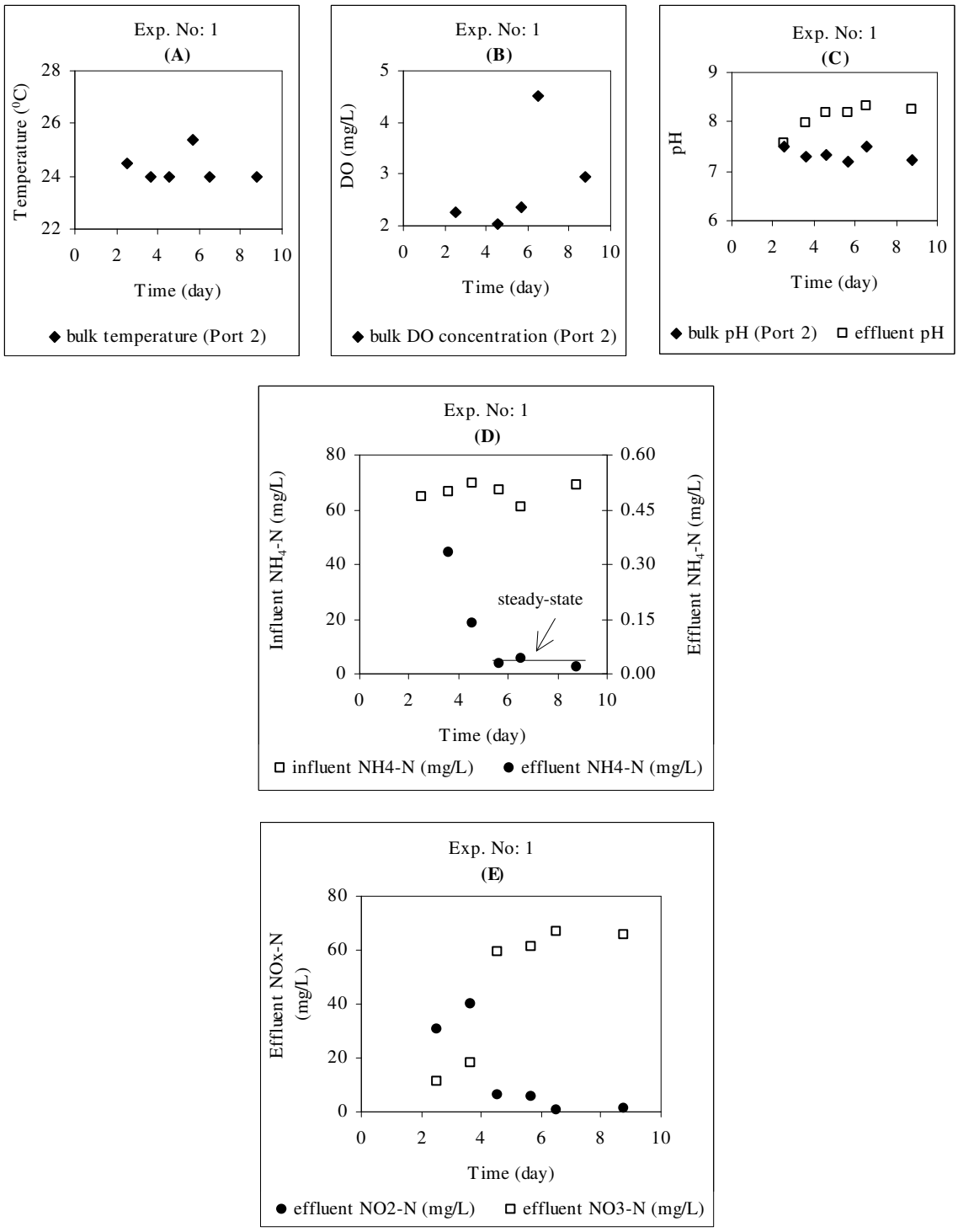

Figure R.1. Preliminary continuous-flow experiment No:1 measurements for (a) T, (b) DO, (c) pH, (d) NH_4-N and (e) NO_x-N

[Feed flowrate = 6L/day, Ave. Feed NH_4-N concentration = 66 mg/L]

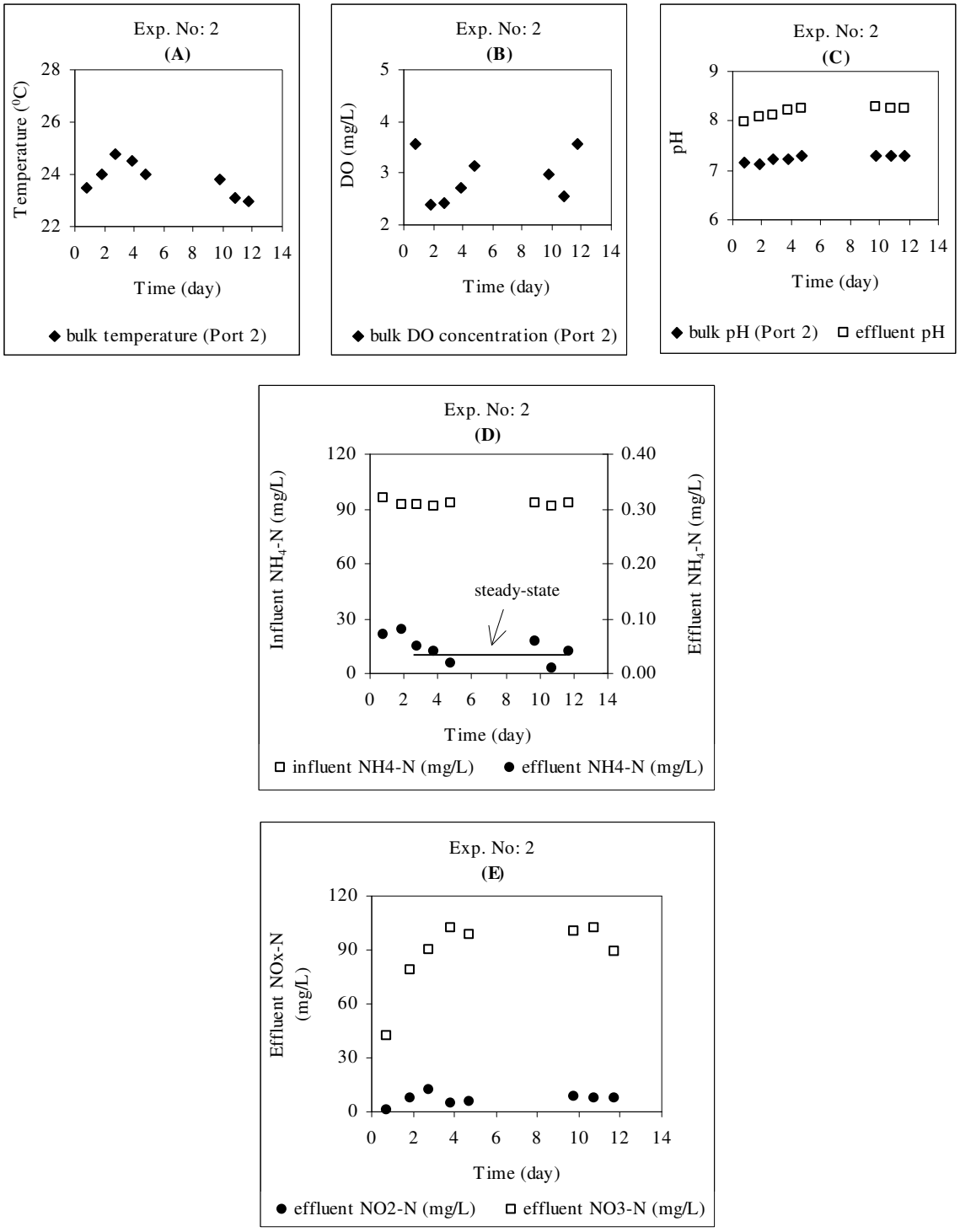

Figure R.2. Preliminary continuous-flow experiment No:2 measurements for (a) T, (b) DO, (c) pH, (d) NH_4-N and (e) NO_x-N

[Feed flowrate = 6L/day, Ave. Feed NH_4-N concentration = 93 mg/L]

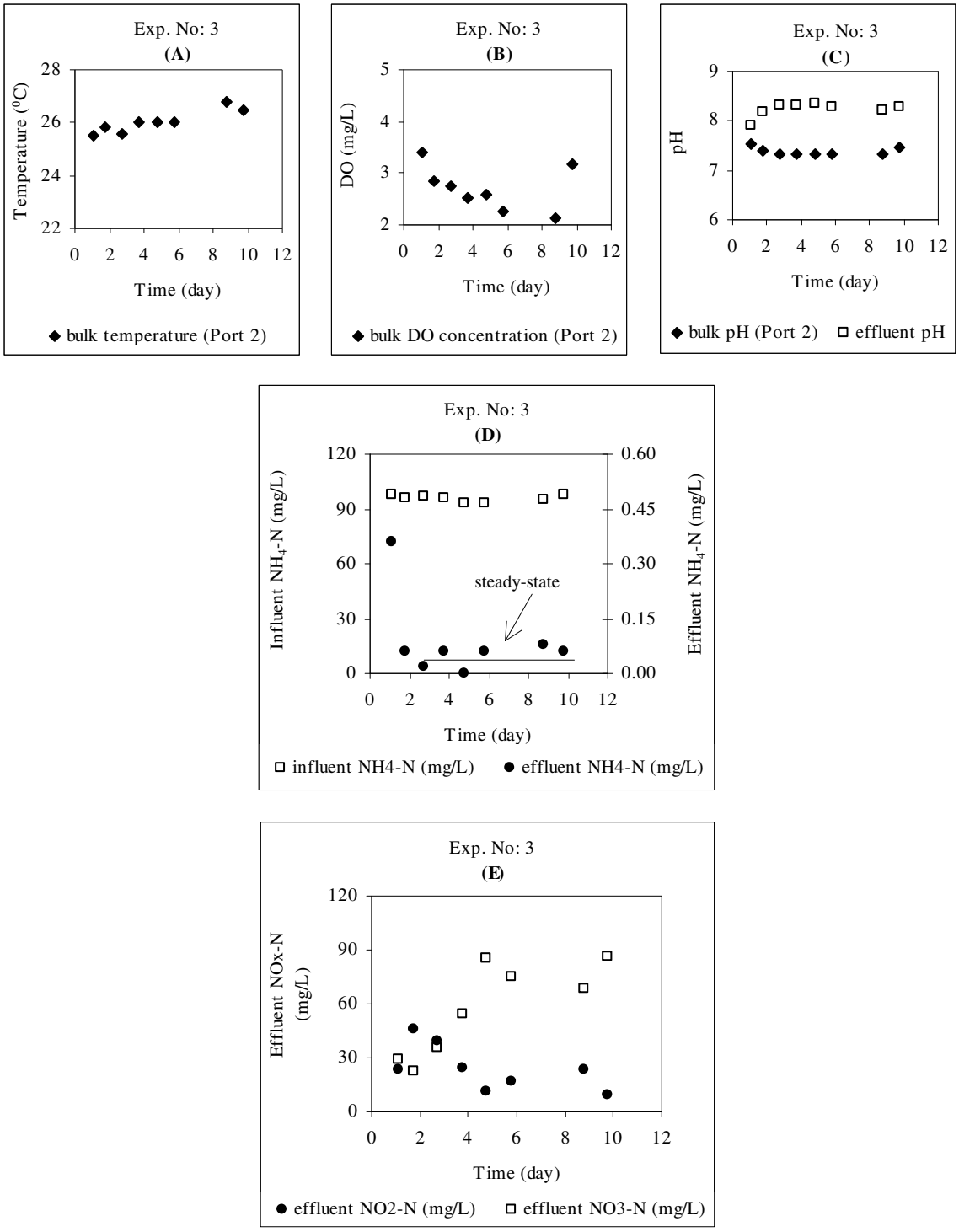

Figure R.3. Preliminary continuous-flow experiment No:3 measurements for (a) T, (b) DO, (c) pH, (d) NH_4-N and (e) NO_x-N

[Feed flowrate = 6L/day, Ave. Feed NH_4-N concentration = 95 mg/L]

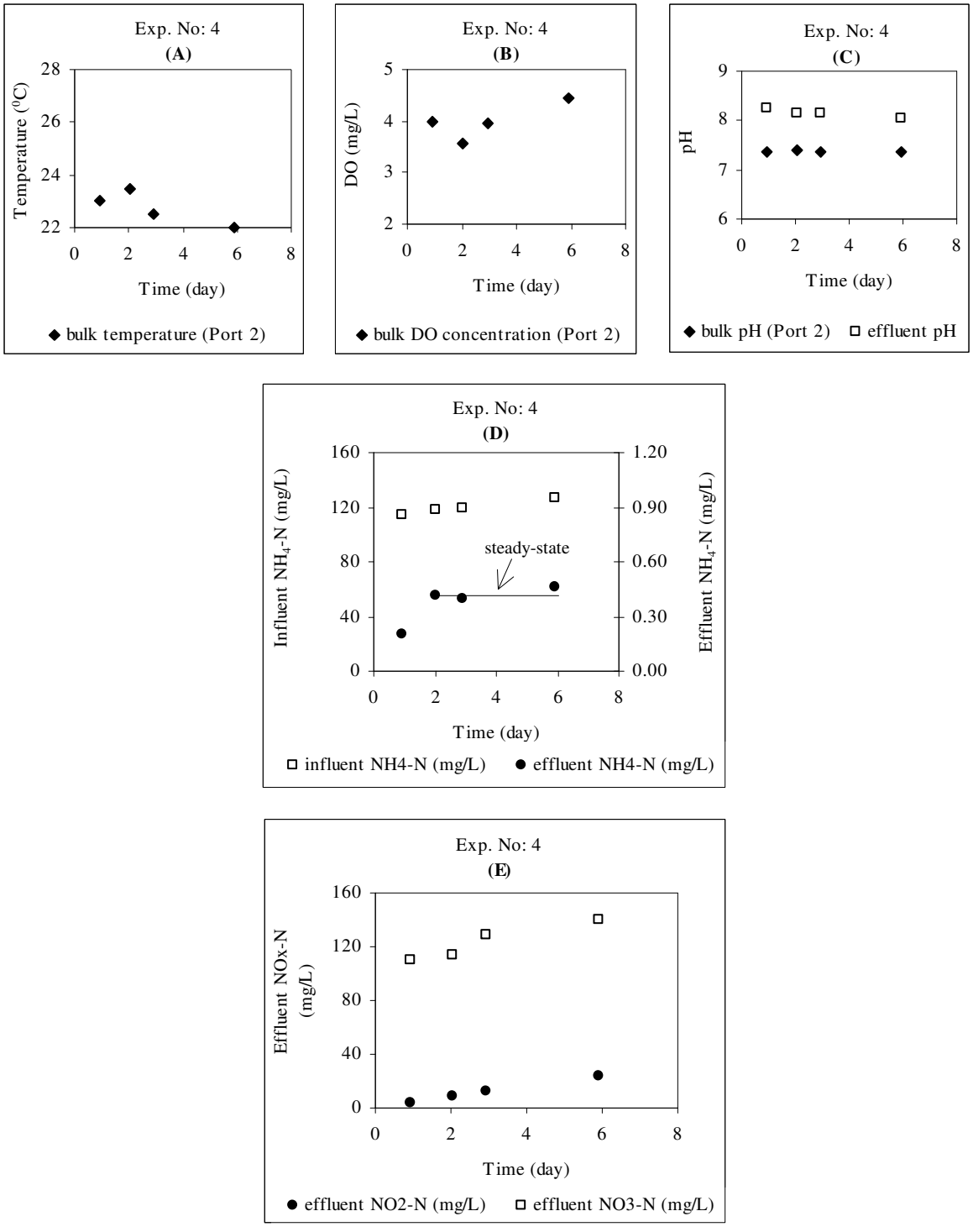

Figure R.4. Preliminary continuous-flow experiment No:4 measurements for (a) T, (b) DO, (c) pH, (d) NH_4-N and (e) NO_x-N

[Feed flowrate = 6L/day, Ave. Feed NH_4-N concentration = 122 mg/L]

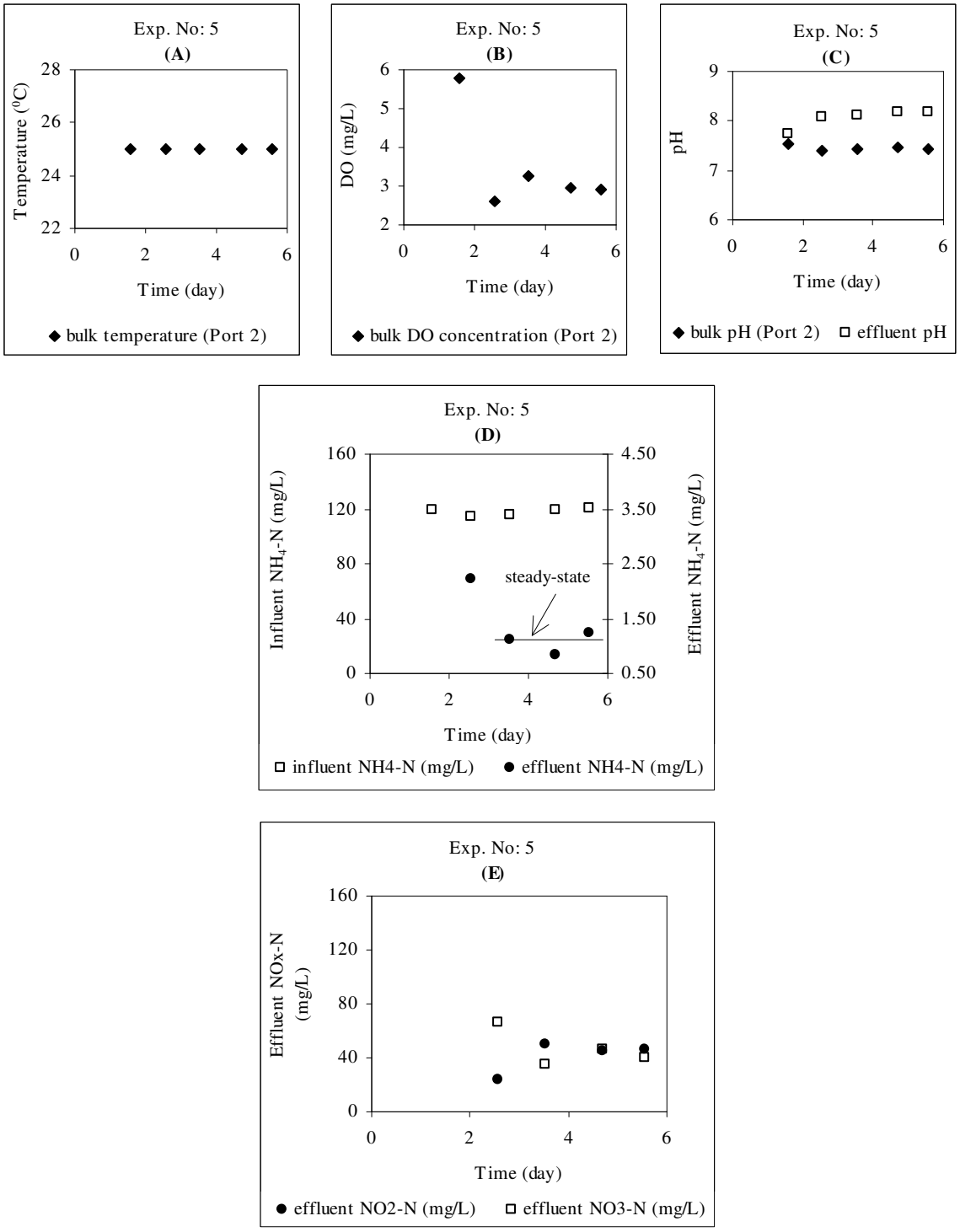

Figure R.5. Preliminary continuous-flow experiment No:5 measurements for (a) T, (b) DO, (c) pH, (d) NH_4-N and (e) NO_x-N

[Feed flowrate = 6L/day, Ave. Feed NH_4-N concentration = 119 mg/L]

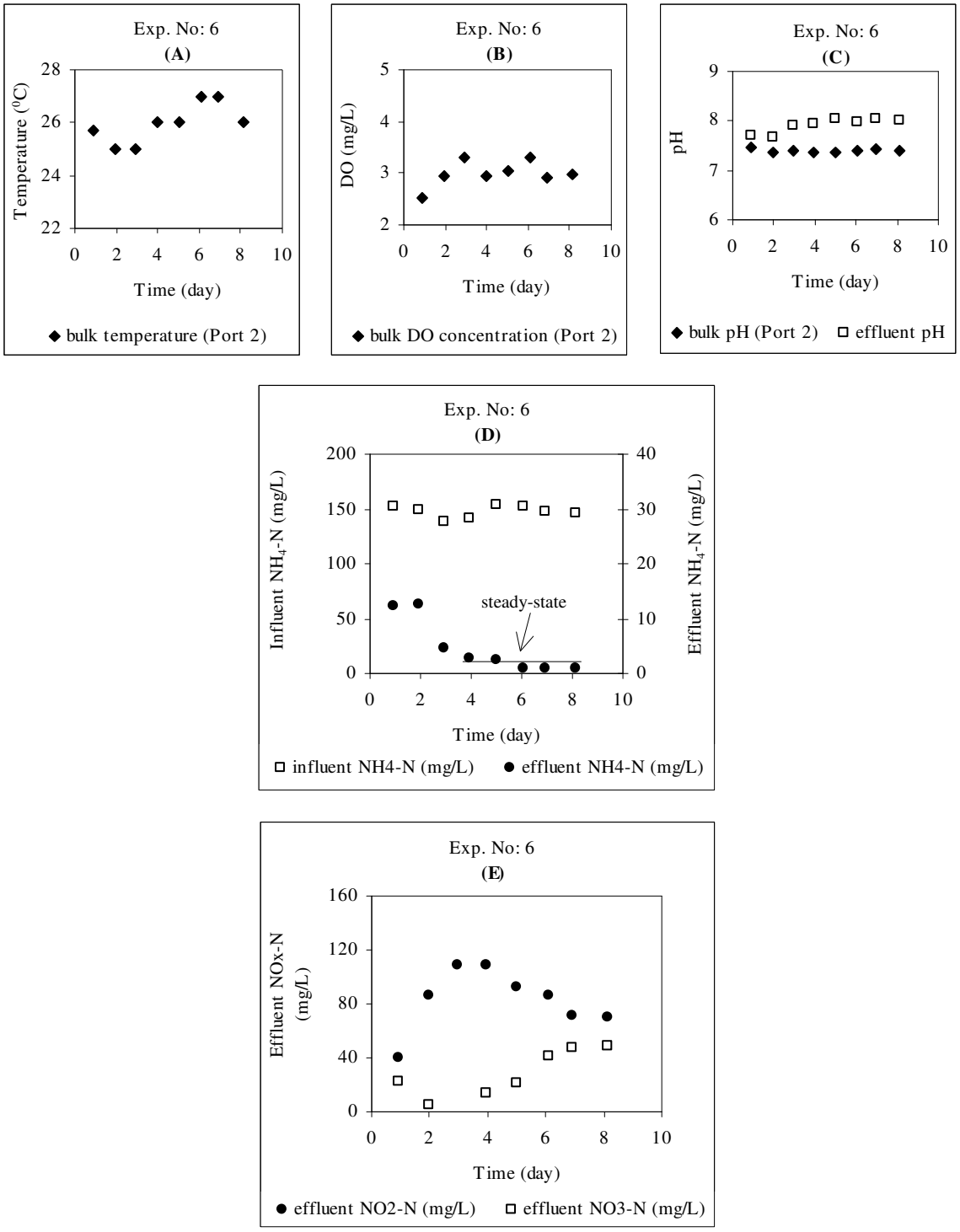

Figure R.6. Preliminary continuous-flow experiment No:6 measurements for (a) T, (b) DO, (c) pH, (d) NH_4-N and (e) NO_x-N

[Feed flowrate = 6L/day, Ave. Feed NH_4-N concentration = 148 mg/L]

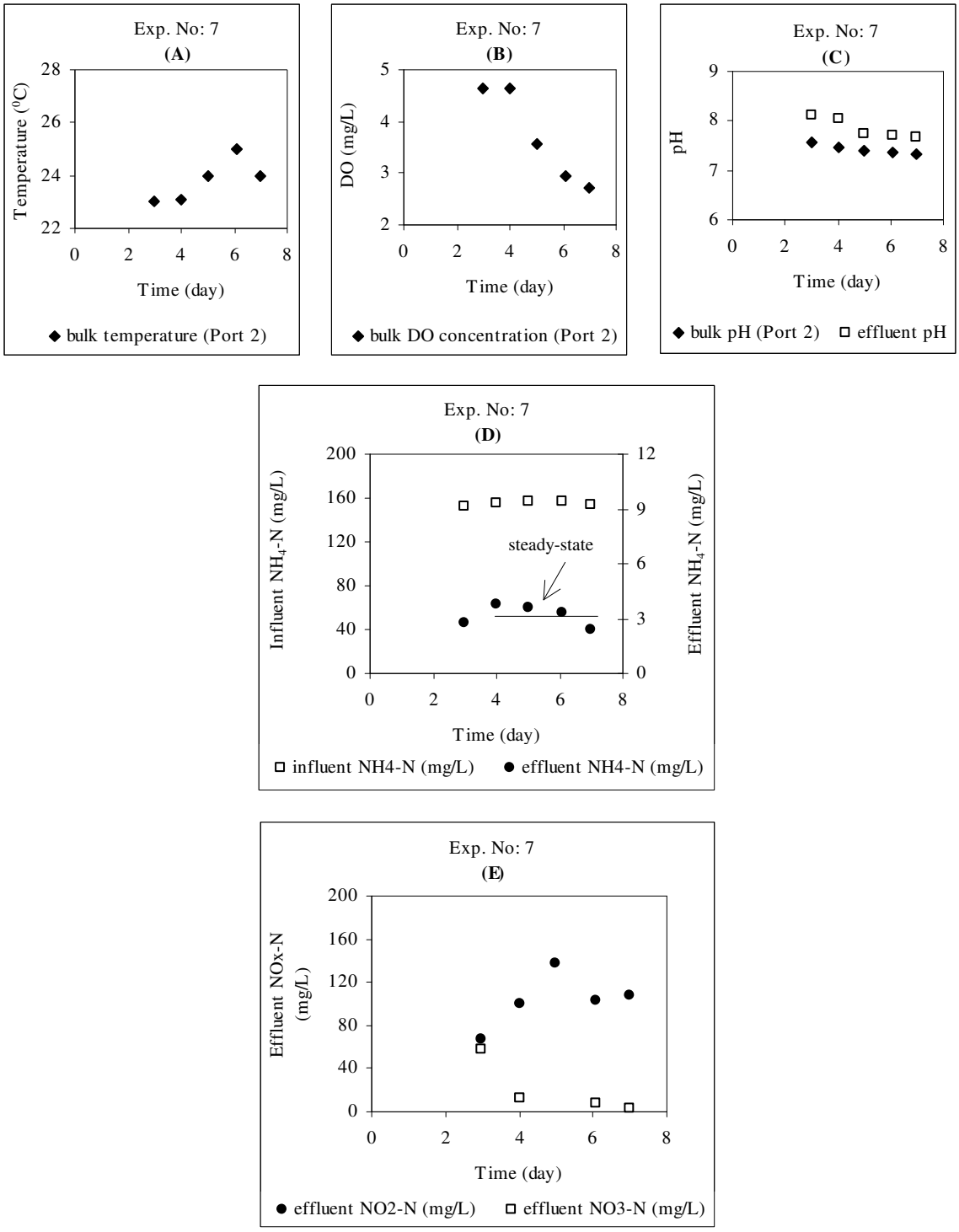

Figure R.7. Preliminary continuous-flow experiment No:7 measurements for (a) T, (b) DO, (c) pH, (d) NH_4-N and (e) NO_x-N

[Feed flowrate = 6L/day, Ave. Feed NH_4-N concentration = 156 mg/L]

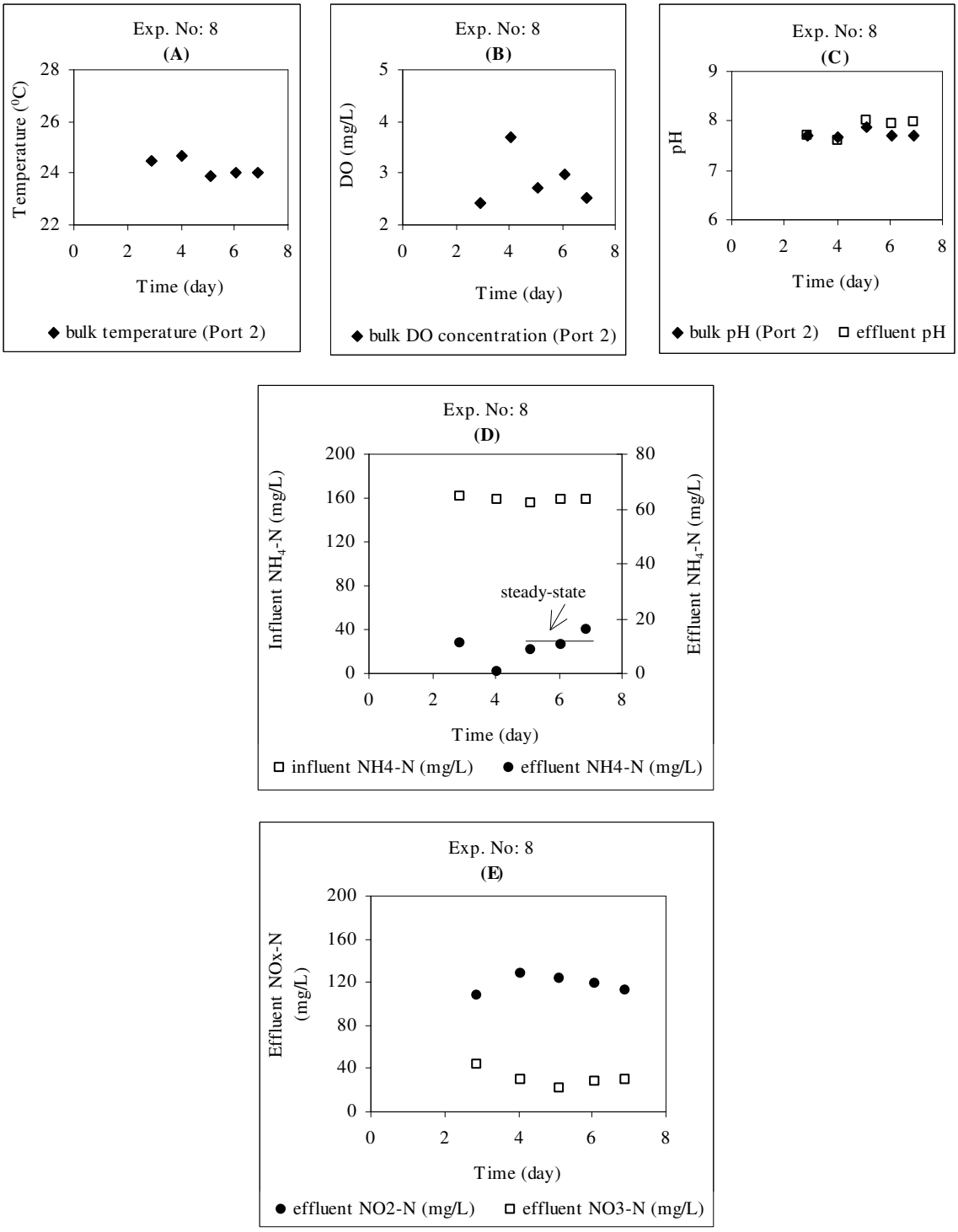

Figure R.8. Preliminary continuous-flow experiment No:8 measurements for (a) T, (b) DO, (c) pH, (d) NH_4-N and (e) NO_x-N

[Feed flowrate = 6L/day, Ave. Feed NH_4-N concentration = 157 mg/L]

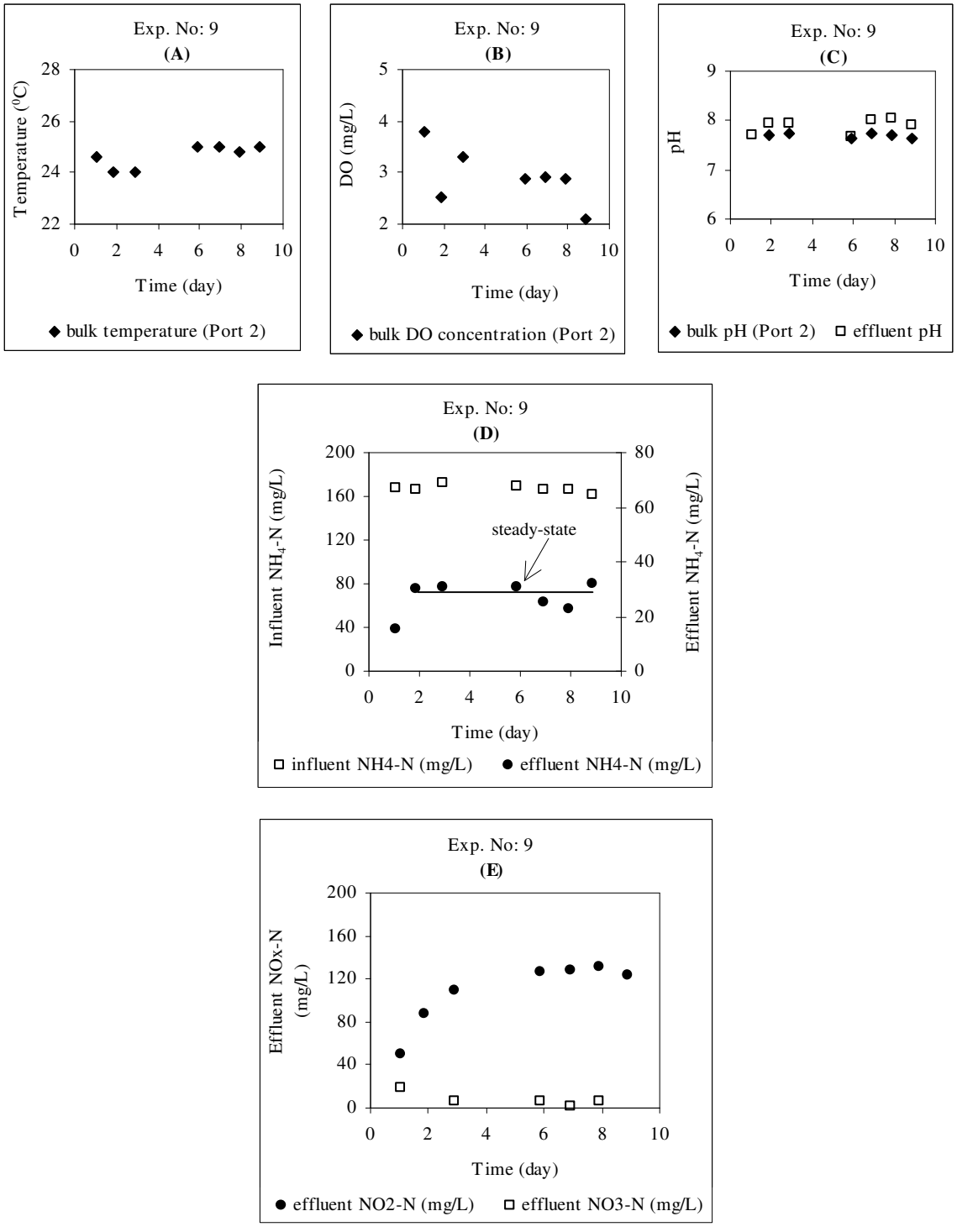

Figure R.9. Preliminary continuous-flow experiment No:9 measurements for (a) T, (b) DO, (c) pH, (d) NH_4-N and (e) NO_x-N

[Feed flowrate = 6L/day, Ave. Feed NH_4-N concentration = 167 mg/L]

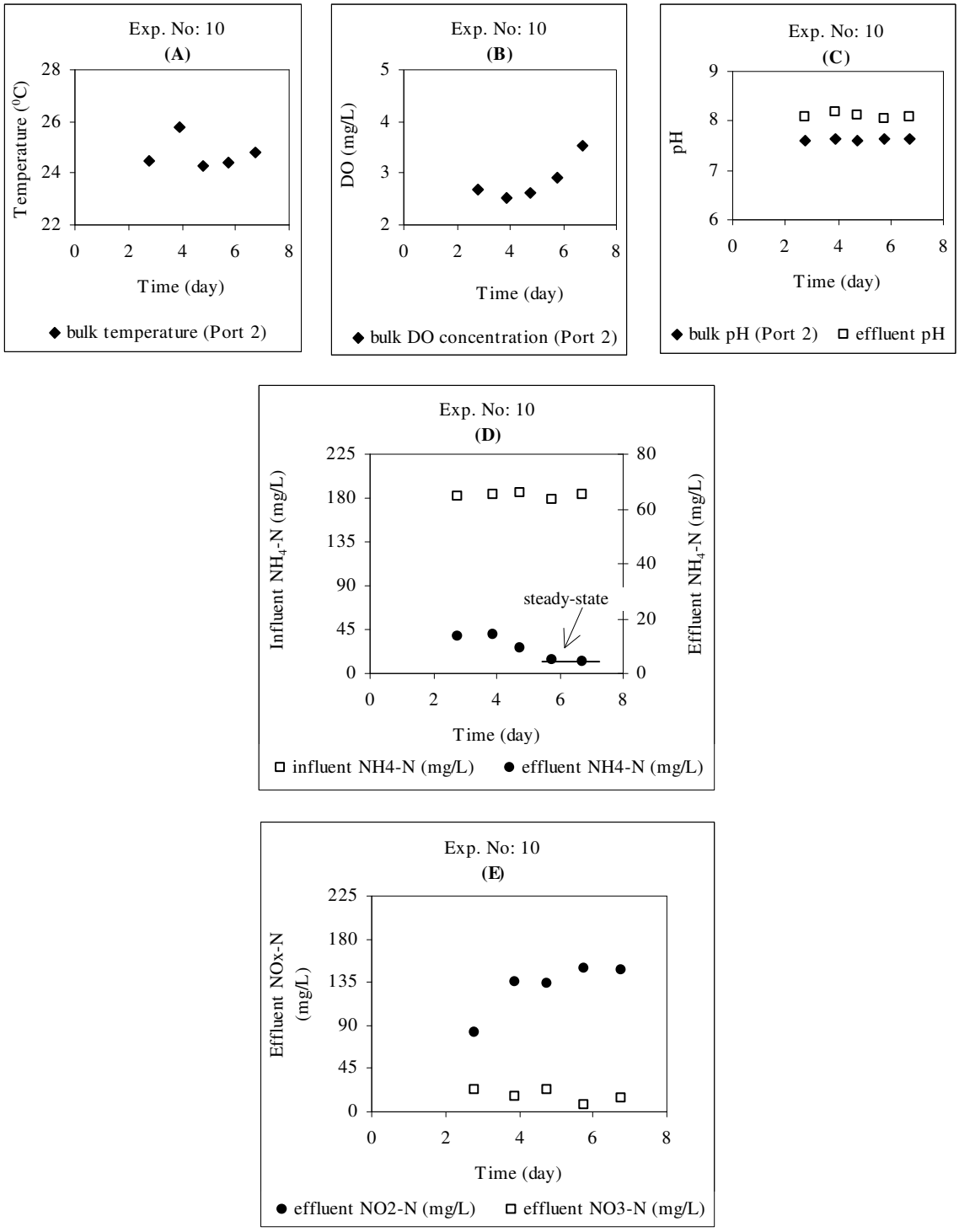

Figure R.10. Preliminary continuous-flow experiment No:10 measurements for (a) T, (b) DO, (c) pH, (d) NH_4-N and (e) NO_x-N

[Feed flowrate = 6L/day, Ave. Feed NH_4-N concentration = 182 mg/L]

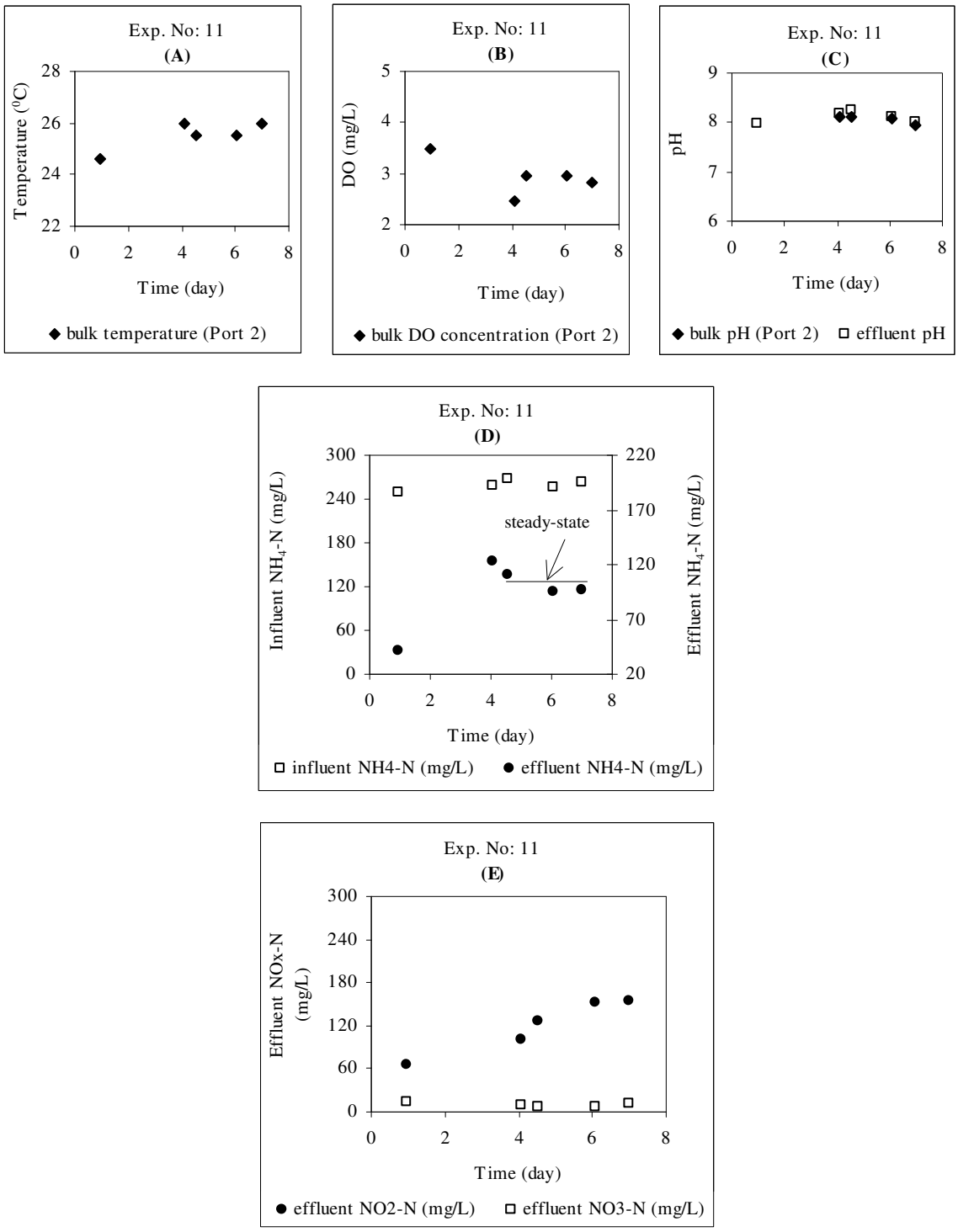

Figure R.11. Preliminary continuous-flow experiment No:11 measurements for (a) T, (b) DO, (c) pH, (d) NH_4-N and (e) NO_x-N

[Feed flowrate = 6L/day, Ave. Feed NH_4-N concentration = 262 mg/L]

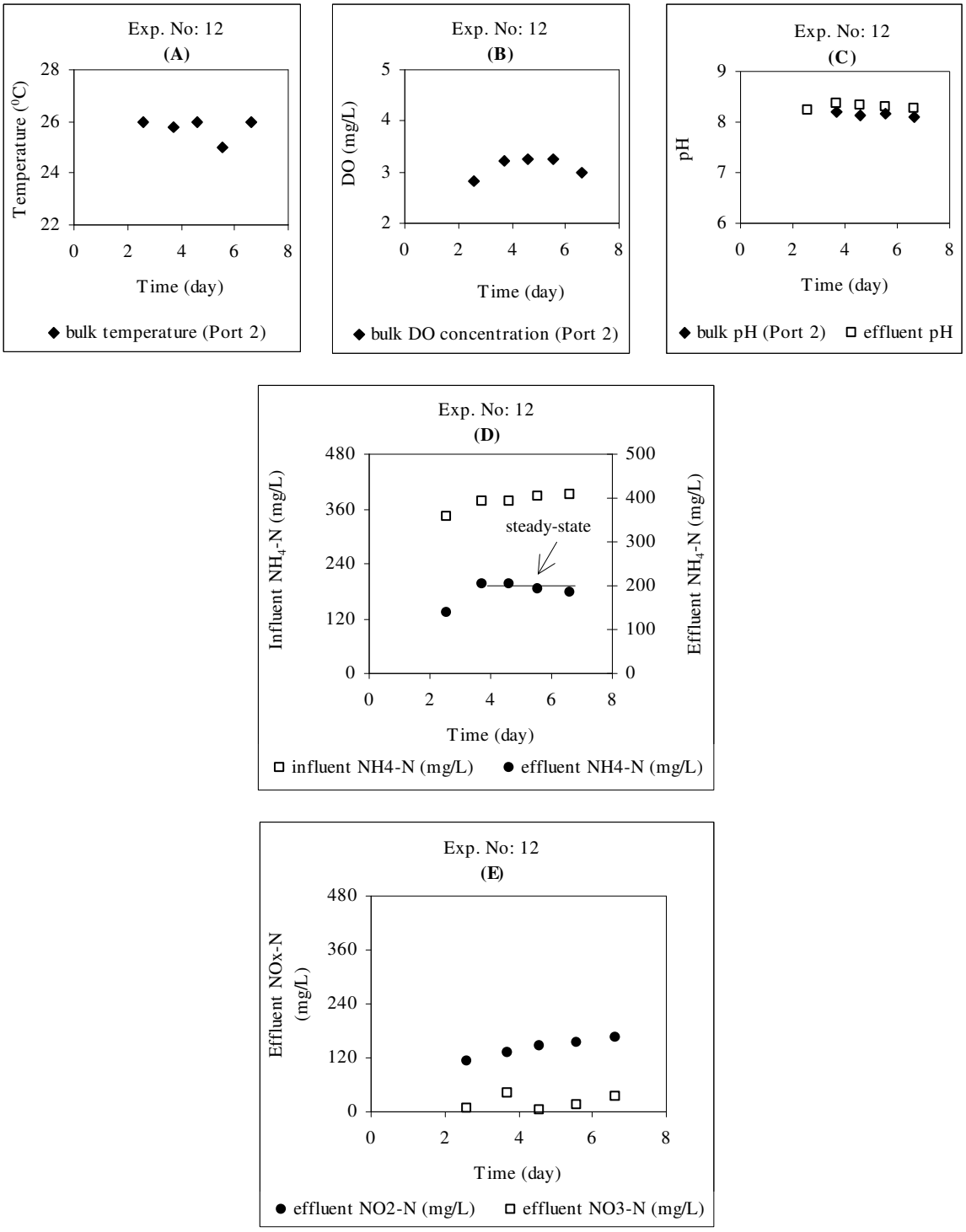

Figure R.12. Preliminary continuous-flow experiment No:12 measurements for (a) T, (b) DO, (c) pH, (d) NH_4-N and (e) NO_x-N

[Feed flowrate = 6L/day, Ave. Feed NH_4-N concentration = 383 mg/L]

APPENDIX S: DAILY MEASUREMENTS IN CONTINUOUS-FLOW BIOFILM EXPERIMENTS WITH 1,2-DCA

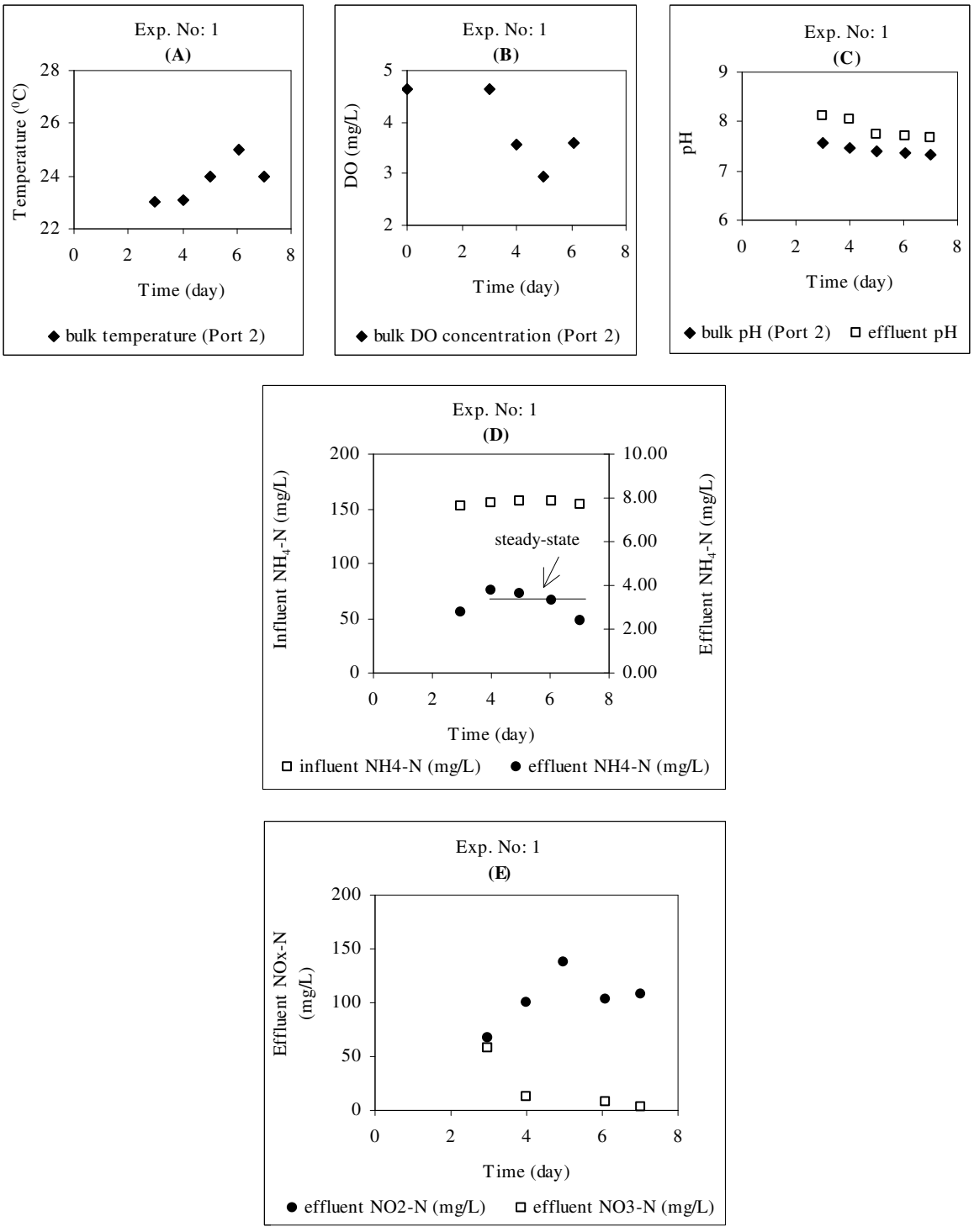

Figure S.1. Continuous–flow experiment with 1,2-DCA No:1 measurements for (a) T, (b) DO, (c) pH, (d) NH_4-N and (e) NO_x-N

[Feed flowrate = 6L/day, Ave. Feed NH_4-N = 156 mg/L, Ave. Feed DCA = 0 ppb]

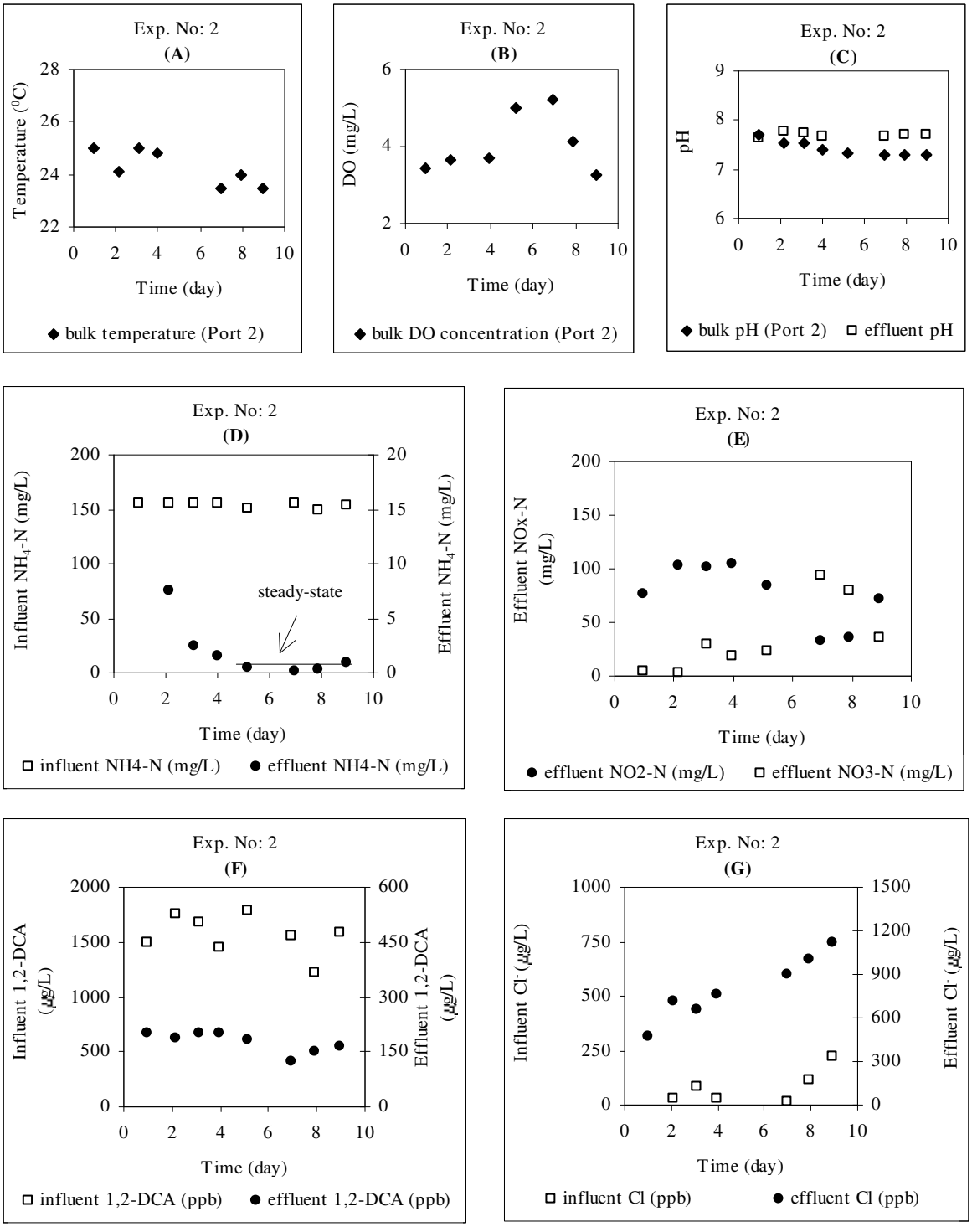

Figure S.2. Continuous–flow experiment with 1,2-DCA No:2 measurements for (a) T, (b) DO, (c) pH, (d) NH_4-N, (e) NO_x-N, (f) 1,2-DCA and (g) Cl^-

[Feed flowrate = 6L/day, Ave. Feed NH_4-N = 153 mg/L, Ave. Feed 1,2-DCA = 1539 ppb]

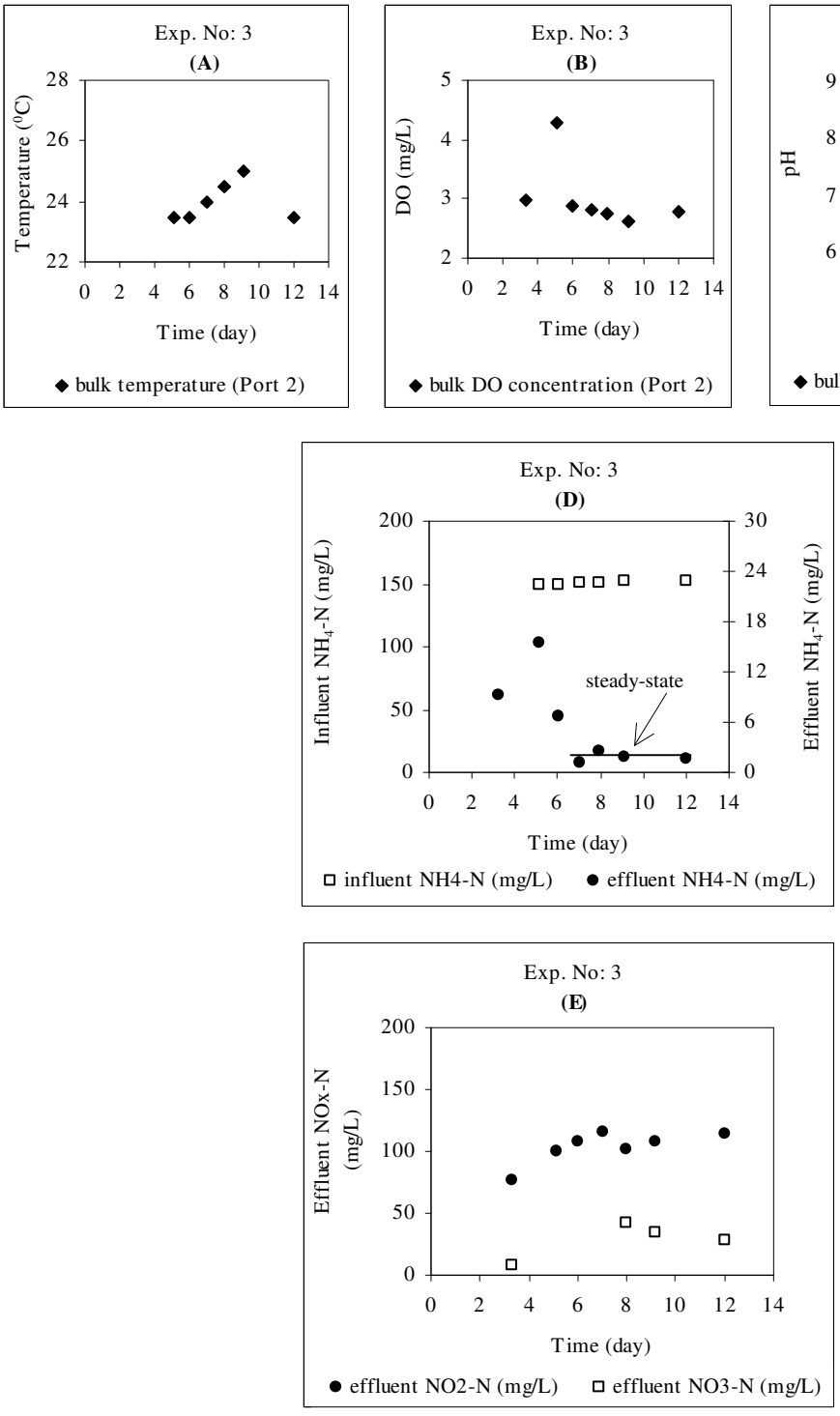

Figure S.3. Continuous–flow experiment with 1,2-DCA No:3 measurements for (a) T, (b) DO, (c) pH, (d) NH_4-N and (e) NO_x-N

[Feed flowrate = 6L/day, Ave. Feed NH_4-N = 152 mg/L, Ave. Feed 1,2-DCA = 0 ppb]

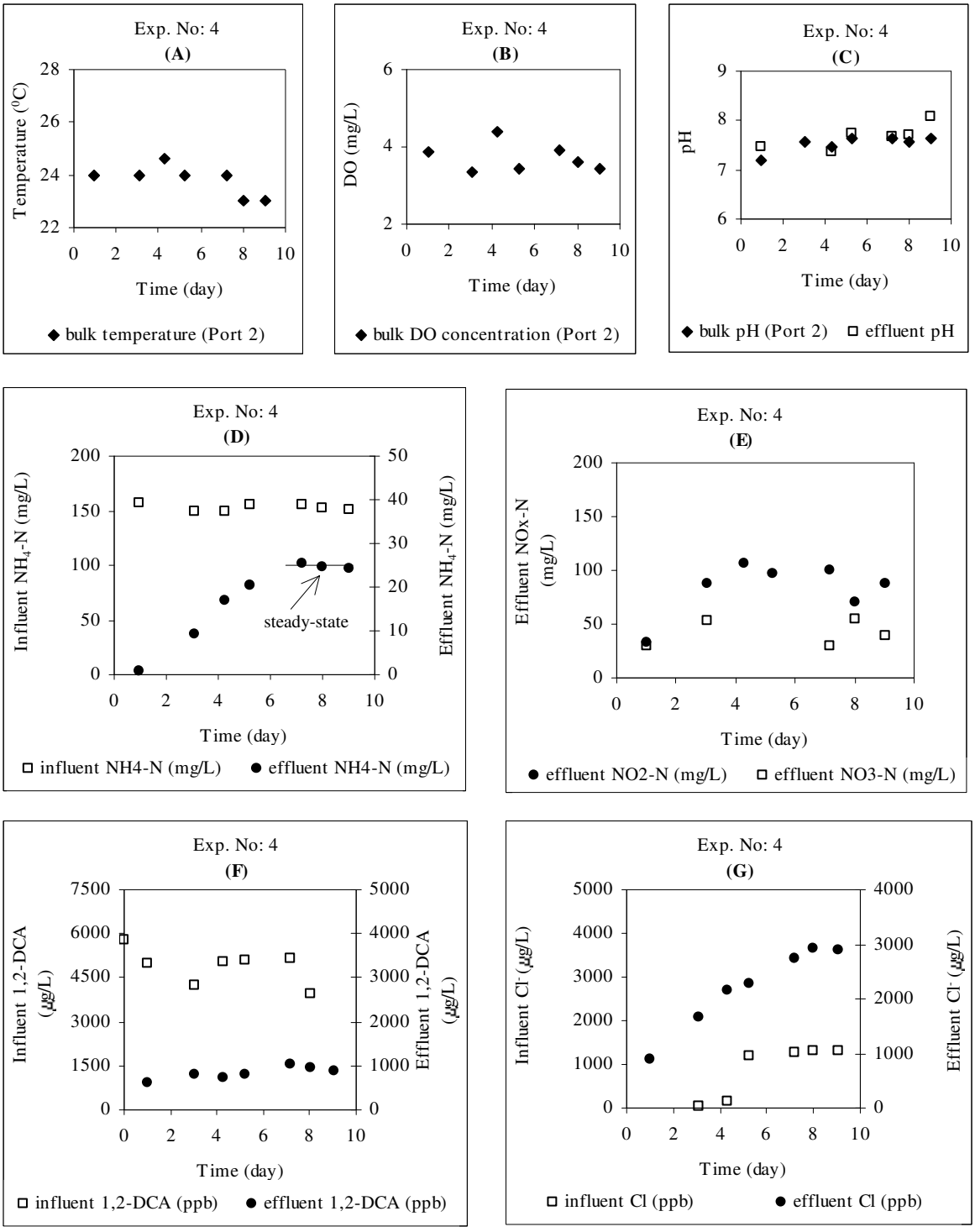

Figure S.4. Continuous–flow experiment with 1,2-DCA No:4 measurements for (a) T, (b) DO, (c) pH, (d) NH_4-N, (e) NO_x-N, (f) 1,2-DCA, and (g) Cl^-

[Feed flowrate = 6L/day, Ave. Feed NH_4-N = 153 mg/L, Ave. Feed 1,2-DCA = 4728 ppb]

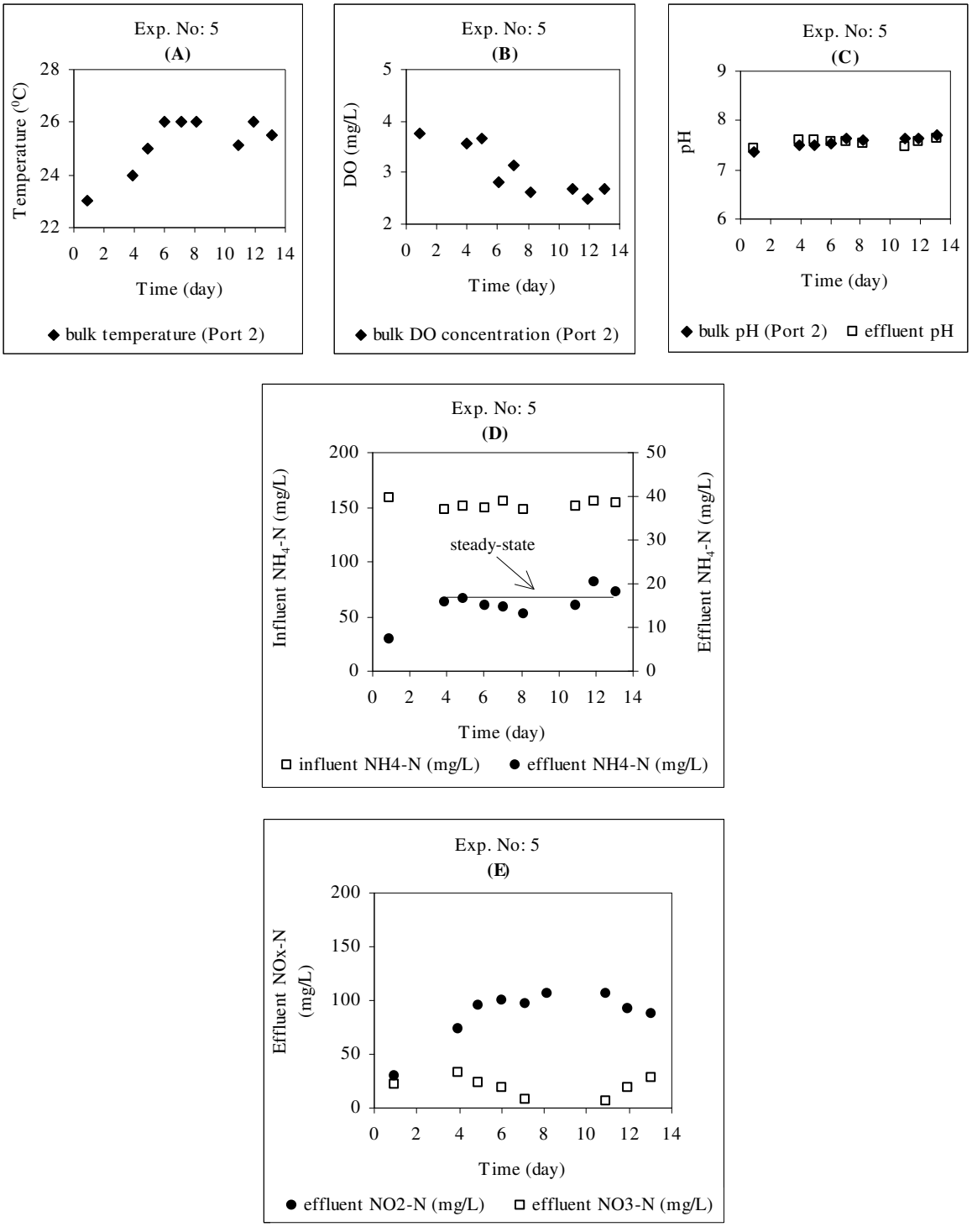

Figure S.5. Continuous–flow experiment with 1,2-DCA No:5 measurements for (a) T, (b) DO, (c) pH, (d) NH_4-N and (e) NO_x-N

[Feed flowrate = 6L/day, Ave. Feed NH_4-N = 151 mg/L, Ave. Feed 1,2-DCA = 0 ppb]

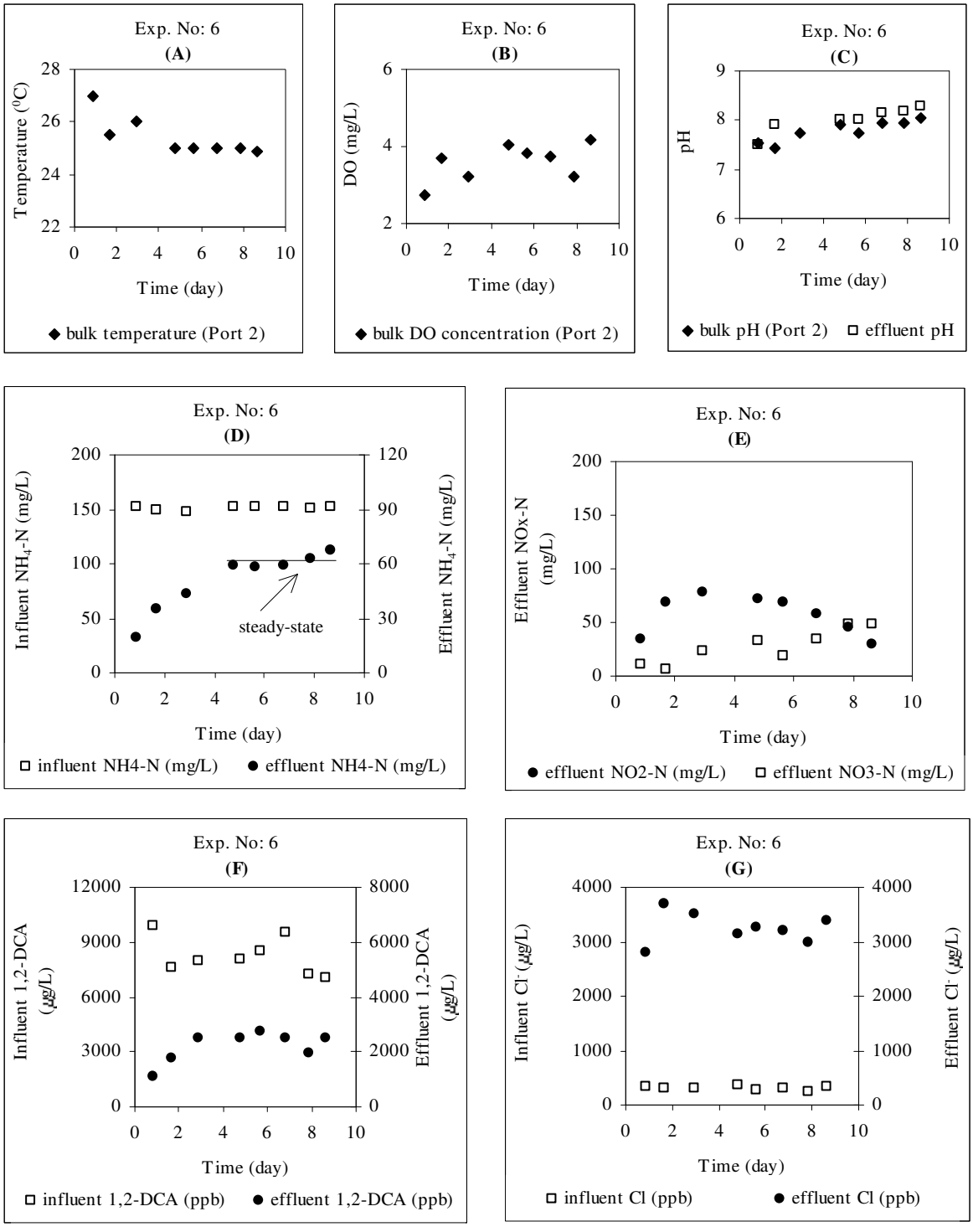

Figure S.6. Continuous–flow experiment with 1,2-DCA No:6 measurements for (a) T, (b) DO, (c) pH, (d) NH_4-N, (e) NO_x-N, (f) 1,2-DCA and (g) Cl^-

[Feed flowrate = 6L/day, Ave. Feed NH_4-N = 152 mg/L, Ave. Feed 1,2-DCA = 8087 ppb]

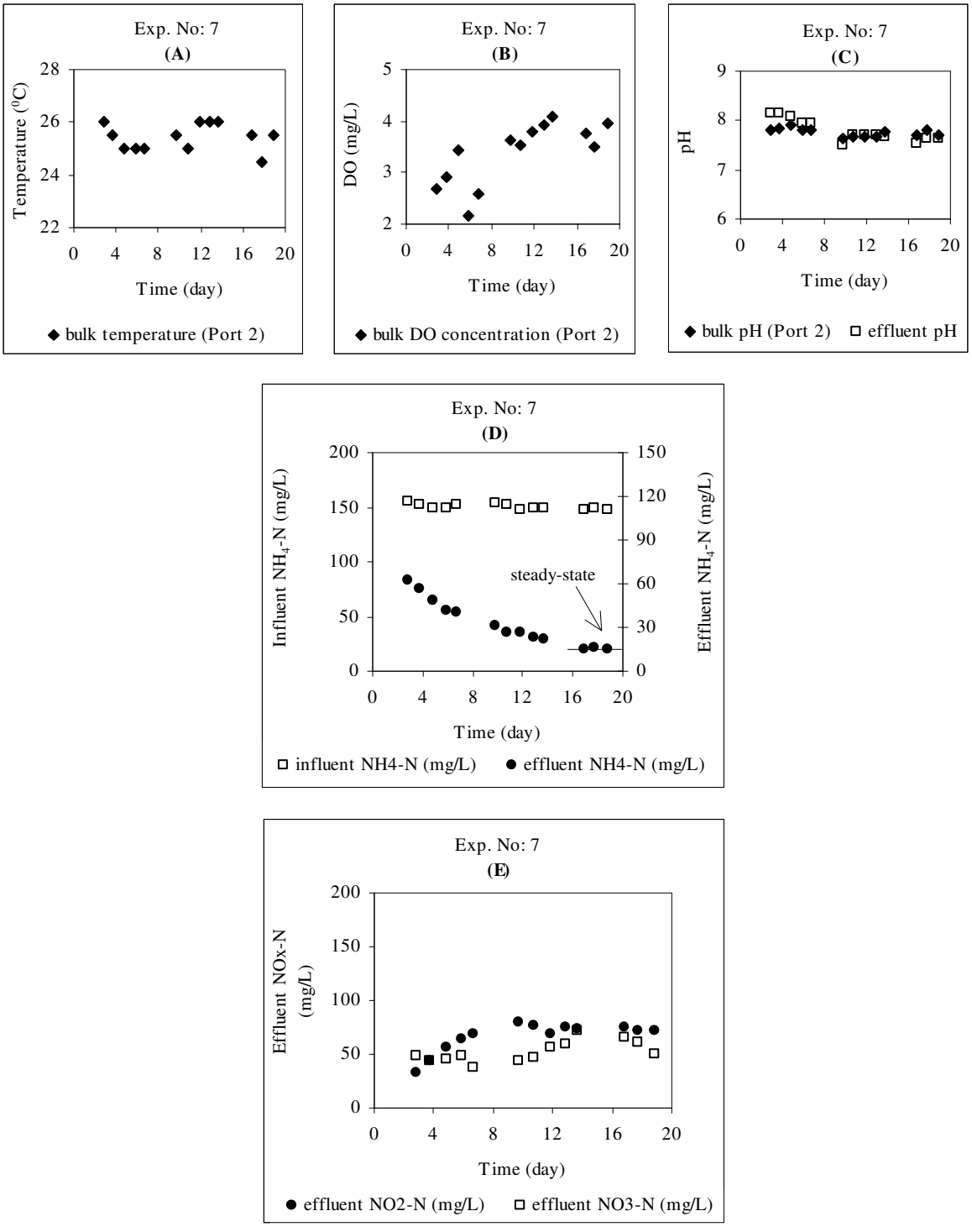

Figure S.7. Continuous–flow experiment with 1,2-DCA No:7 measurements for (a) T, (b) DO, (c) pH, (d) NH_4-N and (e) NO_x-N

[Feed flowrate = 6L/day, Ave. Feed NH_4-N = 149 mg/L, Ave. Feed 1,2-DCA = 0 ppb]

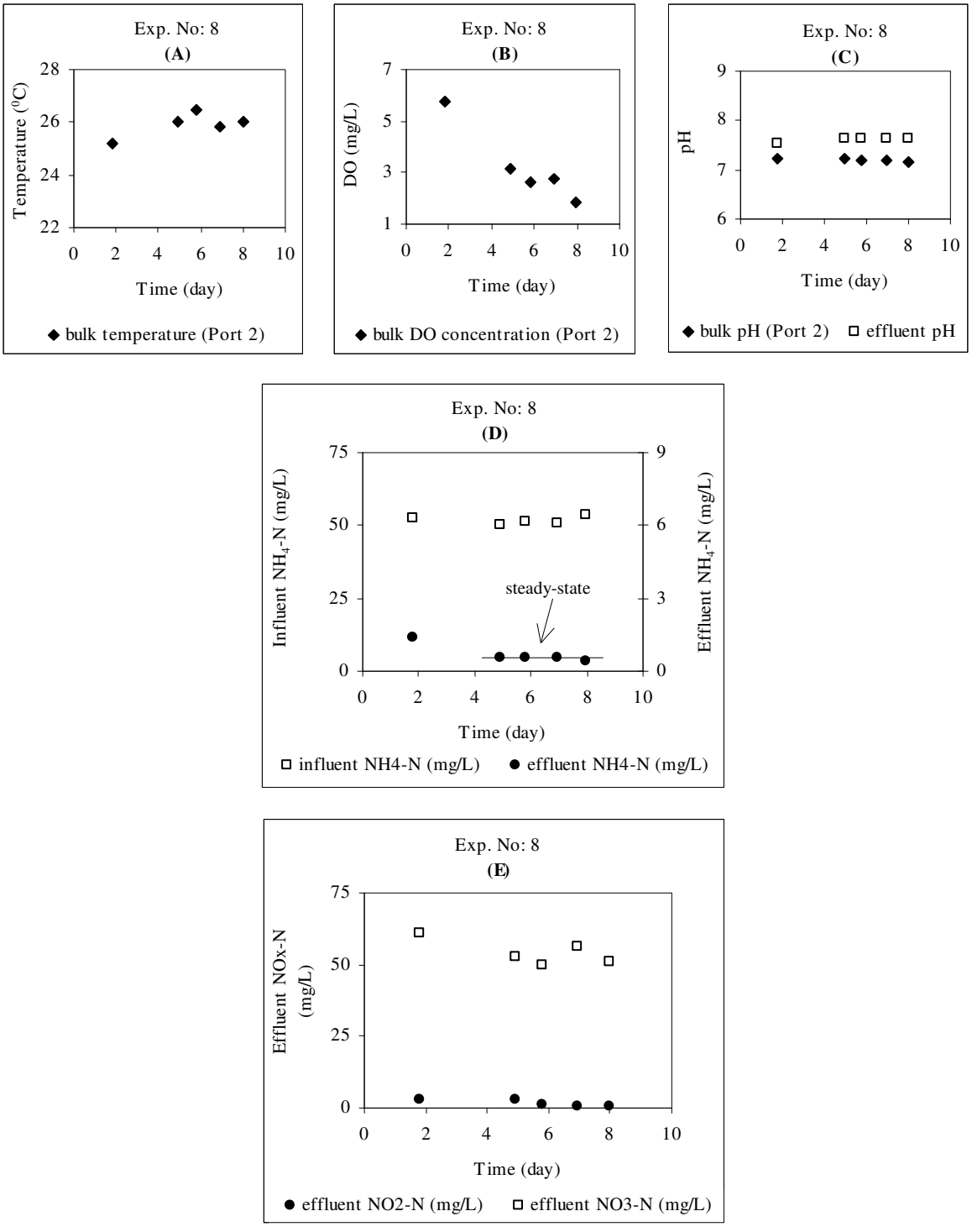

Figure S.8. Continuous–flow experiment with 1,2-DCA No:8 measurements for (a) T, (b) DO, (c) pH, (d) NH_4-N and (e) NO_x-N

[Feed flowrate = 6L/day, Ave. Feed NH_4-N = 52 mg/L, Ave. Feed 1,2-DCA = 0 ppb]

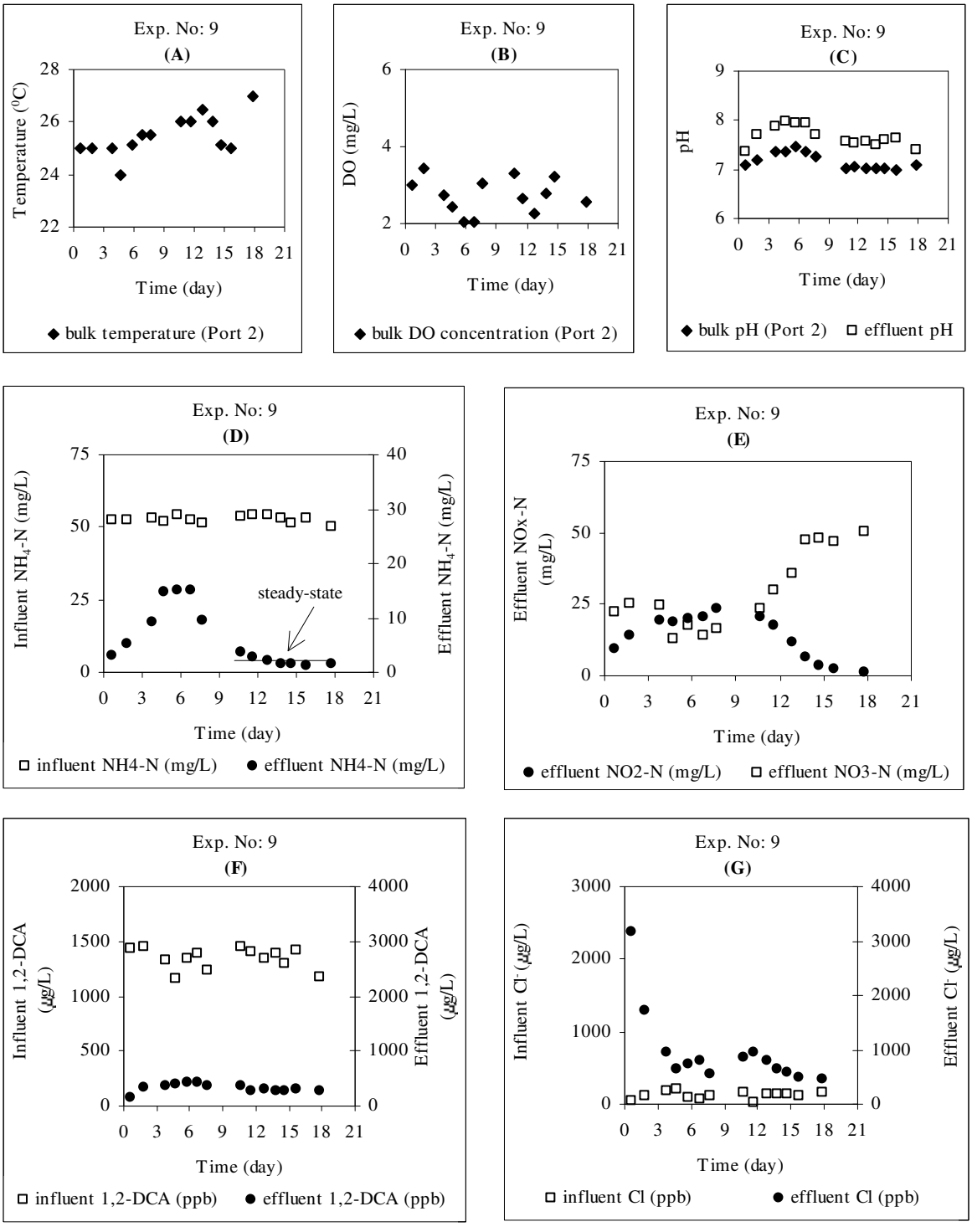

Figure S.9. Continuous–flow experiment with 1,2-DCA No:9 measurements for (a) T, (b) DO, (c) pH, (d) NH_4-N, (e) NO_x-N, (f) 1,2-DCA and (g) Cl^-

[Feed flowrate = 6L/day, Ave. Feed NH_4-N = 53 mg/L, Ave. Feed 1,2-DCA = 1352 ppb]

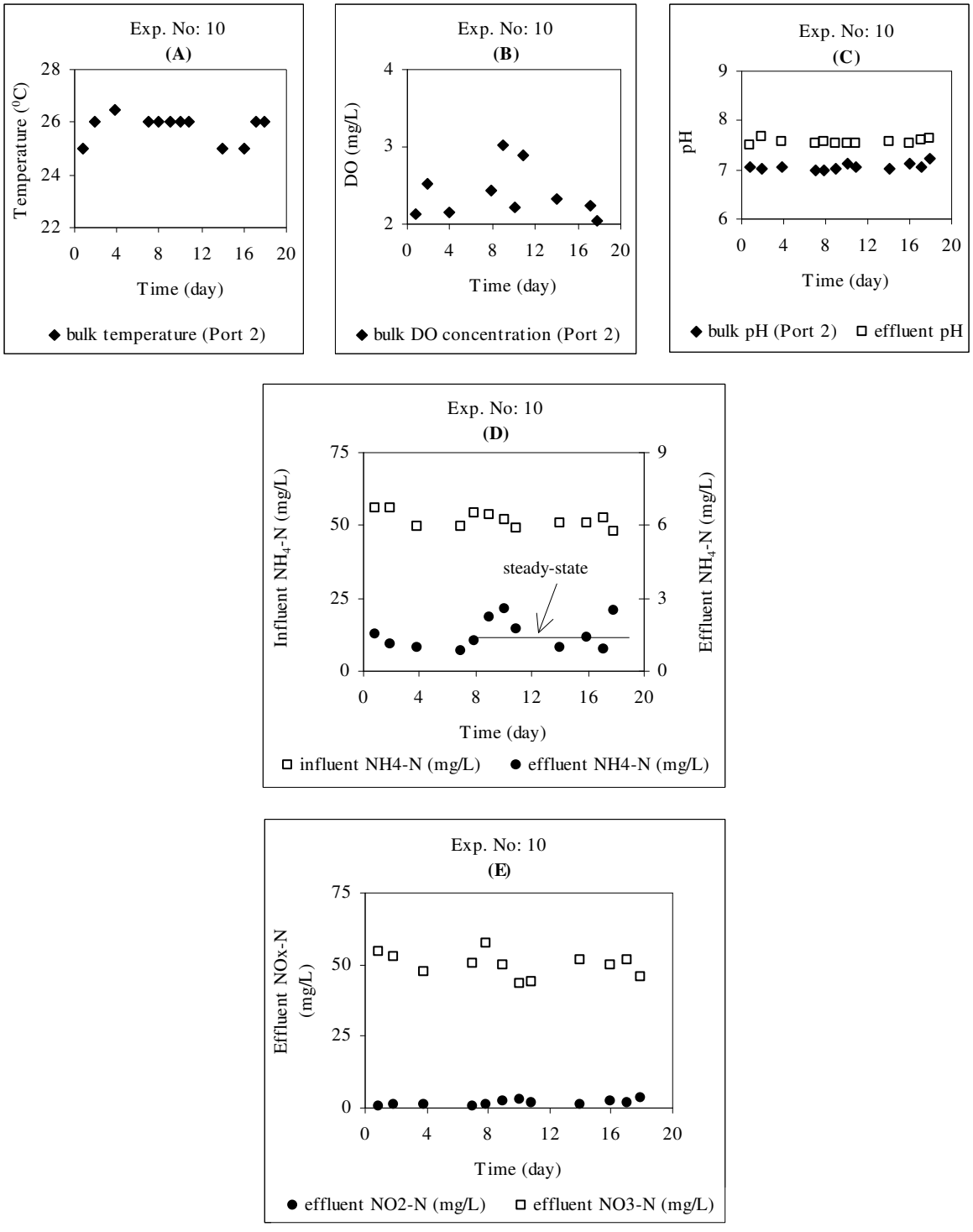

Figure S.10. Continuous–flow experiment with 1,2-DCA No:10 measurements for (a) T, (b) DO, (c) pH, (d) NH_4-N and (e) NO_x-N

[Feed flowrate = 6L/day, Ave. Feed NH_4-N = 51 mg/L, Ave. Feed 1,2-DCA = 0 ppb]

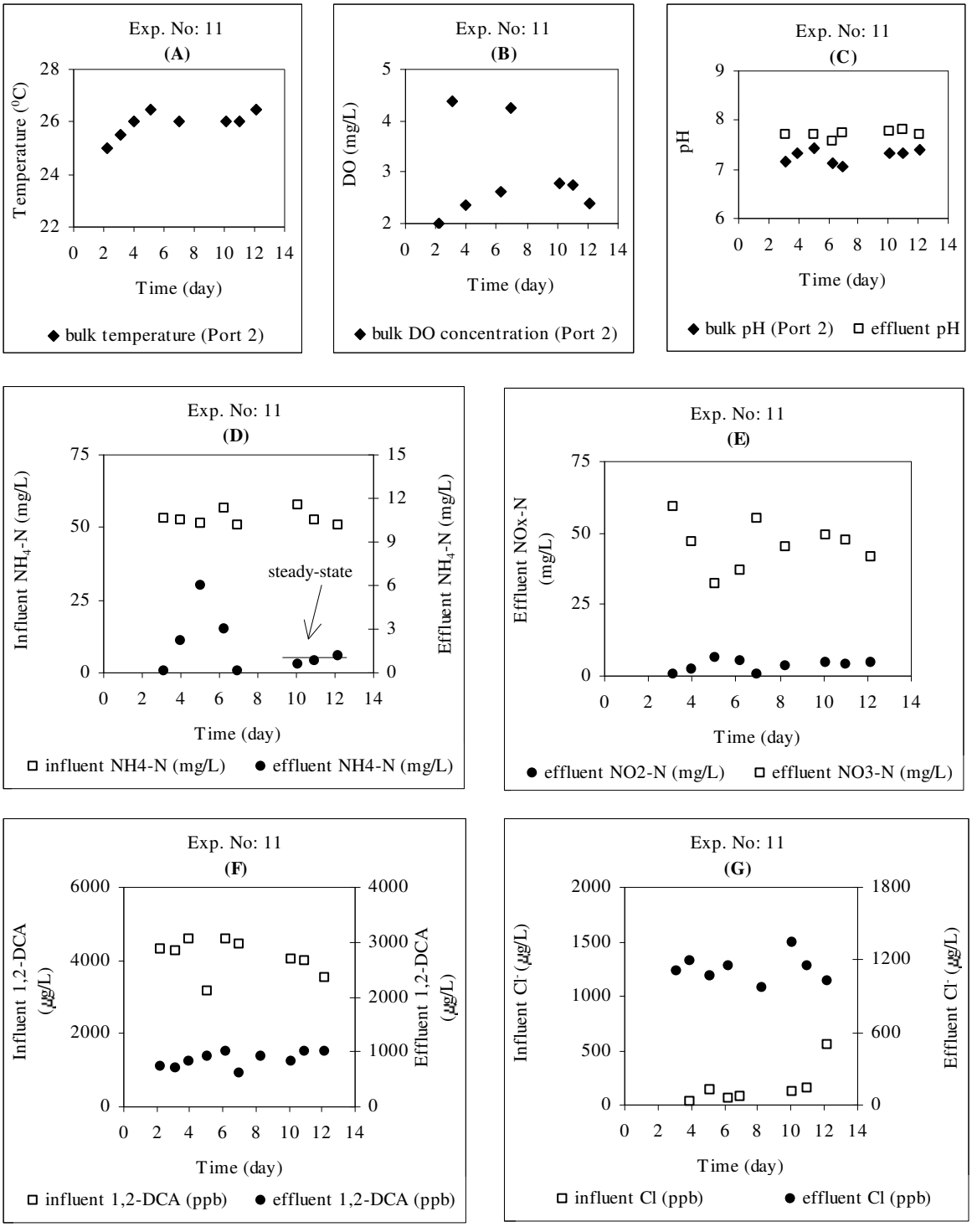

Figure S.11. Continuous–flow experiment with 1,2-DCA No:11 measurements for (a) T, (b) DO, (c) pH, (d) NH_4-N, (e) NO_x-N, (f) 1,2-DCA and (g) Cl^-

[Feed flowrate = 6L/day, Ave. Feed NH_4-N = 54 mg/L, Ave. Feed 1,2-DCA = 3844 ppb]

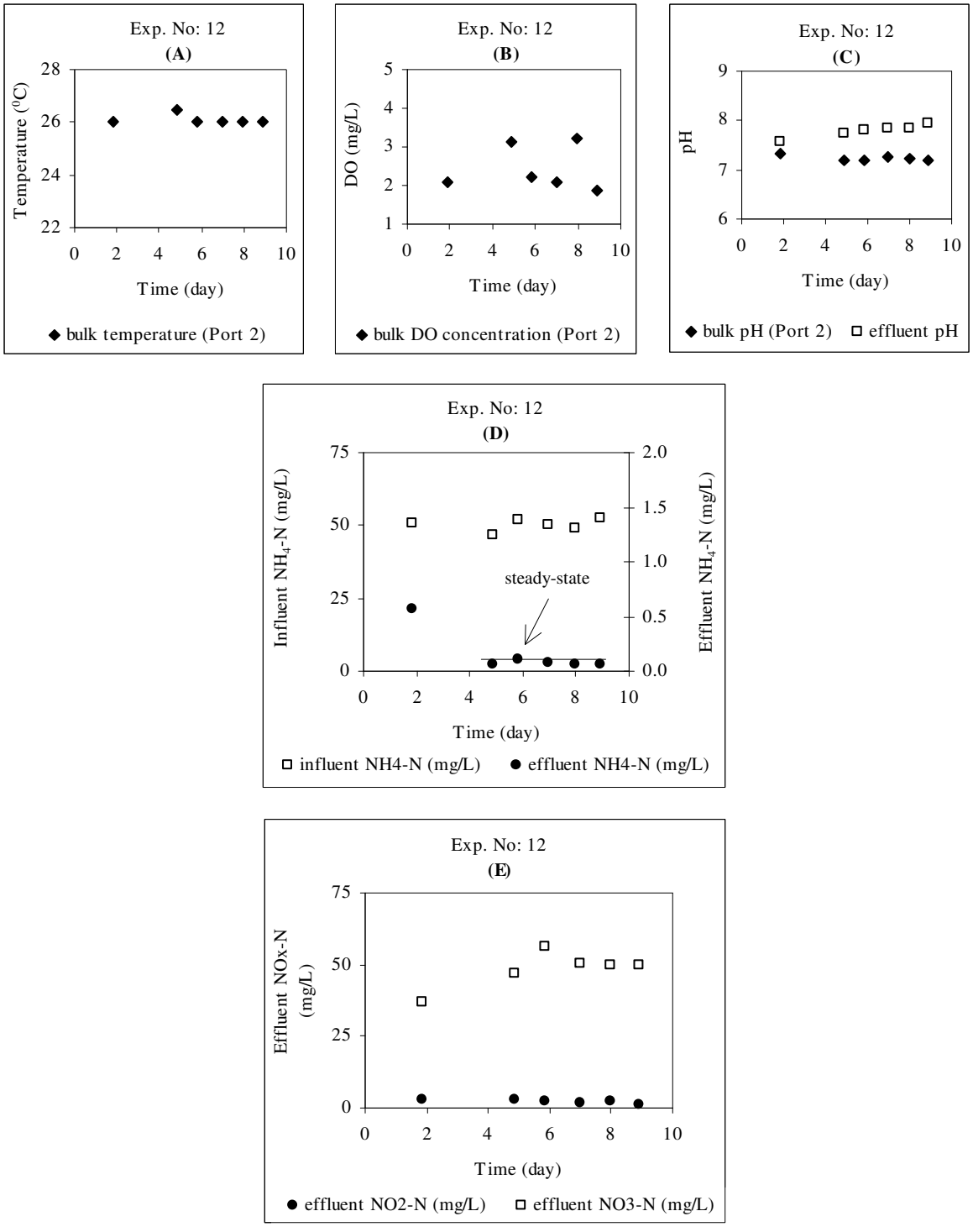

Figure S.12. Continuous–flow experiment with 1,2-DCA No:12 measurements for (a) T, (b) DO, (c) pH, (d) NH_4-N and (e) NO_x-N

[Feed flowrate = 6L/day, Ave. Feed NH_4-N = 50 mg/L, Ave. Feed 1,2-DCA = 0 ppb]

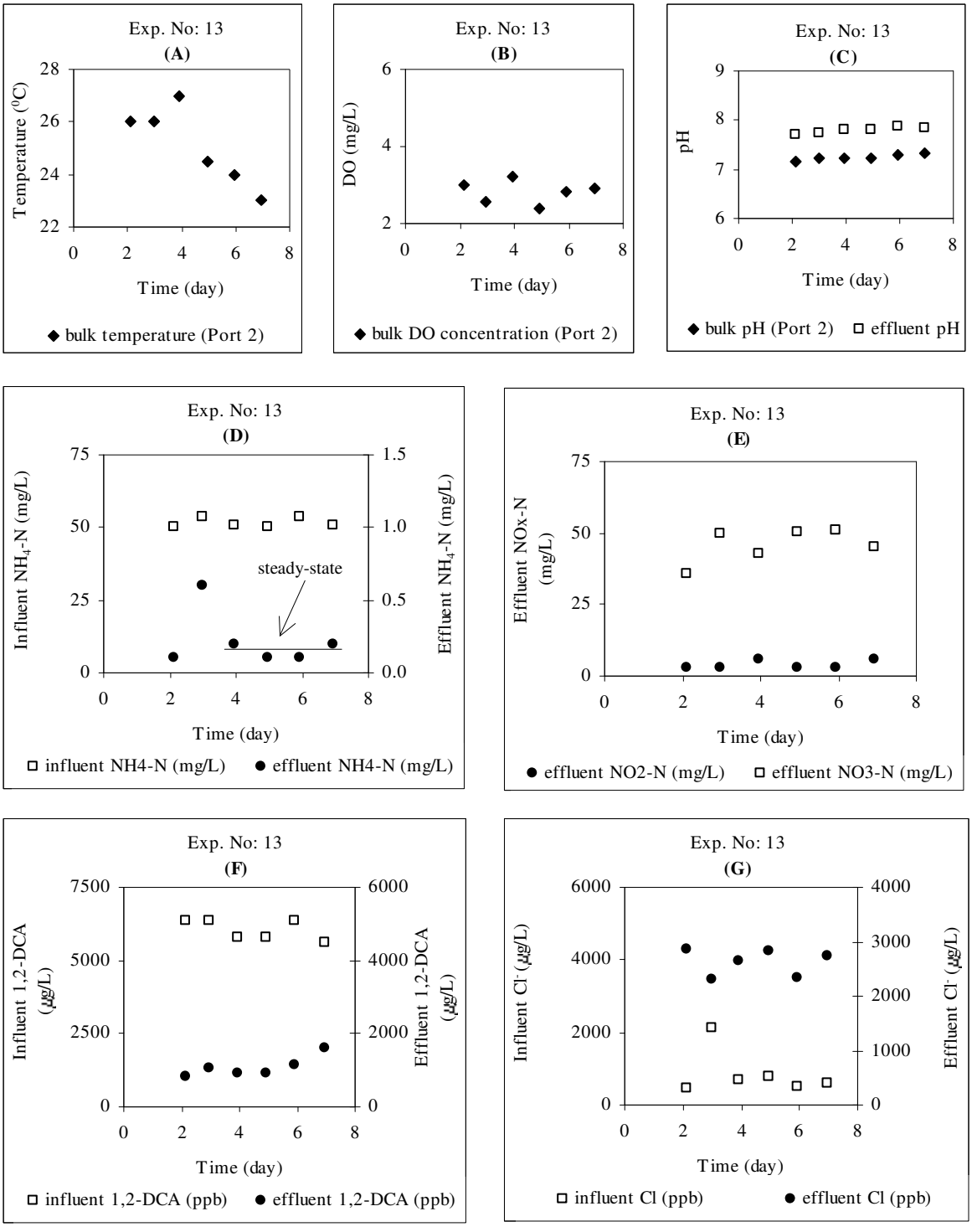

Figure S.13. Continuous–flow experiment with 1,2-DCA No:13 measurements for (a) T, (b) DO, (c) pH, (d) NH_4-N, (e) NO_x-N, (f) 1,2-DCA and (g) Cl^-

[Feed flowrate = 6L/day, Ave. Feed NH_4-N = 51 mg/L, Ave. Feed 1,2-DCA = 5891 ppb]

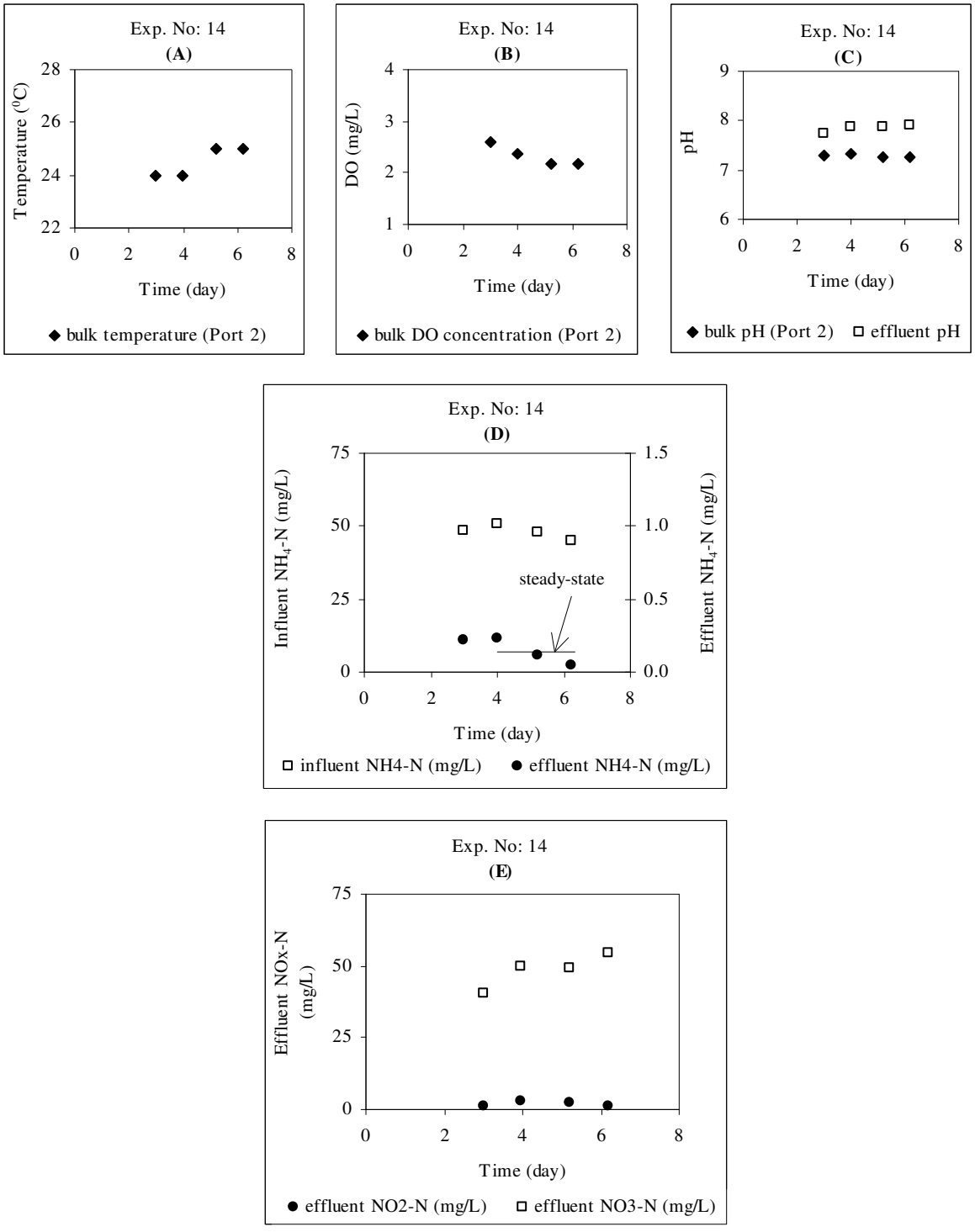

Figure S.14. Continuous–flow experiment with 1,2-DCA No:14 measurements for (a) T, (b) DO, (c) pH, (d) NH_4-N and (e) NO_x-N

[Feed flowrate = 6L/day, Ave. Feed NH_4-N = 48 mg/L, Ave. Feed 1,2-DCA = 0 ppb]

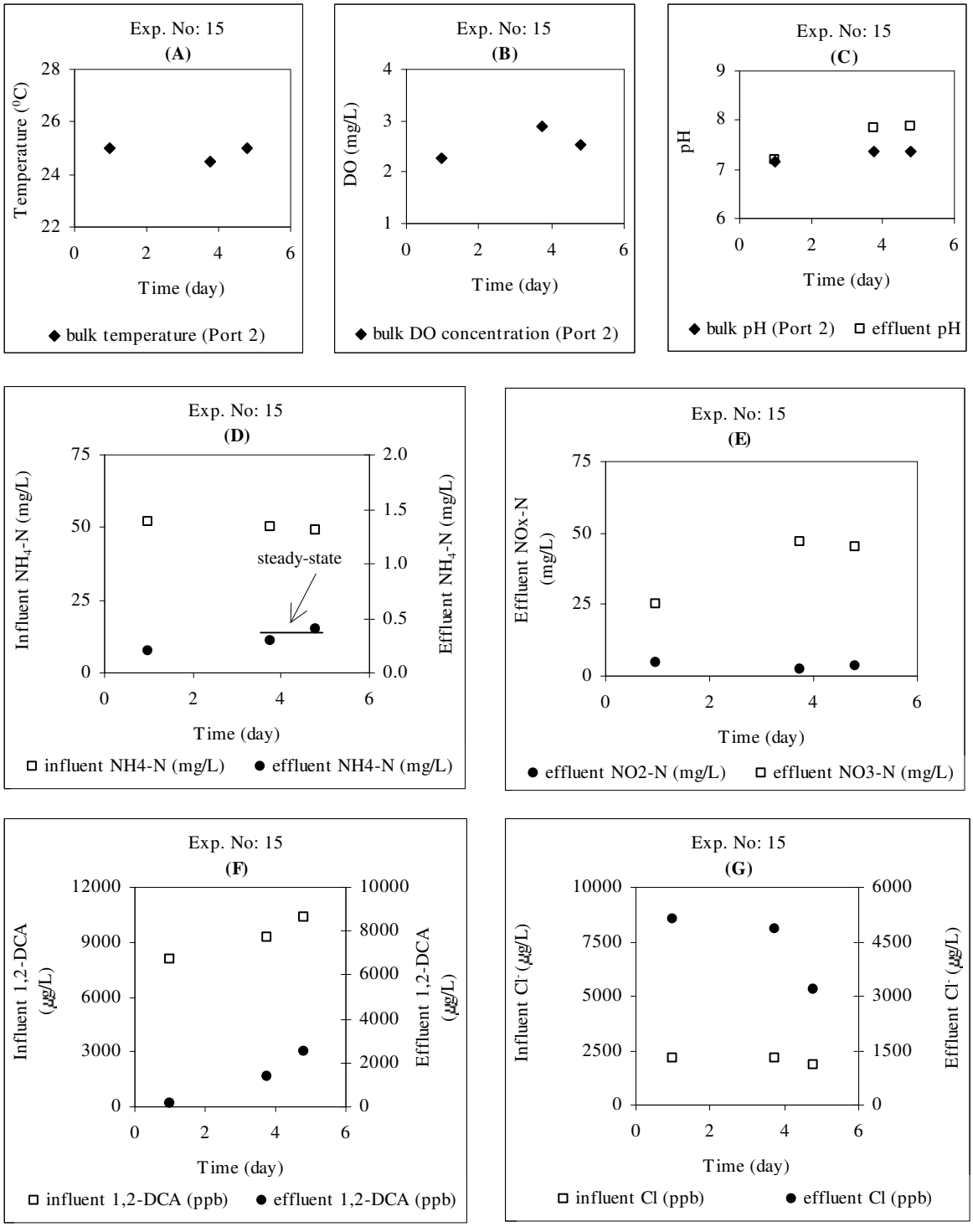

Figure S.15. Continuous–flow experiment with 1,2-DCA No:15 measurements for (a) T, (b) DO, (c) pH, (d) NH_4-N, (e) NO_x-N, (f) 1,2-DCA and (g) Cl^-

[Feed flowrate = 6L/day, Ave. Feed NH_4-N = 50 mg/L, Ave. Feed 1,2-DCA = 9791 ppb]

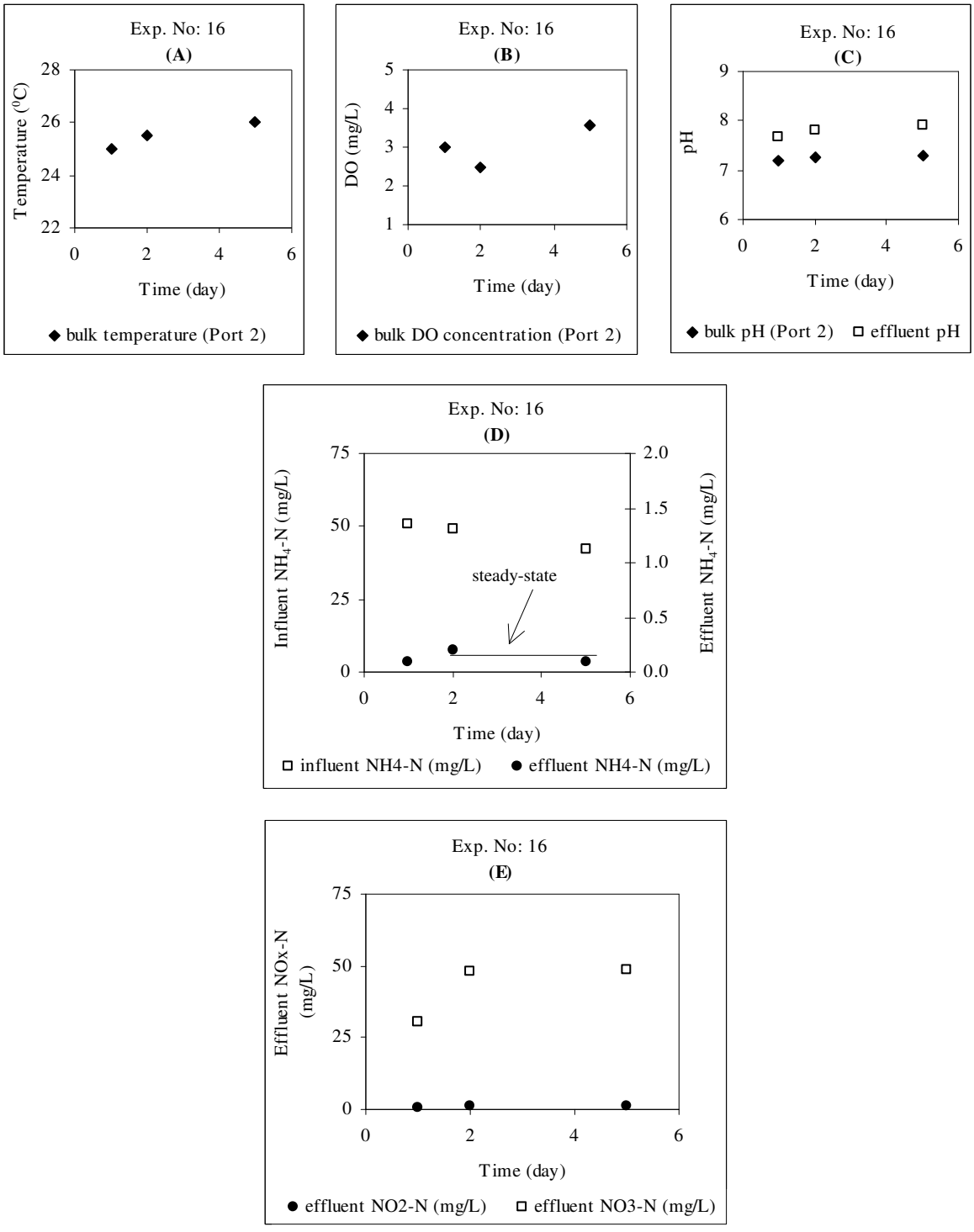

Figure S.16. Continuous–flow experiment with 1,2-DCA No:16 measurements for (a) T, (b) DO, (c) pH, (d) NH_4-N and (e) NO_x-N

[Feed flowrate = 6L/day, Ave. Feed NH_4-N = 46 mg/L, Ave. Feed 1,2-DCA = 0 ppb]

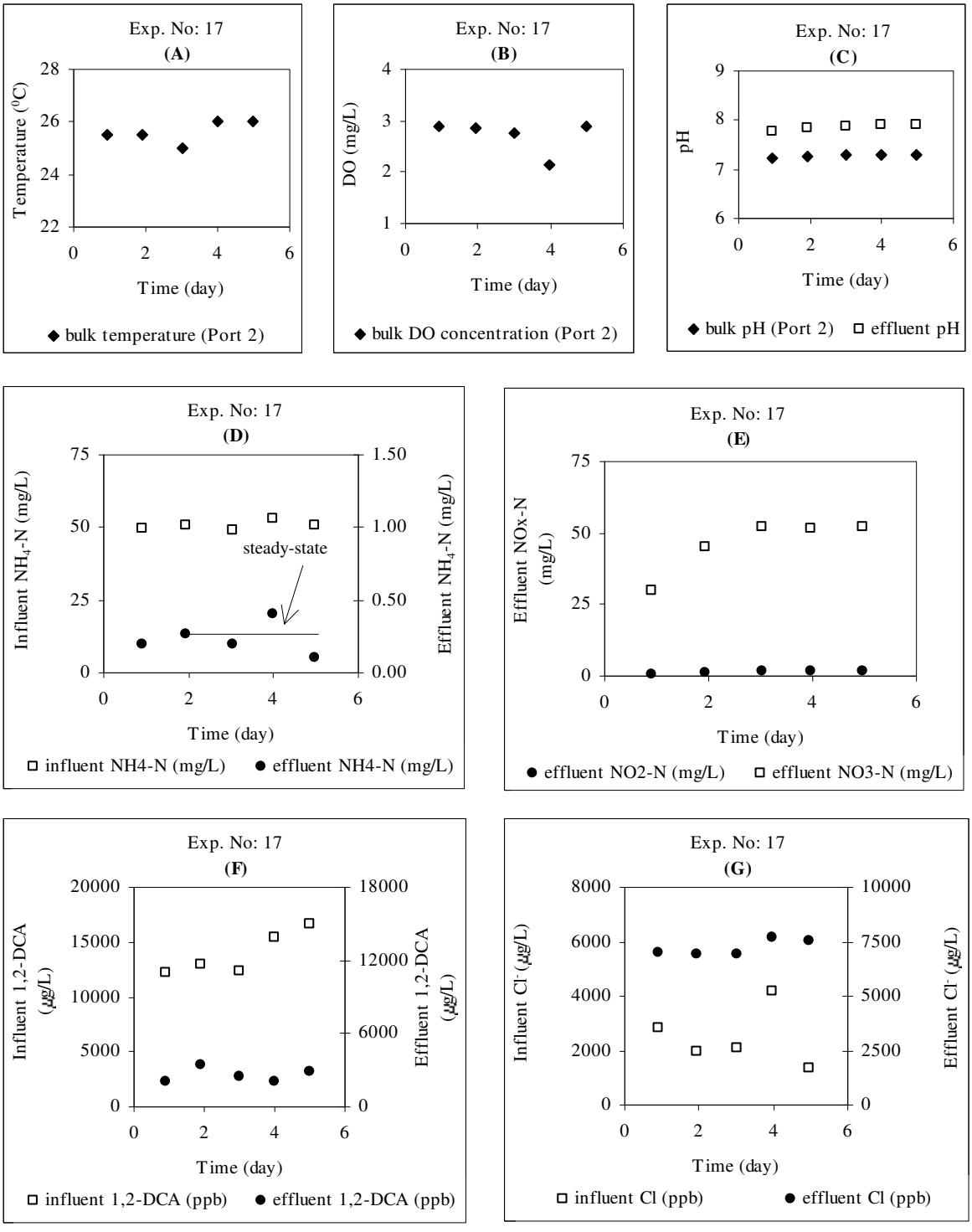

Figure S.17. Continuous–flow experiment with 1,2-DCA No:17 measurements for (a) T, (b) DO, (c) pH, (d) NH_4-N, (e) NO_x-N, (f) 1,2-DCA and (g) Cl^-

[Feed flowrate = 6L/day, Ave. Feed NH_4-N = 51 mg/L, Ave. Feed 1,2-DCA = 14337 ppb]

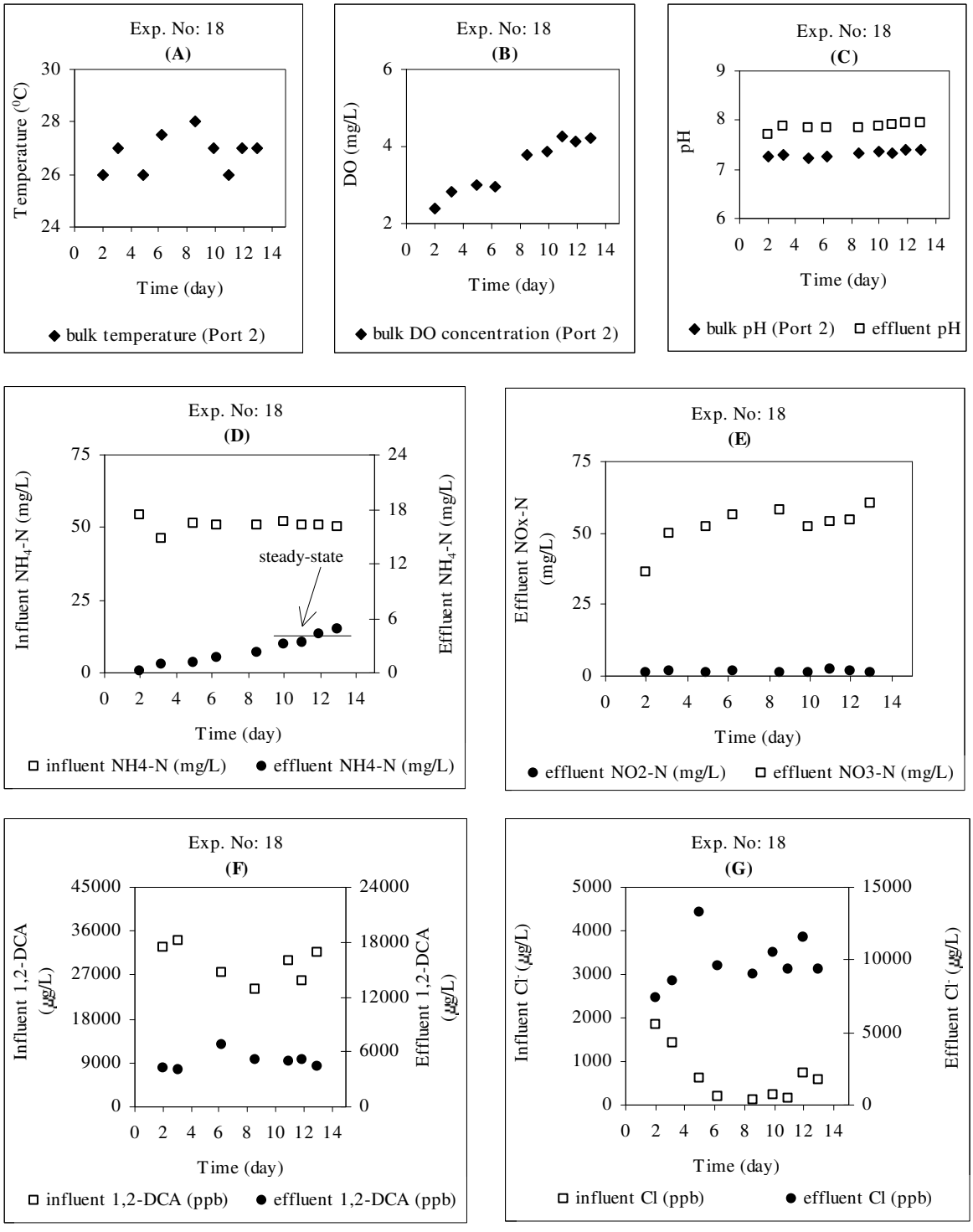

Figure S.18. Continuous–flow experiment with 1,2-DCA No:18 measurements for (a) T, (b) DO, (c) pH, (d) NH_4-N, (e) NO_x-N, (f) 1,2-DCA and (g) Cl^-

[Feed flowrate = 6L/day, Ave. Feed NH_4-N = 51 mg/L, Ave. Feed 1,2-DCA = 29116 ppb]

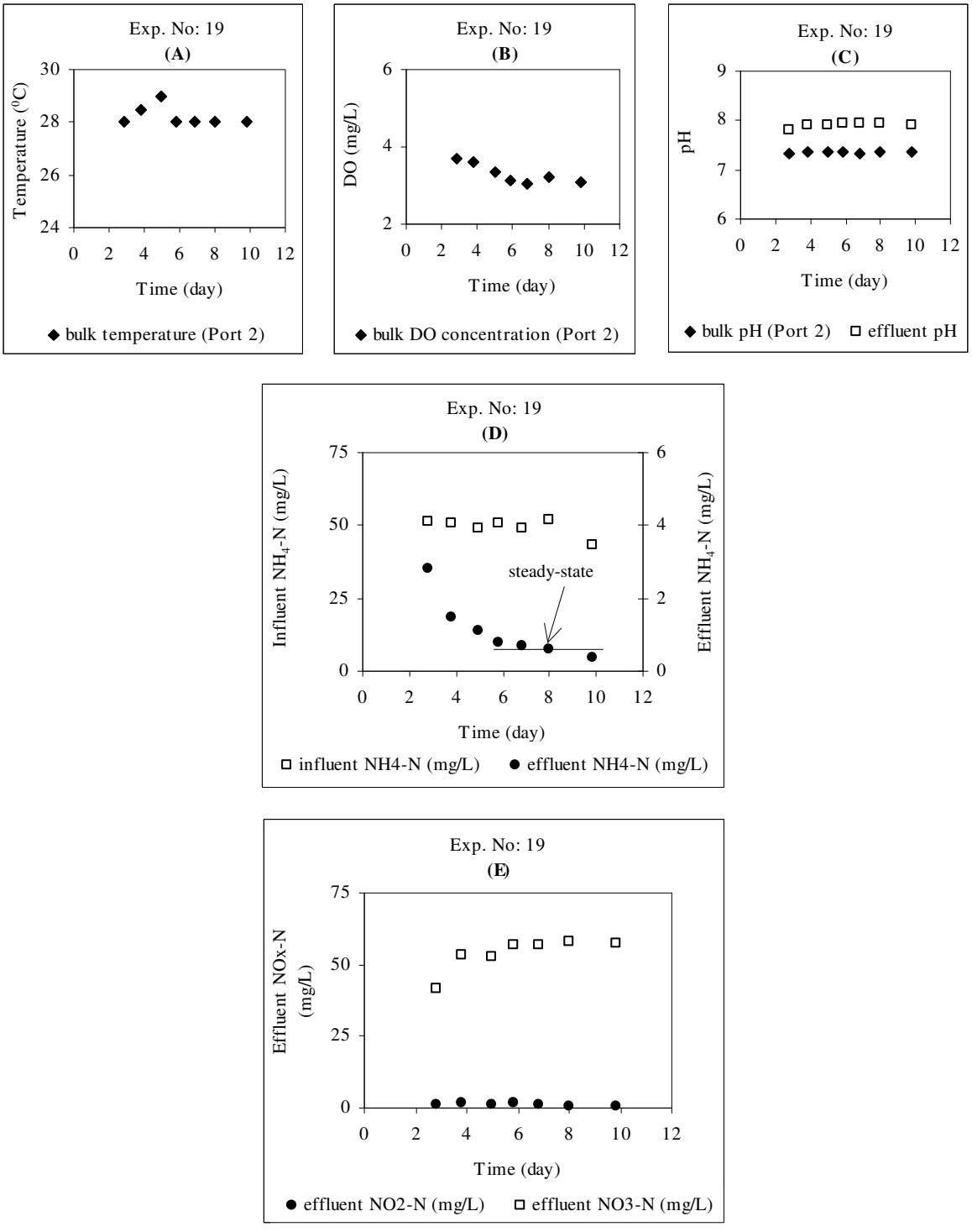

Figure S.19. Continuous–flow experiment with 1,2-DCA No:19 measurements for (a) T, (b) DO, (c) pH, (d) NH_4-N and (e) NO_x-N

[Feed flowrate = 6L/day, Ave. Feed NH_4-N = 49 mg/L, Ave. Feed 1,2-DCA = 0 ppb]

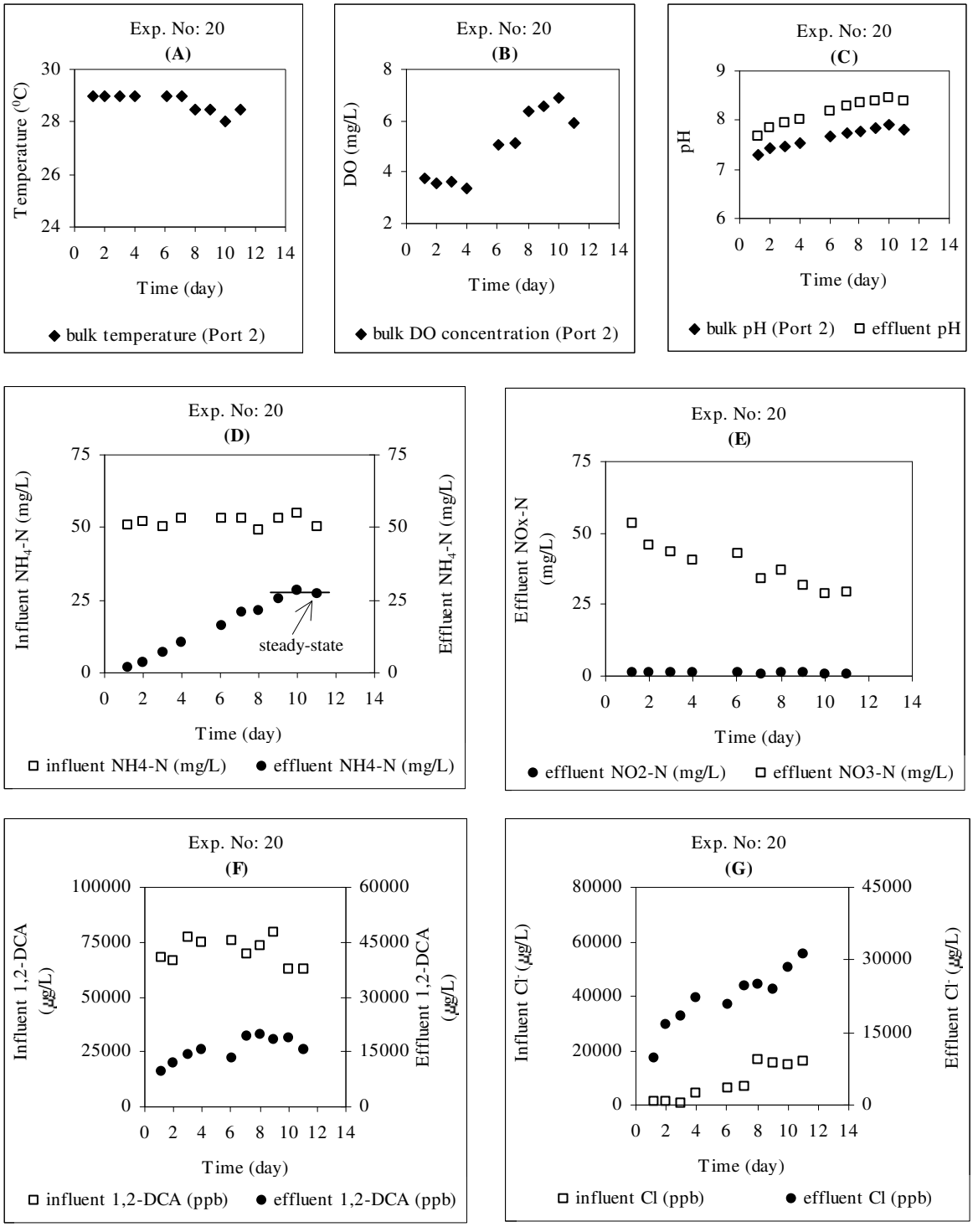

Figure S.20. Continuous–flow experiment with 1,2-DCA No:20 measurements for (a) T, (b) DO, (c) pH, (d) NH_4-N, (e) NO_x-N, (f) 1,2-DCA and (g) Cl^-

[Feed flowrate = 6L/day, Ave. Feed NH_4-N = 53 mg/L, Ave. Feed 1,2-DCA = 68087 ppb]

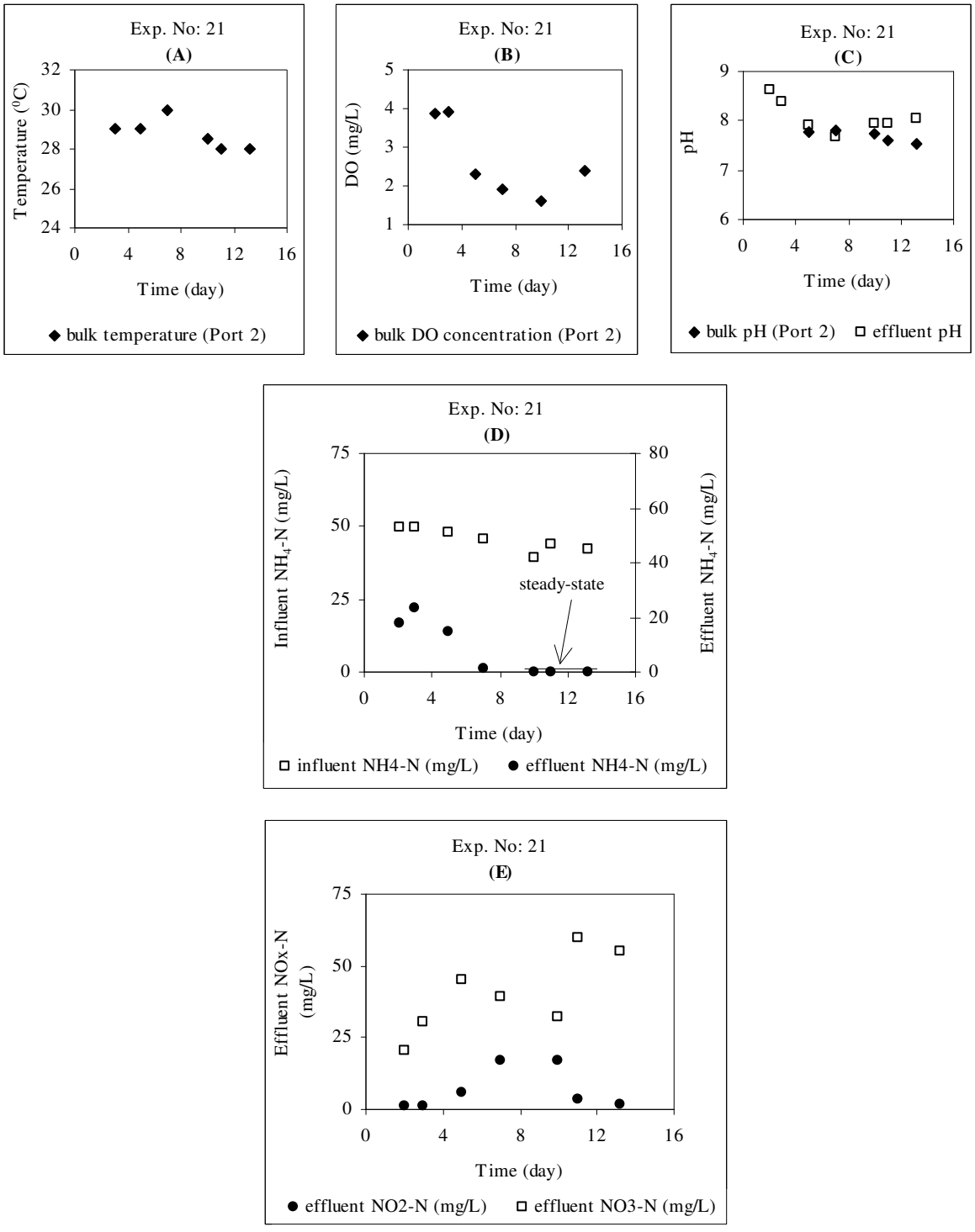

Figure S.21. Continuous–flow experiment with 1,2-DCA No:21 measurements for (a) T, (b) DO, (c) pH, (d) NH_4-N and (e) NO_x-N

[Feed flowrate = 6L/day, Ave. Feed NH_4-N = 42 mg/L, Ave. Feed 1,2-DCA = 0 ppb]

APPENDIX T: STATISTICAL ANALYSIS OF KINETIC MODELS

T.1. Statistical Analysis of Kinetic Models Developed in Section 6.1.1

T.1.1. Residuals Analyses

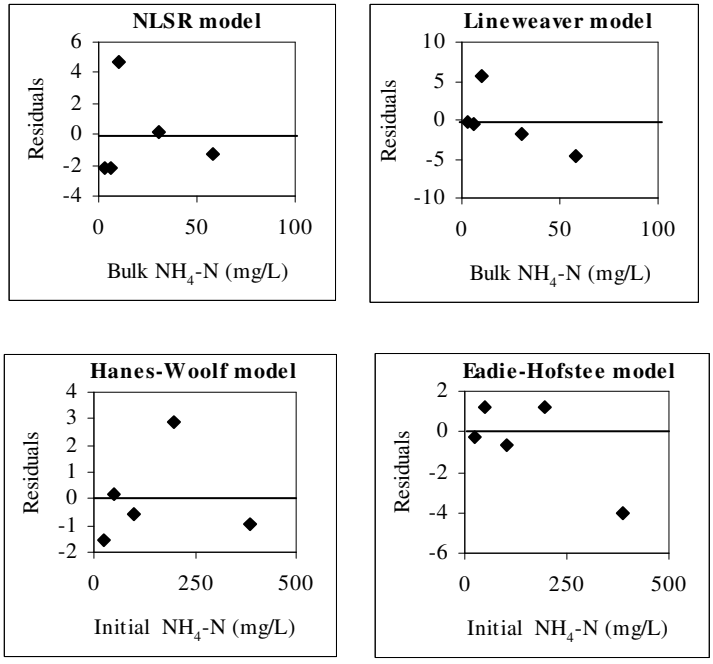

Figure T.1. A few examples of residuals analyses for models developed in Section 6.1.1

T.1.2. Analysis of Variance (ANOVA) outputs

a) with respect to bulk NH_4-N concentrations

```
MINITAB - Two-way ANOVA
Analysis of Variance for q
Source        DF        SS        MS        F        P
m              4      1.14      0.29     0.08    0.988

                        Individual 95% CI
m               Mean    -----+---------+---------+---------+------
1              61.68        (-----------------*-----------------)
2              61.85         (-----------------*-----------------)
3              61.97           (-----------------*-----------------)
4              61.40    (-----------------*-----------------)
5              61.97           (-----------------*-----------------)
                        -----+---------+---------+---------+------
                         60.00     61.00     62.00     63.00
```

b) with respect to initial NH_4-N concentrations

```
MINITAB-Two-way ANOVA
Analysis of Variance for q
Source        DF        SS        MS        F        P
m              4      1.38      0.35     0.27    0.892
Error         16     20.42      1.28
Total         24  11940.55


                        Individual 95% CI
m               Mean    -----+---------+---------+---------+------
1              61.68     (--------------*--------------)
2              61.76      (--------------*---------------)
3              62.19            (--------------*---------------)
4              61.70     (--------------*---------------)
5              62.19            (--------------*---------------)
                        -----+---------+---------+---------+------
                         60.90     61.60     62.30     63.00
```

T.2. Statistical Analysis of Kinetic Models Developed in Section 6.5.2

T.2.1. Residuals Analyses

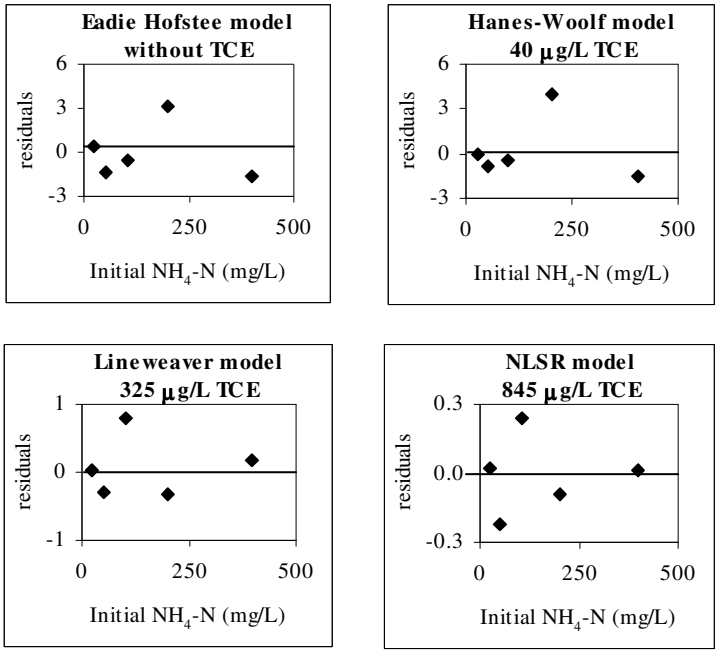

Figure T.2. A few examples of residuals analyses for models developed in Section 6.5.2

T.2.2. Analysis of Variance (ANOVA) outputs

a) without TCE

```
MINITAB- Two-way ANOVA
Analysis of Variance for q
Source        DF        SS        MS        F        P
m              4     0.312     0.078     0.09    0.983


                                  Individual 95% CI
m               Mean   -------+---------+---------+---------+----
1              50.32          (-----------------*-----------------)
2              50.34           (-----------------*-----------------)
3              50.06    (-----------------*----------------)
4              50.36           (-----------------*-----------------)
5              50.29          (-----------------*----------------)
                       -------+---------+---------+---------+----
                          49.50     50.00     50.50     51.00
```

b) 40 µg/L TCE

```
MINITAB- Two-way ANOVA
Analysis of Variance for q
Source        DF        SS        MS        F        P
m              4      1.29      0.32     0.32    0.860


                       Individual 95% CI
m               Mean   ---------+---------+---------+---------+--
1              28.83           (-------------*------------)
2              29.06              (------------*-------------)
3              28.39    (-------------*------------)
4              28.58       (------------*-------------)
5              28.69        (-------------*------------)
                       ---------+---------+---------+---------+--
                            28.00     28.70     29.40     30.10
```

c) 110 µg/L TCE

```
MINITAB- Two-way ANOVA
Analysis of Variance for q
Source        DF        SS        MS        F        P
m              4     0.925     0.231     1.92    0.157


                       Individual 95% CI
m               Mean   -+---------+---------+---------+---------+
1              25.41                     (----------*----------)
2              25.46                       (----------*---------)
3              24.93    (----------*----------)
4              25.36                   (---------*----------)
5              25.39                   (----------*----------)
                       -+---------+---------+---------+---------+
                     24.60     24.90     25.20     25.50     25.80
```

d) 325 µg/L TCE

```
MINITAB- Two-way ANOVA
Analysis of Variance for q
Source        DF        SS        MS        F        P
m              4     0.025     0.006     0.15    0.959


                       Individual 95% CI
m              Mean    ---------+---------+---------+---------+--
1            23.687           (---------------*---------------)
2            23.693           (---------------*----------------)
3            23.613    (---------------*---------------)
4            23.626     (---------------*---------------)
5            23.650       (---------------*---------------)
                       ---------+---------+---------+---------+--
                           23.520    23.640    23.760    23.880
```

e) 845 µg/L TCE

```
MINITAB- Two-way ANOVA
Analysis of Variance for q
Source        DF        SS        MS        F        P
m              4     0.141     0.035     1.64    0.214


                       Individual 95% CI
m              Mean    ---------+---------+---------+---------+--
1            18.097                (-----------*-----------)
2            18.105                 (-----------*-----------)
3            17.913   (-----------*----------)
4            18.115                   (-----------*----------)
5            18.077               (----------*-----------)
                       ---------+---------+---------+---------+--
                           17.880    18.000    18.120    18.240
```

T.3. Statistical Analysis of Kinetic Models Developed in Section 6.8.2

T.3.1. Residuals Analyses

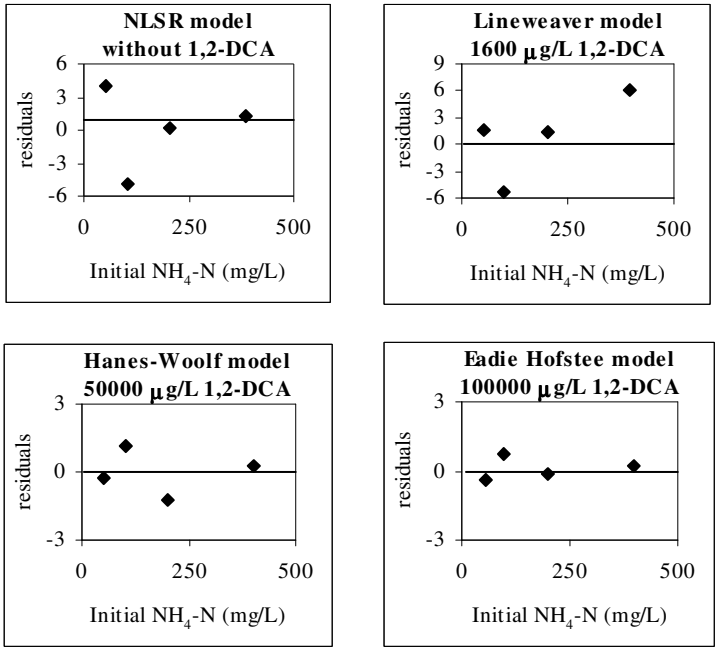

Figure T.3. A few examples of residuals analyses for models developed in Section 6.8.2

T.3.2. Analysis of Varience (ANOVA) outputs

a) without 1,2-DCA

```
MINITAB- Two-way ANOVA
Analysis of Variance for q
Source        DF        SS        MS        F        P
m              4      0.32      0.08     0.02    0.999

                        Individual 95% CI
m               Mean    --+---------+---------+---------+---------
1               85.1       (----------------*----------------)
2               84.9     (----------------*----------------)
3               84.8    (----------------*----------------)
4               85.1       (----------------*----------------)
5               85.0     (----------------*----------------)
                        --+---------+---------+---------+---------
                       82.5      84.0      85.5      87.0
```

b) 1600 µg/L 1,2-DCA

```
MINITAB- Two-way ANOVA
Analysis of Variance for q
Source        DF        SS        MS        F        P
m              4      2.69      0.67     0.13    0.967


                       Individual 95% CI
m               Mean   --+---------+---------+---------+---------
1               78.2          (---------------*----------------)
2               78.0         (---------------*----------------)
3               77.2    (---------------*---------------)
4               78.2          (----------------*---------------)
5               78.1         (----------------*---------------)
                       --+---------+---------+---------+---------
                      75.0      76.5      78.0      79.5
```

c) 15000 µg/L 1,2-DCA

```
MINITAB- Two-way ANOVA
Analysis of Variance for q
Source        DF        SS        MS        F        P
m              4      4.62      1.16     0.31    0.869


                       Individual 95% CI
m               Mean   ---+---------+---------+---------+--------
1              58.52           (-------------*-------------)
2              58.43          (-------------*-------------)
3              57.27    (-------------*-------------)
4              58.57           (-------------*-------------)
5              58.29         (-------------*-------------)
                       ---+---------+---------+---------+--------
                      55.50     57.00     58.50     60.00
```

d) 50000 µg/L 1,2-DCA

```
MINITAB- Two-way ANOVA
Analysis of Variance for q
Source        DF        SS        MS        F        P
m              4     0.066     0.017     0.07    0.989


                       Individual 95% CI
m               Mean   -+---------+---------+---------+---------+
1              42.84      (----------------*----------------)
2              42.82     (----------------*----------------)
3              42.96          (----------------*----------------)
4              42.84     (----------------*----------------)
5              42.80    (----------------*----------------)
                       -+---------+---------+---------+---------+
                   42.30     42.60     42.90     43.20     43.50
```

e) 75000 µg/L 1,2-DCA

```
MINITAB- Two-way ANOVA
Analysis of Variance for q
Source        DF        SS        MS        F        P
m              4     0.121     0.030     0.35    0.840

                        Individual 95% CI
m               Mean    -------+---------+---------+---------+----
1              28.61             (------------*-----------)
2              28.58            (------------*------------)
3              28.42     (------------*------------)
4              28.63              (-----------*------------)
5              28.60            (------------*------------)
                        -------+---------+---------+---------+----
                           28.25     28.50     28.75     29.00
```

f) 100000 µg/L 1,2-DCA

```
MINITAB- Two-way ANOVA
Analysis of Variance for q
Source        DF        SS        MS        F        P
m              4     1.206     0.301     0.74    0.585


                        Individual 95% CI
m               Mean    ----+---------+---------+---------+-------
1              21.62       (-------------*-------------)
2              21.65       (-------------*-------------)
3              22.19                   (-------------*-------------)
4              21.55     (-------------*-------------)
5              21.53     (-------------*-------------)
                        ----+---------+---------+---------+-------
                        21.00     21.50     22.00     22.50
```